

UNIwersYTET JAGIELLOŃSKI W KRAKOWIE

INSTYTUT FIZYKI IM. MARIANA SMOLUCHOWSKIEGO



Stany zreggeizowanych gluonów w chromodynamice kwantowej

JAN KOTAŃSKI

PRACA DOKTORSKA WYKONANA POD KIERUNKIEM
PROF. DR HAB. MICHAŁA PRASZAŁOWICZA

KRAKÓW, MAJ 2005

JAGIELLONIAN UNIVERSITY IN KRAKÓW

MARIAN SMOLUCHOWSKI INSTITUTE OF PHYSICS



Reggeized gluon states in Quantum Chromodynamics

JAN KOTAŃSKI

DOCTORAL DISSERTATION PERFORMED UNDER GUIDANCE OF
PROF. DR HAB. MICHAŁ PRASZAŁOWICZ

KRAKÓW, MAY 2005

Contents

| | | |
|----------|--|-----------|
| 1 | Preface | 13 |
| 2 | Introduction | 17 |
| 2.1 | Hamiltonian for the N -Reggeon states | 17 |
| 2.1.1 | The gluon reggeization | 17 |
| 2.1.2 | Integral equation for the scattering amplitude | 20 |
| 2.1.3 | Impact parameter representation | 22 |
| 2.2 | System with $SL(2, \mathbb{C})$ symmetry | 23 |
| 2.2.1 | Symmetry $SL(2, \mathbb{C})$ | 23 |
| 2.2.2 | Scalar product | 24 |
| 2.2.3 | Conformal charges q_k and the conformal spins | 25 |
| 2.2.4 | Two-dimensional Lorentz spin and the scaling dimension | 27 |
| 2.3 | Conformal charges \hat{q}_k as a differential operators | 28 |
| 2.4 | Other symmetries | 29 |
| 2.5 | Pomeron and odderon | 30 |
| 3 | Baxter Q-operator | 33 |
| 3.1 | Definition of the Baxter Q -operator | 33 |
| 3.2 | Observables | 35 |
| 3.3 | Construction of the eigenfunction | 36 |
| 4 | WKB approximation | 39 |
| 4.1 | WKB approximation for Reggeons | 39 |
| 4.2 | Quantization conditions with WKB | 40 |
| 4.3 | Lattice structure of the conformal charges spectrum | 41 |
| 5 | Eigenfunctions for the conformal charges \hat{q}_k | 43 |
| 5.1 | Solution of the \hat{q}_2 eigenproblem | 43 |
| 5.2 | Various ansatzes | 44 |
| 5.3 | Solutions of the \hat{q}_3 eigenproblem for $N = 3$ | 45 |
| 5.3.1 | Derivation of differential equations for $N = 3$ | 45 |
| 5.3.2 | Solutions for $s = 0$ | 46 |

| | | |
|----------|---|-----------|
| 5.3.3 | Wave-function for $s = \bar{s} = 0$ around $x = \bar{x} = 0^+$ | 47 |
| 5.3.4 | Wave-function for $s = \bar{s} = 0$ around $x = \bar{x} = 1^-$ and $x = \bar{x} = \infty^-$ | 48 |
| 5.3.5 | Transition matrices between solutions around different poles | 49 |
| 5.3.6 | Additional conditions coming from the particle permutation invariance | 50 |
| 5.4 | Set of differential equations for $N = 4$ | 52 |
| 6 | Quantization conditions in the Q-Baxter method | 53 |
| 6.1 | Solution around $z = 0$ | 54 |
| 6.2 | Solution around $z = 1$ | 56 |
| 6.3 | Transition matrices | 58 |
| 7 | Numerical results | 59 |
| 7.0.1 | Trajectories | 59 |
| 7.0.2 | Symmetries | 60 |
| 7.0.3 | Descendent states | 60 |
| 7.1 | Quantum numbers of the $N = 3$ states | 61 |
| 7.1.1 | Lattice structure | 61 |
| 7.1.2 | Trajectories in ν_h | 63 |
| 7.1.3 | Energy and dispersion | 64 |
| 7.1.4 | Descendent states for $N = 3$ | 66 |
| 7.1.5 | Corrections to WKB | 66 |
| 7.2 | Quantum numbers of the $N = 4$ states | 68 |
| 7.2.1 | Descendent states for $N = 4$ | 70 |
| 7.2.2 | Lattice structure for $q_3 = 0$ | 70 |
| 7.2.3 | Resemblant lattices with $\ell_3 = 0$ | 71 |
| 7.2.4 | Winding lattices with $\ell_3 \neq 0$ | 73 |
| 7.2.5 | Corrections to WKB | 76 |
| 7.3 | Quantum numbers of the states with higher N | 78 |
| 7.3.1 | Properties of the ground states | 78 |
| 7.3.2 | Energy for different N | 79 |
| 7.3.3 | Energy dependence on ν_h | 80 |
| 8 | Other quantization conditions | 83 |
| 8.1 | De Vega and Lipatov's solution | 83 |
| 8.1.1 | Three Reggeon states | 85 |
| 9 | Anomalous dimensions | 89 |
| 9.1 | Expansion for the large scale Q | 90 |
| 9.2 | Analytical continuation | 92 |
| 9.2.1 | Two level model | 92 |

| | | |
|-----------|--|------------|
| 9.2.2 | $SL(2, \mathbb{C})$ Heisenberg model for two Reggeons | 93 |
| 9.2.3 | $SL(2, \mathbb{C})$ Heisenberg model for more Reggeons | 94 |
| 9.3 | Spectral surfaces | 95 |
| 9.4 | Energy poles and the anomalous dimensions | 97 |
| 10 | Summary and Conclusions | 101 |
| A | $SL(2, \mathbb{C})$ invariants and other variables | 109 |
| B | Solution of the q_2 eigenproblem | 111 |
| B.1 | Case for $N = 2$ | 111 |
| B.2 | Case for $N = 3$ | 112 |
| B.3 | Case for $N = 4$ | 112 |
| C | Solutions for $N = 3$ | 115 |
| C.1 | Solutions for $s = 0$ around $x = 0^+$ | 115 |
| C.1.1 | Solutions for $q_3 \neq 0$ and $h \notin \mathbb{Z}$ | 115 |
| C.1.2 | Solution with $q_3 = 0$ | 116 |
| C.1.3 | Solution with $q_3 \neq 0$, $q_2 = 0$ and $h = 1$ | 116 |
| C.1.4 | Solution with $q_2 = q_3 = 0$ and $h = 1$ | 117 |
| C.1.5 | Solution with $q_3 \neq 0$, $q_2 = 0$ and $h = 0$ | 118 |
| C.1.6 | Solution with $h = 0$ and $q_2 = q_3 = 0$ | 118 |
| C.1.7 | Solution with $q_3 \neq 0$ and $h = 2$ | 119 |
| C.1.8 | Solution with $q_3 = 0$ and $h = 2$ | 120 |
| C.2 | Solutions for $s = 0$ around $x = 1^-$ | 120 |
| C.2.1 | Solutions for $q_3 \neq 0$ and $h \notin \mathbb{Z}$ | 120 |
| C.2.2 | Solution with $q_3 = 0$ | 121 |
| C.2.3 | Solution with $q_3 \neq 0$, $q_2 = 0$ and $h = 1$ | 121 |
| C.2.4 | Solution with $q_2 = q_3 = 0$ and $h = 1$ | 122 |
| C.2.5 | Solution with $q_3 \neq 0$, $q_2 = 0$ and $h = 0$ | 123 |
| C.2.6 | Solution with $q_2 = q_3 = 0$ and $h = 0$ | 123 |
| C.2.7 | Solution with $q_3 \neq 0$ and $h = 2$ | 124 |
| C.2.8 | Solution with $q_3 = 0$ and $h = 2$ | 125 |
| C.3 | Solutions for $s = 0$ around $x = \infty^-$ | 125 |
| C.3.1 | Solutions for $q_3 \neq 0$ and $h \notin \mathbb{Z}$ | 125 |
| C.3.2 | Solution with $q_3 = 0$ | 126 |
| C.3.3 | Solution with $q_3 \neq 0$, $q_2 = 0$ and $h = 1$ | 127 |
| C.3.4 | Solution with $q_2 = q_3 = 0$ and $h = 1$ | 127 |
| C.3.5 | Solution with $q_3 \neq 0$, $q_2 = 0$ and $h = 0$ | 128 |
| C.3.6 | Solution with $q_2 = q_3 = 0$ and $h = 0$ | 129 |

| | | |
|-------|--|-----|
| C.3.7 | Solution with $q_3 \neq 0$ and $h = 2$ | 129 |
| C.3.8 | Solution with $q_3 = 0$ and $h = 2$ | 130 |

| | | |
|----------|--|------------|
| D | Coefficients in the eigenequations for $N = 4$ | 131 |
|----------|--|------------|

List of Figures

| | | |
|------|--|----|
| 2.1 | Some diagrams which give contribution to the total cross section $\sigma_{2 \rightarrow 2}$ | 17 |
| 2.2 | Diagram symbolizing the scattering amplitude $A_{2 \rightarrow n+2}$ | 19 |
| 2.3 | Illustration of the BFKL equation by means of Feynman diagrams. | 21 |
| 4.1 | The Riemann surface Γ_N with integration cycles, α_j and β_j | 41 |
| 7.1 | The spectrum of $q_3^{1/3}$ for the system of $N = 3$ particles for $h = \frac{1}{2}$ and $h = 1$. . . | 62 |
| 7.2 | The spectrum of $q_3^{1/3}$ for the system of $N = 3$ particles for $h = \frac{3}{2}$ and $h = 2$. . . | 63 |
| 7.3 | The dependence of quantized $q_3(\nu_h; \ell_1, \ell_2)$ on the total spin $h = 1/2 + i\nu_h$ | 64 |
| 7.4 | The trajectories of $q_3^{1/3}$ projected on $\nu_h = 0$ for $n_h = 0$ and $n_h = 1$ | 65 |
| 7.5 | The trajectories of $q_3^{1/3}$ projected on $\nu_h = 0$ for $n_h = 2$ and $n_h = 3$ | 66 |
| 7.6 | The energy spectrum corresponding to three trajectories shown in Figure 7.3 . . | 67 |
| 7.7 | The spectrum of q_4 for $N = 4$ and the total spin $h = 1/2$ | 69 |
| 7.8 | The spectra of the conformal charges for $N = 4$ | 70 |
| 7.9 | The dependence of the energy, $-E_4/4$, and q_4/q_2 with $q_2 = 1/4 + \nu_h^2$ | 71 |
| 7.10 | The spectra of the conformal charges for $N = 4$ with $\theta_4 = 0$, $\ell_3 = 0$ and $\ell_4 = 1$. . | 72 |
| 7.11 | The spectra of the conformal charges for $N = 4$ with $\theta_4 = 0$, $\ell_3 = 0$ and $\ell_4 = 2$. . | 73 |
| 7.12 | The spectra of the conformal charges for $N = 4$ with $\theta_4 = \pi$, $\ell_3 = 0$ and $\ell_4 = 1$. . | 74 |
| 7.13 | The spectra of the conformal charges for $N = 4$ with $\theta_4 = \pi$, $\ell_3 = 0$ and $\ell_4 = 2$. . | 74 |
| 7.14 | The winding spectrum of $\{q_3, q_4\}$ for $N = 4$ with $h = 1/2$, $\theta_4 = -\pi/2$ and $\ell_3 = 1$. . | 75 |
| 7.15 | The winding spectrum of $\{q_3, q_4\}$ for $N = 4$ and $h = 1/2$ with $\theta_4 = 0$ and $\ell_3 = 2$. . | 76 |
| 7.16 | The winding spectrum of $\{q_3, q_4\}$ for $N = 4$ and $h = 1/2$ with $\theta_4 = \pi$ and $\ell_3 = 2$. . | 77 |
| 7.17 | The dependence of $-E_N/4$ on the number of particles N | 80 |
| 7.18 | The dependence of the energy $-E_N(\nu_h)/4$ and $ q_N /q_2$ on $h = 1/2 + i\nu_h$ | 81 |
| 9.1 | Spectral surfaces for the two energy level model | 93 |
| 9.2 | The energy spectrum of the $N = 3$ Reggeon states $E_3(\nu_h; n_h, \ell)$ for $n_h = 0$. . . | 96 |

List of Tables

| | | |
|-----|--|----|
| 7.1 | Comparison of the exact spectrum of $q_3^{1/3}$ with the WKB expression | 65 |
| 7.2 | The fitted coefficient to the series formula of $q_3^{1/3}$ | 68 |
| 7.3 | Comparison of $q_4^{1/4}$ at $q_3 = 0$ and $h = 1/2$ with the WKB expression | 72 |
| 7.4 | The fitted coefficient to the series formula of $q_4^{1/4}$ | 78 |
| 7.5 | The exact quantum numbers, q_N , and the energy, E_N | 80 |

Chapter 1

Preface

The aim of this work is to present a role of the reggeized gluon states in perturbative Quantum Chromodynamics. The reggeized gluon states, also called Reggeons, appear in the Regge limit where the square of the total energy s is large while the transfer of four-momentum t is low and fixed. In this limit the leading contribution to the scattering amplitude of hadrons is dominated by the exchange of intermediate particles, Reggeons, which are the compound states of gluons [1, 2, 3, 4, 5, 6].

Even for the Regge limit in the generalized leading logarithm approximation [7, 8, 9] this problem is technically very complicated due to the non-abelian structure of QCD. Therefore, in order to simplify colour factors the 't Hooft's multi-colour limit [10, 11, 12] is performed, in which a number of colours $N_c \rightarrow \infty$. This causes that the Reggeon wave-functions become the eigenstates of a Hamiltonian which is equivalent to the Hamiltonian for the non-compact Heisenberg $SL(2, \mathbb{C})$ spin magnet. Because of this symmetry the multi-Reggeon system with N particles is completely solvable [13, 14]. Thus, it possesses a complete set of integrals of motion, conformal charges $(q_2, \bar{q}_2, q_3, \bar{q}_3, \dots, q_N, \bar{q}_N)$. The eigenvalues of the $SL(2, \mathbb{C})$ Hamiltonian are also called the energies of the Reggeons. The Schrödinger equation for the lowest non-trivial case, i.e. for $N = 2$ Reggeons, was formulated and solved by Balitsky, Fadin, Kureav and Lipatov [15, 16, 4]. They calculated the energy of the Pomeron state with $N = 2$ Reggeons. An integral equation for three and more Reggeons was formulated in Refs. [7, 8, 17] in 1980. However, it took almost twenty years to obtain the solution for $N = 3$, which corresponds to the QCD odderon [18, 19, 20]. Finally, the solutions for higher $N = 4, \dots, 8$ recently in series of papers [21, 22, 23] written in collaboration with S.É. Derkachov, G.P. Korchemsky and A.N. Manashov.

Description of scattering amplitudes in terms of the reggeized gluon states is most frequently used in two different kinematical regions. The first region appears in calculation of the elastic scattering amplitude of two heavy hadrons whose masses are comparable. Here the amplitude is equal to a sum over the Regge poles. They give behaviour in the Regge limit, $s \rightarrow \infty$ and $t = \text{const}$, like $s^{\alpha(t)}$ where $\alpha(0)$ is called the intercept and its value is close to 1. On the other hand, the intercept is related to the minimum of the Reggeon energy defined by the $SL(2, \mathbb{C})$

Hamiltonian. Thus, evaluating the spectrum of the $SL(2, \mathbb{C})$ XXX Heisenberg model we can calculate the behaviour of the hadron scattering amplitudes.

The second kinematical region is the region of deep inelastic scattering (DIS) where a virtual photon $\gamma^*(Q^2)$ is scattered off a (polarized) hadron with the mass $M^2 = p_\mu^2$, such that $\Lambda_{\text{QCD}}^2 \ll M^2 \ll Q^2$ with $x = Q^2/2(p \cdot q)$ and $q_\mu^2 = -Q^2$. In this case the moments of the structure function $F_2(x, Q^2)$ can be expanded (OPE) in a power series in $1/Q^2$ where the exponents of this expansion are related to the twist of Reggeons and anomalous dimensions of QCD. Analysing the spectrum of the $SL(2, \mathbb{C})$ Hamiltonian one can find a twist related to a given Reggeon wave-function and calculate the corresponding anomalous dimension. This was done for the leading twist $n = 2$ in Ref. [24] and for other twists of two-Reggeon states in Ref. [25]. The anomalous dimension and twists for more than two Reggeons were discussed in Ref. [26].

In this work we present the methods of constructing the Reggeon eigenstates. Moreover, we calculate the reach spectrum of the the Reggeon energy and the conformal charges $\{q_k, \bar{q}_k\}$. Finally, we calculate anomalous dimensions of QCD and twists in operator product expansion (OPE) which are also provided by the Reggeon states. In the first three Chapters we discuss the current state of knowledge. The main results of the present work are collected in Chapters 5–7 and in Chapter 9. For completeness in Chapter 8 we added description of another method presented in Refs. [27, 28].

Thus, in Chapter 2 we explain when the reggeization of the gluon appears [29]. Next, we perform the multi-colour limit [10, 11, 12], discuss the properties of the $SL(2, \mathbb{C})$ symmetry and construct invariants of this symmetry, the conformal charges. In next Chapter we introduce a Baxter Q –operator method [30] with Baxter equations which allows us to solve the Reggeon system, completely. Chapter 4 contains the quasi-classical solution for the Baxter equations [21]. It gives us the WKB approximation for the spectra of the Reggeon energy and the conformal charges. It also explains the structure of these spectra.

In Chapter 5 we show construction of the Reggeon eigenfunctions which consists in solving the the eigenequations of the conformal charges. We systematize the knowledge about the ansatzes for eigenstates of $\{q_k, \bar{q}_k\}$ with an arbitrary number of Reggeons, N , extend the calculations to an arbitrary complex spins s and derive differential eigenequations for the conformal charges with $N = 3, 4$. Moreover, we show solutions to the differential eigenequations with $N = 3$ and $s = 0$ and resum obtained series solutions for the $q_3 = 0$ case. In next Chapter we present an exact solution to the Baxter equations. It consists in rewriting the Baxter equation into the differential equation, which may be solved by a series method, and finding the quantization conditions for $\{q_k, \bar{q}_k\}$ which comes from single-valuedness of the Reggeon wave-function and analytical properties of the Baxter functions. The numerical results of this method for $N = 2, \dots, 8$ Reggeons are shown in Chapter 7 [22, 23]. In the $N = 3$ case we present quantized values of q_3 for different Lorentz spins $n_h = 0, \dots, 3$ as well as corrections to the WKB approximation. For $N = 4$ we show the resemblant and winding structure of the

q_4 and q_3 spectrum and also corrections to the WKB approximation when $q_3 = 0$. At the end we discuss the ground states with $N = 2, \dots, 8$ Reggeons and describe their properties. In Chapter 8 we review another approach to the Baxter equation which was presented in Refs. [27, 28]. We discuss the advantages and disadvantages of this method and compare it with the results presented in previous Chapters. Finally, in Chapter 9 we concentrate on deep inelastic scattering processes. We calculate anomalous dimensions of QCD and twists coming from Reggeized gluon states [26]. One can obtain them by performing an analytical continuation of the Reggeon energy into the complex space of the scaling dimension ν_h and analysing the pole structure of the energy. At the end we make final conclusions.

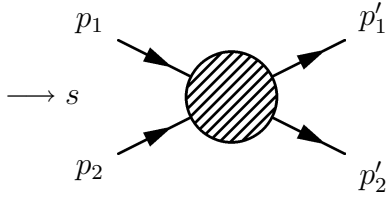
Chapter 2

Introduction

2.1 Hamiltonian for the N -Reggeon states

2.1.1 The gluon reggeization

The Regge limit can be conveniently illustrated by considering the elastic scattering amplitude of two hadrons



$$\text{with } s = (p_1 + p_2)^2, \text{ and } t = (p_1 - p_1')^2, \quad (2.1)$$

in the kinematical region:

$$s \rightarrow \infty, \quad t = \text{const.} \quad (2.2)$$

In this case the largest contribution to the scattering amplitude is provided by a multi-gluon exchange. It was shown in the papers [3, 4, 5, 6, 16, 15, 31] that in the limit (2.2) so called gluon reggeization occurs. It means that the contribution to the scattering amplitude may be written as a sum of ladder diagrams, where compound states of the reggeized gluons, called Reggeons, are exchanged in the t -channel and interact with each other.

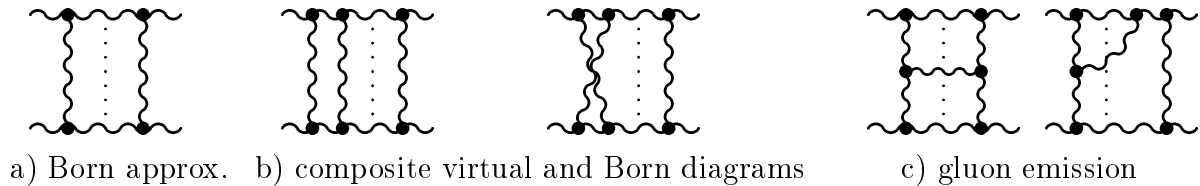


Figure 2.1: Some diagrams of the order g^4 and g^6 which give contribution to the total cross section $\sigma_{2 \rightarrow 2}$.

In order to illustrate what the gluon reggeization is, we show in Figure 1 some diagrams of the order g^4 and g^6 which give contribution to the total cross section $\sigma_{2 \rightarrow 2}$ for two scattered

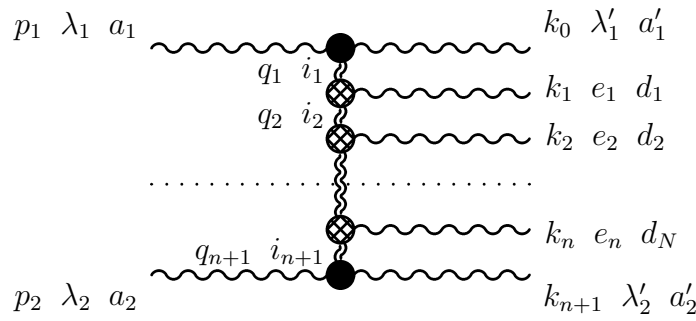


Figure 2.2: Diagram symbolizing the scattering amplitude $A_{2 \rightarrow n+2}$

numbered from 1 to n are characterized by polarization vectors e_j , where $j = 1, \dots, n$. Similarly for the colour indices, the two initial gluons and the two final ones have the colour indices a_i, a'_i where $i = 1, 2$, whereas the indices of the produced gluons are denoted as d_j where $j = 1, \dots, n$. The Reggeons transfer squares of 4-momenta $t_j = q_j^2$ and possess colour indices i_j , where $j = 1, \dots, n+1$.

The total contribution of the diagram from the Figure 2 to the scattering amplitude has the form

$$A_{2 \rightarrow n+2} = 2sg^{n+1} \delta_{\lambda_1 \lambda'_1} \delta_{\lambda_2 \lambda'_2} \times \sum_{i_1 \dots i_n} T_{a'_1 a_1}^{i_1} \frac{s_{0,1}^{\omega(t_1)}}{t_1} T_{i_2 i_1}^{d_1} (e_1 F(q_2, q_1)) \frac{s_{1,2}^{\omega(t_2)}}{t_2} T_{i_3 i_2}^{d_2} (e_2 F(q_3, q_2)) \dots \frac{s_{n,n+1}^{\omega(t_{n+1})}}{t_{n+1}} T_{a'_2 a_2}^{i_{n+1}}, \quad (2.8)$$

where $s_{i,j} = (k_i + k_j)^2$.

One can decompose the momenta k_i in a basis of the scattered particles momenta

$$k_i = \alpha_i p_1 + \beta_i p_2 + k_{i\perp}. \quad (2.9)$$

In the limit (2.2) the largest contribution comes from the kinematical region where $\alpha_{j-1} \gg \alpha_j$, $\beta_{j-1} \ll \beta_j$ and small $q_j^2 \simeq q_{j\perp}^2$. Taking square of the diagram in Figure 2 one can perform integration over longitudinal degrees of freedom. All non-trivial dynamics is then concealed in the 2-dimensional subspace of transverse variables.

In Eq. (2.7) one has to sum over polarizations and colours of intermediate particles. The sum over polarizations gives

$$\sum_i e_{\lambda_i}^\mu F_\mu(q_{i+1}, q_i) e_{\lambda_i}^\nu F_\nu(q'_{i+1}, q'_i) = -F_\mu(q_{i+1}, q_i) g^{\mu\nu} F_\nu(q'_{i+1}, q'_i) \equiv 2K_q(q_i, q_{i+1}), \quad (2.10)$$

where

$$K_q(q_i, q_{i+1}) = q^2 - \frac{q_{i\perp}^2 q'_{i+1\perp}^2 + q_{i+1\perp}^2 q'_{i\perp}^2}{k_{i\perp}^2} \quad (2.11)$$

with $t = q^2$. In order to perform the sum over colours it is convenient to introduce projectors $P^{(R)}$ onto irreducible representation (R) composed of two colour octets in the t -channel:

$$(8) \otimes (8) = (1) \oplus (8)_S \oplus (8)_A \oplus (10) \oplus (\overline{10}) \oplus (27). \quad (2.12)$$

The scattering interaction of two reggeized gluons may be then written as

$$A_{a_2 a'_2, a_1 a'_1}(s, t) = \sum_{(R)} P_{a_2 a'_2, a_1 a'_1}^{(R)} A^{(R)}(s, t), \quad (2.13)$$

where $A^{(R)}(s, t)$ is the amplitude with specified colour state in the t channel. For the i -th intermediate gluon we obtain a colour part in the form

$$\sum_{d_i} T_{b_{i+1}, b_i}^{d_i} (T_{b'_{i+1}, b'_i}^{d_i})^* = -(TT')_{b_{i+1} b_i, b'_{i+1} b'_i} = \sum_R \lambda_R P_{b_{i+1} b_i, b'_{i+1} b'_i}^{(R)}, \quad (2.14)$$

where λ_R is the colour factor.

Summarizing, the absorptive part of the scattering amplitude for two gluons with conservation of helicities is given as [32, 4, 33]

$$\begin{aligned} \text{Im} A^{(R)}(s, t) = \pi \lambda_R^2 s \sum_{n=0}^{\infty} g^{2(n+2)} \int \prod_{i=1}^{n+1} \frac{d^2 q_i ds_{i-1, i}}{16\pi^3} \left(\frac{s_{i-1, i}}{s_0} \right)^{\omega(t_i) + \omega(t'_i)} \frac{1}{t_i t'_i} \\ \times \prod_{i=1}^n 2K_q^{(R)}(q_i, q_{i+1}) \delta\left(\prod_{i=0}^n s_{i, i+1} - s \prod_{i=1}^n |k_{i\perp}^2|\right). \end{aligned} \quad (2.15)$$

The reggeization may only occur in the non-abelian theories. In contrast to the quantum chromodynamics, the reggeization of particles does not appear in such theories as quantum electrodynamics as well as scalar field theories. These theories do possess neither a colour structure nor three-gauge-field vertices, which are responsible for gluon emission, and as a result in these theories $\omega(t) = 0$.

2.1.2 Integral equation for the scattering amplitude

Performing the Mellin transformation on (2.15), the sum over n and introducing new 2-dimensional variables in the transverse subspace:

$$\begin{aligned} l_1 = q_1, \quad l_2 = -q'_1 = q - q_1, \\ l'_1 = q_{n+1}, \quad l'_2 = -q'_{n+1} = q - q_{n+1}, \\ t_i = -l_i^2 < 0, \quad t = -q^2 < 0 \quad \text{for } i = 1, 2, \end{aligned} \quad (2.16)$$

we obtain

$$a_j^{(R)} = \int \frac{ds}{2\pi i} s^{-j-1} \text{Im} A^R(s, t) = 2g^2 \lambda_R^2 \int \frac{d^2 l_1}{16\pi^3 t_1 t_2} \phi_{jq}^{(R)}(l_1), \quad (2.17)$$

where the function $\phi_{jq}^{(R)}(l_1)$ describes the gluon ladder with two external reggeized gluons and with the fixed total angular momentum j and the transferred momentum q . This function satisfies the integral BFKL equation [15, 16, 4]

$$(j - 1 - \omega(t_1) - \omega(t_2)) \phi_{jq}^{(R)}(l_1) = 1 + 2\alpha_s \lambda_R \int \frac{d^2 l'_1}{4\pi^2} V_q(l_1, l'_1) \phi_{jq}^{(R)}(l'_1), \quad (2.18)$$

where $\alpha_s = g^2/4\pi$, and the interaction potential between two Reggeons is

$$\hat{V}_{12} : \quad V_q(l_1, l'_1) = \frac{K_q(l_1, l'_1)}{l_1'^2 l_2'^2} = \left(\frac{l_1^2 l_2'^2 + l_2^2 l_1'^2}{(l_1 - l'_1)^2} - q^2 \right) \frac{1}{l_1'^2} \frac{1}{l_2'^2}. \quad (2.19)$$

Equation (2.18) may be illustrated using the diagrammatic form shown in Figure 3. Notice that Eq. (2.18) does not contain the propagators of out-going gluons related to the momenta l_1 and l_2 .

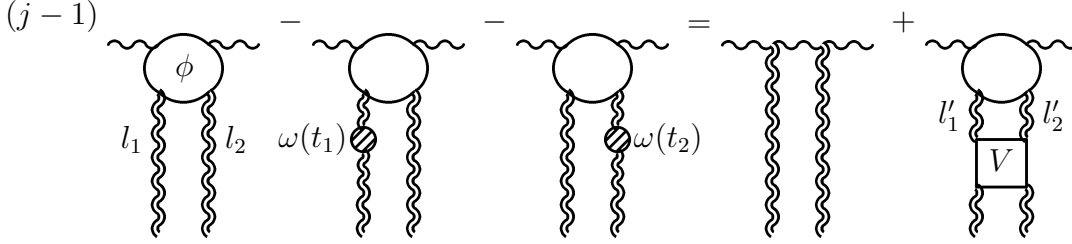


Figure 2.3: Illustration of the BFKL equation by means of Feynman diagrams.

Equation (2.18) contains infrared singularities. The Reggeons in the t -channel may form different colour representations (2.12). For the singlet $\lambda_{R=1} = 3$. In this case, for $q \neq 0$ all infrared singularities cancel. For $q = 0$, the integrand kernel in Eq. (2.18) contains singularities at $l'_1 = l'_2 = 0$. Equation (2.18) describes the process with a gluon of momentum p_2 being a target. In reality we are not interested in the scattering on a gluon, but on a physical colourless particle. In this case thanks to inhomogeneity in Equation (2.18), which describes the Reggeon interaction with a target, all infrared singularities disappear.

Equation (2.18) has the form of the inhomogeneous integral Schrödinger equation

$$(\hat{\mathcal{H}}_2 - \mathcal{E}) \otimes \phi = f, \quad \text{where} \quad \hat{\mathcal{H}}_2 = \omega(t_1) + \omega(t_2) + 2\alpha_s \lambda_1 \hat{V}_{12}, \quad \mathcal{E} = j - 1, \quad (2.20)$$

whereas \otimes means convolution of the Hamiltonian with the wave-function ϕ .

Equation (2.20) describes exchange of two reggeized gluons. It is possible to generalize it to more gluons. The kinetic energy of the i -th Reggeon is equal to $\omega(t_i)$. The potential of the interaction between two Reggeons has the form $6\alpha_s \hat{V}_{12}$, where \hat{V}_{12} (2.19) is an integral operator. For N Reggeons we have

$$(\hat{\mathcal{H}}_N - \mathcal{E}) \otimes \phi = f, \quad (2.21)$$

where the Hamiltonian, which was firstly derived in the works [7, 8, 17] takes a form

$$\begin{aligned} \hat{\mathcal{H}}_N &= \sum_{i=1}^N \omega(t_i) - 2\alpha_s \sum_{i < k=2}^N T_i T_k \hat{V}_{ik} \\ &= -\frac{1}{3} \sum_{i < k=2}^N T_i T_k (\omega(t_i) + \omega(t_k) + 6\alpha_s \hat{V}_{ik}) = -\frac{1}{3} \sum_{i < k=2}^N T_i T_k \hat{H}_{ik}. \end{aligned} \quad (2.22)$$

The interaction potential \hat{V}_{ik} between i -th and k -th reggeized gluons is defined by Eq. (2.19).

2.1.3 Impact parameter representation

The Hamiltonian (2.22) was defined in two-dimensional space of transverse Reggeon momenta. It appears that it is more convenient to perform calculations using variables in the impact parameter space using the transverse spatial coordinates of Reggeons (x_j, y_j) . We pass to this representation performing Fourier transform of Eq. (2.22). After introducing holomorphic and anti-holomorphic complex coordinates for the j -th reggeized gluon

$$z_j = x_j + iy_j, \quad \bar{z}_j = x_j - iy_j \quad (2.23)$$

the Hamiltonian for a pair of Reggeons \hat{H}_{ik} defined in Eq. (2.22) separates into two independent parts:

$$\hat{H}_{ik} = -\frac{\alpha_s}{2\pi}(\hat{H}(z_i, z_k) + \hat{H}(\bar{z}_i, \bar{z}_k)). \quad (2.24)$$

Now, one can see that (2.21) was reduced to two one-dimensional Schrödinger equations.

The holomorphic part and analogously the anti-holomorphic one has the form

$$\hat{H}(z_j, z_k) = -P_j^{-1} \ln(z_{jk}) P_j - P_k^{-1} \ln(z_{jk}) P_k - \ln(P_i P_k) + 2\psi(1), \quad (2.25)$$

where $P_j = -i\partial_{z_j}$, and $z_{jk} = z_j - z_k$.

The Hamiltonian (2.25) is $SL(2, \mathbb{C})$ conformal invariant. It means that is invariant under translation, scaling and inversion operation [25]. An eigenstate of the full Hamiltonian (2.22) may be written as the bilinear form $\Phi = \bar{\Psi} \times \Psi$. In this work we demand that this function is single-valued and normalized.

The colour factor $T_i T_k$ in the Hamiltonian (2.22) may be calculated exactly for $N = 2$ (i.e. the leading order of Pomeron exchange) and for $N = 3$ (i.e. the leading order of odderon and the next to leading order of Pomeron exchange). For $N > 3$ we use an approximation $N_c \rightarrow \infty$. Finally we obtain the Hamiltonian of the nearest neighbour interaction

$$\hat{\mathcal{H}}_N = \hat{H}_N + \hat{\bar{H}}_N = \frac{\bar{\alpha}_s}{4} \sum_{k=1}^N \left[\hat{H}(z_k, z_{k+1}) + \hat{H}(\bar{z}_k, \bar{z}_{k+1}) \right] \quad (2.26)$$

with $\bar{\alpha}_s = \alpha_s N_c / \pi$ where N_c is the number of colours, and z_1 and z_{N+1} correspond to the same Reggeon.

The total cross section for the exchange of two reggeized gluons in the singlet representation (Pomeron) is proportional to $s^{\omega(t)}$. This behaviour is in contradiction with unitarity of the S matrix. There is a conjecture [7, 34] that in order to conserve unitarity one has to sum up diagrams for all N -Reggeon exchanges. Additionally, as discussed in the papers [35, 36, 34] the multiple Pomeron exchanges, so called the fan diagrams, are more likely to unitarize the total hadronic cross section [37]. In the latter diagrams the number of the Reggeons varies in the t -channel. Those diagrams are beyond the scope of this work.

2.2 System with $SL(2, \mathbb{C})$ symmetry

2.2.1 Symmetry $SL(2, \mathbb{C})$

The Hamiltonian (2.26) is invariant under the coordinate transformation of the $SL(2, \mathbb{C})$ group

$$z'_k = \frac{az_k + b}{cz_k + d}, \quad \bar{z}'_k = \frac{\bar{a}\bar{z}_k + \bar{b}}{\bar{c}\bar{z}_k + \bar{d}} \quad (2.27)$$

with $k = 1, \dots, N$ and $ad - bc = \bar{a}\bar{d} - \bar{b}\bar{c} = 1$.

Now one may associate with each particle generators of this transformation [38]. This generators are a pair of mutually commuting holomorphic and anti-holomorphic spin operators, $S_\alpha^{(k)}$ and $\bar{S}_\alpha^{(k)}$. They satisfy the standard commutation relations $[S_\alpha^{(k)}, S_\beta^{(n)}] = i\epsilon_{\alpha\beta\gamma}\delta^{kn}S_\gamma^{(k)}$ and similarly for $\bar{S}_\alpha^{(k)}$. The generators act on the quantum space of the k -th particle, $V^{(s_k, \bar{s}_k)}$ as differential operators

$$\begin{aligned} S_0^k &= z_k \partial_{z_k} + s_k, & S_-^{(k)} &= -\partial_{z_k}, & S_+^{(k)} &= z_k^2 \partial_{z_k} + 2s_k z_k, \\ \bar{S}_0^k &= \bar{z}_k \partial_{\bar{z}_k} + \bar{s}_k, & \bar{S}_-^{(k)} &= -\partial_{\bar{z}_k}, & \bar{S}_+^{(k)} &= \bar{z}_k^2 \partial_{\bar{z}_k} + 2\bar{s}_k \bar{z}_k, \end{aligned} \quad (2.28)$$

where $S_\pm^{(k)} = S_1^{(k)} \pm iS_2^{(k)}$ while the complex parameters, s_k and \bar{s}_k , are called the complex spins. Thus, the Casimir operator reads

$$\sum_{j=0}^2 (S_j^{(k)})^2 = (S_0^{(k)})^2 + (S_+^{(k)} S_-^{(k)} + S_-^{(k)} S_+^{(k)})/2 = s_k(s_k - 1) \quad (2.29)$$

and similarly for the anti-holomorphic operator $(\bar{S}^{(k)})^2$. The eigenstates of $SL(2, \mathbb{C})$ invariant system transform as [39, 40]

$$\Psi(z_k, \bar{z}_k) \rightarrow \Psi'(z_k, \bar{z}_k) = (cz_k + d)^{-2s_k} (\bar{c}\bar{z}_k + \bar{d})^{-2\bar{s}_k} \Psi(z'_k, \bar{z}'_k). \quad (2.30)$$

Due to the invariance (2.27) of the system we can rewrite the Hamiltonian (2.26)

$$\mathcal{H}_N = H_N + \bar{H}_N, \quad [H_N, \bar{H}_N] = 0 \quad (2.31)$$

in terms of the conformal spins (2.28)

$$H_N = \sum_{k=1}^N H(J_{k,k+1}), \quad \bar{H}_N = \sum_{k=1}^N H(\bar{J}_{k,k+1}), \quad H(J) = \psi(1 - J) + \psi(J) - 2\psi(1) \quad (2.32)$$

with $\psi(x) = d \ln \Gamma(x)/dx$ being the Euler function and $J_{N,N+1} = J_{N,1}$. Here operators, $J_{k,k+1}$ and $\bar{J}_{k,k+1}$, are defined through the Casimir operators for the sum of the spins of the neighbouring Reggeons

$$J_{k,k+1}(J_{k,k+1} - 1) = (S^{(k)} + S^{(k+1)})^2 \quad (2.33)$$

with $S_\alpha^{(N+1)} = S_\alpha^{(1)}$, and $\bar{J}_{k,k+1}$ is defined similarly.

In statistical physics (2.32) is called the Hamiltonian of the non-compact $SL(2, \mathbb{C})$ XXX Heisenberg spin magnets. It describes the nearest neighbour interaction between N non-compact $SL(2, \mathbb{C})$ spins attached to the particles with periodic boundary conditions.

For the homogeneous spin chain we have to take $s_k = s$ and $\bar{s}_k = \bar{s}$. In QCD values of (s, \bar{s}) depend on a chosen scalar product in the space of the wave-functions (2.30) and they are usually equal to $(0, 1)$ or $(0, 0)$ [38, 27].

2.2.2 Scalar product

In order to find the high energy behaviour of the scattering amplitude we have to solve the Schrödinger equation

$$\mathcal{H}_N^{(s=0, \bar{s}=1)} \Psi(\vec{z}_1, \vec{z}_2, \dots, \vec{z}_N) = E_N \Psi(\vec{z}_1, \vec{z}_2, \dots, \vec{z}_N) \quad (2.34)$$

with the eigenstate $\Psi(\vec{z}_1, \vec{z}_2, \dots, \vec{z}_N)$ being single-valued function on the plane $\vec{z} = (z, \bar{z})$, normalizable with respect to the $SL(2, \mathbb{C})$ invariant scalar product

$$||\Psi||^2 = \langle \Psi | \Psi \rangle = \int d^2 z_1 d^2 z_2 \dots d^2 z_N |\Psi(\vec{z}_1, \vec{z}_2, \dots, \vec{z}_N)|^2, \quad (2.35)$$

where $d^2 z_i = dx_i dy_i = dz_i d\bar{z}_i / 2$ with $\bar{z}_i = z_i^*$.

It is possible to use other scalar products [23]. Let us consider the amplitude for the scattering of two colourless objects A and B . In the Regge limit, the contribution to the scattering amplitude from N -gluon exchange in the t -channel takes the form

$$\mathcal{A}(s, t) = is \sum_N (i\alpha_s)^N \mathcal{A}_N(s, t). \quad (2.36)$$

Using the $SL(2, \mathbb{C})$ scalar product (2.35) we have

$$\mathcal{A}_N(s, t) = s \int d^2 z_0 e^{i\vec{z}_0 \cdot \vec{p}} \langle \tilde{\Phi}_A(\vec{z}_0) | e^{-\bar{\alpha}_s Y \tilde{\mathcal{H}}_N / 4} \left(\vec{\partial}_1^2 \dots \vec{\partial}_N^2 \right)^{-1} | \tilde{\Phi}_B(0) \rangle, \quad (2.37)$$

where $\partial_k = \partial / \partial z_k$, the rapidity $Y = \ln s$ and $\left(\vec{\partial}_1^2 \dots \vec{\partial}_N^2 \right)^{-1}$ are gluon propagators omitted in (2.18). Here the Hamiltonian $\tilde{\mathcal{H}}_N$ is related to (2.26) as $\hat{\mathcal{H}}_N = -\bar{\alpha}_s \tilde{\mathcal{H}}_N / 4$, so it is given by the sum of N BFKL kernels corresponding to nearest neighbour interaction between N reggeized gluons. The wave-functions $|\Phi_{A(B)}(\vec{z}_0)\rangle \equiv \Phi_{A(B)}(\vec{z}_i - \vec{z}_0)$ describe the coupling of N -gluons to the scattered particles. The \vec{z}_0 -integration fixes the momentum transfer $t = -\vec{p}^2$ whereas the operators $1/\vec{\partial}_k^2$ stand for two-dimensional transverse propagators.

Defining the functions $\Phi(\vec{z})$ as

$$\tilde{\Phi}(\vec{z}) = (-i)^N \partial_{z_1} \partial_{z_2} \dots \partial_{z_N} \Phi(\vec{z}) \quad (2.38)$$

the scalar product in the amplitude (2.37) can be rewritten as

$$\langle \tilde{\Phi}_A(\vec{z}_0) | e^{-\bar{\alpha}_s Y \tilde{\mathcal{H}}_N / 4} \left(\vec{\partial}_1^2 \dots \vec{\partial}_N^2 \right)^{-1} | \tilde{\Phi}_B(0) \rangle = \langle \Phi_A(\vec{z}_0) | e^{-\bar{\alpha}_s Y \mathcal{H}_N^{(s=0, \bar{s}=1)} / 4} | \Phi_B(0) \rangle. \quad (2.39)$$

The Hamiltonians, \mathcal{H}_N and $\tilde{\mathcal{H}}_N$ are related to each other as

$$\mathcal{H}_N^{(s=0, \bar{s}=1)} = (\bar{\partial}_1 \dots \bar{\partial}_N) \tilde{\mathcal{H}}_N (\bar{\partial}_1 \dots \bar{\partial}_N)^{-1}. \quad (2.40)$$

From the point of view of the $SL(2, \mathbb{C})$ spin chain

$$\tilde{\mathcal{H}}_N = \mathcal{H}_N^{(s=0, \bar{s}=0)}. \quad (2.41)$$

Indeed, the transformation $\bar{S}_\alpha \rightarrow (\bar{\partial}_1 \dots \bar{\partial}_N) \bar{S}_\alpha (\bar{\partial}_1 \dots \bar{\partial}_N)^{-1}$ maps the $SL(2, \mathbb{C})$ generators of the spin $\bar{s} = 0$ into those with the spin $\bar{s} = 1$. One concludes from (2.41) that the Hamiltonian $\mathcal{H}_N^{(s=0, \bar{s}=1)}$ is advantageous with respect to $\tilde{\mathcal{H}}_N$ as it has the quantum numbers of the principal series representation of the $SL(2, \mathbb{C})$ group.

However, one can also use $\mathcal{H}_N^{(s=0, \bar{s}=0)}$ [27] or even $\mathcal{H}_N^{(s=1, \bar{s}=1)}$ [28]. Then the factor $(\partial_1 \dots \partial_N)^{\mp 1}$ or $(\bar{\partial}_1 \dots \bar{\partial}_N)^{\mp 1}$ may be included into the scalar product, i.e. for $(s = 1, \bar{s} = 1)$ we have

$$||\Psi||^2 = \int d^2 z_1 d^2 z_2 \dots d^2 z_N |(\bar{\partial}_1 \dots \bar{\partial}_N)^{-1} \Psi(\vec{z}_1, \vec{z}_2, \dots, \vec{z}_N)|^2. \quad (2.42)$$

Here the scalar product is no longer in the principal series representation of the $SL(2, \mathbb{C})$ group. All these Hamiltonians with the corresponding scalar products are equivalent up to the zero modes of the $(\partial_1 \dots \partial_N)^{\mp 1}$ and $(\bar{\partial}_1 \dots \bar{\partial}_N)^{\mp 1}$ operators.

2.2.3 Conformal charges q_k and the conformal spins

The Hamiltonian (2.31) possesses a complete set of the integrals of motion $\{\vec{p}, \vec{q}_k\}$ where $\vec{q}_k = \{q_k, \bar{q}_k\}$ with $k = 2, \dots, N$ are called conformal charges while $\vec{p} = \{p, \bar{p}\}$ is the total momentum of the system. In order to construct them we introduce the Lax operators [41, 42, 43, 44] in holomorphic and anti-holomorphic sectors:

$$\begin{aligned} L_k(u) &= u + i(\sigma \cdot S^{(k)}) = \begin{pmatrix} u + iS_0^{(k)} & iS_-^{(k)} \\ iS_+^{(k)} & u - iS_0^{(k)} \end{pmatrix}, \\ \bar{L}_k(\bar{u}) &= \bar{u} + i(\sigma \cdot \bar{S}^{(k)}) = \begin{pmatrix} \bar{u} + i\bar{S}_0^{(k)} & i\bar{S}_-^{(k)} \\ i\bar{S}_+^{(k)} & \bar{u} - i\bar{S}_0^{(k)} \end{pmatrix} \end{aligned} \quad (2.43)$$

with u and \bar{u} being arbitrary complex parameters called the spectral parameters and σ_α being Pauli matrices.

To identify the total set of the integrals of motion of the model, one constructs the auxiliary holomorphic monodromy matrix

$$T_N(u) = L_1(u) L_2(u) \dots L_N(u) \quad (2.44)$$

and similarly for the anti-holomorphic monodromy operator $\bar{T}_N(\bar{u})$. Taking the trace of the monodromy matrix we define the auxiliary transfer matrix (spectral invariants)

$$\hat{t}_N(u) = \text{tr} T_N(u) = 2u^N + \hat{q}_2 u^{N-2} + \dots + \hat{q}_N \quad (2.45)$$

and similarly for $\hat{t}_N(\bar{u})$. We see from (2.45) the advantage of using the transfer matrix $\hat{t}_N(u)$: that is a polynomial in u with coefficients given in terms of conformal charges \hat{q}_k and $\hat{\bar{q}}_k$, which are expressed as linear combinations of the product of k spin operators:

$$\hat{q}_2 = -2 \sum_{i_2 > i_1 = 1}^N \sum_{j_1 = 0}^2 \left(S_{j_1}^{(i_1)} S_{j_1}^{(i_2)} \right) \quad (2.46)$$

$$\hat{q}_4 = - \sum_{i_2 > i_1 = 1}^N \sum_{i_4 > i_3 = 1}^N \sum_{j_1, j_2 = 0}^2 \varepsilon_{i_1 i_2 i_3 i_4} \left(S_{j_1}^{(i_1)} S_{j_1}^{(i_2)} \right) \left(S_{j_2}^{(i_3)} S_{j_2}^{(i_4)} \right) \quad (2.47)$$

$$\begin{aligned} \hat{q}_6 = & -\frac{1}{3} \sum_{i_2 > i_1 = 1}^N \sum_{i_4 > i_3 = 1}^N \sum_{i_6 > i_5 = 1}^N \sum_{j_1, j_2, j_3 = 0}^2 \varepsilon_{i_1 i_2 i_3 i_4 i_5 i_6} \left(S_{j_1}^{(i_1)} S_{j_1}^{(i_2)} \right) \\ & \times \left(S_{j_2}^{(i_3)} S_{j_2}^{(i_4)} \right) \left(S_{j_3}^{(i_5)} S_{j_3}^{(i_6)} \right), \end{aligned} \quad (2.48)$$

where $\varepsilon_{i_1 i_2 \dots i_k}$ is completely anti-symmetric tensor and $\varepsilon_{i_1 i_2 \dots i_k} = 1$ for $i_1 < i_2 < \dots < i_k$. So for even k we have a formula for conformal charges

$$\hat{q}_k = -\frac{2}{(k/2)!} \sum_{\substack{i_2 > i_1 = 1 \\ i_4 > i_3 = 1 \\ \dots \\ i_n > i_{n-1} = 1}}^N \sum_{j_1, j_2, \dots, j_{k/2} = 0}^2 \varepsilon_{i_1 i_2 \dots i_k} \prod_{n=1}^{k/2} \left(S_{j_n}^{(i_{2n-1})} S_{j_n}^{(i_{2n})} \right). \quad (2.49)$$

For odd k 's we have

$$\begin{aligned} \hat{q}_3 &= 2 \sum_{i_1, i_2, i_3 = 1}^N \varepsilon_{i_1 i_2 i_3} \left(S_0^{(i_1)} S_1^{(i_2)} S_2^{(i_3)} \right) \\ &= 2 \sum_{i_3 > i_2 > i_1 = 1}^N \sum_{j_1, j_2, j_3 = 0}^2 \varepsilon_{i_1 i_2 i_3} \varepsilon_{j_1 j_2 j_3} \left(S_{j_1}^{(i_1)} S_{j_2}^{(i_2)} S_{j_3}^{(i_3)} \right), \end{aligned} \quad (2.50)$$

$$\hat{q}_5 = -2 \sum_{i_3, i_2, i_1 = 1}^N \sum_{i_5 > i_4 = 1}^N \sum_{j_4 = 0}^2 \varepsilon_{i_1 i_2 i_3 i_4 i_5} \left(S_0^{(i_1)} S_1^{(i_2)} S_2^{(i_3)} \right) \left(S_{j_4}^{(i_4)} S_{j_4}^{(i_5)} \right), \quad (2.51)$$

$$\begin{aligned} \hat{q}_7 &= \sum_{i_3, i_2, i_1 = 1}^N \sum_{i_5 > i_4 = 1}^N \sum_{i_7 > i_6 = 1}^N \sum_{j_4, j_5 = 0}^2 \varepsilon_{i_1 i_2 i_3 i_4 i_5 i_6 i_7} \left(S_0^{(i_1)} S_1^{(i_2)} S_2^{(i_3)} \right) \\ &\times \left(S_{j_4}^{(i_4)} S_{j_4}^{(i_5)} \right) \left(S_{j_5}^{(i_6)} S_{j_5}^{(i_7)} \right) \end{aligned} \quad (2.52)$$

and the general expression for an odd number of the conformal spins is

$$\begin{aligned} \hat{q}_k &= \frac{2(-1)^{(k+1)/2}}{\left(\frac{k-3}{2}\right)!} \sum_{i_3, i_2, i_1=1}^N \sum_{\substack{i_5 > i_4 = 1 \\ i_7 > i_6 = 1 \\ \dots \\ i_k > i_{k-1} = 1}}^N \sum_{j_1, j_2, \dots, j_{(k-3)/2}=0}^2 \varepsilon_{i_1 i_2 \dots i_k} \left(S_0^{(i_1)} S_1^{(i_2)} S_2^{(i_3)} \right) \\ &\times \prod_{n=1}^{(k-3)/2} \left(S_{j_n}^{(i_{2n+2})} S_{j_n}^{(i_{2n+3})} \right). \end{aligned} \quad (2.53)$$

In the above formulae we have two basic blocks $\left(S_{j_1}^{(i_1)} S_{j_1}^{(i_2)} \right)$ and $\left(S_0^{(i_1)} S_1^{(i_2)} S_2^{(i_3)} \right)$ whose products are summed with antisymmetric tensor $\varepsilon_{i_1 i_2 \dots i_k}$.

2.2.4 Two-dimensional Lorentz spin and the scaling dimension

The Hamiltonian (2.32) is a function of two-particle Casimir operators [38], and, therefore, it commutes with the operators of the total spin $S_\alpha = \sum_k S_\alpha^{(k)}$ and $\bar{S}_\alpha = \sum_k \bar{S}_\alpha^{(k)}$, acting on the quantum space of the system $V_N \equiv V^{(s_1, \bar{s}_1)} \otimes V^{(s_2, \bar{s}_2)} \otimes \dots \otimes V^{(s_N, \bar{s}_N)}$. This implies that the eigenstates can be classified according to the irreducible representations of the $SL(2, \mathbb{C})$ group, $V^{(h, \bar{h})}$, parameterized by spins (h, \bar{h}) [38].

The Hamiltonian depends on differences of particle coordinates so eigenfunctions can be written as

$$\Psi_{\vec{p}}(\vec{z}_1, \vec{z}_2, \dots, \vec{z}_N) = \int d^2 z_0 e^{i \vec{z}_0 \cdot \vec{p}} \Psi(\vec{z}_1 - \vec{z}_0, \vec{z}_2 - \vec{z}_0, \dots, \vec{z}_N - \vec{z}_0). \quad (2.54)$$

The eigenstates $\Psi(\vec{z}_1, \vec{z}_2, \dots, \vec{z}_N)$ belonging to $V^{(h, \bar{h})}$ are labelled by the centre-of-mass coordinate \vec{z}_0 and can be chosen to have the following the $SL(2, \mathbb{C})$ transformation properties

$$\Psi(\{\vec{z}_k' - \vec{z}_0'\}) = (cz_0 + d)^{2h} (\bar{c}\bar{z}_0 + \bar{d})^{2\bar{h}} \left(\prod_{k=1}^N (cz_k + d)^{2s_k} (\bar{c}\bar{z}_k + \bar{d})^{2\bar{s}_k} \right) \Psi(\{\vec{z}_k - \vec{z}_0\}) \quad (2.55)$$

with z_0 and \bar{z}_0 transforming in the same way as z_k and \bar{z}_k , (2.27). As a consequence, they diagonalize the Casimir operators:

$$(S^2 - h(h-1))\Psi(\vec{z}_1, \vec{z}_2, \dots, \vec{z}_N) = 0 \quad (2.56)$$

corresponding to the total spin of the system,

$$S^2 = \sum_{i_2, i_1=1}^N \sum_{j=0}^2 S_j^{(i_1)} S_j^{(i_2)} = -\hat{q}_2 - \sum_{k=1}^N s_k(s_k - 1). \quad (2.57)$$

The complex parameters (s_k, \bar{s}_k) and (h, \bar{h}) parameterize the irreducible representations of the $SL(2, \mathbb{C})$ group. For principal series representation they satisfy the conditions

$$s_k - \bar{s}_k = n_{s_k}, \quad s_k + (\bar{s}_k)^* = 1 \quad (2.58)$$

and have the following form

$$s_k = \frac{1 + n_{s_k}}{2} + i\nu_{s_k}, \quad \bar{s}_k = \frac{1 - n_{s_k}}{2} + i\nu_{s_k} \quad (2.59)$$

with ν_{s_k} being real and n_{s_k} being integer or half-integer. The spins (h, \bar{h}) are given by similar expressions with n_{s_k} and ν_{s_k} replaced by n_h and ν_h , respectively

$$h = \frac{1 + n_h}{2} + i\nu_h, \quad \bar{h} = \frac{1 - n_h}{2} + i\nu_h. \quad (2.60)$$

The parameter n_{s_k} has the meaning of the two-dimensional Lorentz spin of the particle, whereas ν_{s_k} defines its scaling dimension. To see this one can perform a 2π -rotation of the particle on the plane, and find from eigenstates transformations (2.55) that the wave-function acquires a phase. Indeed

$$z_k \rightarrow z_k \exp(2\pi i) \quad \text{and} \quad \bar{z}_k \rightarrow \bar{z}_k \exp(-2\pi i) \quad \text{gives} \quad \Psi(z_k, \bar{z}_k) \rightarrow (-1)^{2n_{s_k}} \Psi(z_k, \bar{z}_k). \quad (2.61)$$

For half-integer n_{s_k} it changes the sign and the corresponding representation is spinorial. Similarly, to define scaling dimension, $s + \bar{s} = 1 + 2i\nu_{s_k}$ one performs the transformation

$$z \rightarrow \lambda z \quad \text{and} \quad \bar{z} \rightarrow \lambda \bar{z} \quad \text{giving} \quad \Psi(z_k, \bar{z}_k) \rightarrow \lambda^{1+2i\nu_{s_k}} \Psi(z_k, \bar{z}_k). \quad (2.62)$$

Because the scale product for the wave-functions is invariant under $SL(2, \mathbb{C})$ transformations, (2.27), the parameter ν_{s_k} is real.

We notice that the holomorphic and anti-holomorphic spin generators as well as Casimir operators (2.33) are conjugated to each other with respect to the scalar product (2.35):

$$[S_\alpha^{(k)}]^\dagger = -\bar{S}_\alpha^{(k)}, \quad [J_k]^\dagger = 1 - \bar{J}_k. \quad (2.63)$$

Moreover, because of the transformation law (2.63), $h^* = 1 - \bar{h}$ ¹. This implies that $H_N^\dagger = \bar{H}_N$ and, as a consequence, the Hamiltonian is hermitian on the space of the functions endowed with the $SL(2, \mathbb{C})$ scalar product, $\mathcal{H}_N^\dagger = \mathcal{H}_N$.

2.3 Conformal charges \hat{q}_k as a differential operators

We noticed in the previous paragraphs that the conformal charge operators \hat{q}_k are given by invariant sum of linear combinations of the product of k spin operators. They can be rewritten as k -th order differential operators acting on (anti)holomorphic coordinates (z, \bar{z}) .

Two particle spin square can be written as

$$\sum_{j_1=0}^2 S_{j_1}^{(i_1)} S_{j_1}^{(i_2)} = -\frac{1}{2}(z_{i_1} - z_{i_2})^2 \partial_{z_{i_1}} \partial_{z_{i_2}} + (z_{i_1} - z_{i_2})(s_{i_2} \partial_{z_{i_1}} + s_{i_1} \partial_{z_{i_2}}) + s_1 s_2. \quad (2.64)$$

¹* – denotes complex conjugation

For homogeneous spins $s = s_1 = s_2 = \dots = s_N$, what is also the QCD case, we have

$$\begin{aligned}
\hat{q}_2 &= -2 \sum_{i_2 > i_1 = 1}^N \left(\sum_{j_1=0}^2 S_{j_1}^{(i_1)} S_{j_1}^{(i_2)} \right) = \sum_{i_2 > i_1 = 1}^N \left((z_{i_2 i_1})^{2(1-s)} \partial_{z_{i_2}} \partial_{z_{i_1}} (z_{i_2 i_1})^{2s} + 2s(s-1) \right), \\
\hat{q}_3 &= 2 \sum_{i_1, i_2, i_3=1}^N \varepsilon_{i_1 i_2 i_3} S_0^{(i_1)} S_1^{(i_2)} S_2^{(i_3)} = i^3 \sum_{i_3 > i_2 > i_1 = 1}^N \left(z_{i_1 i_2} z_{i_2 i_3} z_{i_3 i_1} \partial_{z_{i_3}} \partial_{z_{i_2}} \partial_{z_{i_1}} + \right. \\
&\quad + s z_{i_1 i_2} (z_{i_2 i_3} - z_{i_3 i_1}) \partial_{z_{i_2}} \partial_{z_{i_1}} + s z_{i_2 i_3} (z_{i_3 i_1} - z_{i_1 i_2}) \partial_{z_{i_3}} \partial_{z_{i_2}} \\
&\quad \left. + s z_{i_3 i_1} (z_{i_1 i_2} - z_{i_2 i_3}) \partial_{z_{i_3}} \partial_{z_{i_1}} - 2s^2 z_{i_1 i_2} \partial_{z_{i_3}} - 2s^2 z_{i_2 i_3} \partial_{z_{i_1}} - 2s^2 z_{i_3 i_1} \partial_{z_{i_2}} \right), \quad (2.65)
\end{aligned}$$

where $z_{ij} = z_i - z_j$. Similar relations hold for the anti-holomorphic sector.

In that way one can also construct operators for the higher conformal charges. They have a particularly simple form for the $SL(2, \mathbb{C})$ spins $s = 0$

$$\hat{q}_k = i^k \sum_{1 \leq j_1 < j_2 < \dots < j_k \leq N} z_{j_1 j_2} \dots z_{j_{k-1} j_k} \partial_{z_{j_k}} \dots \partial_{z_{j_2}} \partial_{z_{j_1}} \quad (2.66)$$

as well as for $s = 1$

$$\hat{q}_k = i^k \sum_{1 \leq j_1 < j_2 < \dots < j_k \leq N} \partial_{z_{j_1}} \dots \partial_{z_{j_{k-1}}} \partial_{z_{j_k}} z_{j_1 j_2} \dots z_{j_{k-1} j_k} \quad (2.67)$$

2.4 Other symmetries

The states (2.54) have additional symmetries [38]:

$$\begin{aligned}
\mathbb{P} \Psi_{q, \bar{q}}(\vec{z}_1, \vec{z}_2, \dots, \vec{z}_N) &\stackrel{\text{def}}{=} \Psi_{q, \bar{q}}(\vec{z}_2, \vec{z}_3, \dots, \vec{z}_1) = e^{i\theta_N(q, \bar{q})} \Psi_{q, \bar{q}}(\vec{z}_1, \vec{z}_2, \dots, \vec{z}_N), \\
\mathbb{M} \Psi^\pm(\vec{z}_1, \vec{z}_2, \dots, \vec{z}_N) &\stackrel{\text{def}}{=} \Psi^\pm(\vec{z}_N, \vec{z}_{N-1}, \dots, \vec{z}_1) = \pm \Psi^\pm(\vec{z}_1, \vec{z}_2, \dots, \vec{z}_N)
\end{aligned} \quad (2.68)$$

so called cyclic and mirror permutation where the conformal charges are denoted by $q \equiv (q_2, q_3, \dots, q_n)$ and $\bar{q} \equiv (\bar{q}_2, \bar{q}_3, \dots, \bar{q}_n)$. They generators \mathbb{P} and \mathbb{M} , respectively, commute with the Hamiltonian \mathcal{H} but they do not commute with each other. They satisfy relations

$$\mathbb{P}^N = \mathbb{M}^2 = 1, \quad \mathbb{P}^\dagger = \mathbb{P}^{-1} = \mathbb{P}^{N-1}, \quad \mathbb{M}^\dagger = \mathbb{M}, \quad \mathbb{P} \mathbb{M} = \mathbb{M} \mathbb{P}^{-1} = \mathbb{M} \mathbb{P}^{N-1}. \quad (2.69)$$

The phase $\theta_N(q)$ which is connected with eigenvalues of \mathbb{P} is called the quasimomentum. It takes the following values

$$\theta_N(q, \bar{q}) = 2\pi \frac{k}{N}, \quad \text{for } k = 0, 1, \dots, N-1. \quad (2.70)$$

The eigenstates of the conformal charges \hat{q}_k diagonalize \mathcal{H} and \mathbb{P} .

The transfer matrices (2.45) are invariant under the cyclic permutations $\mathbb{P}^\dagger \hat{t}_N(u) \mathbb{P} = \hat{t}_N(u)$ whereas they transform under the mirror transformation as

$$\mathbb{M} \hat{t}_N(u) \mathbb{M} = (-1)^N \hat{t}_N(-u). \quad (2.71)$$

Substituting (2.45) into (2.71) one derives a transformation law of the conformal charges q_k

$$\mathbb{P}^\dagger \hat{q}_k \mathbb{P} = \hat{q}_k \quad \mathbb{M} \hat{q}_k \mathbb{M} = (-1)^k \hat{q}_k \quad (2.72)$$

and similarly for the anti-holomorphic charges. Since the Hamiltonian (2.32) is invariant under the mirror permutation, it has to satisfy

$$\mathcal{H}(\hat{q}_k, \hat{\bar{q}}_k) = \mathbb{M} \mathcal{H}(\hat{q}_k, \hat{\bar{q}}_k) \mathbb{M} = \mathcal{H}(\mathbb{M} \hat{q}_k \mathbb{M}, \mathbb{M} \hat{\bar{q}}_k \mathbb{M}) = \mathcal{H}((-1)^k \hat{q}_k, (-1)^k \hat{\bar{q}}_k). \quad (2.73)$$

This implies that the eigenstates of the Hamiltonian (2.32) corresponding to two different sets of the quantum number $\{q_k, \bar{q}_k\}$ and $\{(-1)^k q_k, (-1)^k \bar{q}_k\}$ have the same energy

$$E_N(q_k, \bar{q}_k) = E_N((-1)^k q_k, (-1)^k \bar{q}_k). \quad (2.74)$$

Similarly one can derive relation for quasimomentum

$$\theta_N(q_k, \bar{q}_k) = -\theta_N((-1)^k q_k, (-1)^k \bar{q}_k). \quad (2.75)$$

The cyclic and mirror permutation symmetries come from the Bose symmetry and they appear after performing the multi-colour limit [10]. Physical states should possess both symmetries.

2.5 Pomeron and odderon

In the previous Sections we introduced the wave-functions of the Reggeized gluon states. Now, we answer how one can distinguish Pomeron states from odderon states [45]. Since the Pomeron states have conjugation charge parity $C = 1$ and the odderon states have $C = -1$, we have to check the C -parity of studied states. Let us consider for simplicity purely perturbative gluon fields $\mathbf{A}_\mu(x) = A_\mu^a(x) t^a$, where t^a are the generators of the gauge group $SU(N_c)$ and x are coordinates of the gluon. Thus, under a charge conjugation transformation this field transforms as

$$\mathbf{A}_\mu(x) \rightarrow -\mathbf{A}_\mu^T(x), \quad (2.76)$$

where T denotes matrix transposition.

For $N = 2$ we have only one possibility to form a colour singlet state from two gluon operators

$$\mathcal{P}_{\mu\nu}(x, y) = \text{tr}(\mathbf{A}_\mu(x), \mathbf{A}_\nu(y)) = \frac{1}{2} \delta_{ab} A_\mu^a(x) A_\nu^b(y). \quad (2.77)$$

This state is invariant under charge conjugation (2.76) so that it has $C = +1$. Therefore, for two gluons we have only the Pomeron states.

In the $N = 3$ case there are two ways of constructing a colour singlet state. Firstly, one can build

$$\mathcal{P}_{\mu\nu\rho}(x, y, z) = -i \text{tr}([\mathbf{A}_\mu(x), \mathbf{A}_\nu(y)] \mathbf{A}_\rho(z)) = \frac{1}{2} f_{abc} A_\mu^a(x) A_\nu^b(y) A_\rho^c(z) \quad (2.78)$$

with the total antisymmetric structure constants f_{abc} defined via the Lie algebra of $SU(N_c)$:

$$[t^a, t^b] = if_{abc}t^c. \quad (2.79)$$

Using (2.76), we find that $\mathcal{P}_{\mu\nu\rho}(x, y, z)$ have also $C = +1$ so for $N = 3$ the state (2.78) gives a subleading correction to the $N = 2$ Pomeron state.

The other possibility to form colour singlet states is to use the totally symmetric constant

$$d_{abc} = 2 [\text{tr}(t^a t^b t^c) + \text{tr}(t^c t^b t^a)]. \quad (2.80)$$

In this way we obtain a state

$$\mathcal{O}_{\mu\nu\rho}(x, y, z) = \text{tr}(\{\mathbf{A}_\mu(x), \mathbf{A}_\nu(y)\} \mathbf{A}_\rho(z)) = \frac{1}{2} d_{abc} A_\mu^a(x) A_\nu^b(y) A_\rho^c(z). \quad (2.81)$$

Similarly, applying (2.76) we find that (2.81) is the odd under C -parity. Thus, it is the leading contribution to the odderon state. This state only appears for the gauge groups $SU(N_c)$ with $N_c > 2$.

In order to find the eigenstates of the Hamiltonian (2.22) we perform the multi-colour limit (2.26). In this limit the colour factor of the Hamiltonian is reduced to a trivial delta-function. Thus, a solution to the Schrödinger equation (2.34) does not have a colour factor. On the other hand, the Reggeon wave-function should be invariant under Bose symmetry. Adding a proper colour factor into the Reggeon wave-functions we are able to restore Bose symmetry. In the multi-colour limit the Bose symmetry reduce into the cycle and mirror permutation symmetries (2.68). Thus, we have states which under the mirror permutations are either odd or even. For example in the $N = 3$ case it turns out that adding colour factor: corresponding to the antisymmetric constant f_{abc} for the odd-mirror states and the symmetric one d_{abc} for the even-mirror states, we are able to restore Bose symmetry. As we have said in (2.78) and (2.81) f_{abc} corresponds to the Pomeron states while d_{abc} is related to the odderon states. One may expect similar relationship for $N > 3$ states. Therefore, in order to check C -parity of a given state we need to study its parity under the mirror permutation \mathbb{M} . The states Ψ satisfying $\mathbb{M}\Psi = -\Psi$ are the Pomeron states whereas states for which $\mathbb{M}\Psi = +\Psi$ are the odderon states.

Chapter 3

Baxter Q -operator

3.1 Definition of the Baxter Q -operator

The Schrödinger equation (2.34) may be solved applying the powerful method of the Baxter Q -operator [30]. This operator depends on two complex spectral parameters u, \bar{u} and in the following will be denoted as $\mathbb{Q}(u, \bar{u})$. This operator has to satisfy the following relations

- Commutativity:

$$[\mathbb{Q}(u, \bar{u}), \mathbb{Q}(v, \bar{v})] = 0, \quad (3.1)$$

- $Q - t$ relation:

$$[\hat{t}_N(u), \mathbb{Q}(u, \bar{u})] = [\hat{t}_N(\bar{u}), \mathbb{Q}(u, \bar{u})] = 0, \quad (3.2)$$

- Baxter equation:

$$\hat{t}_N(u) \mathbb{Q}(u, \bar{u}) = (u + is)^N \mathbb{Q}(u + i, \bar{u}) + (u - is)^N \mathbb{Q}(u - i, \bar{u}), \quad (3.3)$$

$$\hat{t}_N(\bar{u}) \mathbb{Q}(u, \bar{u}) = (\bar{u} + i\bar{s})^N \mathbb{Q}(u, \bar{u} + i) + (\bar{u} - i\bar{s})^N \mathbb{Q}(u, \bar{u} - i), \quad (3.4)$$

where $\hat{t}_N(u)$ and $\hat{t}_N(\bar{u})$ are the auxiliary transfer matrices (2.45). According to (3.2) the Baxter $\mathbb{Q}(u, \bar{u})$ -operator and the auxiliary transfer matrices as well as the Hamiltonian (2.26) share the common set of the eigenfunctions

$$\mathbb{Q}(u, \bar{u}) \Psi_{q, \bar{q}}(\vec{z}_1, \vec{z}_2, \dots, \vec{z}_N) = Q_{q, \bar{q}}(u, \bar{u}) \Psi_{q, \bar{q}}(\vec{z}_1, \vec{z}_2, \dots, \vec{z}_N). \quad (3.5)$$

The eigenvalues of the Q -operator satisfy the same Baxter equation (3.3) and (3.4) with the auxiliary transfer matrices replaced by their corresponding eigenvalues.

In the paper [38] the Q -operator was constructed as an N -fold integral operator

$$\begin{aligned} \mathbb{Q}(u, \bar{u}) \Psi(\vec{z}_1, \vec{z}_2, \dots, \vec{z}_N) &= \int d^2 w_1 \int d^2 w_2 \dots \\ &\dots \int d^2 w_N Q_{u, \bar{u}}(\vec{z}_1, \vec{z}_2, \dots, \vec{z}_N | \vec{w}_1, \vec{w}_2, \dots, \vec{w}_N) \Psi(\vec{w}_1, \vec{w}_2, \dots, \vec{w}_N), \end{aligned} \quad (3.6)$$

where the integrations are performed over two-dimensional \vec{w}_i -planes. The integral kernel in (3.6) takes two different forms:

$$Q_{u,\bar{u}}^{(+)}(\vec{z}|\vec{w}) = a(2-2s, s+iu, \bar{s}-i\bar{u})^N \pi^N \prod_{k=1}^N \frac{[z_k - z_{k+1}]^{1-2s}}{[w_k - z_k]^{1-s-iu} [w_k - z_{k+1}]^{1-s+iu}} \quad (3.7)$$

and

$$Q_{u,\bar{u}}^{(-)}(\vec{z}|\vec{w}) = \prod_{k=1}^N \frac{[w_k - w_{k+1}]^{2s-2}}{[z_k - w_k]^{s+iu} [z_k - w_{k+1}]^{s-iu}}, \quad (3.8)$$

which appear to be equivalent [38]. In Eqs. (3.7) and (3.8) $a(\dots)$ factorizes as

$$a(\alpha, \beta, \dots) = a(\alpha)a(\beta) \dots \quad \text{and} \quad a(\alpha) = \frac{\Gamma(1-\bar{\alpha})}{\Gamma(\alpha)} \quad (3.9)$$

and $\bar{\alpha}$ is an anti-holomorphic partner of α satisfying $\alpha - \bar{\alpha} \in \mathbb{Z}$. Moreover, the two-dimensional propagators are defined as

$$[z_k - w_k]^{-\alpha} = (z_k - w_k)^{-\alpha} (\bar{z}_k - \bar{w}_k)^{-\bar{\alpha}}. \quad (3.10)$$

In order for the Baxter Q -operators to be well defined, (3.7) and (3.8), should be single-valued functions. In this way we can find that the spectral parameters u and \bar{u} have to satisfy the condition

$$i(u - \bar{u}) = n \quad (3.11)$$

with n being an integer.

The Baxter Q -operator has a defined pole structure. For $\mathbb{Q}^{(+)}(u, \bar{u})$ we have an infinite set of poles of the order not higher than N situated at

$$\{ u_m^+ = i(s-m), \bar{u}_m^+ = i(\bar{s}-\bar{m}) \}; \quad \{ u_m^- = -i(s-m), \bar{u}_m^- = -i(\bar{s}-\bar{m}) \} \quad (3.12)$$

with $m, \bar{m} = 1, 2, \dots$. The behaviour of $Q_{q,\bar{q}}(u, \bar{u})$, i.e. an eigenvalue of $\mathbb{Q}^{(+)}(u, \bar{u})$, in the vicinity of the pole at $m = \bar{m} = 1$ can be parameterized as

$$Q_{q,\bar{q}}(u_1^\pm + \epsilon, \bar{u}_1^\pm + \epsilon) = R^\pm(q, \bar{q}) \left[\frac{1}{\epsilon^N} + \frac{i E^\pm(q, \bar{q})}{\epsilon^{N-1}} + \dots \right]. \quad (3.13)$$

The functions $R^\pm(q, \bar{q})$ fix an overall normalization of the Baxter operator, while the residue functions $E^\pm(q, \bar{q})$ define the energy of the system (see Eqs. (3.21) and (3.24) below). It has also specified asymptotic behaviour. For $|\text{Im}\lambda| < 1/2$ and $\text{Re}\lambda \rightarrow \infty$

$$Q_{q,\bar{q}}(\lambda - in/2, \lambda + in/2) \sim e^{i\Theta_h(q,\bar{q})} \lambda^{h+\bar{h}-N(s-\bar{s})} + e^{-i\Theta_h(q,\bar{q})} \lambda^{1-h+1-\bar{h}-N(s-\bar{s})}, \quad (3.14)$$

where Θ_h is a phase which should not be confused with quasimomentum $\theta_N(q, \bar{q})$.

3.2 Observables

The Hamiltonian (2.31) may be written in terms of the Baxter Q -operator [38]:

$$\mathcal{H}_N = \epsilon_N + i \frac{d}{du} \ln \mathbb{Q}^{(+)}(u + is, \bar{u} + i\bar{s}) \Big|_{u=0} - \left(i \frac{d}{du} \ln \mathbb{Q}^{(+)}(u - is, \bar{u} - i\bar{s}) \Big|_{u=0} \right)^\dagger, \quad (3.15)$$

where the additive normalization constant is given as

$$\epsilon_N = 2N \operatorname{Re}[\psi(2s) + \psi(2 - 2s) - 2\psi(1)]. \quad (3.16)$$

Applying to (3.15) the eigenstate Ψ_q we obtain the energy

$$E_N(q, \bar{q}) = \epsilon_N + i \frac{d}{du} \ln [Q_{q, \bar{q}}(u + is, u + i\bar{s}) (Q_{q, \bar{q}}(u - is, u - i\bar{s}))^*] \Big|_{u=0}, \quad (3.17)$$

or equivalently

$$E_N(q, \bar{q}) = -\operatorname{Im} \frac{d}{du} \ln \left[u^{2N} Q_{q, \bar{q}}(u + i(1 - s), u + i(1 - \bar{s})) \times Q_{-q, -\bar{q}}(u + i(1 - s), u + i(1 - \bar{s})) \right] \Big|_{u=0}, \quad (3.18)$$

where $Q_{q, \bar{q}}(u, \bar{u}) \equiv Q_{q, \bar{q}}^{(+)}(u, \bar{u})$ is eigenvalue of the $\mathbb{Q}_+(u, \bar{u})$ operator, while

$$\pm q = (q_2, \pm q_3, \dots, (\pm)^N q_N) \quad (3.19)$$

are the conformal charges.

It is also possible to rewrite the quasimomentum operator in terms of $\mathbb{Q}_+(u, \bar{u})$:

$$\hat{\theta}_N = -i \ln \mathbb{P} = i \ln \frac{\mathbb{Q}_+(is, i\bar{s})}{\mathbb{Q}_+(-is, -i\bar{s})}. \quad (3.20)$$

Moreover, using the mirror permutation (2.72) one finds the following parity relations for the residue functions $R^+(q, \bar{q})$ defined in (3.13):

$$R^+(q, \bar{q}) / R^+(-q, -\bar{q}) = e^{2i\theta_N(q, \bar{q})} \quad (3.21)$$

and for the eigenvalues of the Baxter operator:

$$Q_{q, \bar{q}}(-u, -\bar{u}) = e^{i\theta_N(q, \bar{q})} Q_{-q, -\bar{q}}(u, \bar{u}), \quad (3.22)$$

where $-q \equiv (q_2, -q_3, \dots, (-1)^n q_n)$ and similarly for \bar{q} . Examining the behaviour of (3.22) around the pole at $u = u_1^\pm$ and $\bar{u} = \bar{u}_1^\pm$ and making use of Eq. (3.13) one gets

$$R^\pm(q, \bar{q}) = (-1)^N e^{i\theta_N(q, \bar{q})} R^\mp(-q, -\bar{q}), \quad E^\pm(q, \bar{q}) = -E^\mp(-q, -\bar{q}). \quad (3.23)$$

To obtain the expression for the energy $E_N(q, \bar{q})$, we apply (3.17) and replace the function $Q_{q, \bar{q}}(u \pm i(1 - s), u \pm i(1 - \bar{s}))$ by its pole expansion (3.13). Then, applying the second relation in (3.23), one finds

$$E_N(q, \bar{q}) = E^+(-q, -\bar{q}) + (E^+(q, \bar{q}))^* = \operatorname{Re} [E^+(-q, -\bar{q}) + E^+(q, \bar{q})], \quad (3.24)$$

where the last relation follows from hermiticity of the Hamiltonian (2.32). We conclude from Eqs. (3.24) and (3.13), that in order to find the energy $E_N(q, \bar{q})$, one has to calculate the residue of $Q_{q, \bar{q}}(u, \bar{u})$ at the $(N - 1)$ -th order pole at $u = i(s - 1)$ and $\bar{u} = i(\bar{s} - 1)$.

3.3 Construction of the eigenfunction

The Hamiltonian eigenstate $\Psi_{\vec{p},\{q,\bar{q}\}}(\vec{z})$ is a common state of the total set of the integrals of motion, \vec{p} and $\{q,\bar{q}\}$ as well as the Baxter Q -operator. Thanks to the method of the Separation of Variables (SoV) developed by Sklyanin [41, 38] we can write the eigenstate using separated coordinates $\vec{x} = (\vec{x}_1, \dots, \vec{x}_{N-1})$ as

$$\Psi_{\vec{p},\{q,\bar{q}\}}(\vec{z}) = \int d^{N-1}\vec{x} \mu(\vec{x}_1, \dots, \vec{x}_{N-1}) U_{\vec{p},\vec{x}_1, \dots, \vec{x}_{N-1}}(\vec{z}_1, \dots, \vec{z}_N) (\Phi_{q,\bar{q}}(\vec{x}_1, \dots, \vec{x}_{N-1}))^* , \quad (3.25)$$

where $U_{\vec{p},\vec{x}}$ is the kernel of the unitary operator while

$$(\Phi_{q,\bar{q}}(\vec{x}_1, \dots, \vec{x}_{N-1}))^* = e^{i\theta_N(q,\bar{q})/2} \prod_{k=1}^{N-1} \left(\frac{\Gamma(s + ix_k) \Gamma(\bar{s} - i\bar{x}_k)}{\Gamma(1 - s + ix_k) \Gamma(1 - \bar{s} - i\bar{x}_k)} \right)^N Q_{q,\bar{q}}(x_k, \bar{x}_k) . \quad (3.26)$$

The functions $Q_{q,\bar{q}}(x_k, \bar{x}_k)$ are eigenstates of the Baxter Q -operator. In contrast to the $\vec{z}_i = (z_i, \bar{z}_i)$ - coordinates, the allowed values of separated coordinates are

$$x_k = \nu_k - \frac{in_k}{2} , \quad \bar{x}_k = \nu_k + \frac{in_k}{2} \quad (3.27)$$

with n_k integer and ν_k real. Integration over the space of separated variables implies summation over integer n_k and integration over continuous ν_k

$$\int d^{N-1}\vec{x} = \prod_{k=1}^{N-1} \left(\sum_{n_k=-\infty}^{\infty} \int_{-\infty}^{\infty} d\nu_k \right) , \quad \mu(\vec{x}) = \frac{2\pi^{-N^2}}{(N-1)!} \prod_{\substack{j,k=1 \\ j>k}}^{N-1} |\vec{x}_k - \vec{x}_j|^2 , \quad (3.28)$$

where $|\vec{x}_k - \vec{x}_j|^2 = (\nu_k - \nu_j)^2 + (n_k - n_j)^2/4$.

The integral kernel $U_{\vec{p},\vec{x}}$ can be written as

$$U_{\vec{p},\vec{x}}(\vec{z}_1, \dots, \vec{z}_N) = c_N(\vec{x}) (\vec{p}^2)^{(N-1)/2} \int d^2 w_N e^{2i\vec{p} \cdot \vec{w}_N} U_{\vec{x}}(\vec{z}_1, \dots, \vec{z}_N; \vec{w}_N) , \quad (3.29)$$

where $2\vec{p} \cdot \vec{w}_N = p w_N + \bar{p} \bar{w}_N$,

$$U_{\vec{x}}(\vec{z}_1, \dots, \vec{z}_N; \vec{w}_N) = \left[\Lambda_{N-1,(\vec{x}_1)}^{(s,\bar{s})} \Lambda_{N-2,(\vec{x}_2)}^{(1-s,1-\bar{s})} \dots \Lambda_{1,(\vec{x}_{N-1})}^{(s,\bar{s})} \right] (\vec{z}_1, \dots, \vec{z}_N | \vec{w}_N) \quad (3.30)$$

for even N , and

$$U_{\vec{x}}(\vec{z}_1, \dots, \vec{z}_N; \vec{w}_N) = \left[\Lambda_{N-1,(\vec{x}_1)}^{(s,\bar{s})} \Lambda_{N-2,(\vec{x}_2)}^{(1-s,1-\bar{s})} \dots \Lambda_{1,(\vec{x}_{N-1})}^{(1-s,1-\bar{s})} \right] (\vec{z}_1, \dots, \vec{z}_N | \vec{w}_N) \quad (3.31)$$

for odd N . Here the convolution involves the product of $(N-1)$ functions $\Lambda_{N-k,(\vec{x}_k)}$ with alternating spins (s, \bar{s}) and $(1-s, 1-\bar{s})$. They are defined as

$$\begin{aligned} \Lambda_{N-n,(\vec{x})}^{(s,\bar{s})}(\vec{z}_n, \dots, \vec{z}_N | \vec{y}_{n+1}, \dots, \vec{y}_N) &= [z_1 - y_2]^{-x+iu} \\ &\times \left(\prod_{k=n+1}^{N-1} [z_k - y_k]^{-x-iu} [z_k - y_{k+1}]^{-x+iu} \right) [z_N - y_N]^{-x-iu} , \end{aligned} \quad (3.32)$$

where the convolution $[\Lambda_{N-k,(\vec{x}_k)}\Lambda_{N-k+1,(\vec{x}_{k-1})}]$ contains $(N-k)$ two-dimensional integrals. The coefficient $c_N(\vec{x})$ is given for $N \geq 3$

$$c_N(\vec{x}) = \prod_{k=1}^{[(N-1)/2]} (a(s + ix_{2k}, \bar{s} - i\bar{x}_{2k}))^{N-k} \prod_{k=1}^{[N/2-1]} (a(s + ix_{2k+1}, \bar{s} - i\bar{x}_{2k+1}))^k \quad (3.33)$$

while the sums goes over integer numbers lower than upper limit. For $N = 2$ we have $c_2(\vec{x}_1) = 1$.

Chapter 4

WKB approximation

4.1 WKB approximation for Reggeons

The WKB approach was presented in a series of papers [46, 47, 21]. We will use this method to find an approximation set of conformal charges as well as to understand the structure of the q_k 's values. In the representation of the separated coordinates (3.25) – (3.27) the Baxter equations (3.3), (3.4) play the role of one-dimensional Schrödinger equations where the eigenfunctions are the eigenvalues of the Baxter operator (3.26). These equations may be solved in the quasi-classical limit [21] which corresponds to large values of the conformal charges, \hat{q}_k and $\hat{\bar{q}}_k$, (2.45).

In order to apply the WKB limit we introduce an auxiliary parameter η and rescale simultaneously the coordinates, $x \rightarrow x/\eta$, and the charges. Thus we define

$$\tilde{t}_N(x) = \eta^N t_N(x/\eta) = 2x^N + \tilde{q}_2 x^{N-2} + \dots + \tilde{q}_N x^N \quad (4.1)$$

with $\tilde{q}_k \equiv q_k \eta^k = \mathcal{O}(\eta^0)$ as $\eta \rightarrow 0$. The small parameter η appears in the Baxter equation

$$(x - i\eta s)^N Q((x - i\eta)/\eta) + (x + i\eta s)^N Q((x + i\eta)/\eta) = Q(x/\eta) \tilde{t}_N(x) \quad (4.2)$$

which allows us to perform the WKB expansion

$$Q(x/\eta) = \exp\left(\frac{i}{\eta} \int_{x_0}^x dx S'(x)\right) \quad \text{with} \quad S(x) = S_0(x) + \eta S_1(x) + \eta^2 S_2(x) + \mathcal{O}(\eta^3), \quad (4.3)$$

where $S'(x) = dS(x)/dx$ and x_0 is an arbitrary reference point. Substituting (4.3) into the Baxter equation (4.2) we obtain relations

$$2 \cosh S'_0(x) = \frac{\tilde{t}_N(x)}{x^N}, \quad S'_1(x) = \frac{i}{2} (\ln \sinh S'_0(x))' + \frac{isN}{x}. \quad (4.4)$$

In this way one can obtain further relations for higher $S_k(x)$.

The first relation in (4.4) can be rewritten as

$$y^2(x) = \tilde{t}_N^2(x) - 4x^{2N}, \quad (4.5)$$

where

$$y(x) = 2x^N \sinh p_x \quad \text{with} \quad p_x = S'_0(x) \quad (4.6)$$

is a hyperelliptic curve. Solving this relation (4.4) we obtain the leading term of (4.3)

$$S_0(x) = \int_{x_0}^x dx p_x = \int_{x_0}^x \frac{dx}{y(x)} (N \tilde{t}_N(x) - x \tilde{t}'_N(x)) + x p_x \Big|_{x_0}^x. \quad (4.7)$$

The hyperelliptic curve, $y(x)$, as well as $S'(x)$, are double-valued functions on the complex x -plane. Two different branches of $S'_0(x)$ will be denoted by (\pm) , so we have $S'_{0,\pm}(x)$. To specify them one makes cuts on the x -plane in an arbitrary way between the $2(N-1)$ branching points σ_j where $y(\sigma_j) = 0$. Taking (4.4) and (4.7) we have the first non-leading correction

$$S'_1(x) = \frac{i}{2} \left(\ln \frac{y(x)}{2x^N} \right)' + \frac{iNs}{x} = \frac{i}{4} \sum_{j=0}^{2N-2} \frac{1}{x - \sigma_j} + \frac{iN}{x} \left(s - \frac{1}{2} \right). \quad (4.8)$$

which is a single-valued function on the complex x -plane.

Combining together (4.7) and (4.8) we obtain two different solutions to the holomorphic Baxter equation (4.2)

$$Q_{\pm}(x/\eta) = \exp \left(\frac{i}{\eta} \int_{x_0}^x dx S'_{\pm}(x) \right), \quad \text{where} \quad S'_{\pm} = S_{0,\pm} + \eta S'_1(x) + \mathcal{O}(\eta^2) \quad (4.9)$$

with asymptotics at $x \rightarrow \infty$:

$$Q_+(x/\eta) \sim x^{1-h-Ns}, \quad Q_-(x/\eta) \sim x^{h-Ns}. \quad (4.10)$$

Similarly, one gets solutions in the anti-holomorphic sector with

$$\overline{Q}_+(\overline{x}/\eta) \sim \overline{x}^{1-\overline{h}-N\overline{s}}, \quad \overline{Q}_-(\overline{x}/\eta) \sim \overline{x}^{\overline{h}-N\overline{s}}, \quad (4.11)$$

as $\overline{x} \rightarrow \infty$.

4.2 Quantization conditions with WKB

The quasi-classical solution of the Baxter equation (4.2) is given as a bilinear combination of the chiral solutions $Q_{\pm}(x/\eta)$ and $\overline{Q}_{\pm}(\overline{x}/\eta)$:

$$Q(x/\eta, \overline{x}/\eta) = c_+ Q_+(x/\eta) \overline{Q}_+(\overline{x}/\eta) + c_- Q_-(x/\eta) \overline{Q}_-(\overline{x}/\eta). \quad (4.12)$$

The cross-terms $Q_{\pm} \overline{Q}_{\mp}$ do not enter (4.12) since they do not satisfy (3.14).

The function (4.12) should not depend on reference point x_0 . This gives condition

$$c_{\pm}(x'_0) = c_{\pm} \exp \left(\frac{i}{\eta} \int_{x_0}^{x'_0} dx S'_{\pm}(x) + \frac{i}{\eta} \int_{\overline{x}_0}^{\overline{x}'_0} d\overline{x} \overline{S}'_{\pm}(\overline{x}) \right) \quad (4.13)$$

with $\overline{x}_0 = x_0^*$. Additionally, taking into account that

$$c_+(\sigma_j) = c_-(\sigma_j) \quad \text{with} \quad j = 1, 2, \dots, 2(N-1) \quad (4.14)$$

one can derive [21] the quantization conditions

$$\operatorname{Re} \oint_{\alpha_k} dx S'_0(x)/\eta = \pi \ell_{2k-1} + \mathcal{O}(\eta), \quad \operatorname{Re} \oint_{\beta_k} dx S'_0(x)/\eta = \pi \ell_{2k} + \mathcal{O}(\eta), \quad (4.15)$$

where $k = 1, \dots, N-2$ and $\ell = (l_1, \dots, l_{2N-4})$ being integer and the integrals are performed over cycles around branching points σ_j , Fig. 4.1. The relations (4.15) give the WKB quantization conditions for the integrals of motion, q_k and \bar{q}_k .

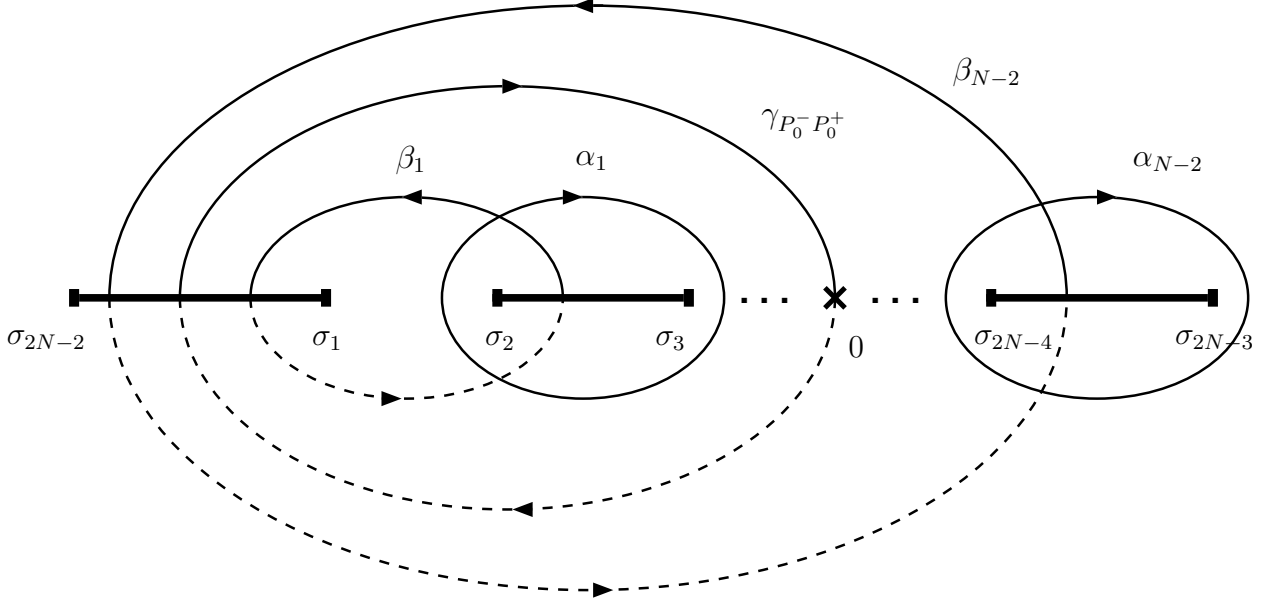


Figure 4.1: The Riemann surface Γ_N with integration cycles, α_j and β_j . The dashed lines represent the contours on the lower sheet [21]. The contour $\gamma_{P_0^- P_0^+}$ used in (4.16), goes from the point $x = 0$ on the lower sheet to $x = 0$ on the upper sheet.

4.3 Lattice structure of the conformal charges spectrum

Additionally [21], one can obtain the quasimomentum, (3.20) as

$$\theta_N = -2\operatorname{Re} \oint_{\gamma_{P_0^- P_0^+}} dx S'_0(x)/\eta = \frac{2\pi}{N} \ell \pmod{2\pi} \quad (4.16)$$

and the energy (3.17) in the WKB approximation

$$\begin{aligned} E_N^{(as)} = 4 \ln 2 + 2\operatorname{Re} \sum_{\operatorname{Im} \lambda_k \geq 0} (\psi(1-s-i\lambda_k) + \psi(s-i\lambda_k) - 2\psi(1)) \\ + 2\operatorname{Re} \sum_{\operatorname{Im} \lambda_k < 0} (\psi(1-s+i\lambda_k) + \psi(s+i\lambda_k) - 2\psi(1)) , \end{aligned} \quad (4.17)$$

where $t_N(\lambda_k) = 0$ for $k = 1, \dots, N$.

The further analysis of (4.15) and (4.16) where we fix $\eta = (q_N/4)^{-1/N}$, which is equivalent to expansion for large conformal charges, gives the system of $(N-2)$ equations for the integrals of motion

$$\begin{aligned} u_N \cdot N \operatorname{B}\left(\frac{1}{2}, \frac{1}{N}\right) - (u_2 u_N)^* \cdot \operatorname{B}\left(\frac{1}{2}, \frac{N-1}{N}\right) &= \pi \sum_{k=1}^N e^{-i\pi(2k-1)/N} n_k, \\ (u_{N+1-m} u_N) \cdot \operatorname{B}\left(\frac{1}{2}, \frac{1}{N}\right) - (u_{N+1-m} u_N)^* \cdot \operatorname{B}\left(\frac{1}{2}, \frac{N-m}{N}\right) &= \pi \sum_{k=1}^N e^{-i\pi(2k-1)m/N} n_k, \end{aligned} \quad (4.18)$$

with $m = 2, \dots, N-2$ and

$$u_n = \frac{q_n}{4} \left(\frac{q_N}{4}\right)^{-n/N} \quad \text{for } n = 2, \dots, N-2, \quad u_N = \left(\frac{q_N}{4}\right)^{1/N}. \quad (4.19)$$

The Euler beta-function $\operatorname{B}(x, y) = \Gamma(x)\Gamma(y)/\Gamma(x+y)$ and n_k are integer numbers related to the quasimomentum (4.16) by

$$\ell = - \sum_{k=1}^N n_k \pmod{N}. \quad (4.20)$$

The equations (4.18) give only $(N-1)$ conditions so the system is underdetermined.

Solving (4.18) one can obtain the quantized values of the highest conformal charge q_N as

$$q_N^{1/N} = \pi \frac{\Gamma(1+2/N)}{\Gamma^2(1/N)} \mathcal{Q}(\mathbf{n}) \left(1 + \frac{q_2^*}{2\pi} \frac{N^2}{(N-2)} \cot(\pi/N) |\mathcal{Q}(\mathbf{n})|^{-2} + \mathcal{O}(|\mathcal{Q}(\mathbf{n})|^{-4}) \right), \quad (4.21)$$

where

$$\mathcal{Q}(\mathbf{n}) = \sum_{k=1}^N n_k e^{-i\pi(2k-1)/N}. \quad (4.22)$$

with $\mathbf{n} = \{n_1, \dots, n_N\}$ integer forming a lattice structure on the spectrum of q_N (4.21).

Chapter 5

Eigenfunctions for the conformal charges

\hat{q}_k

In this Chapter we present the general method of constructing the ansatzes for eigenfunction of the conformal charges \hat{q}_k . These ansatzes have been commonly used before [48, 49, 50, 51]. Here we systematize the knowledge about this ansatzes and extend our calculations to an arbitrary complex spin s . Moreover, we derive differential eigenequations for the conformal charges. Next, we show solutions to the differential equation for $N = 3$ and $s = 0$ using the series method and present derivation of the quantization conditions for the integrals of motion q_k . Finally, we resum obtained series solutions for the $q_3 = 0$ case.

5.1 Solution of the \hat{q}_2 eigenproblem

In this Section we solve the \hat{q}_2 eigenproblem. This gives us not only the solution for the $N = 2$ Pomeron problem but also provides us with a structure of the ansatz for the eigenfunctions of the conformal charges, \hat{q}_k for $N > 2$.

As one can see from Eq. (2.54), the eigenfunctions (2.55) of the Hamiltonian (2.31) depend on differences of coordinates, $z_i - z_0$. They may contain two types of factors. The first ones are arbitrary functions of $(N - 2)$ variables, $x_i = \frac{(z_{i-1} - z_r)(z_{i+1} - z_0)}{(z_{i-1} - z_0)(z_{i+1} - z_r)}$, which are $SL(2, \mathbb{C})$ -invariant. They are defined in Appendix A. The other ones are some products of the coordinate differences that satisfy the transformation law (2.55). Let us consider the general product

$$\prod_{i_2 > i_1 = 0}^N (z_{i_2 i_1})^{k_{i_1 i_2}}, \quad (5.1)$$

where $z_{i_2 i_1} = z_{i_2} - z_{i_1}$ and $k_{i_1 i_2}$ is arbitrary.

It is convenient to parameterize the eigenvalues of the lowest conformal charge as

$$q_2 = -h(h - 1) + \sum_{j=1}^N s_j(s_j - 1), \quad (5.2)$$

where h and s_j are the conformal spins (2.56). Now one can act with the \hat{q}_2 operator (2.65) on the product of holomorphic coordinates (5.1):

$$\hat{q}_2 \prod_{i_2 > i_1 = 0}^N (z_{i_2 i_1})^{k_{i_1 i_2}} = q_2 \prod_{i_2 > i_1 = 0}^N (z_{i_2 i_1})^{k_{i_2 i_1}}. \quad (5.3)$$

In this way we obtain the equation for $k_{i_2 i_1}$ which can be easily solved.

For each N we obtain two sets of solutions: the first ones, with the z_0 coordinate, and the second ones, without the z_0 coordinate. The latter solutions may be calculated by integrating the first ones over z_0 with $\vec{p} = 0$ with the help of (2.54). They don't transform as (2.55) so they will not be further considered. The integration with an arbitrary \vec{p} (2.54) for two Reggeons was performed in [52]. In the first set we obtain two groups of solutions related by the symmetry $h \rightarrow 1 - h$, which comes from that the form of the q_2 eigenvalue (5.2). More detailed studies of this problem are included in Appendix B.

As a result we obtain an ansatz for the eigenfunction. For an arbitrary N it has a form

$$\Psi(z_{10}, z_{20}, \dots, z_{N0}) = \frac{1}{(z_{10})^{2s_1} (z_{20})^{2s_2} \dots (z_{N0})^{2s_N}} \left(\frac{z_{31}}{z_{10} z_{30}} \right)^{h-s_1-s_2-\dots-s_N} F(x_1, x_2, \dots, x_{N-2}). \quad (5.4)$$

For N particles we have $N - 2$ invariant independent variables, x_i . For the homogeneous spin, i.e. with $s_1 = s_2 = \dots = s_N = s$, chains we have

$$\Psi(z_{10}, z_{20}, \dots, z_{N0}) = \frac{1}{(z_{10} z_{20} \dots z_{N0})^{2s}} \left(\frac{z_{31}}{z_{10} z_{30}} \right)^{h-Ns} F(x_1, x_2, \dots, x_{N-2}). \quad (5.5)$$

5.2 Various ansatzes

Using the above ansatzes we can construct other ansatzes which are equivalent to the original ones. For example, for $N = 3$ [51],

$$\Psi(z_{10}, z_{20}, z_{30}) = \frac{1}{(z_{10})^{2s_1} (z_{20})^{2s_2} (z_{30})^{2s_3}} \left(\frac{z_{31}}{z_{10} z_{30}} \right)^{h-s_1-s_2-s_3} F(x), \quad (5.6)$$

where $x = x_2$ we substitute $F(x) = G(x) \left(\frac{(x-1)^2}{-x} \right)^{h/3-s_1/3-s_2/3-s_3/3}$ what gives an ansatz

$$\Psi(z_{10}, z_{20}, z_{30}) = \frac{1}{(z_{10})^{2s_1} (z_{20})^{2s_2} (z_{30})^{2s_3}} \left(\frac{z_{31} z_{12} z_{23}}{(z_{10})^2 (z_{20})^2 (z_{30})^2} \right)^{\frac{h}{3} - \frac{s_1}{3} - \frac{s_2}{3} - \frac{s_3}{3}} G(x) \quad (5.7)$$

or equivalently

$$\begin{aligned} \Psi(z_{10}, z_{20}, z_{30}) = & \left(\frac{(z_{20})^2 (z_{30})^2}{(z_{10})^4 z_{12} z_{23} z_{31}} \right)^{\frac{s_1}{3}} \left(\frac{(z_{10})^2 (z_{30})^2}{(z_{20})^4 z_{12} z_{23} z_{31}} \right)^{\frac{s_2}{3}} \left(\frac{(z_{20})^2 (z_{10})^2}{(z_{30})^4 z_{12} z_{23} z_{31}} \right)^{\frac{s_3}{3}} \\ & \times \left(\frac{z_{31} z_{12} z_{23}}{(z_{10})^2 (z_{20})^2 (z_{30})^2} \right)^{\frac{h}{3}} G(x). \end{aligned} \quad (5.8)$$

As we can see we obtained a totally symmetric ansatz which is equivalent to original one. For the homogeneous spin chains we have

$$\Psi(z_{10}, z_{20}, z_{30}) = \frac{1}{(z_{12}z_{23}z_{31})^s} \left(\frac{z_{31}z_{12}z_{23}}{(z_{10})^2(z_{20})^2(z_{30})^2} \right)^{\frac{h}{3}} G(x). \quad (5.9)$$

Both ansatzes have advantages and disadvantages. The symmetric one (5.8) is appropriate if we want to deal with the particle symmetries. The original one (5.6) has a simpler structure, it contains powers of h (not $h/3$), so we can use it when we want to construct proper single-valuedness conditions. One can easily notice that $z^h \bar{z}^{\bar{h}}$ is single-valued because $h - \bar{h} = n_h \in \mathbb{Z}$.

Similarly, we can go from the original ansatz (5.6) to an ansatz with different permutation of particles

$$\begin{aligned} \Psi(z_{10}, z_{20}, z_{30}) &= \frac{1}{(z_{10})^{2s_1}(z_{20})^{2s_2}(z_{30})^{2s_3}} \left(\frac{z_{31}}{z_{10}z_{30}} \right)^{h-s_1-s_2-s_3} F(x) = \\ &= \frac{1}{(z_{10})^{2s_1}(z_{20})^{2s_2}(z_{30})^{2s_3}} \left(\frac{z_{12}}{z_{10}z_{20}} \right)^{h-s_1-s_2-s_3} H(x) \\ &= \frac{1}{(z_{10})^{2s_1}(z_{20})^{2s_2}(z_{30})^{2s_3}} \left(\frac{z_{32}}{z_{20}z_{30}} \right)^{h-s_1-s_2-s_3} J(x). \end{aligned} \quad (5.10)$$

Now we can generalize our ansatz for different number of particles, N . In this case we have

$$\begin{aligned} \Psi(z_{10}, z_{20}, \dots, z_{N0}) &= \left(\frac{(z_{10})^2(z_{20})^2 \dots (z_{N0})^2}{(z_{10})^{2N} z_{12} z_{23} \dots z_{N1}} \right)^{\frac{s_1}{N}} \left(\frac{(z_{10})^2(z_{20})^2 \dots (z_{N0})^2}{(z_{20})^{2N} z_{12} z_{23} \dots z_{N1}} \right)^{\frac{s_2}{N}} \dots \\ &\dots \left(\frac{(z_{10})^2(z_{20})^2 \dots (z_{N0})^2}{(z_{N0})^{2N} z_{12} z_{23} \dots z_{N1}} \right)^{\frac{s_N}{N}} \left(\frac{z_{12} z_{23} \dots z_{N1}}{(z_{10})^2(z_{20})^2 \dots (z_{N0})^2} \right)^{\frac{h}{N}} G(x_1, x_2, \dots, x_{N-2}). \end{aligned} \quad (5.11)$$

And for the homogeneous spin chains, $s_i = s$, it has a form

$$\Psi(z_{10}, z_{20}, \dots, z_{N0}) = \frac{1}{(z_{12}z_{23} \dots z_{N1})^s} \left(\frac{z_{12}z_{23} \dots z_{N1}}{(z_{10})^2(z_{20})^2 \dots (z_{N0})^2} \right)^{\frac{h}{N}} G(x_1, x_2, \dots, x_{N-2}). \quad (5.12)$$

To sum up, we have many equivalent ansatzes. Here we presented two of them, (5.6) and (5.8). They are most frequently used due to their simplicity and symmetry properties.

5.3 Solutions of the \hat{q}_3 eigenproblem for $N = 3$

In this Section we solve the \hat{q}_3 eigenproblem for three Reggeons. We derive differential equations for the integral of motion q_3 for an arbitrary complex spin s and solve them for $s = \bar{s} = 0$ making use of the series method. We also construct the quantization conditions for q_3 and in the end we resum the series for zero-modes of \hat{q}_3 . We obtain the known solution (5.44) as well as some others with $\text{Log}(x)$ -terms (5.51).

5.3.1 Derivation of differential equations for $N = 3$

In the previous Section we solved the eigenproblem for \hat{q}_2 . However, for N particles there are $N - 1$ conformal charges which commute with the Hamiltonian. Thus, for $N = 3$ we have \hat{q}_2

and \hat{q}_3 . In order to solve the eigenproblem for \hat{q}_3 we can act with \hat{q}_3 on our ansatz

$$\Psi(z_{10}, z_{20}, z_{30}) = \frac{1}{(z_{10})^{2s_1} (z_{20})^{2s_2} (z_{30})^{2s_3}} \left(\frac{z_{32}}{z_{20} z_{30}} \right)^{h-s_1-s_2-s_3} F(x) \quad (5.13)$$

and derive a differential equation for $F(x)$ with $x = x_2 = \frac{(z_1-z_2)(z_3-z_0)}{(z_1-z_0)(z_3-z_2)}$. Thus we obtain

$$\begin{aligned} iq_3 F(x) = & -s_1(s_1 + s_2 + s_3 - h)(h - 1 - s_1 - s_2 + s_3 - 2hx + 2(1 + s_1)x)F(x) + \\ & + ((s_1 + s_2)(1 - h + s_1 + s_2 - s_3) + \\ & - (2 + h^2 + 7s_1 + 3s_2 + (s_1 + s_2)(5s_1 + s_2) - h(3 + 6s_1 + 2s_2) + s_3 - s_3^2)x + \\ & + (h^2 + 2(1 + s_2 + s_3) - h(3 + 6s_1 + s_2 + s_3) + s_1(7 + 5s_1 + 3s_2 + 3s_3))x^2)F'(x) + \\ & - (x - 1)x(2 + 2s_1 + 2s_2 - s_3 - (4 + 4s_1 + s_2 + s_3)x + h(2x - 1))F''(x) + \\ & + (x - 1)^2 x^2 F^{(3)}(x). \end{aligned} \quad (5.14)$$

Using various ansatzes we obtain equivalent differential equations.

For the homogeneous chain our equation looks like

$$\begin{aligned} iq_3 F(x) = & (3s - h)(h - 1 - s)(1 - 2x)F(x) + (((h - 2)(h - 1)(x - 1)x + s^2(2 + 11(x - 1)x) + \\ & + s(2 - 2h(1 - 2x)^2 + 11(x - 1)x))F'(x) + (2 + h - 3s)(1 - x)x(2x - 1)F''(x) + \\ & + (x - 1)^2 x^2 F^{(3)}(x)). \end{aligned} \quad (5.15)$$

From the QCD point of view the most interesting cases are for $s = 0$:

$$iq_3 F(x) = (h - 1)(h - 2)x(x - 1)F'(x) + (h - 2)(x - 1)x(1 - 2x)F''(x) + x^2(x - 1)^2 F^{(3)}(x) \quad (5.16)$$

and for $s = 1$

$$\begin{aligned} iq_3 F(x) = & (h - 3)(h - 2)(2x - 1)F(x) + \\ & + ((4 - 2h - (h - 8)(h - 3)x + (h - 8)(h - 3)x^2)F'(x) + \\ & + (5 - h)(x - 1)x(2x - 1)F''(x) + (x - 1)^2 x^2 F^{(3)}(x)). \end{aligned} \quad (5.17)$$

The first such solution was derived and found numerically in [18].

5.3.2 Solutions for $s = 0$

Now, we will solve the above equations by the series method. All these equations have three regular singular points at $x = 0$, $x = 1$ and $x = \infty$. Let us take an ansatz (5.13) which for $s = 0$ can be rewritten as

$$\Psi(z_{10}, z_{20}, z_{30}) = w^h F(x), \quad (5.18)$$

where w is defined similarly to (A.4) with z_3 , z_2 and z_0 . Thus, we obtained (5.16)

$$iq_3 F(x) = (h - 1)(h - 2)x(x - 1)F'(x) + (x - 1)x(h - 2)(1 - 2x)F''(x) + x^2(x - 1)^2 F^{(3)}(x). \quad (5.19)$$

This equation can be used to obtain solution around $x = 0^+$. To generate solutions around other singular points we exchange variables. For the case $x = 1^-$ we can use a substitution $x = 1 - y$:

$$iq_3 G(y) = (h-1)(h-2)y(1-y)G'(y) + (h-2)(1-y)y(1-2y)G''(y) - y^2(y-1)^2 G^{(3)}(y). \quad (5.20)$$

Moreover, for $x = 1^+$ we can use $x = y + 1$:

$$q_3 G(y) = i(y(y+1)(h-1)(h-2)G'(y) - (y+1)y(h-2)(1+2y)G''(y) + y^2(y+1)^2 G^{(3)}(y)) \quad (5.21)$$

and for $x = \infty^-$ we have $x = 1/y$:

$$q_3 G(y) = i((y-1)(h+1)(h-2y)G'(y) + (y-1)y(2(h+1) - (h+4)y)G''(y) + y(y-1)^2 G^{(3)}(y)) . \quad (5.22)$$

The upper-scripts *plus* and *minus* correspond to case where $\text{Re}[x]$ is above and below the singular point, respectively.

5.3.3 Wave-function for $s = \bar{s} = 0$ around $x = \bar{x} = 0^+$

In order to obtain the full-complex solution containing the holomorphic and anti-holomorphic parts we have to glue together solutions from these parts:

$$\Phi_{q,\bar{q}}(\{z_i\}, \{\bar{z}_i\}) = \bar{u}_{\bar{q}}(\{\bar{z}_i\})^T \cdot A^{(0)}(h, \bar{h}, q_3, \bar{q}_3) \cdot u_q(\{z_i\}), \quad (5.23)$$

where we use a $(N \times N)$ mixing-matrix, $A_{q,\bar{q}}^{(0)}$, [18] which does not depend on particle coordinates but only on $q \equiv \{q_2, q_3\}$. From the QCD point of view we have two possibilities of gluing solutions: $(s = 0, \bar{s} = 0)$ [27] and $(s = 0, \bar{s} = 1)$ [38]. These two cases are equivalent except zero modes of the highest conformal charge \hat{q}_N . Let us consider the first case, $s = \bar{s} = 0$.

The conformal charges are related by conditions $\bar{h} = 1 - h^*$ and $\bar{q}_k = q_k^*$. The wave-function has to be single-valued. This condition defines the structure of the mixing-matrix.

For $h \notin \mathbb{Z}$ and $\hat{q}_3 \neq 0$ we have solutions of the following type

$$\begin{aligned} u_1(x) &= x^h \sum_{n=0}^{\infty} a_{n,r_1} x^n, \\ u_2(x) &= x^1 \sum_{n=0}^{\infty} a_{n,r_2} x^n, \\ u_3(x) &= x^0 \sum_{n=0}^{\infty} b_{n,r_3} x^n + x^1 \sum_{n=0}^{\infty} a_{n,r_2} x^n \text{Log}(x) \end{aligned} \quad (5.24)$$

and similarly in the anti-holomorphic sector. The coefficient recurrence relations for the a_{n,r_i} are given in Appendix C. One can notice that $x^a \bar{x}^b$ is single-valued only if $a - b \in \mathbb{Z}$. Moreover we have also terms with $\text{Log}(x)$ which have to give in a sum $\text{Log}(x\bar{x})$. So in this case we have a mixing matrix of the form

$$A^{(0)}(h, \bar{h}, q_3, \bar{q}_3) = \begin{bmatrix} \alpha & 0 & 0 \\ 0 & \beta & \gamma \\ 0 & \gamma & 0 \end{bmatrix}, \quad (5.25)$$

where α, β, γ are arbitrary. In the above matrix we have $A_{12} = A_{13} = A_{21} = A_{31} = 0$ in order to eliminate multi-valuedness coming from the power-terms, $A_{23} = A_{32}$ to obtain single-valuedness in $\text{Log}(x)$ -terms and $A_{33} = 0$ because the term $\text{Log}(x)\text{Log}(\bar{x})$ is not single-valued on the \vec{x} -plane.

In the case of $q_3 = 0$ and $h \notin \{0, 1\}$ we don't have any $\text{Log}(x)$ -terms so the mixing matrix looks like ¹

$$A^{(0)}(h, \bar{h}, q_3 = 0, \bar{q}_3 = 0) = \begin{bmatrix} \beta & 0 & 0 \\ 0 & \alpha & \delta \\ 0 & \varepsilon & \gamma \end{bmatrix}. \quad (5.26)$$

For $q_3 \neq 0$ and $h \in \mathbb{Z}$ we have a solution with all power in x integer and solutions without Log , with one- Log and with double- Log . The structure of the matrix is

$$A^{(0)}(h \in \mathbb{Z}, \bar{h} \in \mathbb{Z}, q_3, \bar{q}_3) = \begin{bmatrix} \alpha & \beta & \gamma \\ \beta & 2\gamma & 0 \\ \gamma & 0 & 0 \end{bmatrix}. \quad (5.27)$$

In the last case for $q_3 = 0$ and $h \in \{0, 1\}$ we have all powers of x integer and the third solution with one- Log term. The matrix has a form

$$A^{(0)}(h \in \{0, 1\}, \bar{h} \in \{0, 1\}, q_3 = 0, \bar{q}_3 = 0) = \begin{bmatrix} \alpha & \gamma & 0 \\ \beta & \delta & \varepsilon \\ 0 & \varepsilon & 0 \end{bmatrix}. \quad (5.28)$$

5.3.4 Wave-function for $s = \bar{s} = 0$ around $x = \bar{x} = 1^-$ and $x = \bar{x} = \infty^-$

Around the other singular point we construct the wave-function exactly in the same way obtaining matrices $A^{(1^-)}(h, \bar{h}, q_3, \bar{q}_3)$, $A^{(1^+)}(h, \bar{h}, q_3, \bar{q}_3)$ (around 1) and $A^{(\infty^-)}(h, \bar{h}, q_3, \bar{q}_3)$ (around ∞).

Thus, we have the wave-function similar to (5.23). For $h \notin \mathbb{Z}$ and $\hat{q}_3 \neq 0$ we take solutions

$$\begin{aligned} u_1(x) &= (1-x)^h \sum_{n=0}^{\infty} a_{n,r_1} (1-x)^n, \\ u_2(x) &= (1-x)^1 \sum_{n=0}^{\infty} a_{n,r_2} (1-x)^n, \\ u_3(x) &= (1-x)^0 \sum_{n=0}^{\infty} b_{n,r_3} (1-x)^n + (1-x)^1 \sum_{n=0}^{\infty} a_{n,r_2} (1-x)^n \text{Log}(1-x) \end{aligned} \quad (5.29)$$

and similarly in the anti-holomorphic sector. Our the wave-functions have to be single-valued. Thus, the mixing matrices take the following forms

$$A^{(1)}(h, \bar{h}, q_3, \bar{q}_3) = \begin{bmatrix} \alpha & 0 & 0 \\ 0 & \beta & \gamma \\ 0 & \gamma & 0 \end{bmatrix}, \quad A^{(1)}(h, \bar{h}, q_3 = 0, \bar{q}_3 = 0) = \begin{bmatrix} \beta & 0 & 0 \\ 0 & \alpha & \delta \\ 0 & \varepsilon & \gamma \end{bmatrix}, \quad (5.30)$$

¹ *Greek* variables in each A -matrix have different numerical values

$$A^{(1)}(h \in \mathbb{Z}, \bar{h} \in \mathbb{Z}, q_3, \bar{q}_3) = \begin{bmatrix} \alpha & \beta & \gamma \\ \beta & 2\gamma & 0 \\ \gamma & 0 & 0 \end{bmatrix}, \quad (5.31)$$

$$A^{(1)}(h \in \{0, 1\}, \bar{h} \in \{0, 1\}, q_3 = 0, \bar{q}_3 = 0) = \begin{bmatrix} \alpha & \gamma & 0 \\ \beta & \delta & \varepsilon \\ 0 & \varepsilon & 0 \end{bmatrix}. \quad (5.32)$$

Similarly, we proceed around $x = \infty^-$. For $h \notin \mathbb{Z}$ and $\hat{q}_3 \neq 0$ we have solutions of type

$$\begin{aligned} u_1(x) &= (1/x)^0 \sum_{n=0}^{\infty} a_{n,r_1} (1/x)^n, \\ u_2(x) &= (1/x)^{1-h} \sum_{n=0}^{\infty} a_{n,r_2} (1/x)^n, \\ u_3(x) &= (1/x)^{-h} \sum_{n=0}^{\infty} b_{n,r_3} x^n + (1/x)^{1-h} \sum_{n=0}^{\infty} a_{n,r_2} x^n \text{Log}(x) \end{aligned} \quad (5.33)$$

and similarly in the anti-holomorphic region. In this case we have the matrix

$$A^{(\infty)}(h, \bar{h}, q_3, \bar{q}_3) = \begin{bmatrix} \alpha & 0 & 0 \\ 0 & \beta & \gamma \\ 0 & \gamma & 0 \end{bmatrix}, \quad A^{(\infty)}(h, \bar{h}, q_3 = 0, \bar{q}_3 = 0) = \begin{bmatrix} \beta & 0 & 0 \\ 0 & \alpha & \delta \\ 0 & \varepsilon & \gamma \end{bmatrix}, \quad (5.34)$$

$$A^{(\infty)}(h \in \mathbb{Z}, \bar{h} \in \mathbb{Z}, q_3, \bar{q}_3) = \begin{bmatrix} \alpha & \beta & \gamma \\ \beta & 2\gamma & 0 \\ \gamma & 0 & 0 \end{bmatrix}, \quad (5.35)$$

$$A^{(\infty)}(h \in \{0, 1\}, \bar{h} \in \{0, 1\}, q_3 = 0, \bar{q}_3 = 0) = \begin{bmatrix} \alpha & \gamma & 0 \\ \beta & \delta & \varepsilon \\ 0 & \varepsilon & 0 \end{bmatrix}. \quad (5.36)$$

5.3.5 Transition matrices between solutions around different poles

The above solutions around $x = 0, 1, \infty$ have a convergence radius equal to the difference between the two singular points: the points around which the solution is defined and the nearest of the remaining two. In order to define a global solution which is convergent in the entire complex plane we have to glue the solutions defined around different singular points. This can be done by expanding one set of solutions in terms of the other solutions in the overlap region of the two considered solutions. Thus, in the overlap region we can define the transition matrices Δ, Γ , where

$$\begin{aligned} \vec{u}^{(0)}(x, q) &= \Delta(q) \vec{u}^{(1)}(x, q), \\ \vec{u}^{(1)}(x, q) &= \Gamma(q) \vec{u}^{(\infty)}(x, q). \end{aligned} \quad (5.37)$$

Matrices, Δ and Γ , are constructed in terms of the ratios of certain determinants [48]. For example, to calculate the matrix Δ we construct Wronskian

$$W = \begin{vmatrix} u_1^{(1)}(x; q) & u_2^{(1)}(x; q) & u_3^{(1)}(x; q) \\ u_1'^{(1)}(x; q) & u_2'^{(1)}(x; q) & u_3'^{(1)}(x; q) \\ u_1''^{(1)}(x; q) & u_2''^{(1)}(x; q) & u_3''^{(1)}(x; q) \end{vmatrix}. \quad (5.38)$$

Next we construct determinants W_{ij} which are obtained from W by replacing j -th column by the i -th solution around $x = 0$, i.e. for $i = 1$ and $j = 2$ we have

$$W_{12} = \begin{vmatrix} u_1^{(1)}(x; q_3) & u_1^{(0)}(x; q_3) & u_3^{(1)}(x; q_3) \\ u_1'^{(1)}(x; q_3) & u_1'^{(0)}(x; q_3) & u_3'^{(1)}(x; q_3) \\ u_1''^{(1)}(x; q_3) & u_1''^{(0)}(x; q_3) & u_3''^{(1)}(x; q_3) \end{vmatrix}. \quad (5.39)$$

The matrix elements Δ_{ij} are given by

$$\Delta_{ij} = \frac{W_{ij}}{W}. \quad (5.40)$$

Matrix Δ does not depend on x , but only on q_k . In the similar way we can get the matrices Γ and their anti-holomorphic equivalents: $\overline{\Delta}$, $\overline{\Gamma}$.

Substituting equation (5.37) into the wave-function (5.23), one finds the following conditions for continuity of the matrix $A(\overline{q}, q)$:

$$\overline{\Delta}^T(\overline{q}_3)A^{(0)}(\overline{q}_3, q_3)\Delta(q_3) = A^{(1)}(\overline{q}_3, q_3), \quad (5.41)$$

$$\overline{\Gamma}^T(\overline{q}_3)A^{(1)}(\overline{q}_3, q_3)\Gamma(q_3) = A^{(\infty)}(\overline{q}_3, q_3). \quad (5.42)$$

Each Equation, (5.41,5.42), consists of nine equations. Solving them numerically, we obtain values of parameters $\alpha, \beta, \gamma, \dots$ as well as quantized values of the conformal charges, q_k and \overline{q}_k . Numerical calculations tell us that the spectrum of q_k obtained using this method is equivalent to the spectrum obtained using the Baxter Q -operator method which is presented in next Chapter.

5.3.6 Additional conditions coming from the particle permutation invariance

Our states have additional symmetries: the cyclic and mirror permutation (2.68). The conformal charges commute only with \mathbb{P} . Thus, our eigenstates are hardly ever eigenstates of \mathbb{M} , so they usually have mixed C -parity.

For $q_3 = 0$ we can easily resum the series solutions, see Appendix C. Let us take a case for $h \notin \{0, 1\}$. The eigenequation for the cyclic permutation with a quasimomentum $\theta_3(q)$ gives a following condition

$$\begin{aligned} & w^h \overline{w}^{\overline{h}} \left(\beta + \gamma(-x)^h(-\overline{x})^{\overline{h}} + \alpha(x-1)^h(\overline{x}-1)^{\overline{h}} + \delta(-x)^h(\overline{x}-1)^{\overline{x}} + \varepsilon(x-1)^h(-\overline{x})^{\overline{h}} \right) = \\ & = e^{i\theta_3(q)} w^h \overline{w}^{\overline{h}} \left(\alpha + \beta(-x)^h(-\overline{x})^{\overline{h}} + \gamma(x-1)^h(\overline{x}-1)^{\overline{h}} + \delta(x-1)^h + \varepsilon(\overline{x}-1)^{\overline{h}} \right). \end{aligned} \quad (5.43)$$

Here we have used cyclic transformation laws (A.6).

Comparing these two lines we obtain conditions: $\alpha = e^{-i\theta_3(q)}\beta$, $\beta = e^{-i\theta_3(q)}\gamma$, $\gamma = e^{-i\theta_3(q)}\alpha$ and $\delta = \varepsilon = 0$. One can derive that $\exp(3i\theta_3(q)) = 1$ so $\theta_3(q) = \frac{2k\pi}{3}$ where $k = 0, 1, 2$ ($k = 0$ for physical states). Thus we have an eigenstate of \mathbb{P} [53]

$$\Psi(\vec{z}_{10}, \vec{z}_{20}, \vec{z}_{30}) = w^h \overline{w}^{\overline{h}} \left(1 + \exp(i\frac{2\pi k}{3})(-x)^h(-\overline{x})^{\overline{h}} + \exp(i\frac{4\pi k}{3})(x-1)^h(\overline{x}-1)^{\overline{h}} \right), \quad (5.44)$$

where we have omitted the normalization constant.

Now we can act with a mirror permutation operator on (5.44) and test its eigenequation (2.68). Using the mirror transformations (A.7), similarly to (5.43), we obtain the following relation

$$\begin{aligned} w^h \bar{w}^{\bar{h}} (-1)^{n_h} \left(\exp(i\frac{2\pi k}{3}) + (-x)^h (-\bar{x})^{\bar{h}} + \exp(i\frac{4\pi k}{3})(x-1)^h (\bar{x}-1)^{\bar{h}} \right) = \\ = \pm w^h \bar{w}^{\bar{h}} \left(1 + \exp(i\frac{2\pi k}{3})(-x)^h (-\bar{x})^{\bar{h}} + \exp(i\frac{4\pi k}{3})(x-1)^h (\bar{x}-1)^{\bar{h}} \right). \end{aligned} \quad (5.45)$$

Comparing both sides of (5.45) gives $(-1)^{n_h} \exp(i\frac{2\pi k}{3}) = \pm 1$, $(-1)^{n_h} = \pm \exp(i\frac{2\pi k}{3})$ and $(-1)^{n_h} = \pm 1$ where the $SL(2, \mathbb{C})$ Lorentz spins $n_h = h - \bar{h}$. These conditions are consistent with $k = 0, \frac{3}{2}$. Only the first case agrees with the cyclic permutation condition. As we can see for odd n_h we have *minus* sign, so taking into account colour factors $(-1)^N$, solution (5.45) is C-even. For even n_h we have *plus* sign thus solution is C-odd. The last case is unnormalizable because when $x \rightarrow 0$ or $x \rightarrow 1$ it does not vanish so the norm, with $(s = 0, \bar{s} = 0)$, is divergent [53].

Using the duality symmetry [51, 53, 54, 55, 56], which corresponds to $h \rightarrow 1 - h$, Bartels, Lipatov and Vacca constructed an eigenstate with $q_3 = 0$ and $C = -1$

$$\Psi(\vec{z}_{10}, \vec{z}_{20}, \vec{z}_{30}) = w^h \bar{w}^{\bar{h}} x(1-x)\bar{x}(1-\bar{x}) \left(\delta^{(2)}(x) - \delta^{(2)}(1-x) + \frac{x^h \bar{x}^{\bar{h}}}{x^3 \bar{x}^3} \delta^{(2)}\left(\frac{1}{x}\right) \right). \quad (5.46)$$

This wave-function cannot be constructed using the method described here because it contains non-analytical functions, the Dirac delta $\delta(x)$.

Now, let us take the second wave-function with five parameters i.e. for $q_3 = 0$ and $h \in \{0, 1\}$. Choosing $h = 1$ we have

$$u(x) = [1, (-x), (-x)\text{Log}(-x) + (x-1)\text{Log}(x-1)]^T \quad (5.47)$$

and for $\bar{h} = 0$ it is

$$\bar{u}(\bar{x}) = [\text{Log}(\bar{x}-1), 1, \text{Log}(-\bar{x})]^T. \quad (5.48)$$

Combining them we obtain

$$\begin{aligned} \Psi(\vec{z}_{10}, \vec{z}_{20}, \vec{z}_{30}) = & w^h \bar{w}^{\bar{h}} (\alpha \text{Log}(\bar{x}-1) + \beta + \gamma(-x)\text{Log}(\bar{x}-1) + \delta(-x) + \\ & + \varepsilon((-x)\text{Log}(-\bar{x}) + (-x)\text{Log}(-x) + (x-1)\text{Log}(x-1))) . \end{aligned} \quad (5.49)$$

Like in the previous case we write the eigenequation for the cyclic permutation

$$\begin{aligned} w^{h(=1)} \bar{w}^{\bar{h}(=0)} ((\alpha - \gamma - \varepsilon)\text{Log}(x-1) + (\delta - \beta) + \alpha(-x)\text{Log}(\bar{x}-1) + (-\beta)(-x) + \\ + \varepsilon(-x)\text{Log}(-x) + \alpha(x-1)\text{Log}(-\bar{x}) + \varepsilon(-x)\text{Log}(-x) + \\ + \gamma\text{Log}(-\bar{x}) + \varepsilon(x-1)\text{Log}(x-1)) = \\ = e^{i\theta_3(q)} w (\alpha \text{Log}(\bar{x}-1) + \beta + \gamma(-x)\text{Log}(\bar{x}-1) + \delta(-x) + \\ + \varepsilon((-x)\text{Log}(-\bar{x}) + (-x)\text{Log}(-x) + (x-1)\text{Log}(x-1))) . \end{aligned} \quad (5.50)$$

Thus we get conditions: $\alpha = e^{-i\theta_3(q)}(\alpha - \gamma - \varepsilon)$, $\beta = e^{-i\theta_3(q)}(\delta - \beta)$, $\gamma = e^{-i\theta_3(q)}\alpha$, $\delta = e^{-i\theta_3(q)}(-\beta)$, $0 = e^{-i\theta_3(q)}(\gamma - \alpha)$ and $\varepsilon = e^{-i\theta_3(q)}\varepsilon$. We have two types of solutions.

The first one with $\theta_3(q) = 0$ when $\alpha = \gamma = -\varepsilon$ and $\beta = \delta = 0$. It has a form

$$\Psi(\vec{z}_{10}, \vec{z}_{20}, \vec{z}_{30}) = w((-x)\text{Log}((-\bar{x})(-x)) + (x-1)\text{Log}((\bar{x}-1)(x-1))) . \quad (5.51)$$

We obtained in this way solutions with $\text{Log}(x)$ -terms which have not been presented before. The similar expressions were shown in [27] as asymptotics of the \hat{q}_3 eigenfunction. Acting with the mirror permutation operator on (5.51) we get

$$\begin{aligned} \mathbb{M}w((-x)\text{Log}((-\bar{x})(-x)) + (x-1)\text{Log}((\bar{x}-1)(x-1))) &= \\ = -w((-x)\text{Log}((-\bar{x})(-x)) + (x-1)\text{Log}((\bar{x}-1)(x-1))) . \end{aligned} \quad (5.52)$$

We obtained *minus* sign so this state is also symmetric under C parity.

Other solutions have $\theta_3(q) = 2\pi/3, 4\pi/3$. Thus, $\alpha = \gamma = \varepsilon = 0$ and $\delta = -e^{-i\theta_3(q)}\beta$. The wave-function has a form

$$\Psi(\vec{z}_{10}, \vec{z}_{20}, \vec{z}_{30}) = w(1 + x e^{i\theta_3(q)}) . \quad (5.53)$$

These solutions are not eigenstates of the \mathbb{M} operator.

5.4 Set of differential equations for $N = 4$

Similarly to the case for three particles we can derive a set of differential equations for more particles. For $N = 4$ with the following ansatz

$$\begin{aligned} \Psi(z_{10}, z_{20}, z_{30}, z_{40}) &= \frac{1}{z_{10}^{2s_1} z_{20}^{2s_2} z_{30}^{2s_3} z_{40}^{2s_4}} \left(\frac{z_{31}}{z_{10} z_{30}} \right)^{h-s_1-s_2-s_3-s_4} \\ &\times F\left(x_1 = \frac{z_{20} z_{41}}{z_{21} z_{40}}, x_2 = \frac{z_{12} z_{30}}{z_{10} z_{32}}\right) \end{aligned} \quad (5.54)$$

we have two equations for \hat{q}_3 and for \hat{q}_4 . Acting with \hat{q}_3 we obtain

$$\begin{aligned} t_{0,0}F^{(0,0)}(x_1, x_2) + t_{1,0}F^{(1,0)}(x_1, x_2) + t_{0,1}F^{(0,1)}(x_1, x_2) + t_{2,0}F^{(2,0)}(x_1, x_2) + \\ + t_{1,1}F^{(1,1)}(x_1, x_2) + t_{0,2}F^{(0,2)}(x_1, x_2) + t_{3,0}F^{(3,0)}(x_1, x_2) + t_{2,1}F^{(2,1)}(x_1, x_2) + \\ + t_{1,2}F^{(1,2)}(x_1, x_2) + t_{0,3}F^{(0,3)}(x_1, x_2) = 0 , \end{aligned} \quad (5.55)$$

where coefficients are defined in Appendix D.

Moreover, acting with \hat{q}_4 on our ansatz we have

$$\begin{aligned} f_{0,0}F^{(0,0)}(x_1, x_2) + f_{1,0}F^{(1,0)}(x_1, x_2) + f_{0,1}F^{(0,1)}(x_1, x_2) + f_{2,0}F^{(2,0)}(x_1, x_2) + \\ + f_{1,1}F^{(1,1)}(x_1, x_2) + f_{0,2}F^{(0,2)}(x_1, x_2) + f_{3,0}F^{(3,0)}(x_1, x_2) + f_{2,1}F^{(2,1)}(x_1, x_2) + \\ + f_{1,2}F^{(1,2)}(x_1, x_2) + f_{0,3}F^{(0,3)}(x_1, x_2) + f_{4,0}F^{(0,2)}(x_1, x_2) + f_{3,1}F^{(3,0)}(x_1, x_2) + \\ + f_{2,2}F^{(2,1)}(x_1, x_2) + f_{1,3}F^{(1,2)}(x_1, x_2) + f_{0,4}F^{(3,0)}(x_1, x_2) = 0 . \end{aligned} \quad (5.56)$$

These equations are not symmetric in x_1, x_2 because the ansatz is also not symmetric.

Equations, (5.55) and (5.56), are very hard to solve even numerically, thus for the states with $N \geq 4$ we use the Q -Baxter method.

Chapter 6

Quantization conditions in the Q -Baxter method

In Ref. [23] the authors describe a construction of the solution to the Baxter equations, (3.3) and (3.4), which satisfies additionally the conditions, (3.12) and (3.14). This can be done by means of the following integral representation for $Q_{q,\bar{q}}(u, \bar{u})$

$$Q_{q,\bar{q}}(u, \bar{u}) = \int \frac{d^2 z}{z\bar{z}} z^{-iu} \bar{z}^{-i\bar{u}} Q(z, \bar{z}), \quad (6.1)$$

where we integrate over the two-dimensional \bar{z} -plane with $\bar{z} = z^*$ and $Q(z, \bar{z})$ depends on $\{q, \bar{q}\}$. The advantages of this ansatz are:

- the functional Baxter equation on $Q_{q,\bar{q}}(u, \bar{u})$ is transformed into the N -th order differential equation for the function $Q(z, \bar{z})$

$$\left[z^s (z\partial_z)^N z^{1-s} + z^{-s} (z\partial_z)^N z^{s-1} - 2(z\partial_z)^N - \sum_{k=2}^N i^k q_k (z\partial_z)^{N-k} \right] Q(z, \bar{z}) = 0. \quad (6.2)$$

A similar equation holds in the anti-holomorphic sector with s and q_k replaced by $\bar{s} = 1-s^*$ and $\bar{q}_k = q_k^*$, respectively.

- the condition (3.11) is automatically satisfied since the z -integral in the r.h.s. of (6.1) is well-defined only for $i(u - \bar{u}) = n$.
- the remaining two conditions for the analytical properties and asymptotic behaviour of $Q_{q,\bar{q}}(u, \bar{u})$, Eqs. (3.12) and (3.14), become equivalent to a requirement for $Q(z, \bar{z} = z^*)$ to be a single-valued function on the complex z -plane.

Analogically to the eigenequations for \hat{q}_3 (5.15), the differential equation (6.2) is of Fuchsian type. It possesses three regular singular points located at $z = 0$, $z = 1$ and $z = \infty$. Moreover, it has N linearly independent solutions, $Q_a(z)$. The anti-holomorphic equation has also N independent solutions, $\bar{Q}_b(\bar{z})$.

Now, similarly to (5.23), we construct the general expression for the function $Q(z, \bar{z})$ as

$$Q(z, \bar{z}) = \sum_{a,b=1}^N Q_a(z) C_{ab} \bar{Q}_b(\bar{z}), \quad (6.3)$$

where C_{ab} is an arbitrary mixing matrix. The functions $Q_a(z)$ and $\bar{Q}_b(\bar{z})$ have a nontrivial monodromy¹ around three singular points, $z, \bar{z} = 0, 1$ and ∞ . In order to be well-defined on the whole plane, functions $Q(z, \bar{z} = z^*)$ should be single-valued and their monodromy should cancel in the r.h.s. of (6.3). This condition allows us to determine the values of the mixing coefficients, C_{ab} , and also to calculate the quantized values of the conformal charges q_k .

The differential equation (6.2) is also symmetric under the transformation $z \rightarrow 1/z$ and $q_k \rightarrow (-1)^k q_k$. This property is related to Eq. (3.22) and leads to

$$Q_{q,\bar{q}}(z, \bar{z}) = e^{i\theta_N(q,\bar{q})} Q_{-q,-\bar{q}}(1/z, 1/\bar{z}), \quad (6.4)$$

where $\pm q = (q_2, \pm q_3, \dots, (\pm)^N q_N)$ denotes the integrals of motion corresponding to the function $Q(z, \bar{z})$. The above formula allows us to define the solution $Q(z, \bar{z})$ around $z = \infty$ from the solution at $z = 0$. Thus, applying (6.4) we are able to find $Q(z, \bar{z})$ and analytically continue it to the whole z -plane.

6.1 Solution around $z = 0$

We find a solution $Q(z) \sim z^a$ by the series method. The indicial equation for the solution of Eq. (6.2) around $z = 0$ reads as follows

$$(a - 1 + s)^N = 0. \quad (6.5)$$

and the solution, $a = 1 - s$, is N -times degenerate. This leads to terms $\sim \text{Log}^k(z)$ with $k \leq N - 1$. We define the fundamental set of linearly independent solutions to (6.2) around $z = 0$ as

$$\begin{aligned} Q_1^{(0)}(z) &= z^{1-s} u_1(z), \\ Q_m^{(0)}(z) &= z^{1-s} \left[u_1(z) \text{Log}^{m-1}(z) + \sum_{k=1}^{m-1} c_{m-1}^k u_{k+1}(z) \text{Log}^{m-k-1}(z) \right], \end{aligned} \quad (6.6)$$

with $2 \leq m \leq N$ and where for the later convenience $c_{m-1}^k = (m-1)!/(k!(m-k-1)!)$. The functions $u_m(z)$ are defined inside the region $|z| < 1$ and have a form

$$u_m(z) = 1 + \sum_{n=1}^{\infty} z^n u_n^{(m)}(q). \quad (6.7)$$

¹The monodromy matrix around $z = 0$ is defined as $Q_n^{(0)}(z e^{2\pi i}) = M_{nk} Q_k^{(0)}(z)$ and similarly for the other singular points.

Inserting (6.6) and (6.7) into (6.2), one derives recurrence relations for $u_n^{(m)}(q)$. However, in order to save space, we do not show here their explicit form.

In the anti-holomorphic sector the fundamental set of solutions can be obtained from (6.6) by substituting s and q_k by $\bar{s} = 1 - s^*$ and $\bar{q}_k = q_k^*$, respectively. Sewing the two sectors we obtain the general solution for $Q(z, \bar{z})$ around $z = 0$ as

$$Q(z, \bar{z}) \stackrel{|z| \rightarrow 0}{=} \sum_{m, \bar{m}=1}^N Q_m^{(0)}(z) C_{m\bar{m}}^{(0)} \bar{Q}_{\bar{m}}^{(0)}(\bar{z}). \quad (6.8)$$

The above solution (6.8) should be single-valued on the z -plane. Thus, similarly to (5.23) we find a structure of the mixing matrix $C_{m\bar{m}}^{(0)}$ which for $n + m \leq N + 1$

$$C_{nm}^{(0)} = \frac{\sigma}{(n-1)!(m-1)!} \sum_{k=0}^{N-n-m+1} \frac{(-2)^k}{k!} \alpha_{k+n+m-1} \quad (6.9)$$

with $\sigma, \alpha_1, \dots, \alpha_{N-1}$ being arbitrary complex parameters and $\alpha_N = 1$. Below the main anti-diagonal, that is for $n + m > N + 1$, $C_{nm}^{(0)}$ vanish.

The mixing matrix $C_{m\bar{m}}^{(0)}$ depends on N arbitrary complex parameters σ and α_k . However, two parity relations, Eqs. (3.21) and (6.4), fix $\sigma = \exp(i\theta_N(q, \bar{q}))$, with $\theta_N(q, \bar{q})$ being the quasimomentum, and lead to the quantization of the quasimomentum. Later, we will use (6.4) to calculate the eigenvalues of $\theta_N(q, \bar{q})$ (see Eq. (6.24)).

The leading asymptotic behaviour of $Q(z, \bar{z})$ for $z \rightarrow 0$ can be obtained by substituting (6.9) and (6.6) into (6.8). It has a form

$$Q_{q, \bar{q}}(z, \bar{z}) = z^{1-s} \bar{z}^{1-\bar{s}} e^{i\theta_N(q, \bar{q})} \left[\frac{\text{Log}^{N-1}(z\bar{z})}{(N-1)!} + \frac{\text{Log}^{N-2}(z\bar{z})}{(N-2)!} \alpha_{N-1} + \dots + \frac{\text{Log}(z\bar{z})}{1!} \alpha_2 + \alpha_1 \right] (1 + \mathcal{O}(z, \bar{z})). \quad (6.10)$$

Making use of the integral identity

$$\int_{|z| < \rho} \frac{d^2 z}{z \bar{z}} z^{-iu} \bar{z}^{-i\bar{u}} \ln^n(z\bar{z}) z^{m-s} \bar{z}^{\bar{m}-\bar{s}} = \pi \delta_{m-s-iu, \bar{m}-\bar{s}-i\bar{u}} \left[\frac{(-1)^n n!}{(m-s-iu)^{n+1}} + \mathcal{O}((m-s-iu)^0) \right], \quad (6.11)$$

with m and \bar{m} positive integer, we can calculate the contribution of the small- z region to the eigenvalue of the Baxter equation (6.1). The function $Q_{q, \bar{q}}(u, \bar{u})$ has poles of the order N in the points $u = i(s-m)$ and $\bar{u} = i(\bar{s}-\bar{m})$ what agrees with (3.12). For $m = \bar{m} = 1$ one finds from (6.10)

$$Q_{q, \bar{q}}(u_1^+ + \epsilon, \bar{u}_1^+ + \epsilon) = -\frac{\pi e^{i\theta_N(q, \bar{q})}}{(i\epsilon)^N} \left[1 + i\epsilon \alpha_{N-1} + \dots + (i\epsilon)^{N-2} \alpha_2 + (i\epsilon)^{N-1} \alpha_1 + \mathcal{O}(\epsilon^N) \right], \quad (6.12)$$

where u_1^+ and \bar{u}_1^+ are defined in (3.12). One can see that the integration in (6.1) over the region of large z with (6.4) and (6.10) gives the second set of poles for $Q_{q, \bar{q}}(u, \bar{u})$ located at $u = -i(s-m)$ and $\bar{u} = -i(\bar{s}-\bar{m})$.

Comparing (6.12) with (3.13) one obtains

$$R^+(q, \bar{q}) = -\frac{\pi}{i^N} e^{i\theta_N(q, \bar{q})}, \quad E^+(q, \bar{q}) = \alpha_{N-1}(q, \bar{q}). \quad (6.13)$$

Now, we may derive expression for the energy

$$E_N(q, \bar{q}) = \text{Re} [\alpha_{N-1}(-q, -\bar{q}) + \alpha_{N-1}(q, \bar{q})]. \quad (6.14)$$

The arbitrary complex parameters α_n , defined in (6.9), will be fixed by the quantization conditions below.

In this Section we have obtained following Ref. [23] the expression for the energy spectrum $E_N(q, \bar{q})$, as a function of the matrix elements of the mixing matrix (6.9) in the fundamental basis (6.6). Moreover, we have defined the solution to the Baxter equation $Q(u, \bar{u})$ and reproduced the analytical properties of the eigenvalues of the Baxter operator, Eq. (3.12).

6.2 Solution around $z = 1$

Looking for a solution of (6.2) around $z = 1$ in a form $Q(z) \sim (z - 1)^b$ we obtain the following indicial equation

$$(b + 1 + h - Ns)(b + 2 - h - Ns) \prod_{k=0}^{N-3} (b - k) = 0, \quad (6.15)$$

where h is the total $SL(2, \mathbb{C})$ spin defined in (5.2). Although the solutions $b = k$ with $k = 0, \dots, N - 3$ differ from each other by an integer, for $h \neq (1 + n_h)/2$, no logarithmic terms appear. The $\text{Log}(z)$ -terms are only needed for $\text{Im}h = 0$ where the additional degeneration occurs.

Thus, we define the fundamental set of solutions to Eq. (6.2) around $z = 1$. For $\text{Im}h \neq 0$ it has the form

$$\begin{aligned} Q_1^{(1)}(z) &= z^{1-s}(1 - z)^{Ns-h-1}v_1(z), \\ Q_2^{(1)}(z) &= z^{1-s}(1 - z)^{Ns+h-2}v_2(z), \\ Q_m^{(1)}(z) &= z^{1-s}(1 - z)^{m-3}v_m(z), \end{aligned} \quad (6.16)$$

with $m = 3, \dots, N$. The functions $v_i(z)$ ($i = 1, 2$) and $v_m(z)$ given by the power series

$$v_i(z) = 1 + \sum_{n=1}^{\infty} (1 - z)^n v_n^{(i)}(q), \quad v_m(z) = 1 + \sum_{n=N-m+1}^{\infty} (1 - z)^n v_n^{(m)}(q), \quad (6.17)$$

which converge inside the region $|1 - z| < 1$ and where the expansion coefficients $v_n^{(i)}$ and $v_n^{(m)}$ satisfy the N -term recurrence relations² with respect to the index n . For $h = (1 + n_h)/2 \in 2\mathbb{Z} + 1$, one $\text{Log}(z)$ -terms appears so for $n_h \geq 0$,

$$Q_1^{(1)}(z) \Big|_{h=(1+n_h)/2} = z^{1-s}(1 - z)^{Ns-(n_h+3)/2} [(1 - z)^{n_h} \text{Log}(1 - z) v_2(z) + \tilde{v}_1(z)], \quad (6.18)$$

²The factor z^{1-s} was included in the r.h.s. of (6.16) and (6.18) to simplify the form of the recurrence relations.

where the function $v_2(z)$ is the same as before, $\tilde{v}_1(z) = \sum_{k=0}^{\infty} \tilde{v}_k z^k$ and the coefficients \tilde{v}_k satisfy the N -term recurrence relations with the boundary condition $\tilde{v}_{n_h} = 1$. For $h \in \mathbb{Z}$ we have two additional terms: $\text{Log}(z)$ and $\text{Log}^2(z)$.

Similar calculations have to be performed in the anti-holomorphic sector with s and h replaced by $\bar{s} = 1 - s^*$ and $\bar{h} = 1 - h^*$, respectively. A general solution for $Q(z, \bar{z})$ for $\text{Im}(h) \neq 0$ with respect to the single-valuedness can be constructed as

$$Q(z, \bar{z}) \stackrel{|z| \rightarrow 1}{=} \beta_h Q_1^{(1)}(z) \bar{Q}_1^{(1)}(\bar{z}) + \beta_{1-h} Q_2^{(1)}(z) \bar{Q}_2^{(1)}(\bar{z}) + \sum_{m, \bar{m}=3}^N Q_m^{(1)}(z) \gamma_{m\bar{m}} \bar{Q}_{\bar{m}}^{(1)}(\bar{z}). \quad (6.19)$$

Here the parameters β_h and $\gamma_{m\bar{m}}$ build the $C^{(1)}$ matrix where $Q(z, \bar{z}) = Q_m^{(1)} C_{m\bar{m}}^{(1)} \bar{Q}_{\bar{m}}^{(1)}$. The β -coefficients depend, in general, on the total spin h (and $\bar{h} = 1 - h^*$). They are chosen in (6.19) in such a way that the symmetry of the eigenvalues of the Baxter operator under $h \rightarrow 1 - h$ becomes manifest. Thus, the mixing matrix $C^{(1)}$ defined in (6.19) depends on $2 + (N - 2)^2$ complex parameters β_h, β_{1-h} and $\gamma_{m\bar{m}}$ which are some functions of the integrals of motion (q, \bar{q}) , so, they can be fixed by the quantization conditions.

For $h = (1 + n_h)/2$ the first two terms in the r.h.s. of (6.19) look differently in virtue of (6.18)

$$Q(z, \bar{z}) \Big|_{h=(1+n_h)/2} = \beta_1 \left[Q_1^{(1)}(z) \bar{Q}_2^{(1)}(\bar{z}) + Q_2^{(1)}(z) \bar{Q}_1^{(1)}(\bar{z}) \right] + \beta_2 Q_2^{(1)}(z) \bar{Q}_2^{(1)}(\bar{z}) + \dots, \quad (6.20)$$

where ellipses denote the remaining terms. Substituting (6.19) into (6.1) and performing integration over the region of $|1 - z| \ll 1$, one can find the asymptotic behaviour of $Q(u, \bar{u})$ at large u .

Let us consider the duality relation (6.4). Using the function $Q(z, \bar{z})$ we evaluate (6.19) in the limit $|z| \rightarrow 1$. In this way, we obtain set of relations for the functions $\beta_i(q, \bar{q})$ and $\gamma_{m\bar{m}}(q, \bar{q})$. The derivation is based on the following property

$$Q_a^{(1)}(1/z; -q) = \sum_{b=1}^N S_{ab} Q_b^{(1)}(z; q), \quad (6.21)$$

with $\text{Im}(1/z) > 0$ and where the dependence on the integrals of motion was explicitly indicated. Here taking limit $z \rightarrow 1$ in (6.16) and (6.17) and substituting them to (6.21) we are able to evaluate the S -matrix

$$S_{11} = e^{-i\pi(Ns-h-1)}, \quad S_{22} = e^{-i\pi(Ns+h-2)}, \quad S_{k,k+m} = (-1)^{k-3} \frac{(k-2s-1)_m}{m!} \quad (6.22)$$

with $(x)_m \equiv \Gamma(x+m)/\Gamma(x)$, $3 \leq k \leq N$ and $0 \leq m \leq N - k$. Similar relations hold in the anti-holomorphic sector,

$$\bar{S}_{11} = e^{i\pi(N\bar{s}-\bar{h}-1)}, \quad \bar{S}_{22} = e^{i\pi(N\bar{s}+\bar{h}-2)}, \quad \bar{S}_{k,k+m} = (-1)^{k-3} \frac{(k-2\bar{s}-1)_m}{m!}. \quad (6.23)$$

The S -matrix does not depend on z because the Q -functions on the both sides of relation (6.21) satisfy the same differential equation (6.2).

Now, substituting (6.19) and (6.21) into (6.4), we find

$$\begin{aligned}\beta_h(q, \bar{q}) &= e^{i\theta_N(q, \bar{q})} (-1)^{Nn_s+n_h} \beta_h(-q, -\bar{q}), \\ \gamma_{m\bar{m}}(q, \bar{q}) &= e^{i\theta_N(q, \bar{q})} \sum_{n, \bar{n} \geq 3}^N S_{nm} \gamma_{n\bar{n}}(-q, -\bar{q}) \bar{S}_{\bar{n}\bar{m}}.\end{aligned}\quad (6.24)$$

In this way, similarly to the energy, Eq. (6.14), which was calculated from the mixing matrix at $z = 0$, the eigenvalues of the quasimomentum, $\theta_N(q, \bar{q})$, maybe calculated from the mixing matrix at $z = 1$, from the first relation in (6.24). In the special case when $q_{2k+1} = \bar{q}_{2k+1} = 0$ ($k = 1, 2, \dots$), this means $\beta_h(q, \bar{q}) = \beta_h(-q, -\bar{q})$, the quasimomentum is equal to

$$e^{i\theta_N(q, \bar{q})} = (-1)^{Nn_s+n_h}. \quad (6.25)$$

6.3 Transition matrices

In the previous Sections we constructed the solutions $Q(z, \bar{z})$ to (6.2) in the vicinity of $z = 0$ and $z = 1$. Now, we sew these solutions inside the region $|1 - z| < 1$, $|z| < 1$ and, then analytically continue the resulting expression for $Q(z, \bar{z})$ into the whole complex z -plane by making use of the duality relation (6.4).

The sewing procedure is similar to that described by (5.37)–(5.41). Firstly, we define the transition matrices $\Omega(q)$ and $\bar{\Omega}(\bar{q})$:

$$Q_n^{(0)}(z) = \sum_{m=1}^N \Omega_{nm}(q) Q_m^{(1)}(z), \quad \bar{Q}_n^{(0)}(\bar{z}) = \sum_{m=1}^N \bar{\Omega}_{nm}(\bar{q}) \bar{Q}_m^{(1)}(\bar{z}). \quad (6.26)$$

which are uniquely fixed (5.40). The resulting expressions for the matrices $\Omega(q)$ and $\bar{\Omega}(\bar{q})$ take the form of infinite series in q and \bar{q} , respectively. Substituting (6.26) into (6.8) and matching the result into (6.19), we find the following relation

$$C^{(1)}(q, \bar{q}) = [\Omega(q)]^T C^{(0)}(q, \bar{q}) \bar{\Omega}(\bar{q}). \quad (6.27)$$

The above matrix equation allows us to determine the matrices $C^{(0)}$ and $C^{(1)}$ and provides the quantization conditions for the integrals of motion, q_k and \bar{q}_k with $k = 3, \dots, N$. Therefore, we can evaluate the eigenvalues of the Baxter \mathbb{Q} -operator, Eq. (6.1). Formula (6.27) contains N^2 equations with:

- $(N - 1)$ α -parameters inside the matrix $C^{(0)}$,
- $2 + (N - 2)^2$ parameters $\beta_{1,2}$ and $\gamma_{m\bar{m}}$ inside the matrix $C^{(1)}$,
- $(N - 2)$ integrals of motion q_3, \dots, q_N where $\bar{q}_k = q_k^*$

Thus, we obtain $(2N - 3)$ nontrivial consistency conditions.

The solutions to the quantization conditions (6.27) will be presented in details in next Sections.

Chapter 7

Numerical results

In this Chapter we present the spectra of the conformal charges obtained by numerical calculations [23, 50]. To this end we resum solutions (6.7) and (6.17) numerically, and using them we solve the quantization conditions (6.27). First we discuss the numerical results obtained in Refs. [50, 23] for $N = 3, 4$ and for the ground states for $N = 5, \dots, 8$. Moreover, we present some results which were never published before, i.e. quantized values of q_3 for $N = 3$ and $n_h > 0$, resemblant and winding spectra of q_3, q_4 for $N = 4$ and corrections to the WKB approximation for $N = 3$ and $N = 4$.

7.0.1 Trajectories

Solving quantization conditions (6.27) we obtain continuous trajectories in the space of conformal charges. They are built of points, $(q_2(\nu_h), \dots, q_N(\nu_h))$ which satisfy (6.27) and depend on a continuous real parameter ν_h entering q_2 , (5.2) and (2.60). In order to label the trajectories we introduce the set of the integers

$$\ell = \{\ell_1, \ell_2, \dots, \ell_{2(N-2)}\} \quad (7.1)$$

which parameterize one specified point on each trajectory for given h . Specific examples in the following Sections will further clarify this point.

Next we calculate the observables along these trajectories, namely the energy (6.14) and the quasimomentum (6.24). The quasimomentum is constant (2.70) for all points situated on a given trajectory. The minimum of the energy, which means the maximal intercept, for almost all trajectories is located at $\nu_h = 0$. It turns out that the energy behaves around $\nu_h = 0$ like

$$E_N(\nu_h; \ell^{\text{ground}}) = E_N^{\text{ground}} + \sigma_N \nu_h^2 + \mathcal{O}(\nu_h^2) \quad (7.2)$$

Thus, the ground state along its trajectory is gapless and the leading contribution to the scattering amplitude around ν_h may be rewritten as a series in the strong coupling constant:

$$\mathcal{A}(s, t) \sim -is \sum_{N=2}^{\infty} (i\bar{\alpha}_s)^N \frac{s^{-\bar{\alpha}_s E_N^{\text{ground}}/4}}{(\bar{\alpha}_s \sigma_N \ln s)^{1/2}} \xi_{A,N}(t) \xi_{B,N}(t), \quad (7.3)$$

where $\overline{\alpha}_s = \alpha_s N_c / \pi$ and $\xi_{X,N}(t)$ are the impact factors corresponding to the overlap between the wave-functions of scattered particle with the wave-function of N -Reggeons, whereas σ_N measures the dispersion of the energy on the trajectory around $\nu_h = 0$.

On the other hand, the energy along the trajectories grows with ν_h and for $|\nu_h| \rightarrow \infty$ and finally, we have $E_N(\nu_h; \ell) \sim \ln \nu_h^2$. These parts of the trajectory give the lowest contribution to the scattering amplitude.

7.0.2 Symmetries

The spectrum of quantized charges q_2, \dots, q_N is degenerate. This degeneration is caused by two symmetries:

$$q_k \leftrightarrow (-1)^k q_k \quad (7.4)$$

which comes from invariance of the Hamiltonian under mirror permutations of particles, (2.68), and

$$q_k \leftrightarrow \overline{q}_k \quad (7.5)$$

which is connected with the symmetry under interchange of the z - and \overline{z} -sectors. Therefore, the four points, $\{q_k\}$, $\{(-1)^k q_k\}$, $\{q_k^*\}$ and $\{(-1)^k q_k^*\}$ with $k = 2, \dots, N$, are related and all of them satisfy the quantization conditions (6.27) and have the same energy.

7.0.3 Descendent states

Let us first discuss the spectrum along the trajectories with the highest conformal charge q_N equal zero for arbitrary $\nu_h \in \mathbb{R}$. It turns out [55, 51, 53, 23] that the wave-functions of these states are built of $(N-1)$ -particle states. Moreover, their energies [57] are also equal to the energy of the ancestor $(N-1)$ -particle states:

$$E_N(q_2, q_3, \dots, q_N = 0) = E_{N-1}(q_2, q_3, \dots, q_{N-1}). \quad (7.6)$$

Thus, we call them the descendent states of the $(N-1)$ -particle states.

Generally, for odd N , the descendent state $\Psi_N^{(q_N=0)}$ with the minimal energy $E_N(q_N = 0) = 0$ has for $q_2 = 0$, i.e. for $h = 0, 1$, the remaining integrals of motion $q_3 = \dots = q_N = 0$ as well. For $h = 1 + i\nu_h$, i.e. $q_2 \neq 0$, the odd conformal charges $q_{2k+1} = 0$ with $k = 1, \dots, (N-1)/2$ while the even ones $q_{2k} \neq 0$ and depend on ν_h .

On the other hand, for even N , the eigenstate with the minimal energy $\Psi_N^{(q_N=0)}$ is the descendent state of the $(N-1)$ -particle state which has minimal energy with $q_{N-1} \neq 0$. Thus, $E_N^{min}(q_N = 0) = E_{N-1}^{min}(q_{N-1} \neq 0) > 0$.

Studying more exactly this problem one can obtain [55, 23] a relation between the quasimomentum θ_N of the descendent state and the ancestor one θ_{N-1} , which takes the following form

$$e^{i\theta_N} \Big|_{q_N=0} = -e^{i\theta_{N-1}} = (-1)^{N+1}. \quad (7.7)$$

Additionally, one can define linear operator Δ [55, 23] that maps the subspace $V_{N-1}^{(q_{N-1}-1)}$ of the $(N-1)$ -particle ancestor eigenstates with the quasimomentum $\theta_{N-1} = \pi N$ into the N -particle descendent states with $q_N = 0$ and $\theta_N = \pi(N+1)$ as

$$\Delta : V_{N-1}^{(\theta_{N-1}=\pi N)} \rightarrow V_N^{(\theta_N=\pi(N+1))} . \quad (7.8)$$

It turns out that this operator is nilpotent for the eigenstates which form trajectories [55], i.e. $\Delta^2 \Psi = 0$. Thus, the descendent-state trajectory can not be ancestor one for $(N+1)$ -particle states. However, it is possible to build a single state [23] with $q_2 = q_3 = \dots = q_N = 0$, i.e. for only one point $\nu_h = 0$, that has $E_N = 0$ and the eigenvalue of Baxter Q -operator defined as

$$Q_N^{q=0}(u, \bar{u}) \sim \frac{u - \bar{u}}{\bar{u}^N} , \quad (7.9)$$

where a normalization factor was omitted. For $N = 3$ this state corresponds to the wavefunction defined in (5.51).

Additional examples of the descendent states for $N = 3$ and $N = 4$ will be described later in the next Sections.

7.1 Quantum numbers of the $N = 3$ states

In this section we present the spectrum of q_3 for three reggeized gluons. For the first time such solutions for $\text{Re}[q_3] = 0$ were obtained in [48]. The authors of Ref. [48] used the method of the \hat{q}_3 eigenfunctions described in Chapter 5. Similar quantization condition was also constructed in [51]. Solutions with $\text{Re}[q_3] \neq 0$ were found in [49, 50]. Moreover, in the latter paper the solutions with $n_h \neq 0$ are described.

The first solution using the Baxter Q -operator method was described in Ref. [23]. Later, similar results were also obtained in Ref. [28]. It turns out that the Baxter Q -operator method [23] for $N = 3$ is equivalent to the method of the \hat{q}_3 eigenfunctions described in Chapter 5. For higher $N > 3$ only the Baxter Q -operator method was used to find the quantization values of q_N and the energy.

7.1.1 Lattice structure

Solving the quantization conditions (6.27) for $N = 3$ and for $h = \frac{1+n_h}{2}$, i.e. with $\nu_h = 0$, we reconstruct the full spectrum of q_3 . It is convenient to show the spectrum in terms of $q_3^{1/3}$ rather than q_3 . Since $q_3^{1/3}$ is a multi-valued function of complex q_3 , each eigenstate is represented on the complex $q_3^{1/3}$ -plane by $N = 3$ different points. Thus, the spectrum is symmetric under the transformation

$$q_3^{1/3} \leftrightarrow \exp(2\pi i k/3) q_3^{1/3}, \quad \text{where } 0 < k < 3 . \quad (7.10)$$

Additionally, symmetry (7.4) gives a more regular structure. For the total $SL(2, \mathbb{C})$ spin of the system $h = 1/2$, which means $n_h = 0$ and $\nu_h = 0$, we present the spectrum in Figure

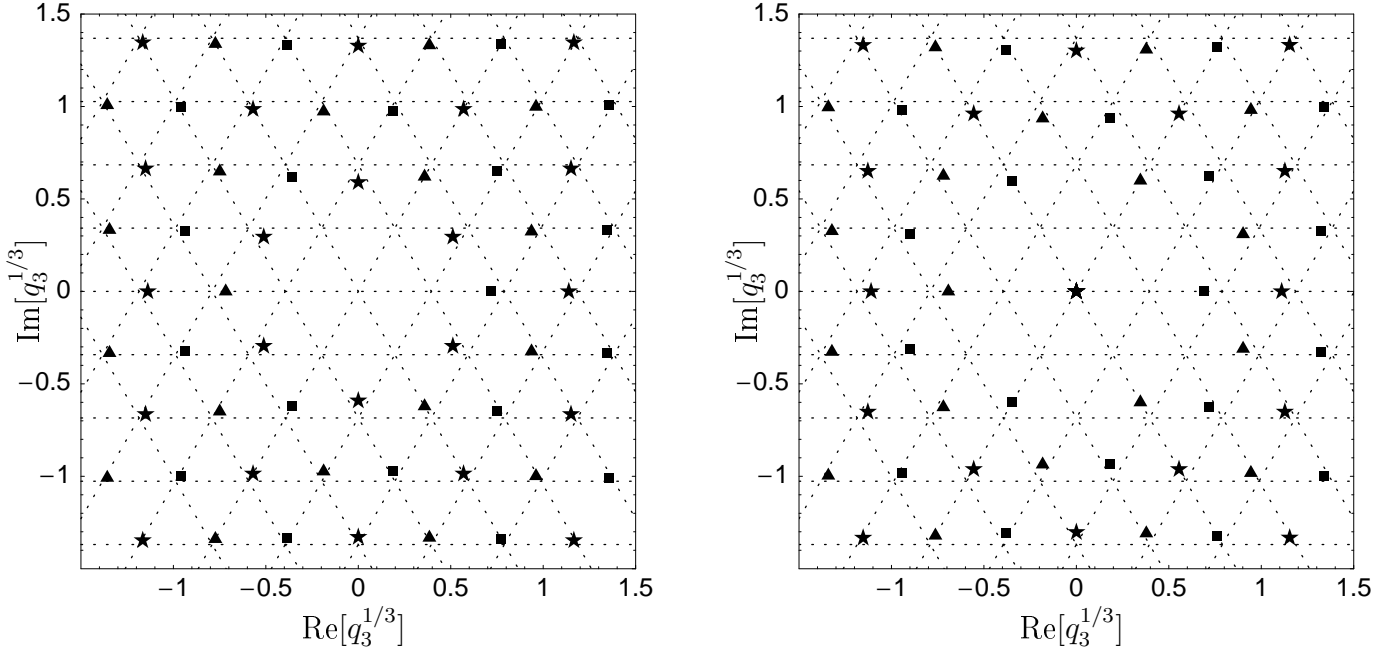


Figure 7.1: The spectrum of quantized $q_3^{1/3}$ for the system of $N = 3$ particles. On the left the total $SL(2, \mathbb{C})$ spin of the system is equal to $h = \frac{1}{2}$, while on the right $h = 1$. Different symbols stand for different quasimomenta θ_3 : *stars* $\theta_3 = 0$ *boxes* $\theta_3 = 4\pi/3$ *triangles* $\theta_3 = 2\pi/3$.

7.1. One can easily notice that the spectrum has the structure close to the equilateral triangle lattice of the leading order WKB approximation (4.21). Indeed, apart from a few points close to the origin, the quantized values of $q_3^{1/3}$ are located almost exactly at the vertices of the WKB lattice. The WKB formula [21] gives

$$[q_3^{\text{WKB}}(\ell_1, \ell_2)]^{1/3} = \Delta_{N=3} \cdot \left(\frac{1}{2}\ell_1 + i\frac{\sqrt{3}}{2}\ell_2 \right), \quad (7.11)$$

where ℓ_1 and ℓ_2 are integers, such that their sum $\ell_1 + \ell_2$ is even. Here the lattice spacing is denoted by

$$\Delta_3 = \left[\frac{3}{4^{1/3}\pi} \int_{-\infty}^1 \frac{dx}{\sqrt{1-x^3}} \right]^{-1} = \frac{\Gamma^3(2/3)}{2\pi} = 0.395175\dots \quad (7.12)$$

The lattice of $q_3^{1/3}$ extends on the whole complex plane except the interior of the disk with the radius Δ_3 :

$$|q_3^{1/3}| > \Delta_3 \quad (7.13)$$

situated at $q_3 = 0$.

In accordance with (7.11), a pair of integers ℓ_1 and ℓ_2 parameterize the quantized values of $q_3^{1/3}$. Going further, one can calculate the quasimomentum as a function of ℓ_1 and ℓ_2 . It has a following form

$$\theta_3(\ell_1, \ell_2) = \frac{2\pi}{3}\ell_1 \pmod{2\pi}. \quad (7.14)$$

Thus, as we can see states with the same value of $\text{Re}[q_3^{1/3}]$ have the same quasimomentum. In Figure 7.1, different quasimomenta are distinguished by *stars*, *boxes* and *triangles*.

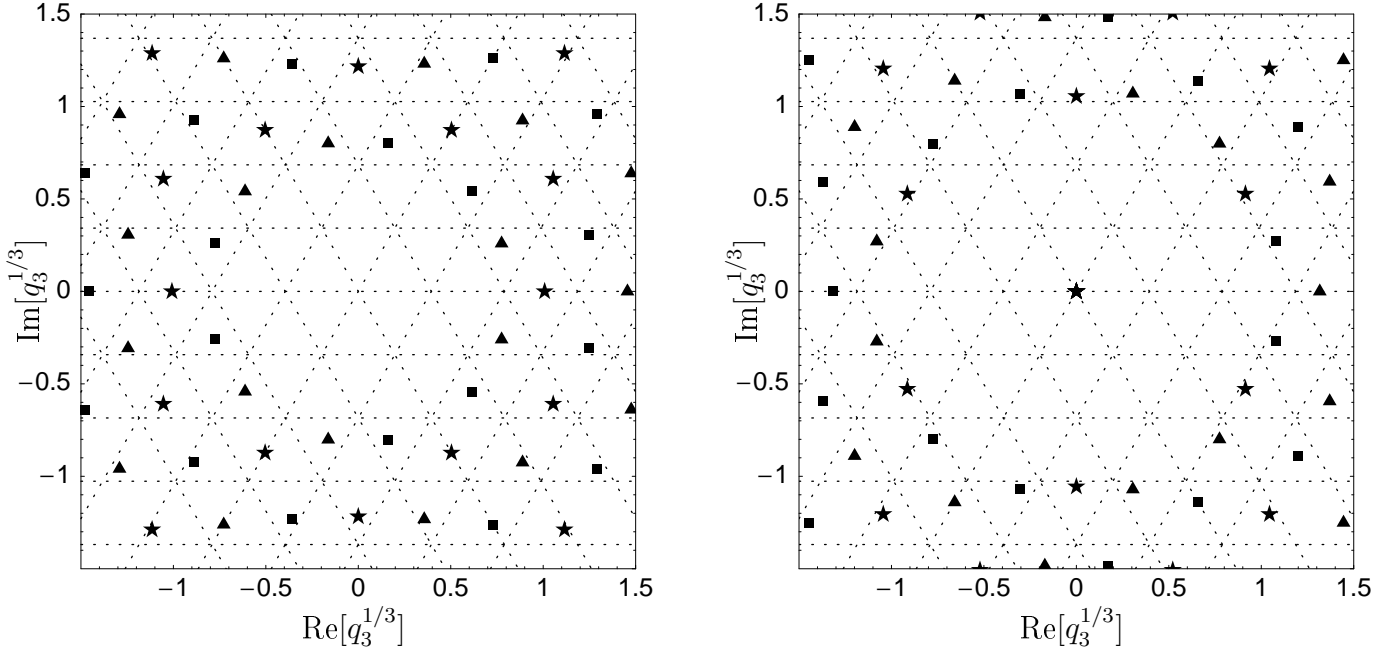


Figure 7.2: The spectrum of quantized $q_3^{1/3}$ for the system of $N = 3$ particles. On the left the total $SL(2, \mathbb{C})$ spin of the system is equal to $h = \frac{3}{2}$, while on the right $h = 2$. Different symbols stand for different quasimomenta θ_3 : *stars* $\theta_3 = 0$ *boxes* $\theta_3 = 4\pi/3$ *triangles* $\theta_3 = 2\pi/3$.

The same lattice structure is exhibited by other spectra with different n_h . However, they have different corrections to the leading order WKB approximation for $q_3^{1/3}$. These spectra are presented in Figures 7.1-7.2. The corrections to the lattice structure depend on q_2 as seen in (4.21). Since the WKB lattice is obtained in the leading order of the expansion for large conformal charges, $1 \ll |q_2^{1/2}| \ll |q_3^{1/3}|$, the corrections are bigger for lower $|q_3^{1/3}|$. Later, we shall discuss some other features of the corrections to the WKB leading order approximation.

As we can see in Figs. 7.1-7.2 for $h \in \mathbb{Z}$ we have additionally trajectories with $q_3 = 0$. They are called the descendent states because their spectra are related to the spectra for the $N - 1 = 2$ Reggeon states. We discuss this point further in next Sections.

7.1.2 Trajectories in ν_h

In the previous Section we considered the dependence of q_3 on n_h for $\nu_h = 0$. However, the spectrum of conformal charges also depends on the continuous parameter ν_h with $h = \frac{1+n_h}{2} + i\nu_h$. It turns out that the spectrum is built of trajectories parameterized by real parameter ν_h . Each trajectory crosses one point (*star*, *box*, *triangle*) in Figs. 7.1-7.2. An example of three trajectories is presented in Figure 7.3. They are numbered by $(\ell_1, \ell_2) = (0, 2)$, $(2, 2)$ and $(4, 2)$ whereas they quasimomentum $\theta_3(\ell_1, \ell_2) = 0, 4\pi/3$ and $2\pi/3$, respectively.

The trajectories cumulate at $\nu_h = 0$. When we increase ν_h , $q_3^{1/3}$ tends to infinity and the structure of quantized charges starts to be less regular, especially for trajectories with lower $|q_3^{1/3}|$. We can see this in Figures 7.4 where we project trajectories with $h = \frac{1}{2} + i\nu_h$ on the $\nu_h = 0$ plane. Here *stars* denote point with $\nu_h = 0$, *boxes* with $\nu_h = 1$ and *circles* $\nu_h = 2$. Grey

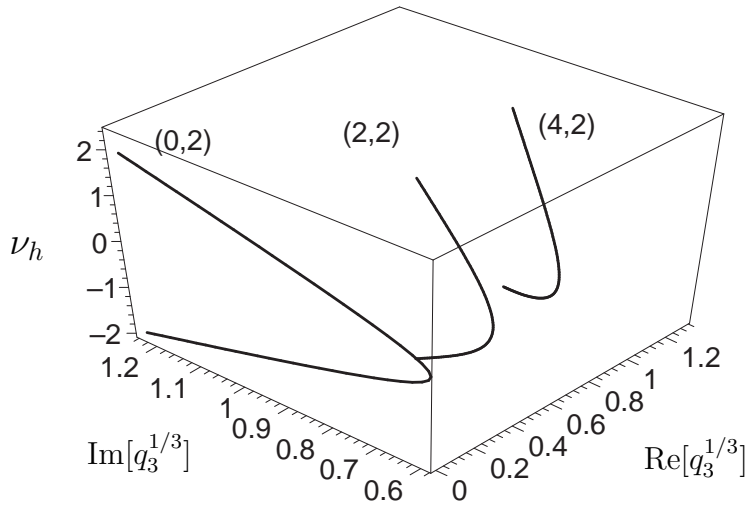


Figure 7.3: The dependence of quantized $q_3(\nu_h; \ell_1, \ell_2)$ on the total spin $h = 1/2 + i\nu_h$. Three curves correspond to the trajectories with $(\ell_1, \ell_2) = (0, 2), (2, 2)$ and $(4, 2)$.

lines are drawn to show the projection of the trajectories for intermediate values of ν_h .

For $n_h \neq 0$ we notice that the spectra start to rotate with ν_h . In Figures 7.4 and 7.5 we present trajectories with positive $n_h = 0, 1, 2, 3$. Due to the symmetry (7.5), which means $h \rightarrow 1 - h^*$ or $n_h \rightarrow -n_h$ with $q_3 \rightarrow q_3^*$, or equivalently, $\nu_h \rightarrow -\nu_h$ but $q_3 \rightarrow q_3$, the spectrum for the negative n_h is the same as for the positive ones but it rotates in the opposite direction with ν_h .

Some of the results presented in this Section were found in earlier works [58, 50]. Trajectories with quasimomentum $\theta_3 = 0$ and $n_h = 0$ were obtained in Refs. [58, 50]. The case for $h = 2 + i\nu_h$ with quasimomentum $\theta_3 = 0$ was discussed in Ref. [50]. In this thesis we additionally analyse the spectra for $h = 1 + i\nu_h$ and $h = 3/2 + i\nu_h$.

7.1.3 Energy and dispersion

For all trajectories in (q_2, q_3) -space we can calculate the energy of the reggeized gluons using Eq. (6.14). Example of the energy spectrum for trajectories from Figure 7.3 with $h = \frac{1}{2} + i\nu_h$ is shown in Figure 7.6.

The energy along the trajectories is a continuous gapless function of ν_h . As we can see the energy E_3 grows with rising $|\nu_h|$. For $n_h = 0$ it has a minimum value $\min_{\nu_h} E_3(\nu_h; \ell_1, \ell_2)$ at $\nu_h = 0$. In the case $n_h \neq 0$, due the bending of the trajectories some minima of the energy are moved away from $\nu_h = 0$ [50]. However, the ground state corresponds to the point(s) on the plane of $q_3^{1/3}$ (see Figure 7.1) closest to the origin. For $N = 3$ the ground state is located on the $(0, 2)$ -trajectory at $\nu_h = 0$ and $n_h = 0$ with quasimomentum equal $\theta_3 = 0$. Due to the symmetry (7.4) it is doubly-degenerated and its conformal charge and energy take the following values:

$$iq_3^{\text{ground}} = \pm 0.20526 \dots, \quad E_3^{\text{ground}} = 0.98868 \dots \quad (7.15)$$

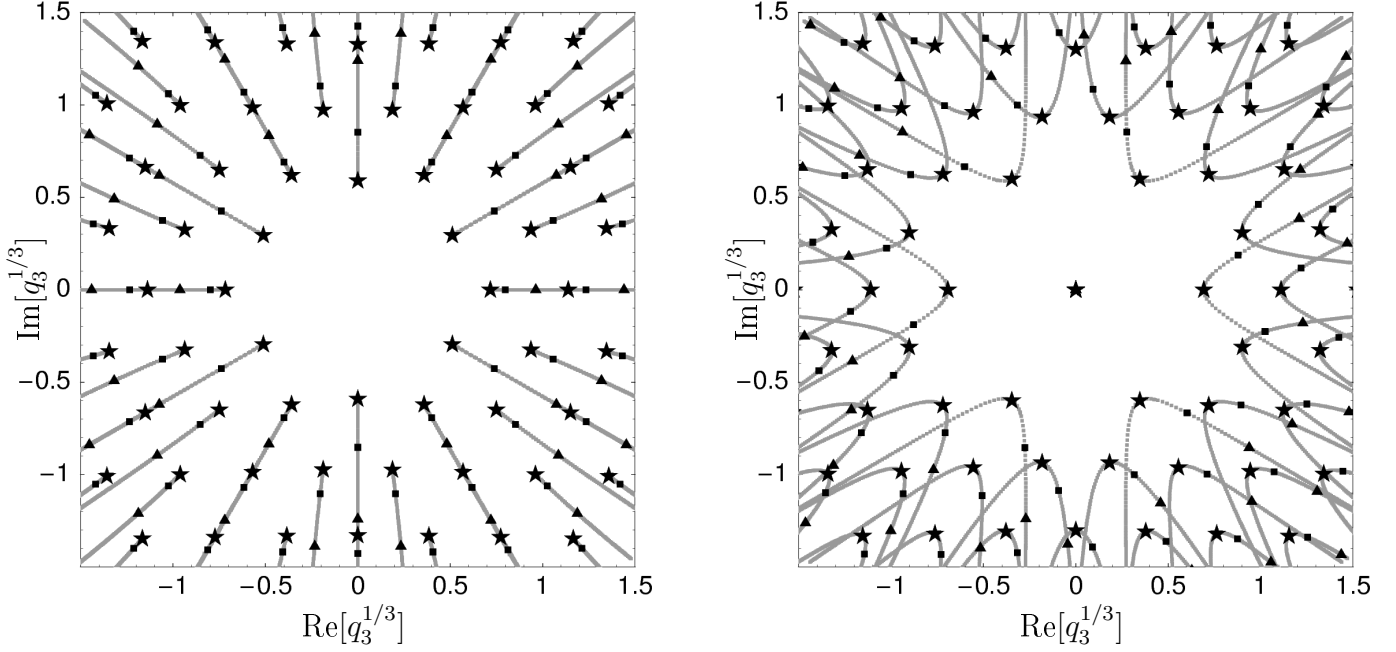


Figure 7.4: The trajectories of $q_3^{1/3}$ projected on $\nu_h = 0$. On the left panel $h = \frac{1}{2} + i\nu_h$, while on the right one $h = 1 + i\nu_h$. *stars* denotes $\nu_h = 0$, *boxes* $\nu_h = 1$ and *triangles* $\nu_h = 2$.

In the vicinity of $\nu_h = 0$ the accumulation of the energy levels is described by the dispersion parameter σ_3 (7.2) given below in the Table 7.5.

We show comparison the WKB result of Eq. (7.11) with the exact expressions for q_3 at $h = 1/2$ in Figure 7.1 and Table 7.1. One can find that the expression (7.11) describes the excited eigenstates with good accuracy. In the case where the eigenstates have smaller q_3 agreement becomes less accurate. Thus, for the ground state with $i q_3 = 0.20526 \dots$ the accuracy of (7.11) is $\sim 20\%$. Obviously, in the region where the WKB expansion is valid, i.e. $|q_3^{1/3}| \gg |q_2^{1/2}|$, Eq. (7.11) can be systematically improved by including subleading WKB corrections.

| (ℓ_1, ℓ_2) | $(q_3^{\text{exact}})^{1/3}$ | $(q_3^{\text{WKB}})^{1/3}$ | $-E_3/4$ |
|--------------------|------------------------------|----------------------------|----------|
| (0, 2) | 0.590 i | 0.684 i | -0.2472 |
| (2, 2) | 0.358 + 0.621 i | 0.395 + 0.684 i | -0.6910 |
| (4, 2) | 0.749 + 0.649 i | 0.790 + 0.684 i | -1.7080 |
| (6, 2) | 1.150 + 0.664 i | 1.186 + 0.684 i | -2.5847 |
| (8, 2) | 1.551 + 0.672 i | 1.581 + 0.684 i | -3.3073 |
| (10, 2) | 1.951 + 0.676 i | 1.976 + 0.684 i | -3.9071 |

Table 7.1: Comparison of the exact spectrum of $q_3^{1/3}$ at $h = 1/2$ with the approximate WKB expression (7.11). The last line defines the corresponding energy $E_3(0; \ell_1, \ell_2)$.

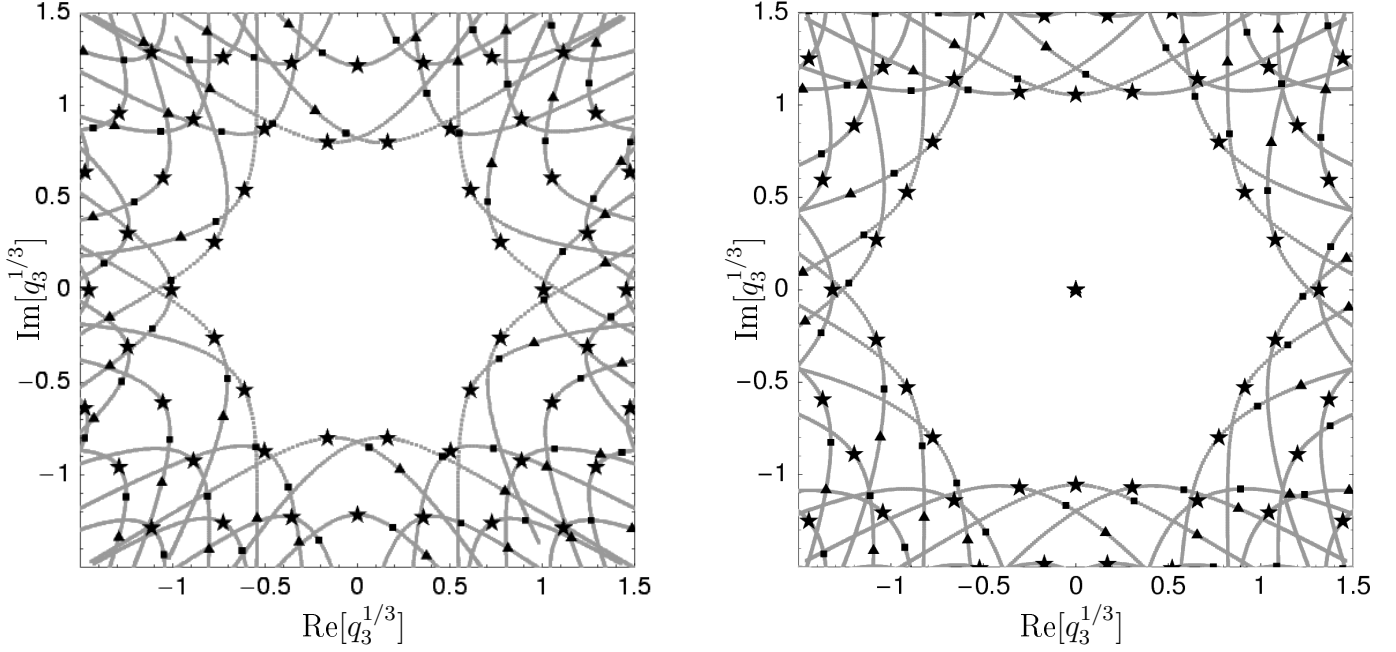


Figure 7.5: The trajectories of $q_3^{1/3}$ projected on $\nu_h = 0$. On the left panel $h = \frac{3}{2} + i\nu_h$, while on the right one $h = 2 + i\nu_h$. *stars* denotes $\nu_h = 0$, *boxes* $\nu_h = 1$ and *triangles* $\nu_h = 2$.

7.1.4 Descendent states for $N = 3$

One also can notice in Figures 7.4 and 7.5 that for odd n_h we have states with $q_3 = 0$. For $n_h = 0$ and $\nu_h = 0$ it has the energy $E_3 = 0$, so it is lower than (7.15). These states are descendants of the states with two Reggeons [51, 53, 54, 55, 23]. We constructed them using the \hat{q}_3 eigenfunction method. The wave-functions of these states are described by (5.44), (5.46), (5.51) and (5.53). These states have the same properties and the energy as the corresponding states with $N - 1 = 2$ particles, $E_3(q_2, q_3 = 0) = E_2(q_2)$, with [15, 16]:

$$E_2(q_2) = 4 \operatorname{Re}[\psi(1 - h) + \psi(h) - 2\psi(1)] = 8 \operatorname{Re} \left[\psi \left(\frac{1 + |n_h|}{2} + i\nu_h \right) - \psi(1) \right], \quad (7.16)$$

where $\psi(x) = \frac{d}{dx} \ln \Gamma(x)$ and $q_2 = -h(h - 1)$. Moreover, their wave-functions are built of the two-Reggeon states [55, 23] and the quasimomentum $\theta_3 = 0$. Contrary to the states with $q_3 \neq 0$, the states with $q_3 = 0$ (5.46) couple to a point-like hadronic impact factors [59, 60, 61], like the one for the $\gamma^* \rightarrow \eta_c$ transition.

7.1.5 Corrections to WKB

The WKB formula for the lattice structure of the conformal charge q_3 was derived in paper [21]. This formula tells us that for $q_3 \rightarrow \infty$

$$q_3^{1/3} = \frac{\Gamma^3(2/3)}{2\pi} \mathcal{Q}(\mathbf{n}) \left[1 + \frac{b}{|\mathcal{Q}(\mathbf{n})|^2} - \left(\frac{b}{|\mathcal{Q}(\mathbf{n})|^2} \right)^2 + \sum_{k=3}^{\infty} a_k \left(\frac{b}{|\mathcal{Q}(\mathbf{n})|^2} \right)^k \right], \quad (7.17)$$

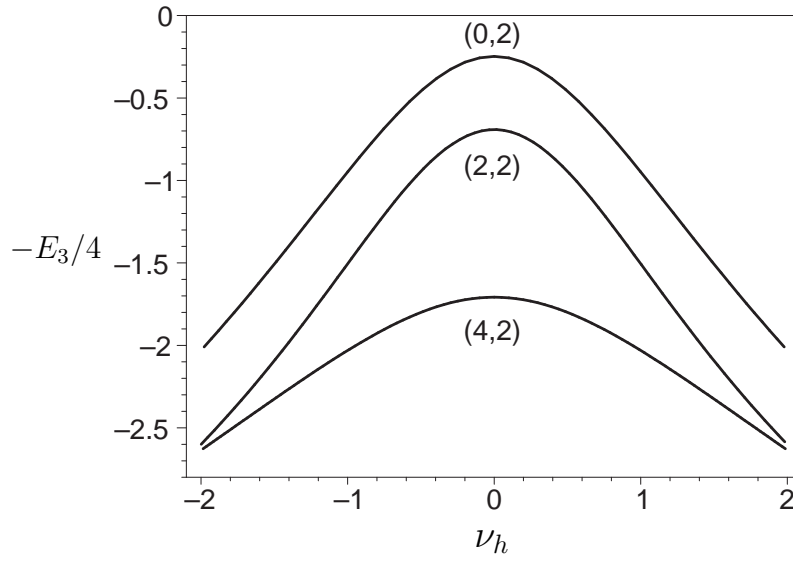


Figure 7.6: The energy spectrum corresponding to three trajectories shown in Figure 7.3. The ground state is located on the $(0, 2)$ –trajectory at $\nu_h = 0$.

where

$$\mathcal{Q}(\mathbf{n}) = \frac{1}{2}(l_1 + l_2) + i\frac{\sqrt{3}}{2}(l_1 - l_2) = \sum_{k=1}^3 n_k e^{i\pi(2k-1)/3} \quad (7.18)$$

and $l_1, l_2, \mathbf{n} = \{n_1, \dots, n_N\}$ are integers, while the coefficient

$$b = \frac{3\sqrt{3}}{2\pi} q_2^*, \quad (7.19)$$

where *star* denotes complex conjugation.

After numerical calculations we have noticed that better agreement with the exact results is obtained for

$$b = \frac{3\sqrt{3}}{2\pi} \left(q_2^* - \frac{2}{3} \right). \quad (7.20)$$

In order to show this, we calculated the values of the conformal charge q_3 for $h = \frac{1+n_h}{2}$ for $n_h = 0, 1, \dots, 19$. We evaluated numerically q_3 with $\text{Im}[q_3] = 0$, i.e. $a_k^{(r)}$, and separately with $\text{Re}[q_3] = 0$, i.e. $a_k^{(i)}$ where the superscript (i) and (r) refers to imaginary and real parts, respectively. Then we fitted expansion coefficients $a_k^{(r,i)}$ for large $|q_3|$ in the range $0 \dots 5000$ with high numerical precision. In order to save space in Table 7.2 we present results only for $n_h = 0, 1, 2$ and 3 .

Coefficients a_k for $k = 0, \dots, 2$ agree with formula (7.17), i.e. $a_0 = 1$, $a_1 = 1$ and $a_2 = -1$, but as we previously mentioned in (7.19) and (7.20), the expansion parameter $b/|\mathcal{Q}(\mathbf{n})|^2$ is different. This difference comes from the fact that the series formula (7.17) with (7.19) is derived in the limit $1 \ll |q_2^{1/2}| \ll |q_3^{1/3}|$. Since in (7.20) the value of q_2^* is much bigger than $2/3$ the value of the parameter b from (7.20) in the above limit goes to (7.19). One may suppose that therefore the factor $2/3$ in Eq. (7.20) as subleading was omitted in the derivation presented in Ref. [21].

| n_h | coef. | $k = 3$ | $k = 4$ | $k = 5$ | $k = 6$ | $k = 7$ |
|-------|-------------------------|-----------------|---------------|-------------|-----------|---------|
| 0 | $a_k^{(r)}$ | 0.509799695633 | -10.065761318 | -76.722084 | -1508.927 | -44580. |
| | $a_k^{(i)}$ | 3.490200304367 | 20.065761318 | 104.722084 | -600.068 | -40411. |
| | $a_k^{(r)} + a_k^{(i)}$ | 4.000000000000 | 10.000000000 | 28.000000 | -2108.995 | -84991. |
| 1 | $a_k^{(r)}$ | -2.585231705744 | -34.383865187 | -209.366287 | -1828.065 | -26404. |
| | $a_k^{(i)}$ | 6.585231705744 | 44.383865187 | 237.366287 | 340.913 | -16641. |
| | $a_k^{(r)} + a_k^{(i)}$ | 4.000000000000 | 10.000000000 | 28.000000 | -1487.152 | -43046. |
| 2 | $a_k^{(r)}$ | 1.336317342408 | 1.2054728742 | -3.08256385 | -31.51219 | -196.87 |
| | $a_k^{(i)}$ | 2.663682657592 | 8.7945271258 | 31.08256385 | 110.89046 | 377.64 |
| | $a_k^{(r)} + a_k^{(i)}$ | 4.000000000000 | 10.000000000 | 28.00000000 | 79.37827 | 180.77 |
| 3 | $a_k^{(r)}$ | 2.250754858908 | 6.7220206127 | 22.76106772 | 79.325249 | 268.13 |
| | $a_k^{(i)}$ | 1.749245141092 | 3.2779793873 | 5.23893228 | -0.430149 | -75.81 |
| | $a_k^{(r)} + a_k^{(i)}$ | 4.000000000000 | 10.000000000 | 28.00000000 | 78.895100 | 192.32 |

Table 7.2: The fitted coefficient to the series formula of $q_3^{1/3}$ (7.17) with $n_h = 0, 1, 2$ and 4

Secondly, we see that the coefficients a_k with $k > 2$ start to depend on n_h . Thus, to describe the behaviour of $q_3^{1/3}$ properly, we have to introduce a second expansion parameter, for example q_2 . We can also notice that for $k > 2$ for a few first coefficients $a_k^{(i)} + a_k^{(r)} \in \mathbb{Z}$ and this sum does not depend on n_h .

Moreover, we can see that after the numerical fitting we obtain two different sets of the expansion coefficient, $\{a_k^{(r)}\}$ and $\{a_k^{(i)}\}$, defined in (7.17), for real and imaginary $q_3^{1/3}$, respectively. Thus, in order to describe full-complex values of $q_3^{1/3}$ in terms of the series (7.17) we have to use both sets of coefficients, one for real and one for imaginary part of $q_3^{1/3}$. Alternatively, we can perform expansion with two small parameters, i.e. $q_2^*/|\mathcal{Q}(\mathbf{n})|^2$ and $1/|\mathcal{Q}(\mathbf{n})|^2$. Since the leading terms, i.e. with a_0 , a_1 and a_2 , for real and imaginary $q_3^{1/3}$ are equal and known analytically, good approximation is obtained using Eq. (7.17) with (7.20) and neglecting higher order terms with $a_{k \geq 3}$.

7.2 Quantum numbers of the $N = 4$ states

In this Section we present the spectrum for four Reggeons. Earlier, some results for $N = 4$ were only presented in [23] and some numerical results in Ref. [28]. Here we show much more data and we present more detailed analysis of this spectrum.

For four Reggeons the spectrum of the conformal charges is much more complicated than in the three-Reggeon case. Indeed we have here the space of three conformal charges (q_2, q_3, q_4) . Thus, apart from the lattice structure in $q_4^{1/4}$ we have also respective lattice structures in q_3 -space. Here we consider the case for $n_h = 0$ so that $h = \frac{1}{2} + i\nu_h$. This spectrum includes the

ground states. For clarity we split these spectra into several parts. We perform this separation by considering spectra with different quasimomenta $\theta_4(q, \bar{q})$ as well as a different quantum number ℓ_3 , which will be defined in the solution (7.22)–(7.23) of two quantization conditions (4.18) for $N = 4$ from Ref. [21].

From the first quantization condition (4.18) one can get the WKB approximation of the charge q_4 as

$$q_4^{1/4} = \frac{\Gamma^2(3/4)}{4\sqrt{\pi}} \left[\frac{1}{\sqrt{2}}\ell_1 + \frac{i}{\sqrt{2}}\ell_2 \right] \quad (7.21)$$

and the quasimomentum is equal to

$$\theta_4 = -\frac{\pi}{2}\ell = \frac{\pi}{2}(\ell_2 + \ell_3 - \ell_1) \pmod{2\pi}, \quad (7.22)$$

where ℓ_1, ℓ_2 and ℓ_3 are even for even ℓ and odd for odd ℓ . Thus, we have two kinds of lattices: with $\theta_4 = 0, \pi$ and with $\theta_4 = \pm\pi/2$. They are presented in Fig. 7.7. In these pictures gray lines show the WKB lattice (7.21) with vertices at $\ell_1, \ell_2 \in \mathbb{Z}$. To find the leading approximation for the charge q_3 , we apply the second relation in (4.18) with $m = 2$ which gives

$$\text{Im} \frac{q_3}{q_4^{1/2}} = (\ell_1 - \ell_2 - \ell) = \ell_3. \quad (7.23)$$

Notice that the system (7.21) and (7.23) is underdetermined and it does not fix the charge q_3 completely [21].

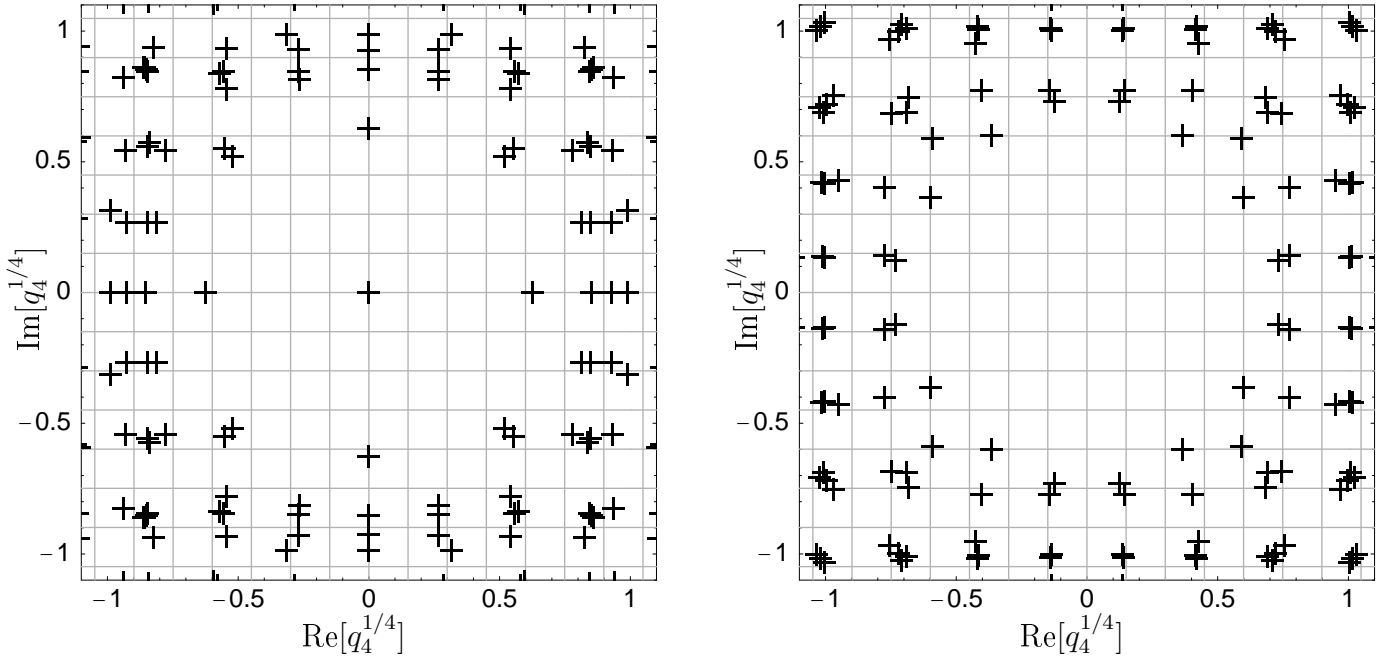


Figure 7.7: The spectrum of the integrals of motion q_4 for $N = 4$ and the total spin $h = 1/2$. The left and right panels correspond to the eigenstates with different quasimomenta $e^{i\theta_4} = \pm 1$ and $\pm i$, respectively.

It turns out that after choosing one value of θ_4 , the lattice in $q_4^{1/4}$ -space is still spuriously degenerated¹ and this degeneration also corresponds to different lattices in $q_3^{1/2}$. The parameter ℓ_3 which is defined in (7.23) will be used to distinguish these different lattices.

¹degeneration in the leading order of the WKB approximation

7.2.1 Descendent states for $N = 4$

One can notice that for $N = 4$ and $n_h = 0$ we have the descendent states. They appear in sector with the quasimomentum $\theta_4 = \pi$, which agree with (7.7). The wave-functions of the descendent states are built of three-particle eigenstates with $\theta_3 = 0$. These three-Reggeon states correspond to the lattice depicted by stars in Fig. 7.1. On the other hand, the lattice for the descendent state for $N = 4$ is presented in Fig. 7.8 on the left panel. Thus, one can compare the both lattices and notice that they are exactly the same. Moreover, the energy of these descendent state and the corresponding three-Reggeon states are also the same (7.6).

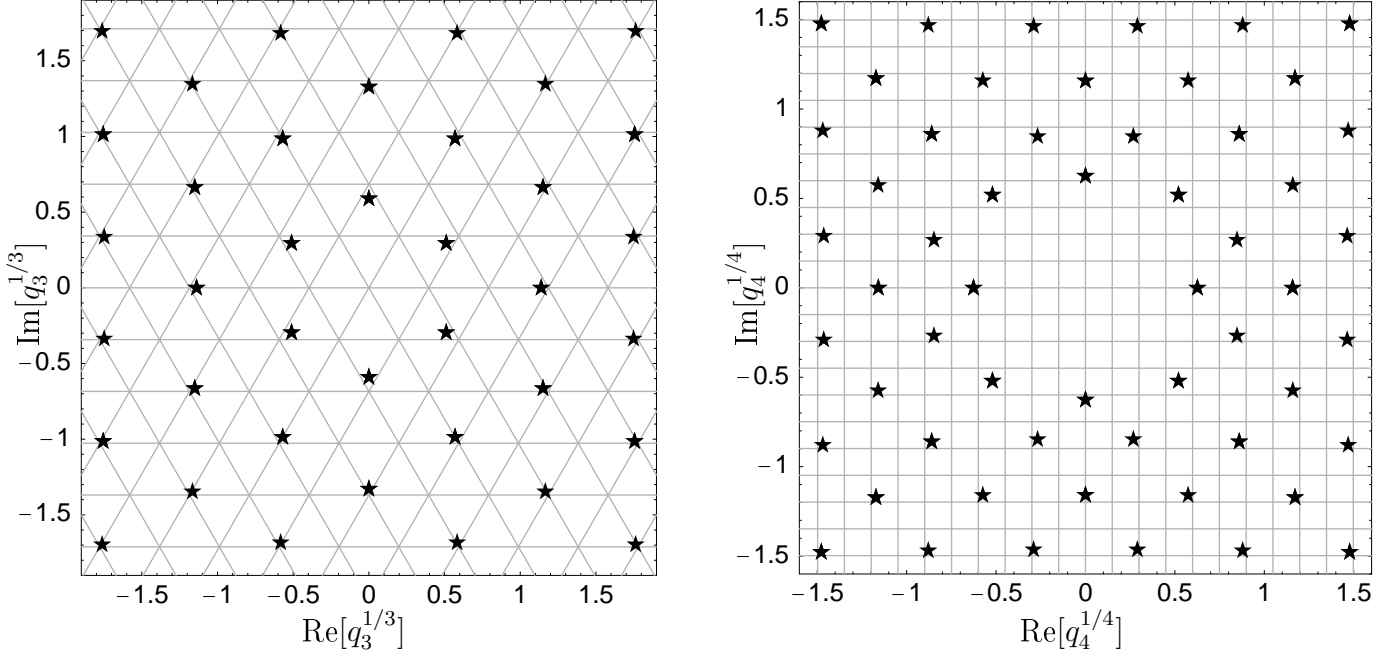


Figure 7.8: The spectra of the conformal charges for $N = 4$ and comparison to the WKB expansion. On the left panel, the spectrum of q_3 with $q_4 = 0$ corresponding to the descendent states with $\theta_4 = \pi$. On the right panel, the spectrum of q_4 for $h = 1/2$ and $q_3 = 0$ with $\theta_4 = 0$. The WKB lattices are denoted by the grey lines.

7.2.2 Lattice structure for $q_3 = 0$

Let us consider the spectrum with $q_4 \neq 0$ and $q_3 = 0$, see the right panel of Fig 7.8. In this case the quasimomentum $\theta_4 = 0$ and the lattice structure include vertices that correspond to the ground state.

Similarly to the $N = 3$ case we have in the $q_4^{1/4}$ -space a lattice with a square-like structure described by (7.21). In this case even numbers ℓ_1 and ℓ_2 satisfy $\ell_1 + \ell_2 \in 4\mathbb{Z}$. Thus, we have the WKB formula

$$[q_4^{\text{WKB}}(\ell_1, \ell_2)]^{1/4} = \Delta_{N=4} \cdot \left(\frac{\ell_1}{2\sqrt{2}} + i \frac{\ell_2}{2\sqrt{2}} \right), \quad (7.24)$$

where the vertices are placed outside a disk around the origin of the radius

$$\Delta_4 = \left[\frac{4^{3/4}}{\pi} \int_{-1}^1 \frac{dx}{\sqrt{1-x^4}} \right]^{-1} = \frac{\Gamma^2(3/4)}{2\sqrt{\pi}} = 0.423606 \dots \quad (7.25)$$

As before, the leading-order WKB formula (7.24) is valid only for $|q_4^{1/4}| \gg |q_2^{1/2}|$.

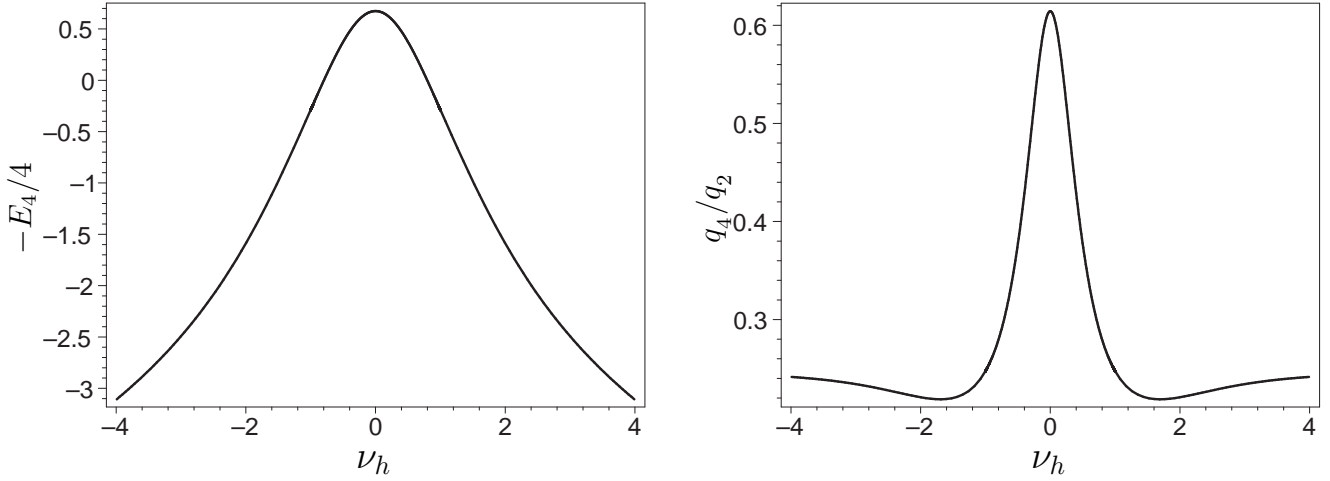


Figure 7.9: The dependence of the energy, $-E_4/4$, and the quantum number, q_4/q_2 , with $q_2 = 1/4 + \nu_h^2$, on the total spin $h = 1/2 + i\nu_h$ along the ground state trajectory for $N = 4$.

The energy is lower for points which are nearer to the origin. Similarly to the $N = 3$ case, the spectrum is also built of trajectories which extend in the (ν_h, q_3, q_4) -space. Namely, each point on the $q_4^{1/4}$ -lattice belongs to one specific trajectory parameterized by the set of integers $\{\ell_1, \ell_2, \dots\}$.

The ground state for $N = 4$ is situated on a trajectory with $(\ell_1, \ell_2) = (4, 0)$. We find that for this trajectory $q_3 = \text{Im } q_4 = 0$, whereas $\text{Re}[q_4]$ and E_4 vary with ν_h as we show in Figure 7.9. An accumulation of the energy levels in the vicinity of $\nu_h = 0$ is described by Eq. (7.2) with the dispersion parameter σ_4 given below in Table 7.5.

On the $q_4^{1/4}$ -plane the ground state is represented by four points with the coordinates $(\ell_1, \ell_2) = (\pm 4, 0)$ and $(0, \pm 4)$. Due to a residual symmetry $q_4^{1/4} \leftrightarrow \exp(ik\pi/2)q_4^{1/4}$, they describe a single eigenstate with

$$q_3^{\text{ground}} = 0, \quad q_4^{\text{ground}} = 0.153589\dots, \quad E_4^{\text{ground}} = -2.696640\dots \quad (7.26)$$

with $h = 1/2$. It has the quasimomentum $\theta_4 = 0$ and, in contrast to the $N = 3$ case, it is unique.

The comparison of (7.24) with the exact results for q_4 at $h = 1/2$ is shown in Figure 7.8 and Table 7.3. One can see that the WKB formula (7.24) describes the spectrum with a good accuracy.

7.2.3 Resemblant lattices with $\ell_3 = 0$

In the previous Section we introduced the parameter ℓ_3 which helps us to distinguish different lattices. This parameter takes even values for $\theta_4 = 0, \pi$ and odd ones for $\theta_4 = \pm\pi/2$. Let us take $\ell_3 = 0$. It turns out that in this case the spectrum lattice in the $q_3^{1/2}$ -space is similar

| $(\ell_1/2, \ell_2/2)$ | $(q_4^{\text{exact}})^{1/4}$ | $(q_4^{\text{WKB}})^{1/4}$ | $-E_4/4$ |
|------------------------|------------------------------|----------------------------|----------|
| (2, 0) | 0.626 | 0.599 | 0.6742 |
| (2, 2) | $0.520 + 0.520 i$ | $0.599 + 0.599 i$ | -1.3783 |
| (3, 1) | $0.847 + 0.268 i$ | $0.899 + 0.299 i$ | -1.7919 |
| (4, 0) | 1.158 | 1.198 | -2.8356 |
| (3, 3) | $0.860 + 0.860 i$ | $0.899 + 0.899 i$ | -3.1410 |
| (4, 2) | $1.159 + 0.574 i$ | $1.198 + 0.599 i$ | -3.3487 |

Table 7.3: Comparison of the exact spectrum of $q_4^{1/4}$ at $q_3 = 0$ and $h = 1/2$ with the approximate WKB expression 7.24. The last column shows the exact energy E_4 .

to the corresponding lattice in the $q_4^{1/4}$ -space, i.e. considering only the leading order of the WKB approximation the $q_3^{1/2}$ -lattice in comparison to the $q_4^{1/4}$ -lattice is rescaled by some real number. An example of such a lattice for $\theta_4 = 0$ is shown in Figure 7.10. One can notice that the non-leading corrections to the WKB approximation cause the bending of the lattice structure in Fig. 7.10: for $q_4^{1/4}$ concave whereas for $q_3^{1/2}$ convex. Moreover, we can see the $q_4^{1/4}$ -lattice as well as $q_3^{1/2}$ -one have a similar structure to the lattice with $q_3 = 0$ presented in Fig. 7.8. These lattices also do not have the vertices inside the disk at the origin $q_3 = q_4 = 0$.

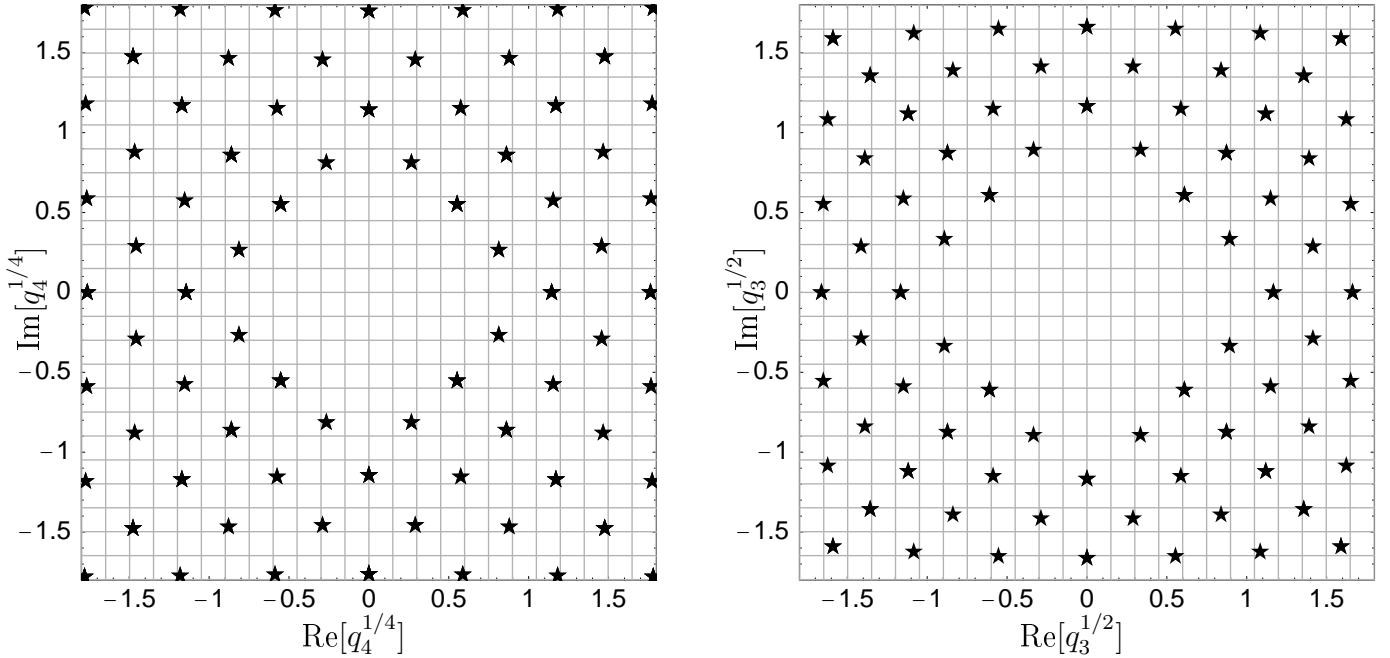


Figure 7.10: The spectra of the conformal charges for $N = 4$ with $\theta_4 = 0$, $\ell_3 = 0$ and $\ell_4 = 1$. On the left panel the spectrum of $q_4^{1/4}$, while on the right panel the spectrum of $q_3^{1/2}$.

Substituting

$$q_3^{1/2} = r_3 e^{i\phi_3} \quad \text{and} \quad q_4^{1/4} = r_4 e^{i\phi_4} \quad (7.27)$$

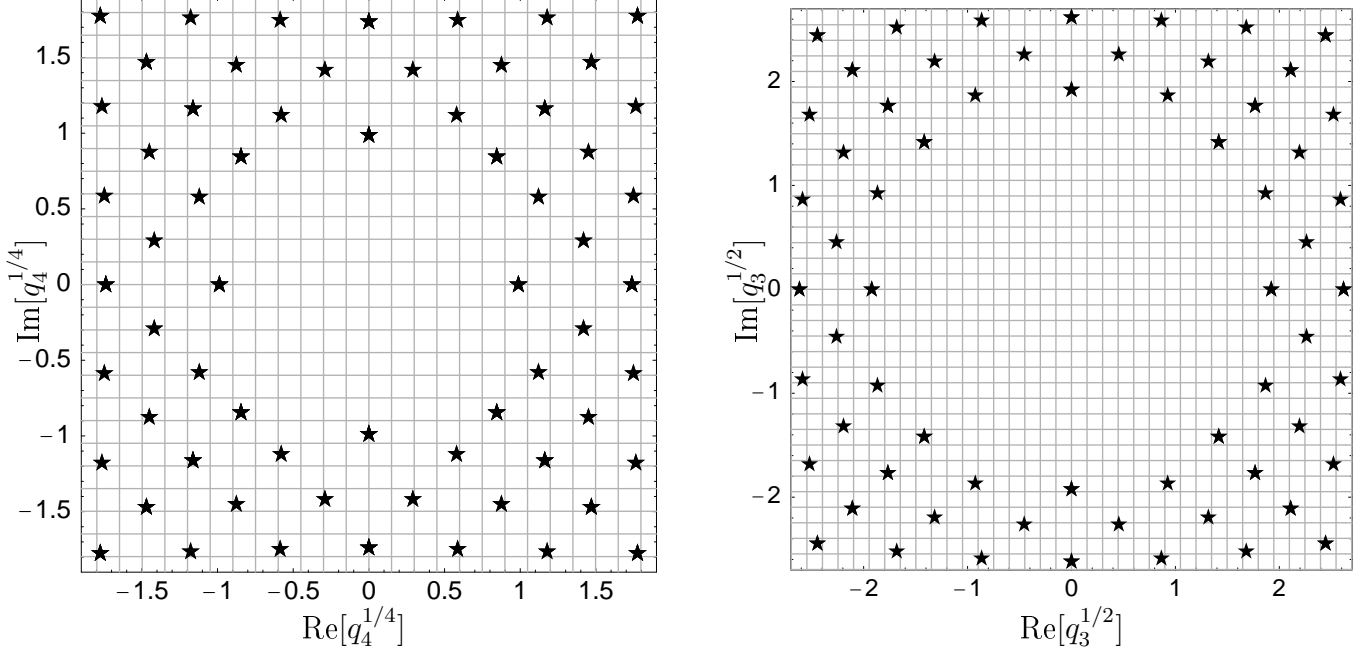


Figure 7.11: The spectra of the conformal charges for $N = 4$ with $\theta_4 = 0$, $\ell_3 = 0$ and $\ell_4 = 2$. On the left panel the spectrum of $q_4^{1/4}$, while on the right panel the spectrum of $q_3^{1/2}$

into (7.23) we obtain a condition for the leading order of the WKB approximation

$$\ell_3 = \left(\frac{r_3}{r_4} \right)^2 \sin(2(\phi_3 - \phi_4)). \quad (7.28)$$

Thus, for $\ell_3 = 0$ and for a scale $\lambda = r_3/r_4 > 0$ we have $\phi_3 = \phi_4$. This means that the vertices on the $q_3^{1/2}$ -lattice have the same angular coordinates as those from the $q_4^{1/4}$ -lattice. Looking at the numerical results in Figure 7.10 we notice that the missing quantization condition for $\ell_3 = 0$ in the leading WKB order should have a form similar to

$$\text{Re} \frac{q_3}{q_4^{1/2}} = \lambda_{\ell_4}^2, \quad (7.29)$$

where $\lambda_{\ell_4} = r_3/r_4 \in \mathbb{R}$ is a constant scale for a given lattice ℓ_4 .

It turns out that for a specified quasimomentum we have an infinite number of such lattices. They differ from each other by a given scale λ_{ℓ_4} . For example for $\theta_4 = 0$ we have another lattice, shown in Fig 7.11. Its scale λ_2 differs from the scale λ_1 of the lattice from Fig. 7.10. The resemblant $q_4^{1/4}$ -lattices for $\theta_4 = 0$ are described by (7.21) with the integer parameters ℓ_1 and ℓ_2 satisfying $\ell_1 + \ell_2 \in 4\mathbb{Z}$.

The similar lattices also exist in the sector with the quasimomentum $\theta_4 = \pi$. Some of them are presented in Figures 7.12 and 7.13. For $\theta_4 = \pi$ the resemblant $q_4^{1/4}$ -lattices are also described by (7.21) but the integer parameters ℓ_1 and ℓ_2 satisfy $\ell_1 + \ell_2 \in 4\mathbb{Z} + 2$.

7.2.4 Winding lattices with $\ell_3 \neq 0$

In the case with $\ell_3 \neq 0$ we have much more complicated situation than for $\ell_3 = 0$. According to (7.28) the angles ϕ_3 and ϕ_4 defined in (7.27) are no more equal. Moreover, they start to

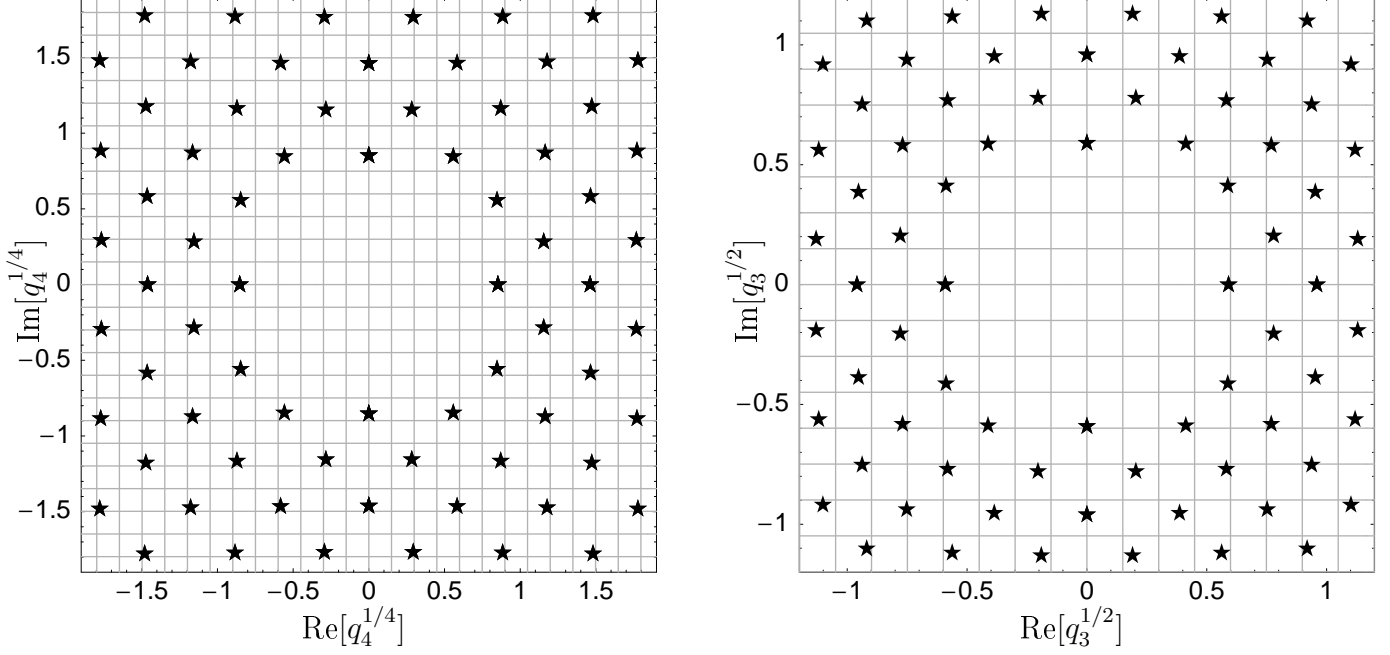


Figure 7.12: The spectra of the conformal charges for $N = 4$ with $\theta_4 = \pi$, $\ell_3 = 0$ and $\ell_4 = 1$. On the left panel the spectrum of $q_4^{1/4}$, while on the right panel the spectrum of $q_3^{1/2}$

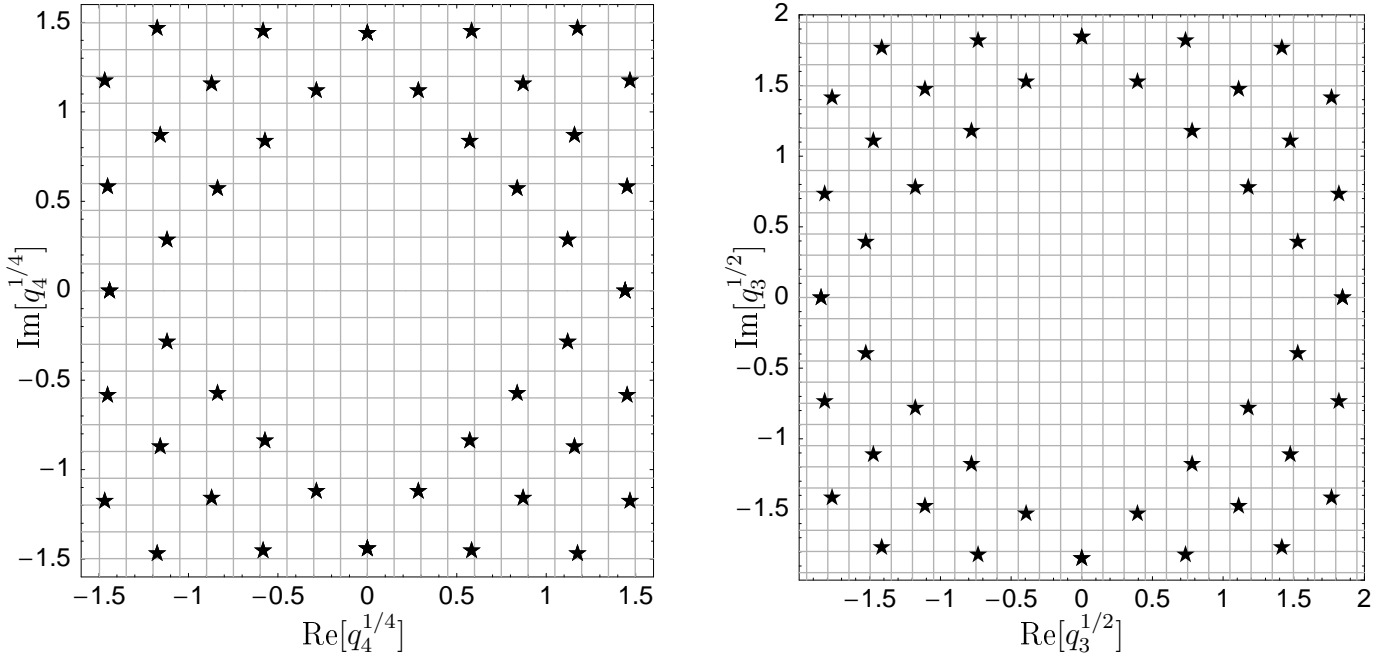


Figure 7.13: The spectra of the conformal charges for $N = 4$ with $\theta_4 = \pi$, $\ell_3 = 0$ and $\ell_4 = 2$. On the left panel the spectrum of $q_4^{1/4}$, while on the right panel the spectrum of $q_3^{1/2}$

depend on the scale $\lambda = r_3/r_4$.

An example of such a lattice, with $\ell_3 = 1$ and $\theta_4 = -\pi/2$ we show in Figure 7.14. For this case, the $q_4^{1/4}$ -lattice is defined by (7.21) with ℓ_1 and ℓ_2 odd integer numbers satisfying $\ell_1 + \ell_2 \in 4\mathbb{Z}$. In Figure 7.14, in order to present the correspondence between the $q_3^{1/2}$ - and $q_4^{1/4}$ -lattice, we depict only some vertices of the lattice which extends in the whole plane of the conformal charges except the place nearby the origin $q_4 = q_3 = 0$. As we can see the $q_3^{1/2}$ -lattice is still a square-like one but it winds around the origin $q_3^{1/2} = 0$. Looking at Figure

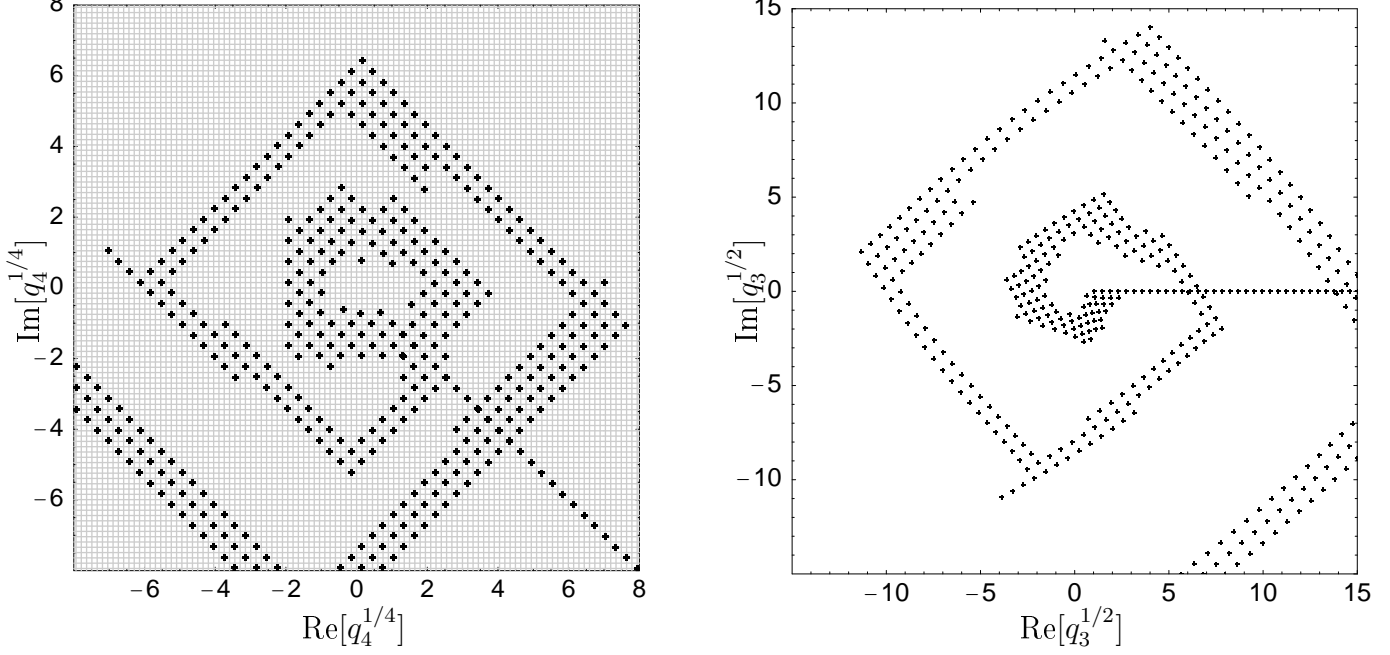


Figure 7.14: The winding spectrum of the conformal charges for $N = 4$ and $h = 1/2$ with $\theta_4 = -\pi/2$ and $\ell_3 = 1$. On the left panel the spectrum of $q_4^{1/4}$, while on the right panel the spectrum of $q_3^{1/2}$

7.14, let us start from $\phi_3 = 0$ and $\phi_4 = -\pi/4$ where ϕ_3 and ϕ_4 are defined in (7.27). Thus, the difference $\phi_3 - \phi_4 = \pi/4$ so that our scale at the beginning is $\lambda = \sqrt{2}$. In this region the vertices of the $q_3^{1/2}$ -lattice are in the nearest place to the origin. When we go clockwise around the origin of the lattices by decreasing ϕ_4 , we notice that ϕ_3 also decreases but much slower. Thus, according to (7.28) the difference $\phi_3 - \phi_4$ changes. Moreover, due to (7.28), the scale λ also continuously rises. Therefore, the $q_3^{1/2}$ -lattice winds in a different way than the $q_4^{1/4}$ -lattice. After one revolution the vertices of the $q_4^{1/4}$ -lattices are at similar places as those with ϕ_4 decreased by 2π . This provides additional spurious degeneration in $q_4^{1/4}$. However, after revolution by the angle 2π , the vertices in $q_3^{1/2}$ -space have completely different conformal charges q_3 . The spurious degeneration in the $q_3^{1/2}$ -lattice does not appear.

We have to add that we obtain the second symmetric structure when we go in the opposite direction, i.e. anti-clockwise. Moreover, the winding lattice, like all other lattices, extends to infinity on the $q_3^{1/2}$ - and $q_4^{1/4}$ -plane and does not have vertices in vicinity of the origin, $q_3 = q_4 = 0$. However, the radii of these empty spaces grow with $\phi_{3,4}$.

Additionally, due to symmetry of the spectrum (7.5) we have a twin lattice with $q_k \rightarrow q_k^*$. Furthermore, the second symmetry (7.4) produces another lattice rotated in the $q_3^{1/2}$ -space by an angle $\pi/2$. Notice that this symmetry (7.4) exchanges quasimomentum $\theta_4 \leftrightarrow 2\pi - \theta_4 \pmod{2\pi}$. Thus, the spectrum for $\theta_4 = \pi/2$ is congruent with the spectrum of $\theta_4 = -\pi/2$ but it is rotated in the $q_3^{1/2}$ -space by $\pi/2$.

As we said before for $\theta_4 \pm \pi/2$ we have winding spectra with odd ℓ_3 . Similarly, for even $\ell_3 \neq 0$ we have winding spectra with $\theta_4 = 0, \pi$, thus, the lattice with the lowest non-zero ℓ_3 corresponds to $|\ell_3| = 2$. We present some points of this spectrum in Fig. 7.15, for which ℓ_1, ℓ_2

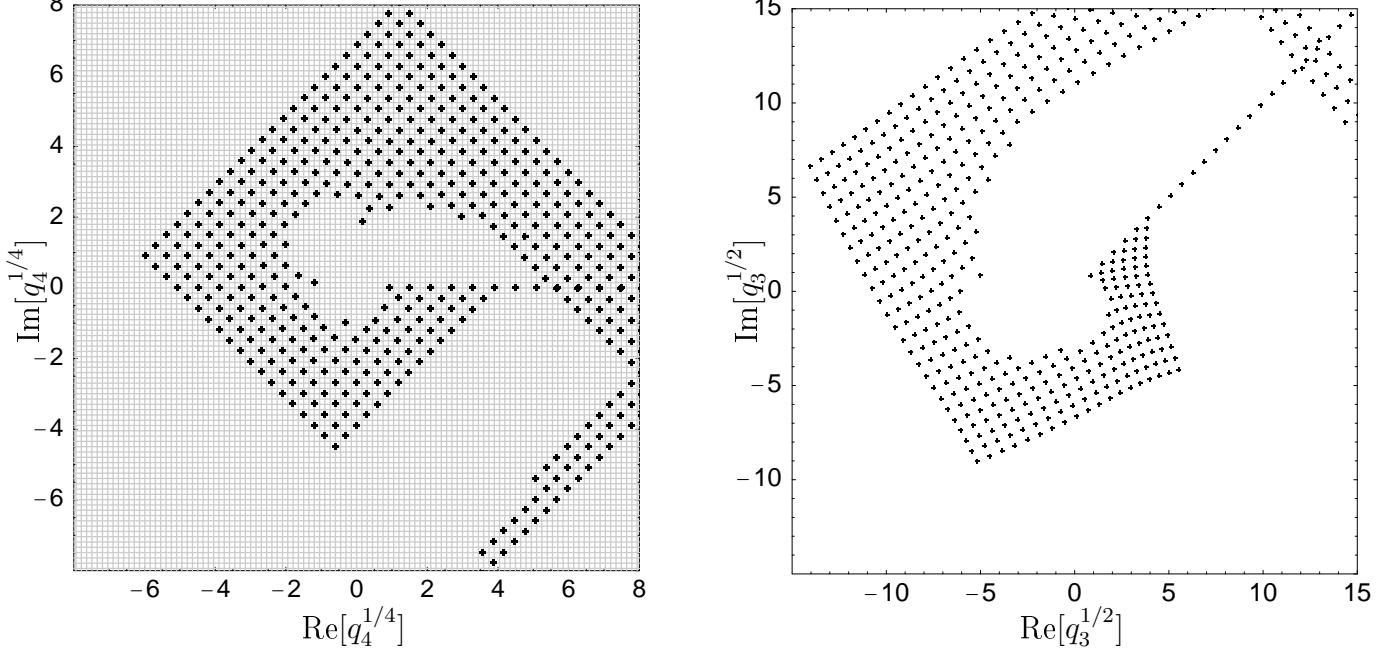


Figure 7.15: The winding spectrum of the conformal charges for $N = 4$ with $h = 1/2$, $\theta_4 = 0$ and $\ell_3 = 2$. On the left panel the spectrum of $q_4^{1/4}$ while on the right panel the spectrum of $q_3^{1/2}$

in (7.21) are even and $\ell_1 + \ell_2 \in 4\mathbb{Z} + 2$. In this case we start with $\phi_3 = \pi/4$ and $\phi_4 = 0$ which implies the beginning scale $\lambda = \sqrt{2}$. The spectra wind as in the previous case.

Similarly, for $\theta_4 = \pi$ we have also spectrum with the lowest $|\ell_3| = 2$. It is defined by (7.21) with ℓ_1, ℓ_2 even and $\ell_1 + \ell_2 \in 4\mathbb{Z}$. In this case the angles $\phi_3 = 0$ and $\phi_4 = -\pi/4$ so we also have the beginning scale $\lambda = \sqrt{2}$, as depicted in Figure 7.16. In order to describe the winding spectra better we may introduce an integer parameter ℓ_4 which helps us to number the overlapping winding planes of the spectra and name spuriously-degenerated vertices in the $q_4^{1/4}$ -plane.

To sum up, even for a given quasimomentum we have many lattices which overlap, so that vertices of the lattices, especially in $q_3^{1/2}$ -space, make an impression of being randomly distributed. However, as we have shown above, those spectra may be distinguished and finally described by (7.21) and (7.23). Still, there is a lack of one nontrivial WKB condition which would uniquely explain the structure of the resemblant and winding lattices.

7.2.5 Corrections to WKB

Let us consider the spectrum of the conformal charge q_4 for $N = 4$ with $q_3 = 0$ and $h = \frac{1+n_h}{2}$. It turns out that for $n_h \neq 0$ it has similar square-like lattice structure like that with $n_h = 0$, see Fig. 7.8 on the right panel. Similarly to the case with three reggeized gluons we have evaluated the conformal charges q_4 with even n_h with high precision. We have done it separately for q_4 with $\text{Im}[q_4] = 0$ and $\text{Re}[q_4] = 0$. Next, we have fitted coefficient expansion of the WKB series, $a_k^{(r)}$ and $a_k^{(i)}$, respectively.

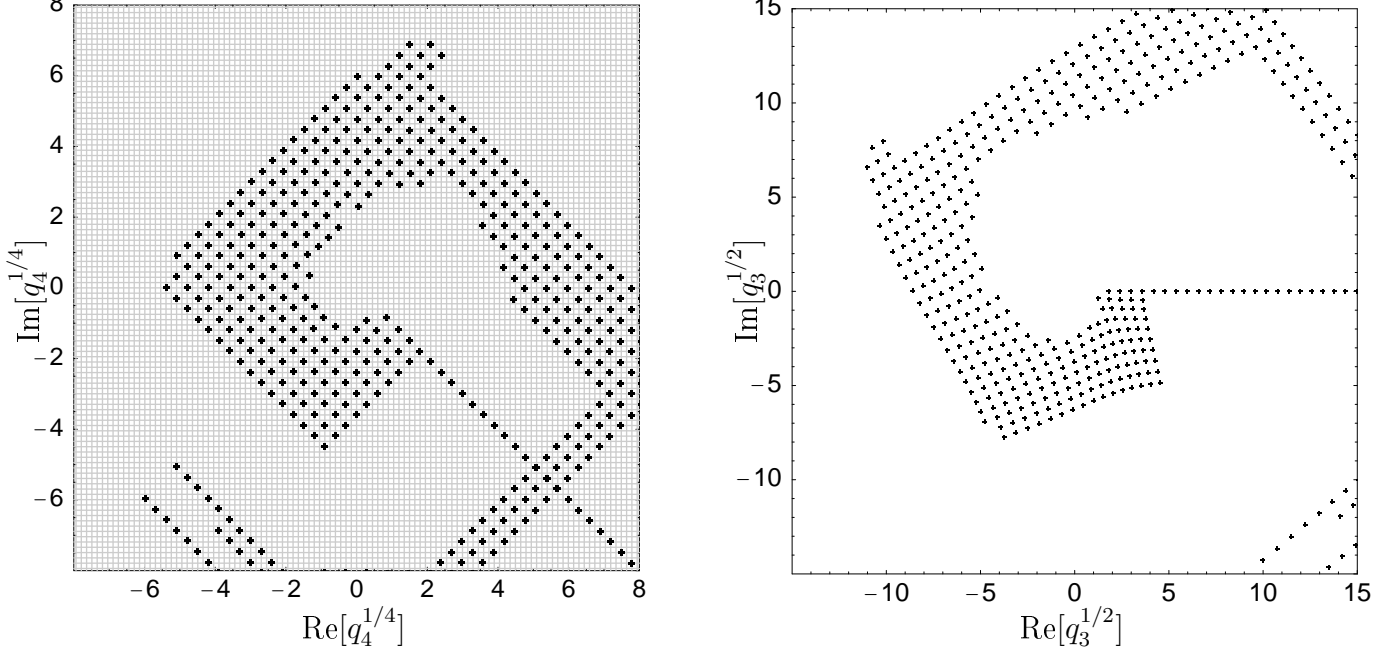


Figure 7.16: The winding spectrum of the conformal charges for $N = 4$ with $h = 1/2$, $\theta_4 = \pi$ and $\ell_3 = 2$. On the left panel the spectrum of $q_4^{1/4}$ while on the right panel the spectrum of $q_3^{1/2}$

In [21] the series formula for $q_4^{1/4}$ looks as follows

$$q_4^{1/4} = \frac{\pi^{3/2}}{2\Gamma^2(1/4)} \mathcal{Q}(\mathbf{n}) \left[1 + \frac{b}{|\mathcal{Q}(\mathbf{n})|^2} + \sum_{k=2}^{\infty} a_k \left(\frac{b}{|\mathcal{Q}(\mathbf{n})|^2} \right)^k \right], \quad (7.30)$$

where

$$\mathcal{Q}(\mathbf{n}) = \sum_{k=1}^4 n_k e^{i\pi(2k-1)/4} = \left(\frac{\ell_1}{\sqrt{2}} + i \frac{\ell_2}{\sqrt{2}} \right) \quad (7.31)$$

and ℓ_1, ℓ_2 , $\mathbf{n} = \{n_1, \dots, n_N\}$ are integer.

Here for $N = 4$, similarly to the $N = 3$ case (7.20), we have a different expansion parameter $b/|\mathcal{Q}(\mathbf{n})|^2$ and in this case the parameter

$$b = \frac{4}{\pi} \left(q_2^* - \frac{5}{4} \right) \quad (7.32)$$

is decreased by $5/4$. The expansion coefficients of the series (7.30) are shown in Table 7.4. Similarly to [21] the coefficients $a_0 = 1$ and $a_1 = 1$. The remaining coefficients depend on n_h . Moreover, the coefficients a_k with $k > 1$ are different for real $q_4^{1/4}$ and for imaginary $q_4^{1/4}$ but one may notice that for $k = 1, 2$ the sum $a_k^{(r)} + a_k^{(i)} \in \mathbb{Z}$ and does not depend on n_h . Thus, to describe the quantized values of $q_4^{1/4}$ more generally one has to use both sets of the coefficients, $a_k^{(r)}$ and $a_k^{(i)}$, or perform the expansion with two small independent parameters, i.e. $q_2^*/|\mathcal{Q}(\mathbf{n})|^2$ and $1/|\mathcal{Q}(\mathbf{n})|^2$.

Using the series (7.30) with (7.32) and coefficients from Table 7.4 gives good approximation of the conformal charges q_4 with $q_3 = 0$. However, if someone wants to have a better precision one has to introduce an additional expansion parameter.

| n_h | coef. | $k = 2$ | $k = 3$ | $k = 4$ | $k = 5$ |
|-------|-------------------------|---------------|------------|----------|---------|
| 0 | $a_k^{(r)}$ | 2.9910566246 | -24.021689 | 91.591 | 645.5 |
| | $a_k^{(i)}$ | -4.9910566246 | 28.021689 | -148.830 | 1656.7 |
| | $a_k^{(r)} + a_k^{(i)}$ | -2.0000000000 | 4.000000 | -57.239 | 2302.2 |
| 2 | $a_k^{(r)}$ | -1.3991056625 | 4.674008 | -4.516 | -95.7 |
| | $a_k^{(i)}$ | -0.6008943375 | -0.674008 | 20.388 | -200.8 |
| | $a_k^{(r)} + a_k^{(i)}$ | -2.0000000000 | 4.000000 | 15.872 | -296.5 |
| 4 | $a_k^{(r)}$ | -1.351212983 | 3.462323 | -11.322 | 43.164 |
| | $a_k^{(i)}$ | -0.648787017 | 0.537677 | -0.096 | 0.611 |
| | $a_k^{(r)} + a_k^{(i)}$ | -2.0000000000 | 4.000000 | -11.418 | 43.775 |
| 6 | $a_k^{(r)}$ | -0.8882504145 | 1.883461 | -5.4248 | 18.081 |
| | $a_k^{(i)}$ | -1.1117495855 | 2.116539 | -4.8117 | 12.091 |
| | $a_k^{(r)} + a_k^{(i)}$ | -2.0000000000 | 4.000000 | -10.2365 | 30.172 |
| 8 | $a_k^{(r)}$ | -0.6326570719 | 1.197694 | -2.94579 | 8.3372 |
| | $a_k^{(i)}$ | -1.3673429281 | 2.802305 | -5.96129 | 12.1238 |
| | $a_k^{(r)} + a_k^{(i)}$ | -2.0000000000 | 4.000000 | -8.90708 | 20.4610 |

Table 7.4: The fitted coefficient to the series formula of $q_4^{1/4}$ (7.30) with $n_h = 0, 2, 4, 6$ and 8

7.3 Quantum numbers of the states with higher N

In the previous Sections we presented the spectra for $N = 3$ and $N = 4$ particles. One can notice that the latter spectrum is much more complicated than the one for $N = 3$. This complexity grows for larger N . Thus, in this Section we discuss only the ground states for $N = 2, \dots, 8$ which we have obtained after solving numerically the quantization conditions (6.27) [22, 23].

For more than $N = 8$ Reggeons numerical problems appear. Firstly, the $\{q_k\}$ -space becomes more dimensional, i.e. it has $(2N - 2)$ real dimensions. This means that the method of solving non-linear equations [50] for higher N needs far more time. Secondly, in the case $N > 8$ the series (6.7) and (6.17) become less convergent and recurrence relations for their coefficients, which include differences of large numbers, start to require bigger precision. Thus, in order to overcome this problem one have to use multi-precision libraries.

7.3.1 Properties of the ground states

Performing the numerical calculations we found for each sector from $N = 2$ to 8 states which have the minimum energy. It turns out that these states have common properties for even N . However, the properties of states with even N are different than the ones with odd N .

For even N the ground states are in sector where $n_h = 0$ so that $h = \frac{1}{2} + i\nu_h$. They are

situated on the trajectories where the odd conformal charges vanish,

$$q_3 = q_5 = \dots = q_{N-1} = 0, \quad (7.33)$$

while the even conformal charges are purely real,

$$\text{Im}[q_2] = \text{Im}[q_4] = \dots = \text{Im}[q_N] = 0. \quad (7.34)$$

The minimal energies for these trajectories are at $\nu_h = 0$. The states are symmetric under (7.4) and (7.5). However, due to (7.33) and (7.34) the ground states for even N are not degenerated. Moreover, the ground states with even N have negative energies $E_N < 0$.

For odd N we have two types of the ground states: the descendent ones and the others that have $q_N \neq 0$.

The descendent ground states are in the sector with $n_h = 0$ so that $h = 1 + i\nu_h$ and they energies $E_N(q_N = 0) = 0$ vanish. Along all trajectories $q_N = 0$ so these states are compositions of $(N - 1)$ -particle states.

On the other hand, the ground state trajectories for odd N with $q_N \neq 0$ are in the sector with $n_h = 0$ so $h = \frac{1}{2} + i\nu_h$. For these trajectories even conformal charges are real,

$$\text{Im}[q_2] = \text{Im}[q_4] = \dots = \text{Im}[q_{N-1}] = 0 \quad (7.35)$$

while the odd conformal charges are imaginary,

$$\text{Re}[q_3] = \text{Re}[q_5] = \dots = \text{Re}[q_N] = 0. \quad (7.36)$$

Similarly to the case with even N , these ground states are situated at $\nu_h = 0$. However, they have positive energies $E_N(q_N \neq 0) > 0$. Moreover, due to (7.4) and (7.5) the ground state is double-degenerated. We show exact values of the conformal charges and the energies for the ground states with $q_N \neq 0$ in Table 7.5. Because of the degeneration for odd N we have two equivalent sets of the ground states with $q_k \leftrightarrow (-1)^k q_k$.

7.3.2 Energy for different N

In order to analyse the dependence of the energy as a function of the number of particles N we plot this dependence in Figure 7.17. As we can see we have two cases: one for odd N and one for even N .

For even N the lowest energy is for the ground state with $N = 2$ and it grows with N as

$$E_N^{\text{even}} \sim \frac{1.8402}{N - 1.3143}. \quad (7.37)$$

Contrary to the even N case, for odd N we have the highest energy for the ground state with $N = 3$ and it falls down with N as

$$E_N^{\text{odd}} \sim \frac{-2.0594}{N - 1.0877}. \quad (7.38)$$

In the both formulae for large N we obtain the limit of the ground-state energy as

$$|E_N| \sim \frac{1}{N} \xrightarrow{N \rightarrow \infty} 0. \quad (7.39)$$

| | $\pm iq_3$ | q_4 | $\pm iq_5$ | q_6 | $\pm iq_7$ | q_8 | $-E_N/4$ | $\sigma_N/4$ |
|---------|------------|----------|------------|----------|------------|----------|----------|--------------|
| $N = 2$ | | | | | | | 2.77259 | 16.829 |
| $N = 3$ | 0.205258 | | | | | | -0.24717 | 0.908 |
| $N = 4$ | 0 | 0.153589 | | | | | 0.67416 | 1.318 |
| $N = 5$ | 0.267682 | 0.039452 | 0.060243 | | | | -0.12752 | 0.493 |
| $N = 6$ | 0 | 0.281825 | 0 | 0.070488 | | | 0.39458 | 0.564 |
| $N = 7$ | 0.313072 | 0.070993 | 0.128455 | 0.008494 | 0.019502 | | -0.08141 | 0.319 |
| $N = 8$ | 0 | 0.391171 | 0 | 0.179077 | 0 | 0.030428 | 0.28099 | 0.341 |

Table 7.5: The exact quantum numbers, q_N , and the energy, E_N , of the ground state of N reggeized gluons in multi-colour QCD. The dispersion parameter, σ_N , defines the energy of the lowest excited states, Eq. (7.2).

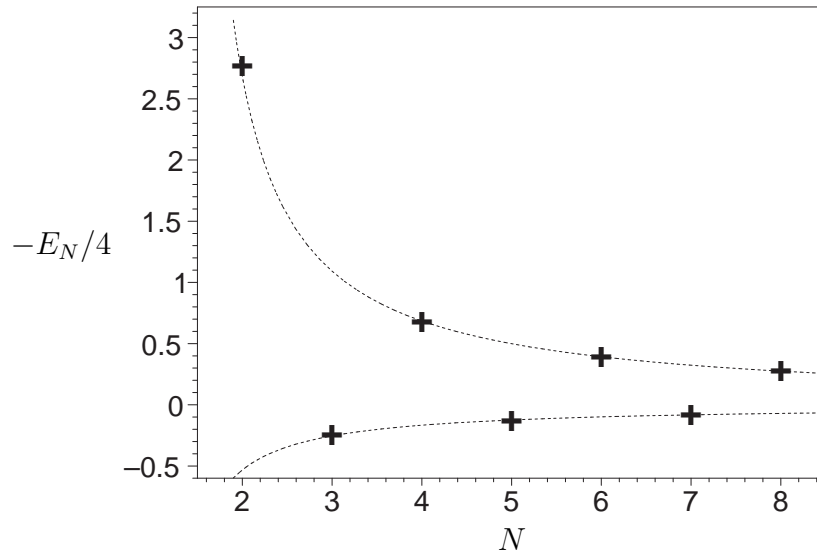


Figure 7.17: The dependence of the ground state energy, $-E_N/4$, on the number of particles N . The exact values of the energy are denoted by crosses. The upper and the lower dashed curves stand for the functions $1.8402/(N - 1.3143)$ and $-2.0594/(N - 1.0877)$, respectively.

7.3.3 Energy dependence on ν_h

The ground states are situated on the ground-state trajectories which are parameterized by a continuous parameter ν_h . Let us consider the dependence of the energy $E_N(\nu_h)$ along these trajectories, which are plotted in Figure 7.18.

We noticed in the previous Section that we have minima of the energy at $\nu_h = 0$ and these energies satisfy inequality

$$E_2 < E_4 < E_6 < E_8 < 0 < E_7 < E_5 < E_3. \quad (7.40)$$

These values of $E_N(\nu_h = 0)$ coincide with those depicted by crosses in Figure 7.17. Thus for ν_h ,

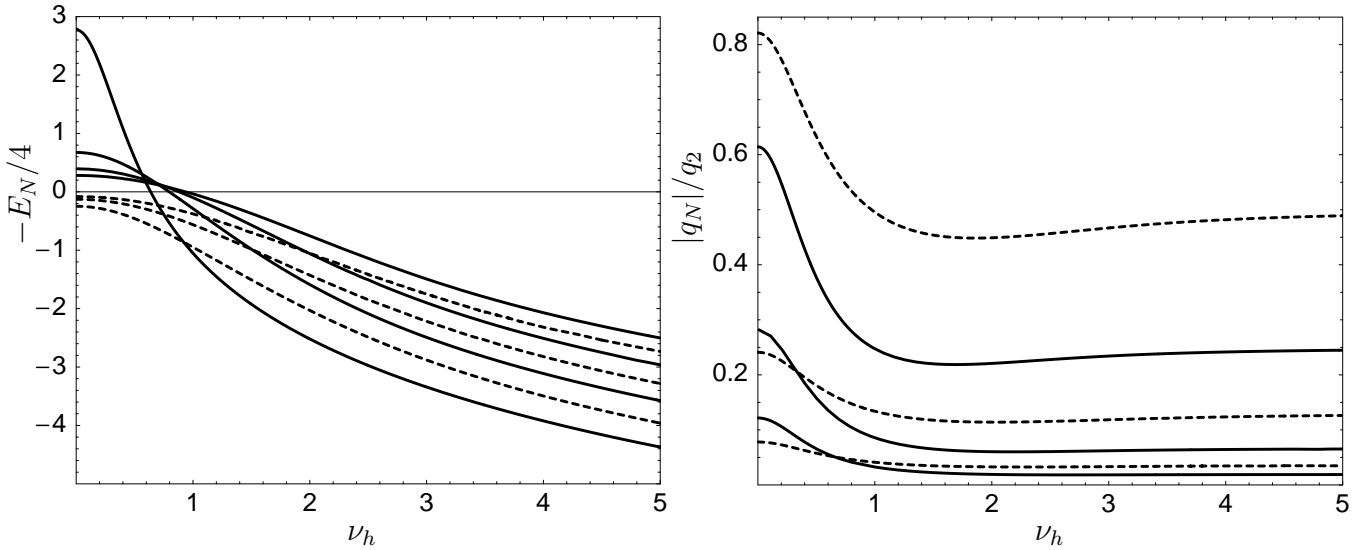


Figure 7.18: The dependence of the energy $-E_N(\nu_h)/4$ and the “highest” integral of motion $|q_N|/q_2$ with $q_2 = (1/4 + \nu_h^2)$ on the total spin $h = 1/2 + i\nu_h$ along the ground state trajectory for different number of particles $2 \leq N \leq 8$. At large ν_h , $-E_8 > \dots > -E_3 > -E_2$ on the left panel and $|q_8/q_2| < \dots < |q_3/q_2|$ on the right panel. Dashed lines correspond to odd N whereas solid lines to even N .

the order of the energy levels tell us that we have anti-ferromagnetic system². In the vicinity of $\nu_h = 0$ the energies behave as (7.2) where σ_N measure accumulation of the energies. The values of σ_N are shown in Table 7.5.

Going to the larger ν_h we notice that the energies grow. For $\nu_h \sim 1$ we have a quantum phase transition. The energies of our system reorder and for the large ν_h the ground-state energies of our system satisfy

$$0 < E_2 < E_3 < E_4 < E_5 < E_6 < E_7 < E_8. \quad (7.41)$$

The reason for this behaviour is that for the total $SL(2, \mathbb{C})$ spin $h = 1/2 + i\nu_h$ with the large ν_h the system approaches a quasi-classical regime [46, 62, 47], in which the energy $E_N(\nu_h)$ and the quantum numbers q_N have a universal scaling behaviour

$$E_N(\nu_h) \sim 4 \text{Log}|q_N|, \quad |q_N| \sim C_N \nu_h^2, \quad (7.42)$$

with C_N decreasing with N . As can be seen from the right panels in Figures 7.9 and 7.18, this regime starts already at $\nu_h \approx 2$ [23].

²In anti-ferromagnetic systems we have two different sectors: with odd and even N numbers of particles. For example: in the simplest anti-ferromagnetic periodic spin-chain with two possible spin orientations: *up* and *down*, for odd N the lowest energy is when the neighbouring spins have opposite orientations. Since for odd N we have always one pair of neighbouring spins with the same orientation the ground states for odd N has higher energies than the the ground states for even N .

Chapter 8

Other quantization conditions

In this Chapter we show for completeness another solution to the Baxter Equation (3.3) that has been presented in Refs. [27, 28] by de Vega and Lipatov. In their method two additional conditions were assumed: the conformal charges should satisfy $\text{Im}[i^k q_k] = 0$ and the holomorphic energy of each from N linearly independent solutions of the pertinent Baxter equation should be equal. As was explained in Ref. [23] these conditions are too strong.

8.1 De Vega and Lipatov's solution

In the papers [27, 28] the authors consider the Baxter equations (3.3) and (3.4) with complex spins ($s = 1, \bar{s} = 1$). The equal values of the complex spins cause that the Baxter equations in the holomorphic and anti-holomorphic sectors are identical. However, in this case the complex spins ($s = 1, \bar{s} = 1$) do not satisfy (2.58) so we have to use the different form of the scalar product given by (2.42).

It has been shown in Ref. [27] that the simplest N -Reggeon solution to the Baxter equation (3.3) may be conveniently written in a form of a sum over poles of orders 1 up to $N - 1$ situated in the upper semi-plane of complex variable u :

$$Q^{(N-1)}(u; h, q) = \sum_{r=0}^{\infty} \frac{P_{r;h,q}^{(N-2)}(u)}{(u - ir)^{N-1}} = \sum_{r=0}^{\infty} \left[\frac{\tilde{a}_r(q)}{(u - ir)^{N-1}} + \frac{\tilde{b}_r(q)}{(u - ir)^{N-2}} + \dots + \frac{\tilde{z}_r(q)}{(u - ir)} \right], \quad (8.1)$$

where $q = \{q_2, q_3, \dots, q_N\}$ and $P_{r;h,q}^{(N-2)}(u)$ are polynomials in u of degree $N - 2$, whereas $\tilde{a}_r(q), \tilde{b}_r(q), \dots$ are some residual coefficients. Substituting (8.1) to (3.3) we obtain the recurrence relations between the polynomials $P_{r;h,q}^{(N-2)}(u)$ which allows us to calculate them successively starting from $P_{0;h,q}^{(N-2)}(u)$.

The solution (8.1) is normalized by the constraint

$$\lim_{u \rightarrow 0} P_{0;h,q}^{(N-2)}(u) = \tilde{a}_r(q) = 1 \quad (8.2)$$

and the remaining coefficients of the polynomial $P_{0;h,q}^{(N-2)}(u)$, or equivalently the coefficients $b_r(q)$,

$c_r(q), \dots$, are calculated from the condition

$$\lim_{u \rightarrow \infty} Q^{(N-1)}(u; h, q) \sim u^{h-N} \quad (8.3)$$

which ensures [27] that the solution (8.1) satisfies the Baxter equation (3.3) for $u \rightarrow \infty$. The condition (8.3) leads to

$$\lim_{u \rightarrow \infty} u^{N-2} \frac{P_{r;h,q}^{(N-2)}(u)}{(u - ir)^{N-1}} = 0 \quad (8.4)$$

which gives $N - 2$ equations and with (8.2) fixes all the polynomial coefficients $P_{0;h,q}^{(N-2)}(u)$, or equivalently $\tilde{a}_0(q), \tilde{b}_0(q), \dots$.

The second independent solution may be written in terms of the first one as

$$Q^{(0)}(u; h, q) = Q^{(N-1)}(-u; h, -q) = \sum_{r=0}^{\infty} \frac{P_{r;h,-q}^{(N-2)}(-u)}{(-u - ir)^{N-1}}, \quad (8.5)$$

where $-q = (q_2, -q_3, \dots, (-)^N q_N)$.

It turns out, that there is a set of Baxter functions $Q^{(t)}(u)$ with $t = 0, 1, \dots, N - 1$ which have poles both in the upper and lower half- u planes:

$$Q^{(t)}(u; h, q) = \sum_{r=0}^{\infty} \left[\frac{P_{r;h,q}^{(t-1)}(u)}{(u - ir)^t} + \frac{P_{r;h,-q}^{(N-2-t)}(-u)}{(-u - ir)^{N-1-t}} \right], \quad (8.6)$$

where the polynomials $P_{r;h,q}^{(t-1)}(u)$ and $P_{r;h,-q}^{(N-2-t)}(-u)$ are fixed by the recurrence relations following from the Baxter equation and from the condition that the solution should decrease at infinity more rapidly than u^{-N+2} .

Using these functions in both holomorphic and anti-holomorphic sectors it is possible to construct the Baxter function

$$Q_{q,\bar{q}}(u, \bar{u}) = \sum_{t,l} C_{t,l} Q^{(t)}(u; h, q) Q^{(l)}(\bar{u}; \bar{h}, \bar{q}) \quad (8.7)$$

choosing the coefficients $C_{t,l}$, appropriately.

In this method the coefficients $C_{t,l}$ are fixed by the normalization condition [27]. It leads to the requirement that $Q_{q,\bar{q}}(u, \bar{u})$ do not have poles at

$$u = im \quad \text{and} \quad \bar{u} = -im \quad \text{for} \quad |m| > 0. \quad (8.8)$$

The pole at $u = \bar{u} = 0$ is removed by the measure of the $(s = 1, \bar{s} = 1)$ scalar product (2.42). Because in the bilinear solution we have products of the poles $(u - ir)^{-s}$ and $(\bar{u} - ir')^{-s'}$ we expand $Q_{q,\bar{q}}(u, \bar{u})$ around the spurious poles (8.8) and we equate the residual expansion coefficients to zero. This results in the quantization conditions for the conformal charges q and \bar{q} .

The authors of Refs. [27, 28] claim that the same conditions are given by imposing equality of holomorphic energies

$$\epsilon_t = i \lim_{u \rightarrow i} \frac{\partial}{\partial u} \ln \left[u^N P_{1;h,q}^{(t-1)}(u) \right] \quad (8.9)$$

for all solutions $Q^{(t)}(u)$. However, our system is two-dimensional and the holomorphic energy is not a physical observable and it may depend on a calculation method. The real observable is the total energy defined as

$$E = 2i \lim_{u, \bar{u} \rightarrow i} \frac{\partial}{\partial u} \frac{\partial}{\partial \bar{u}} \ln \left[(u - i)^{N-1} (\bar{u} - i)^{N-1} u^N \bar{u}^N Q_{q, \bar{q}}(u, \bar{u}) \right]. \quad (8.10)$$

8.1.1 Three Reggeon states

For simplicity, let us consider the $N = 3$ Reggeon case. The Baxter equation (3.3) with $s = 1$ reduces to

$$\begin{aligned} B_3(u; h, q_3) &\equiv [2u^3 - h(h-1)u + q_3] Q(u; h, q_3) \\ &\quad - (u+i)^3 Q(u+i; h, q_3) - (u-i)^3 Q(u-i; h, q_3) = 0. \end{aligned} \quad (8.11)$$

Here the authors of Refs. [27, 28] claim that iq_3 should be real in order to obtain single-valued wave-functions. However, we have already shown (5.23)–(7.11) that it is possible to construct a single-valued function without this assumption.

To find polynomial coefficients in $Q^{(t)}(u, \bar{u})$ we define auxiliary functions f_r , which look as follows

$$\begin{aligned} f_2(u; h, q_3) &= \sum_{l=0}^{\infty} \left[\frac{a_l(h, q_3)}{(-iu - l)^2} + \frac{b_l(h, q_3)}{-iu - l} \right], \\ f_1(u; h, q) &= \sum_{l=0}^{\infty} \frac{a_l(h, q_3)}{-iu - l}. \end{aligned} \quad (8.12)$$

They help us to impose the conditions coming from behaviour of $Q(u; h, q_3)$ at $u \rightarrow \infty$. Substituting (8.12) to (8.11) we obtain the recurrence relations for the residua of (8.12):

$$\begin{aligned} (r+1)^3 a_{r+1}(h, q_3) &= [2r^3 + h(h-1)r + iq_3] a_r(h, q_3) - (r-1)^3 a_{r-1}(h, q_3) \\ (r+1)^3 b_{r+1}(h, q_3) &= [2r^3 + h(h-1)r + iq_3] b_r(h, q_3) - (r-1)^3 b_{r-1}(h, q_3) \\ &\quad + [6r^2 + h(h-1)] a_r(h, q_3) - 3(r+1)^2 a_{r+1}(h, q_3) - 3(r-1)^2 a_{r-1}(h, q_3). \end{aligned} \quad (8.13)$$

We can choose,

$$a_0(h, q_3) = 1 \quad \text{and} \quad b_0(h, q_3) = 0 \quad (8.14)$$

what gives as

$$a_1(h, q_3) = iq_3, \quad b_1(h, q_3) = h(h-1) - 3iq_3. \quad (8.15)$$

Thus, we can calculate all the coefficients $a_r(h, q_3)$ and $b_r(h, q_3)$.

Now, we can construct $Q^{(t)}(u, \bar{u})$ as a linear combinations of the auxiliary functions (8.12) in a form

$$\begin{aligned} Q^{(2)}(u; h, q_3) &= f_2(u; h, q) + B(h, q_3) f_1(u; h, q), \\ Q^{(1)}(u; h, q_3) &= f_1(u; h, q) + C(h, q_3) f_1(-u; h, -q_3), \end{aligned} \quad (8.16)$$

where $B(h, q_3)$ and $C(h, q_3)$ are coefficients we will fix using the condition (8.4) by demanding that the Baxter equation is satisfied at infinity. Taking the limit $u \rightarrow \infty$ of (8.11) with (8.16) we obtain

$$B_3(\infty; h, q_3) = [h(h-1) - 2] \lim_{u \rightarrow \infty} [u Q(u; m, \mu)] . \quad (8.17)$$

Applying (8.17) to (8.16) we get the coefficients in a form

$$B(h, q_3) = -\frac{\sum_{r=0}^{\infty} b_r(h, q_3)}{\sum_{r=0}^{\infty} a_r(h, q_3)} \quad \text{and} \quad C(h, q_3) = \frac{\sum_{r=0}^{\infty} a_r(h, q_3)}{\sum_{r=0}^{\infty} a_r(h, -q_3)} . \quad (8.18)$$

Therefore, the solutions $Q^{(2)}(u; h, q_3)$ and $Q^{(1)}(u; h, q_3)$ are completely determined.

Due to the symmetry (7.4) we can construct the third solution

$$Q^{(0)}(u; h, q_3) = Q^{(2)}(-u; h, -q_3) . \quad (8.19)$$

Moreover, if we multiply a solution of the Baxter equation by a periodic function of iu with period 1 the result is also a solution of the Baxter equation (8.11). For instance

$$Q^{(1)}(u; h, q_3) \pi \cot(i\pi u) \quad (8.20)$$

is also the solution to (8.11) and thanks to $\cot(i\pi u)$ it has second order poles at $u = im$ for $|m| > 0$.

All these solutions are related by the equation [27, 28]

$$[X(h, q_3) - \coth(\pi u)] Q^{(1)}(u; h, q_3) = Q^{(2)}(u; h, q_3) - C(h, q_3) Q^{(0)}(u; h, q_3) , \quad (8.21)$$

where $X(h, q_3)$ can be obtained by performing the Laurent expansion of (8.21) around the poles (8.8). In Refs. [27, 28] it is shown that it is possible to construct the solution (8.7) with $h = \bar{h}$ and $q_3 = -\bar{q}_3$ for which poles at (8.8) disappear. It has the following form

$$Q_{q, \bar{q}}(u, \bar{u}) = Q^{(2)}(u; h, q_3) Q^{(2)}(\bar{u}; \bar{h}, \bar{q}_3) - Q^{(0)}(u; h, q_3) Q^{(0)}(\bar{u}; \bar{h}, \bar{q}_3) . \quad (8.22)$$

Moreover, in Refs. [27, 28] the authors assume that the condition $X(h, q_3) = 0$ gives quantization of q_3 . Accidentally, for solutions with $X(h, q_3) = 0$ the holomorphic energies (8.9) of the solutions $Q^{(2)}(u; h, q_3)$ and $\pi \cot(iu\pi) Q^{(1)}(u; h, q_3)$ are equal what gives equivalent condition to $X(h, q_3) = 0$ which looks like

$$B(h, q_3) - b_1(h, q_3) - \frac{1}{iq_3} + \frac{1}{iq_3} \sum_{r=2}^{\infty} \frac{a_r(h, q_3)}{r-1} + \frac{C(h, q_3)}{iq_3} \sum_{r=0}^{\infty} \frac{a_r(h, -q_3)}{r+1} = 0 . \quad (8.23)$$

However, the way of cancelling poles presented in [27, 28] is not unique. Indeed, the condition (8.23) is too strong and it is only satisfied for some solutions with $\text{Re } q_3 = 0$. There are other solutions, for example with $\text{Im } q_3 = 0$, for which the holomorphic energies are not equal.

In Refs. [27, 28] for $N = 4$ Reggeons the quantization conditions are also introduced by the equality of the holomorphic energies. Similarly to the $N=3$ case, the numerical values of

the conformal charges which result from these conditions agree with Refs. [23] only for $h = \overline{h}$, $\text{Re } q_3 = 0$ and $\text{Im } q_4 = 0$.

Contrary to the solutions described in [23] the solutions presented in this Chapter have a simple pole structure, so they look much simpler than those defined by (6.1)–(6.16). However, the series in (8.12) are much slower convergent than the series defined in (6.7) and (6.17). Moreover, in [23] the quantisation conditions (6.27) come from single-valuedness and normalization of the Reggeon wave-functions explicitly, whereas in [27, 28] except for the normalization condition, the quantization conditions (8.23) follow from the quality of the holomorphic energies (8.9).

Thus, if one wants to find a spectrum of the conformal charges numerically the method presented in [23] is much more convenient.

Chapter 9

Anomalous dimensions

In the preceding Chapters we used the reggeized gluon states to describe the elastic scattering amplitude of strongly interacting hadrons. It turns out that the Reggeon states might be also used to describe deep inelastic scattering of a virtual photon $\gamma^*(q_\mu)$ off a (polarized) hadron with momentum p_μ [26, 28]. In this case we also perform calculations in the limit of the low Björken x but in the region where

$$M^2 \ll Q^2 \ll s^2 = (p_\mu + q_\mu)^2 = \frac{Q^2(1-x)}{x}, \quad (9.1)$$

with

$$Q^2 = -q_\mu^2 \quad M^2 = p_\mu^2. \quad (9.2)$$

Notice that in the previous case (2.2) there was only one hard scale present, namely the mass of the scattering particles which were assumed to be similar.

In the limit (9.1), similarly to (2.2), the moments of the structure function $F_2(x, Q^2) \equiv F(x, Q^2)$ may be rewritten as a power series in the strong coupling constant α_s :

$$\tilde{F}(j, Q^2) \equiv \int_0^1 dx x^{j-2} F(x, Q^2) = \sum_{N=2}^{\infty} \bar{\alpha}_s^{N-2} \tilde{F}_N(j, Q^2), \quad (9.3)$$

where $\bar{\alpha}_s = \alpha_s N_c / \pi$.

The leading contribution comes from the Reggeon states with the intercept $j \rightarrow 1$ and in this limit

$$\tilde{F}_N(j, Q^2) = \sum_{\mathbf{q}} \frac{1}{j-1 + \bar{\alpha}_s E_N(\mathbf{q})/4} \beta_{\gamma^*}^{\mathbf{q}}(Q) \beta_p^{\mathbf{q}}(M), \quad (9.4)$$

where the conformal charges are denoted by $\mathbf{q} = (q_2, \bar{q}_2, q_3, \bar{q}_3, \dots, q_N, \bar{q}_N)$ and $\beta_{\gamma^*}^{\mathbf{q}}(Q)$, $\beta_p^{\mathbf{q}}(M)$ are the impact factors of virtual photon and scattered hadron, respectively, while the energies E_N are the eigenvalues of the Reggeon Hamiltonian (2.31).

Performing the operator product expansion (OPE) one may expand the moments of the structure function $\tilde{F}_N(x, Q^2)$ in inverse powers of hard scale Q

$$\tilde{F}(j, Q^2) = \sum_{n=2,3,\dots} \frac{1}{Q^n} \sum_a C_n^a(j, \alpha_s(Q^2)) \langle p | \mathcal{O}_{n,j}^a(0) | p \rangle, \quad (9.5)$$

where the expansion coefficients are the forward matrix elements of Wilson operators $\mathcal{O}_{n,j}^a(0)$ of increasing twist $n \geq 2$ and they satisfy renormalization group equations

$$Q^2 \frac{d}{dQ^2} \langle p | \mathcal{O}_{n,j}^a(0) | p \rangle = \gamma_n^a(j) \langle p | \mathcal{O}_{n,j}^a(0) | p \rangle \quad (9.6)$$

with the anomalous dimensions of QCD $\gamma_n^a(j)$. The parameter a enumerates operators with the same twist n . It also appears in (9.5) where $C_n^a(j, \alpha_s)$ denote the coefficient functions.

The anomalous dimensions $\gamma_n^a(j)$ may be written as a power series

$$\gamma_n^a(j) = \sum_{k=1}^{\infty} \gamma_{k,n}^a(j) (\alpha_s(Q^2)/\pi)^k. \quad (9.7)$$

For small Björken x ($j \rightarrow 1$), the moments of the structure function $\tilde{F}_N(j, Q^2)$ take a form

$$\tilde{F}(j, Q^2) = \frac{1}{Q^2} \sum_{n=2,3,\dots} \sum_a \tilde{C}_n^a(j, \alpha_s(Q^2)) \left(\frac{M}{Q} \right)^{n-2-2\gamma_n^a(j)}. \quad (9.8)$$

It turns out that solving the Schrödinger equation (2.34) we are able to find poles which give the main contribution to (9.4). Moreover, combining (9.8) and (9.4) we are able to find the dependence of $\gamma_{k,n}^a(j)$ on the strong coupling constant near $j \rightarrow 1$. In this Chapter we show the way one can find this dependence using techniques developed in the previous Chapters.

9.1 Expansion for the large scale Q

The moments of the structure function are defined in (9.3). In the limit $j \rightarrow 1$ they can be rewritten as (9.4) where the impact factors are given by

$$\beta_{\gamma^*}^{\mathbf{q}}(Q) = \int d^2 z_0 \langle \Psi_{\gamma^*} | \Psi_{\mathbf{q}}(\vec{z}_0) \rangle, \quad \beta_p^{\mathbf{q}}(M) = \int d^2 z_0 \langle \Psi_{\mathbf{q}}(\vec{z}_0) | \Psi_p \rangle \quad (9.9)$$

and the functions $\Psi_{\mathbf{q}}(\vec{z}_0)$ are orthonormal with respect to the scalar product (2.35):

$$\langle \Psi_{\mathbf{q}}(\vec{z}_0) | \Psi_{\mathbf{q}'}(\vec{z}_0') \rangle \equiv \int \prod_{k=1}^N d^2 z_k \Psi_{\mathbf{q}}(\{\vec{z}\}; \vec{z}_0) (\Psi_{\mathbf{q}'}(\{\vec{z}\}; \vec{z}_0'))^* = \delta^{(2)}(z_0 - z_0') \delta_{\mathbf{q}\mathbf{q}'}, \quad (9.10)$$

where $\delta_{\mathbf{q}\mathbf{q}'} = \delta(\nu_h - \nu_h') \delta_{n_h n_h'} \delta_{\ell \ell'}$ with $\ell = \{\ell_2, \ell_3, \dots, \ell_{2(N-2)}\}$ defined in (7.1). Due to the scaling symmetry of the reggeized gluon states

$$\Psi_{\mathbf{q}}(\lambda \vec{z}_1, \lambda \vec{z}_2, \dots, \lambda \vec{z}_N) = \lambda^{2-h-\bar{h}} \Psi_{\mathbf{q}}(\vec{z}_1, \vec{z}_2, \dots, \vec{z}_N) \quad (9.11)$$

we are able to calculate dimensions of the impact factors (9.9)

$$\beta_{\gamma^*}^{\mathbf{q}}(Q) = C_{\gamma^*}^{\mathbf{q}} Q^{-1-2i\nu_h}, \quad \beta_p^{\mathbf{q}}(M) = C_p^{\mathbf{q}} M^{-1+2i\nu_h}, \quad (9.12)$$

where $C_{\gamma^*}^{\mathbf{q}}$ and $C_p^{\mathbf{q}}$ are dimensionless. Substituting (9.12) into (9.4) and expanding in powers of the ratio (M/Q)

$$\tilde{F}_N(j, Q^2) = \frac{1}{Q^2} \sum_{\ell} \sum_{n_h \geq 0} \int_{-\infty}^{\infty} d\nu_h \frac{C_{\gamma^*}^{\mathbf{q}} C_p^{\mathbf{q}}}{j-1 + \bar{\alpha}_s E_N(\mathbf{q})/4} \left(\frac{M}{Q} \right)^{-1+2i\nu_h}, \quad (9.13)$$

where $\mathbf{q} = \mathbf{q}(\nu_h; h_n, \boldsymbol{\ell})$. We shall calculate the integral in (9.13) by performing analytical continuation in ν_h . Next, we shall close the integration contour in the ν_h -complex plane and integrate by summing residua closed by the contour. The corresponding poles come from the denominator of (9.13) so they are placed at ν_h where

$$j - 1 = \bar{\alpha}_s E_N(\mathbf{q}(\nu_h; n_h, \boldsymbol{\ell}))/4 \quad (9.14)$$

is satisfied. Here the parameters n_h and $\boldsymbol{\ell} = \{\ell_1, \ell_2, \dots, \ell_{2(N-2)}\}$ are integer numbers and they enumerate the quantized energy levels. The formula for (9.13) is valid for $j > j_N = 1 - \bar{\alpha}_s \min_q E_N(\mathbf{q})/4$.

In this way a contribution to the moments of $F(x, Q^2)$ coming from a given pole in ν_h takes the following form

$$\tilde{F}_N(j, Q^2) \sim \frac{1}{Q^2} \left(\frac{M}{Q} \right)^{-1+2i\nu_h(j)}, \quad (9.15)$$

where we show the dependence on j explicitly. Comparing exponents in (9.8) and (9.15) we obtain relation

$$\gamma_n(j) = (n-1)/2 - i\nu_h(j) = [n - (h(j) + \bar{h}(j))]/2, \quad (9.16)$$

where $h(j)$ and $\bar{h}(j)$ are the $SL(2, \mathbb{C})$ spins defined in (2.60) and $\gamma_n(j)$ is the anomalous dimension of the twist- n operator (9.6).

Now we can calculate $\gamma_n(j)$ which with $\alpha_s(j) \rightarrow 0$ behave as $\gamma_n(j) \rightarrow 0$

$$\gamma_n(j) = \gamma_n^{(0)} \frac{\bar{\alpha}_s}{j-1} + \mathcal{O}(\bar{\alpha}_s^2). \quad (9.17)$$

Substituting (9.14) into (9.17) one finds that $\gamma_n(j) \rightarrow 0$ corresponds to $E_N(\nu_h) \rightarrow \infty$. Thus, we can combine the expansion of the energy $E_N(\nu_h)$ around its poles in the complex ν_h -plane:

$$E_N(\mathbf{q}) = -4 \left[\frac{c_{-1}}{\epsilon} + c_0 + c_1 \epsilon + \dots \right] \quad (9.18)$$

with the small anomalous dimensions $\gamma_n(j) = -\epsilon$ where according to (9.17) $i\nu_h = i\nu_h^{\text{pole}} + \epsilon$. Inverting the series (9.18) and using (9.14) we obtain

$$\gamma_n(j) = -c_{-1} \left[\frac{\bar{\alpha}_s}{j-1} + c_0 \left(\frac{\bar{\alpha}_s}{j-1} \right)^2 + (c_1 c_{-1} + c_0^2) \left(\frac{\bar{\alpha}_s}{j-1} \right)^3 + \dots \right], \quad (9.19)$$

where coefficients $c_k = c_k(n, n_h, \boldsymbol{\ell})$ in Eqs. (9.19) and (9.18) are identical. Thus, evaluating these coefficient for the energy (9.18) we may calculate coefficients for the anomalous dimension expansion in the coupling constant $\bar{\alpha}_s$.

Moreover, we can notice that the positions of the energy poles

$$E_N(\mathbf{q}) \sim \frac{\gamma_n^{(0)}}{i\nu_h - (n-1)/2} \quad (9.20)$$

determines the twist n of $\gamma_n^{(0)}$

$$i\nu_h = (n-1)/2 \quad \text{with} \quad n \geq N + n_h \quad (9.21)$$

with the number of Reggeons N and the Lorentz spin n_h .

For $N = 2$ formula for the energy [15, 4] is given by an analytical expression

$$E_2(\nu_h, n_h) = 4 \left(\psi \left(\frac{1+n_h}{2} + i\nu_h \right) + \psi \left(\frac{1+n_h}{2} - i\nu_h \right) - 2\psi(1) \right), \quad (9.22)$$

where n_h are nonnegative integers. In this case the anomalous dimensions for the leading twist $n = 2$ have been calculated in [24]:

$$\gamma_2(j) = \frac{\bar{\alpha}_s}{j-1} + 2\zeta(3) \left(\frac{\bar{\alpha}_s}{j-1} \right)^4 + 2\zeta(5) \left(\frac{\bar{\alpha}_s}{j-1} \right)^6 + \mathcal{O}(\bar{\alpha}_s^8), \quad (9.23)$$

where $\zeta(k)$ is the Riemann zeta-function. The general formula for $N = 2$ and arbitrary $n \geq 2$ and n_h has been obtained in [25]:

$$\gamma_n(j) = \frac{\bar{\alpha}_s}{j-1} + (2\psi(1) - \psi(1 + |n_h| + n) - \psi(1 + n)) \left(\frac{\bar{\alpha}_s}{j-1} \right)^2 + \mathcal{O}(\bar{\alpha}_s^3). \quad (9.24)$$

9.2 Analytical continuation

The reggeized gluon functions $\Psi(\vec{z}_k)$ defined in (2.54) are normalized with respect to the scalar product (9.10). Performing the analytical continuation in ν_h it turns out that the normalization condition (2.63) is no longer satisfied. The quantization conditions (2.63) and (6.27) become relaxed. Thus, conditions $\bar{q}_k = q_k$ are not necessarily satisfied so that $\bar{h} \neq 1 - h^*$. However, we still have the conditions coming from the single-valuedness of the Reggeon wave-functions. The latter condition (6.27) ensures that the two-dimensional integrals (9.9) are well defined. In (3.18) the energy $E_N(\nu_h)$ is a smooth function of real ν_h . After the analytical continuation into the complex ν_h -plane the energy spectrum exposes pole structure at $\text{Re}[\nu_h] = 0$.

In Quantum Mechanics the problem of analytical continuation of energy $E(g)$ as a function of a coupling constant g has been studied in various models [63, 64, 65]. In our case ν_h plays a role of such a coupling constant g .

Generally, the energy $E(g)$ is a multi-valued function of g . It turns out that the number of energy levels for real g is equal to the number of branches in the complex g -plane. In order to analyse the global spectrum one may glue together different sheets corresponding to its branches and study $E(g)$ as a single-valued function on the resulting Riemann surface. Thus, the models may have a complicated structure of spectrum in the complex g -plane. Additionally, these spectra may consist of a few disconnected parts due to some additional symmetry [64].

9.2.1 Two level model

In order to understand the analytical continuation more clearly let us consider the simple model with two energy levels ϵ_1 and ϵ_2 :

$$\hat{H} = \begin{pmatrix} \epsilon_1 & g \\ g & \epsilon_2 \end{pmatrix}, \quad (9.25)$$

where we add interaction by introducing a small coupling constant g .

The energy eigenvalues of the interacting Hamiltonian (9.25) are given by

$$E_{\pm}(g) = \frac{\epsilon_1 + \epsilon_2}{2} \pm \sqrt{\left(\frac{\epsilon_1 - \epsilon_2}{2}\right)^2 + g^2}. \quad (9.26)$$

Here we have two branches $E_+(g)$ and $E_-(g)$ which are shown in Fig 9.1 where for illustration we have chosen with $\epsilon_1 = 0$ and $\epsilon_2 = 1$. For the real g the energy levels $E_{\pm}(g)$ do not cross.

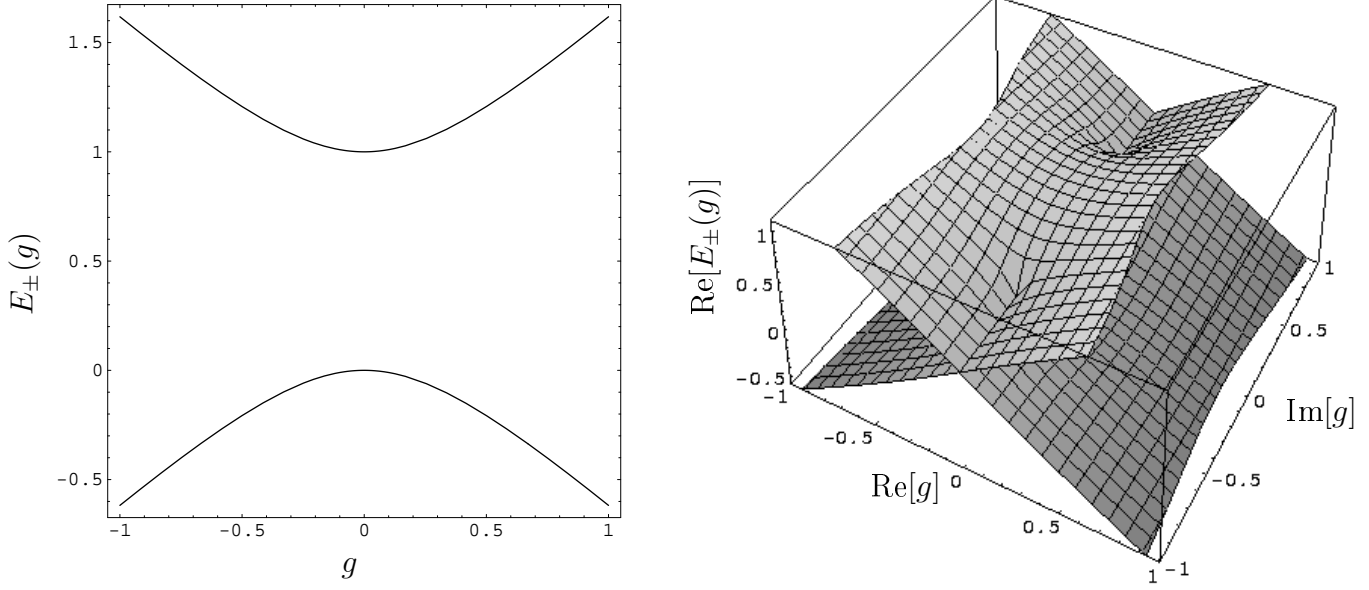


Figure 9.1: Spectral surfaces for two energy level model. On the left panel energy levels as a function of a real coupling constant g . On the right panel real energy surfaces as function of complex g

However, we have two branching points at $g_{\pm} = \pm \frac{i}{2}(\epsilon_1 - \epsilon_2)$ for which $E_+(g_{\pm}) = E_-(g_{\pm}) = \frac{\epsilon_1 + \epsilon_2}{2}$. The energy is a smooth two-valued function of complex g . The spectral surfaces cross each other for $\text{Re}[g] = 0$ where $-ig > -ig_+$ or $-ig < -ig_-$. Going around these branching points we can pass from one surface to the other one. In this case, the spectral curve, which is a function defined on one complicated Riemann surface, consists of two branches $E_+(g)$ and $E_-(g)$.

One has to add that in this model the energy does not have any poles which occur in our $SL(2, \mathbb{C})$ Heisenberg model.

9.2.2 $SL(2, \mathbb{C})$ Heisenberg model for two Reggeons

The energy for two Reggeons with nonnegative n_h is defined by (9.22). We notice that analytical continuation of (9.22) exhibits the poles at

$$i\nu_h = \pm \frac{n-1}{2} \quad \text{with the twist} \quad n \geq 2 + n_h. \quad (9.27)$$

The residua of these poles are related to the anomalous dimensions given by (9.24). The leading twist $n = 2$ corresponds to the pole at $\nu_h = -i/2$ with $n_h = 0$.

The energy (9.22) does not have any branching points. Thus, the spectral surfaces numbered by the Lorentz spin n_h do not mix with each other in the complex ν_h -plane. The spectral surfaces are functions defined on trivial separated Riemann surfaces.

9.2.3 $SL(2, \mathbb{C})$ Heisenberg model for more Reggeons

For the case with more than two Reggeons the energy spectrum is much more complicated. The energy $E_N(\nu_h; n_h, \ell)$ depends not only on ν_h and n_h but also on $2(N-2)$ integer numbers $\ell = \{\ell_1, \ell_2, \dots, \ell_{2(N-2)}\}$. Similarly to the $N = 2$ case the energy surfaces for $N > 2$ possess poles for imaginary ν_h . Additionally, they also have branching points. Thus, the energy spectrum consists of infinite number of spectral surfaces, which are functions of complex ν_h with complicated Riemann structure.

The energy in (3.18) is a smooth function of real ν_h . In this region we have quantization conditions coming from the single-valuedness of the Reggeon wave-function as well as the normalization condition which ensure that Hamiltonian (2.32) is hermitian. The latter condition gives conjugation relations between the conformal charges

$$q_k = \bar{q}_k^* \quad \text{with} \quad k = 2, \dots, N. \quad (9.28)$$

Performing the analytical continuation into the complex ν_h -plane we have to relax the quantization conditions (2.63). The single-valuedness condition survives. However, the normalization condition is not valid anymore. Thus, the relations (9.28) in complex ν_h are not valid, so that, q_k and \bar{q}_k may be independent.

We notice that the N -Reggeon spectrum contains the states with given n_h and ℓ for which

$$\bar{q}_k(\nu_h; n_h, \ell) = \pm q_k(\nu_h; n_h, \ell). \quad (9.29)$$

These states satisfy (9.29) on the whole complex ν_h -plane. They are of utmost interest because they give the higher order contribution to the structure function (9.3). Other interesting states are the descendent states.

For $N \geq 3$ the energy $E_N(\nu_h; n_h, \ell)$ is a multi-valued function of ν_h parameterized by n_h and ℓ which number the spectral surfaces. In the complex ν_h -plane the spectrum possesses poles at

$$i\nu_h = \pm \frac{n-1}{2} \quad \text{with the twist} \quad n \geq N + n_h. \quad (9.30)$$

It turns out that it also possesses the infinite set of branching points which are square-like type similarly to (9.26). In order to construct the complex curves $E_N(\nu; n_h, \ell)$ we apply Eqs. (3.18) developed in Refs. [38, 23]. After analytical continuation we get

$$E_N = [\varepsilon(h, q) + \varepsilon(h, -q) + (\varepsilon(1 - \bar{h}^*, \bar{q}^*))^* + (\varepsilon(1 - \bar{h}^*, -\bar{q}^*))^*], \quad (9.31)$$

where the $SL(2, \mathbb{C})$ spins h and \bar{h} are given by (2.60) and the conformal charges are denoted as $q = \{q_k\}$, $\bar{q} = \{\bar{q}_k\}$, $-q = \{(-1)^k q_k\}$ and $-\bar{q} = \{(-1)^k \bar{q}_k\}$. As one can see $E_N(-q, -\bar{q}) =$

$E_N(q, \bar{q})$. Since for real ν_h we have $h = 1 - \bar{h}^*$ and $q = \bar{q}^*$ the energy $E_N(q, \bar{q})$ takes real values on the real ν_h -axis.

The function $\varepsilon(h, q)$ in (9.31) is defined for arbitrary complex h and q by

$$\varepsilon(h, q) = i \frac{d}{d\epsilon} \ln [\epsilon^N Q(i + \epsilon; h, q)] \Big|_{\epsilon=0}, \quad (9.32)$$

where $Q(u; h, q)$ has a form

$$Q(u; h, q) = \int_0^1 dz z^{iu-1} Q_1(z). \quad (9.33)$$

Going further, $Q_1(z)$ satisfies the differential equation (6.2) which comes from the Baxter equation (3.3). Around $z = 1$ the function $Q_1(z)$ corresponds to one of the solutions in (6.16) with asymptotics $Q_1(z) \sim (1 - z)^{(-h-1)}$ and around $z = 0$ from (6.6) with $Q_1(z) \sim \ln^{N-1} z$. It is convenient to normalize $Q(u; h, q)$ as

$$Q(i + \epsilon; h, q) = \frac{1}{\epsilon^N} - i \frac{\varepsilon(h, q)}{\epsilon^{N-1}} + \mathcal{O}\left(\frac{1}{\epsilon^{N-2}}\right). \quad (9.34)$$

where the function $\varepsilon(h, q)$ appears in (9.31).

Thus, solving the quantization conditions (6.27) and using (3.18) and (9.31) we are able to evaluate the energy $E_N(\nu_h)$ on the whole complex ν_h -plane. Then, we find the poles which appear only for $\text{Re}[\nu_h] = 0$, and we evaluate expansion coefficients of $E_N(\nu_h)$ around its poles. Next, using (9.18) and (9.19) we calculate expansion coefficients of the anomalous dimensions (9.19) in the strong coupling constant α_s . These numerical results will be presented in the next sections.

9.3 Spectral surfaces

The two-Reggeon energy spectrum is described by the analytical formula (9.22). It is a meromorphic function of ν_h and depends on the integer conformal Lorentz spin n_h . It possesses poles at (9.27).

For higher $N \geq 3$ we do not have an analytical formula, so we have to calculate the spectrum numerically using Eqs. (9.31)–(9.34). The energy $E_N(\nu_h, n_h, \ell)$ is a multi-valued function and its branches are numerated by Lorentz spin n_h and integer parameters $\ell = \{\ell_1, \ell_2, \dots, \ell_{2(N-2)}\}$. These spectra, comparing to the $N = 2$ case, except the poles at (9.30), have additionally an infinite set of branching points at $\nu_h^{\text{br}, k} = \nu_h$ which allows us to glue some branches along their cuts. This causes that the spectrum consists of a set of complicated spectral curves. Thus, we consider the energy $E_N(\nu_h; n_h, \ell)$ as a multi-valued function on complicated Riemann surfaces. The states from a given Riemann surface have the same quantum numbers, i.e. Lorentz spin n_h , C -parity, quasimomentum, Bose symmetry. These numbers impose additional rules for parameters ℓ which describe a single spectral curve on one Riemann surface.

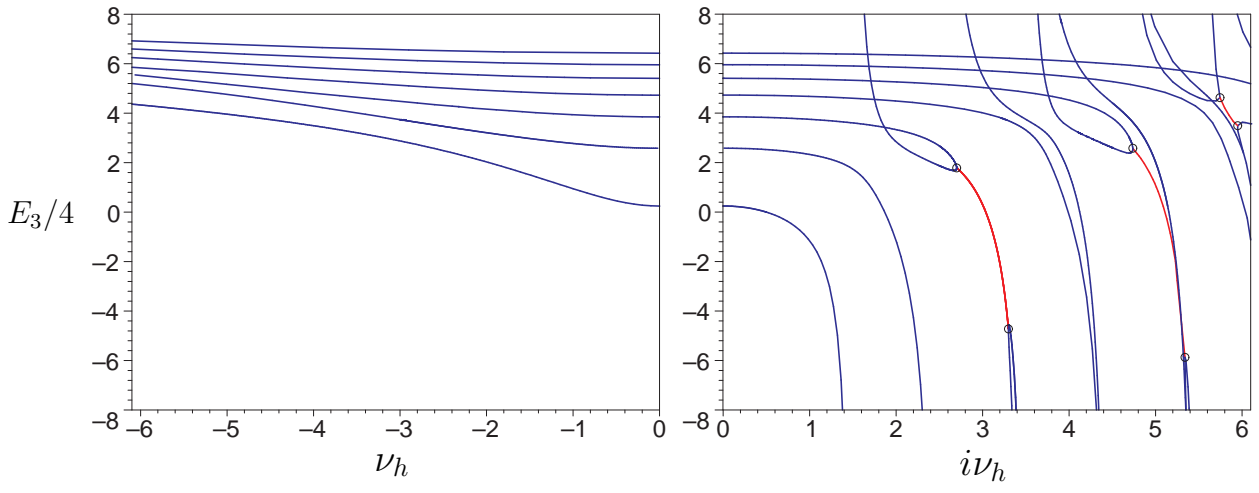


Figure 9.2: The energy spectrum of the $N = 3$ Reggeon states $E_3(\nu_h; n_h, \ell)$ for $n_h = 0$ and $\ell = (0, \ell_2)$, with $\ell_2 = 2, 4, \dots, 14$ from the bottom to the top (on the left). Analytical continuation of the energy along the imaginary ν_h -axis (on the right). The branching points are indicated by open circles. The lines connecting the branching points represent $\text{Re } E_3$.

Let us consider the $N = 3$ Reggeon state along the spectral curves labelled with $\ell_1 = 0$ and $\ell_2 = \text{even positive numbers}$. This gives condition $\bar{q}_k + q_k = 0$. An example of these states is presented in Figure 9.2. On the left panel we plot the energy levels along the real ν_h -axis whereas on the right panel we continue them analytically. Here we show the states for imaginary ν_h only.

For real ν_h the energy is real and the energy levels are smooth functions of real ν_h . Even though that we have only one slice of the spectral curve we are able to observe that, firstly, we have poles at $i\nu_h^{\text{pole}} = 3/2, 5/2, 7/2, 9/2, 11/2$ and, secondly, different energy levels collide at $i\nu_h^{\text{br}} = 2.70, 3.29, 4.73, 5.34, 5.74, 5.94$, which are denoted by circles in Fig. 9.2. Moreover, we have also branching points at complex $i\nu_h^{\text{br}} = 1.723 + i.248$ where the ground state $\ell_2 = 2$ collide with the next state $\ell_2 = 4$. Thus, all these energy levels are glued in the complex ν_h -plane and they form one multi-valued spectral surface.

The complex branching point values ν_h^{br} imply that the contribution of the corresponding square-root cuts to the integral (9.4) scales as $1/[Q^{1+2i\nu_h^{\text{br}}} \ln^{3/2} Q]$ and, therefore, it breaks the OPE expansion (9.5). Although such corrections are present in (9.13) for given n_h and ℓ , they cancel against each other in the sum over all states [26].

Another interesting example of spectral surfaces are $N = 3$ Reggeon states with the Lorentz spin $n_h = 1$ and $q_3 = \bar{q}_3 = 0$. They are descendent states and their energy levels coincide with the levels for $N = 2$ Reggeon states. Performing analytical continuation we notice that $q_3(\nu_h) = \bar{q}_3(\nu_h) = 0$ and $E_{3,d}(\nu_h) = E_2(\nu_h, 1)$ on the whole complex ν_h -plane, where $E_2(\nu_h; 1)$ is defined by (9.22).

Therefore, the energy of this state $E_{3,d}(\nu_h)$ is a single-valued meromorphic function on the complex ν_h -plane. At $\nu_h = 0$ the energy $E_{3,d}(\nu_h)$ vanishes and at this point we have the

“physical” ground state for the system of $N = 3$ Reggeons. Similarly to the $N = 2$ case, the descendent states have poles at (9.27).

In the above example of the $N = 3$ Reggeon states we have presented two special states $E_3(\nu_h = 0, \nu_h = 1) = 0$ and $E_3(\nu_h = 0, \nu_h = 0)/4 = 0.24717$, which are considered as the ground states for the odderon in QCD with the intercept $j_0 = 1 - \bar{\alpha}_s E_3$ [18, 53]. We notice that the minimal twist corresponds to the position of the energy pole in the complex ν_h -plane which is the nearest to the origin, $q_k = \bar{q}_k = 0$.

Thus, for $n_h = 1$ we have the minimal twist $n_{min} = 3$ whereas for $n_h = 0$ we have the minimal twist $n_{min} = 4$. Therefore, the leading contribution to the structure function (9.3) with the intercepts $j_0 = 1$ and $j_0 < 1$ scales at large Q^2 as $\sim 1/Q^3$ and $\sim 1/Q^4$, respectively.

9.4 Energy poles and the anomalous dimensions

In order to evaluate the anomalous dimensions of N Reggeon states around $\gamma_a(\alpha_s = 0) = 0$ we work out the Laurent expansion of the energy function around its poles (9.18). As we said before the energy possesses the poles at $i\nu_h = (n - 1)/2$ with the twist $n \geq N + n_h$ and the Lorentz spin n_h .

Firstly, let us consider the descendent states for $N = 3$ Reggeons with $n_h = 1$. They are related to $N = 2$ Reggeon states, so they have equal energies $E_{3,d}(\nu_h) = E_2(\nu_h, 1)$ defined in (9.22). The pole which is the closest to the origin is located at $i\nu_h = 1$. Thus, $(h, \bar{h}) = (2, 1)$ and the twist $n = h + \bar{h} = 3$. Expanding (9.22) around this pole we get

$$E_{3,d}(2 + \epsilon) = 4 \left(\frac{1}{\epsilon} + 1 - \epsilon - (2\zeta(3) - 1) \epsilon^2 + \dots \right). \quad (9.35)$$

Next, using (9.35) and (9.18) with (9.19) we find the twist-3 anomalous dimension corresponding to the odderon state with the intercept $j_0 = 1$ as

$$\gamma_3^{(N=3)}(j) = \frac{\bar{\alpha}_s}{j-1} - \left(\frac{\bar{\alpha}_s}{j-1} \right)^2 + (2\zeta(3) + 1) \left(\frac{\bar{\alpha}_s}{j-1} \right)^4 + \dots, \quad (9.36)$$

where the subscript and the superscript denote the twist and the number of Reggeons in the given state, respectively.

For the $N = 3$ case with $q_3 \neq 0$ we do not have analytical formula for the energy. However, applying (9.31)- (9.34) we are able to fit numerically the expansion coefficients of the energy around its poles.

Let us consider the spectral surfaces with $n_h = 0$, which we show in Fig. 9.2. Applying (9.31)- (9.34), we expand the energy in the vicinity of the poles at $h = 1/2 + i\nu_h = 2, 3, 4, 5$ with $E_3 = E_3(h + \epsilon)$:

$$E_3(2 + \epsilon) = 4 \left(\epsilon^{-1} + \frac{1}{2} - \frac{1}{2} \epsilon + 1.7021 \epsilon^2 + \dots \right),$$

$$\begin{aligned}
E_3(3 + \epsilon) &= 4 \left(2\epsilon^{-1} + \frac{15}{8} - 1.6172 \epsilon + 0.719 \epsilon^2 + \dots \right), \\
E_3^{(a)}(4 + \epsilon) &= 4 \left(\epsilon^{-1} + \frac{11}{12} - 0.6806 \epsilon - 1.966 \epsilon^2 + \dots \right), \\
E_3^{(b)}(4 + \epsilon) &= 4 \left(2\epsilon^{-1} + \frac{15}{4} - 3.2187 \epsilon + 3.430 \epsilon^2 + \dots \right), \\
E_3^{(a)}(5 + \epsilon) &= 4 \left(2\epsilon^{-1} + \frac{125}{48} - 2.0687 \epsilon + 1.047 \epsilon^2 + \dots \right), \\
E_3^{(b)}(5 + \epsilon) &= 4 \left(2\epsilon^{-1} + \frac{53}{12} - 2.4225 \epsilon + 0.247 \epsilon^2 + \dots \right). \tag{9.37}
\end{aligned}$$

Here $\epsilon \rightarrow 0$ and ellipses denote $\mathcal{O}(\epsilon^3)$ terms. Since the energy is defined on complicated Riemann surfaces, therefore for one Riemann surface at the same given ν_h we have many branches and at some given ν_h we may have many poles. Thus, we introduce the superscripts (a) and (b) to distinguish different branches of spectral curves as well as different poles at the same ν_h .

In this case the nearest pole is at $\nu_h = 3/2$. Therefore, the minimal twist equals $n = h + \bar{h} = 4$. Now applying (9.18) and (9.19) we find from the first relation in (9.37) the anomalous dimension corresponding to the odderon state with the intercept $j_0 < 1$ as

$$\gamma_4^{(N=3)}(j) = \frac{\bar{\alpha}_s}{j-1} - \frac{1}{2} \left(\frac{\bar{\alpha}_s}{j-1} \right)^2 - \frac{1}{4} \left(\frac{\bar{\alpha}_s}{j-1} \right)^3 - 1.0771 \left(\frac{\bar{\alpha}_s}{j-1} \right)^4 + \dots \tag{9.38}$$

Similarly, we may calculate the other anomalous dimensions from (9.37). However, to save the space we do not present them here.

All expansion series formulae for the energies around its poles may be written as

$$E_3(h + \epsilon) = 4 \left(\frac{R}{\epsilon} + \gamma(h) + \mathcal{O}(\epsilon) \right), \tag{9.39}$$

where the parameter R is integer and it is equal to 1 or 2. Moreover, the function $\gamma(h)$ is a rational number and is related to the energy of the Heisenberg $SL(2, \mathbb{R})$ magnet model. More details concerning the properties of $\gamma(h)$ can be found in Refs. [66, 67]. Because it is not the topic of this thesis we omit this interesting subject.

Now, let us consider cases with $N \geq 4$ Reggeon states. For even N the main contributions comes from the sector with $n_h = 0$. The closest poles to the origin are located at $i\nu_h = (N-1)/2$ so the lowest twist $n = N$. These states build Pomeron states. For instance, the expansion series of the energy for $N = 4$ and $N = 6$ states which give the highest contribution look as follows

$$\begin{aligned}
E_4(2 + \epsilon) &= 4 \left(\frac{2}{\epsilon} + 1 - \frac{1}{2} \epsilon - 1.2021 \epsilon^2 + \dots \right), \\
E_6(3 + \epsilon) &= 4 \left(\frac{4}{\epsilon} + \frac{3}{2} - \frac{7}{16} \epsilon - 0.238 \epsilon^2 + \dots \right). \tag{9.40}
\end{aligned}$$

Applying Eqs. (9.18) and (9.19), we obtain the twist- N anomalous dimensions of the N -Reggeon states

$$\begin{aligned}\gamma_4^{(N=4)}(j) &= 2\frac{\bar{\alpha}_s}{j-1} + 2\left(\frac{\bar{\alpha}_s}{j-1}\right)^2 - 13.6168\left(\frac{\bar{\alpha}_s}{j-1}\right)^4 + \dots, \\ \gamma_6^{(N=6)}(j) &= 4\frac{\bar{\alpha}_s}{j-1} + 6\left(\frac{\bar{\alpha}_s}{j-1}\right)^2 + 2\left(\frac{\bar{\alpha}_s}{j-1}\right)^3 - 33.23\left(\frac{\bar{\alpha}_s}{j-1}\right)^4 + \dots\end{aligned}\quad (9.41)$$

The higher corrections are large and grow with N so the expansion series (9.40) has finite radius of convergence and its value decreases with N . This agrees with the fact that the intercept of N -Reggeon state scales at large N as $|j_N - 1| \sim 1/N$ [23].

In the case with odd N , we consider two interesting sectors: with $n_h = 0$ and $n_h = 1$. In the first sector the pole closest to the origin is located at $i\nu_h = N/2$. These gives the minimal twist $n = N + 1$. For $N = 3$ we have written expression for the energies and the anomalous dimensions in (9.37) and (9.38). For $N = 5$ they look like

$$\begin{aligned}E_5(3 + \epsilon) &= 4\left(\frac{3}{\epsilon} + \frac{7}{6} - \frac{101}{216}\epsilon - 0.1136\epsilon^2 + \dots\right), \\ \gamma_6^{(N=5)}(j) &= 3\frac{\bar{\alpha}_s}{j-1} + \frac{7}{2}\left(\frac{\bar{\alpha}_s}{j-1}\right)^2 - \frac{1}{8}\left(\frac{\bar{\alpha}_s}{j-1}\right)^3 - 13.032\left(\frac{\bar{\alpha}_s}{j-1}\right)^4 + \dots\end{aligned}\quad (9.42)$$

These states possess the odderon quantum numbers and have intercepts $j_{\mathbb{O}} = 1 - \bar{\alpha}_s E_5^{(\text{br})}$ lower than 1.

In the second sector, with odd N and $n_h = 1$ the minimal twists are smaller and they are equal to $n = N$. It corresponds to the poles of the energy at $i\nu_h = (N - 1)/2$. At $N = 5$ we have the Laurent expansions as follows

$$\begin{aligned}E_{5,d}(3 + \epsilon) &= 4\left(\frac{3 + \sqrt{5}}{2\epsilon} + 1.36180 - 0.4349\epsilon - 0.315\epsilon^2 + \dots\right), \\ \gamma_5^{(N=5)}(j) &= \frac{3 + \sqrt{5}}{2}\frac{\bar{\alpha}_s}{j-1} + 3.56524\left(\frac{\bar{\alpha}_s}{j-1}\right)^2 + 1.8743\left(\frac{\bar{\alpha}_s}{j-1}\right)^3 - 11.219\left(\frac{\bar{\alpha}_s}{j-1}\right)^4 + \dots\end{aligned}\quad (9.43)$$

For $N = 3$ the results are shown in (9.35)–(9.36). The poles belong to the same spectral surfaces that contain the ground states for given odd number of particles N . Because, these ground states are descendent ones, they have minimum energy $E_N = 0$, the intercept $j_{\mathbb{O}} = 1$ and finally they have the odderon quantum numbers.

Chapter 10

Summary and Conclusions

In this work we have considered the scattering processes in the Regge limit (2.2) where the compound reggeized gluon states, i.e. Reggeons, propagate in the t -channel and interact with each other. We have performed calculations in the generalized leading logarithm approximation (GLLA) [7, 8, 9], in which a number of Reggeons in the t -channel is constant. In this approach the reggeized gluon states appear in two different kinematical regions. Thus, we have considered both of them, i.e. the elastic scattering processes (2.1) as well as the deep inelastic scattering processes (9.1). We attempted to find a scattering amplitude of the above processes with multi-Reggeon exchange. However, a structure of reggeized gluon states as well as their properties have turned out to be so reach, complicated and interesting that in this work we have focused on description of the Reggeon state properties as well as on analysing the spectra of the energy and integrals of motion.

In order to simplify the problem we have applied the multi-colour limit [10], which makes the N -Reggeon system $SL(2, \mathbb{C})$ (2.26) symmetric (2.27) and completely integrable. In this limit the equation for the N -Reggeon wave-function takes a form of Schrödinger equation (2.34) for the non-compact XXX Heisenberg magnet model of $SL(2, \mathbb{C})$ spins s [68, 44, 69]. Its Hamiltonian describes the nearest neighbour interaction of the Reggeons [13, 14] propagating in the two-dimensional transverse-coordinates space (2.9). The system has a hidden cyclic and mirror permutation symmetry (2.68). It also possesses the set of the $(N - 1)$ of integrals of motion, which are eigenvalues of conformal charges [38], \hat{q}_k and $\hat{\bar{q}}_k$, (2.66)–(2.67). Therefore, the operators of conformal charges commute with each other and with the Hamiltonian and they possess a common set of the eigenstates.

Eigenvalues of the lowest conformal charge, q_2 , may be parameterized (5.2) by the complex spins s and the conformal weight h , where h can be expressed by the integer Lorentz spin n_h and the real parameter ν_h related to the scaling dimension (2.60). Solving the eigenequation for q_2 we have derived ansatzes for N -Reggeons states with an arbitrary number of Reggeons N as well as arbitrary complex spins s (5.11). Since the $N = 3$ Reggeon ansatz separates variables, the q_3 -eignequation can be rewritten as a differential equation of a Fuchsian type with three singular points (5.16) [18]. We have solved this equation by a series method. Gluing

solutions for different singular points, (5.24), (5.29) and (5.33), and taking care for normalization and single-valuedness of the Reggeon wave-function (5.23) we have obtained the quantization conditions (5.41)–(5.42) for integrals of motion $(q_2, \bar{q}_2, q_3, \bar{q}_3)$ which we have solved numerically [23, 50]. For $q_3 = \bar{q}_3 = 0$ the series solutions have a simple form and we are able to resum them. Thus, we have obtained analytical expressions for the three-Reggeon wave-functions with $q_3 = 0$ (5.44)–(5.53). For higher N we obtained a set of $N - 2$ non-separable differential equations which are hard to solve even numerically. We have presented explicitly such equations for $N = 4$ (5.55)–(5.56).

In order to solve the Reggeon problem for more than three particles one can make use of the more sophisticated technique, i.e. the Baxter Q –operator method [38]. It relies on the existence of the operator $\mathbb{Q}(u, \bar{u})$ depending on the pair of complex spectral parameters u and \bar{u} . The Baxter Q –operator has to commute with itself (3.1) and with the conformal charges (3.2). It also has to satisfy the Baxter equations (3.3)–(3.4). Furthermore, the Q –operator has well defined analytical properties, i.e. known pole structure (3.12) and asymptotic behaviour at infinity (3.14). The above conditions fix the Q –operator uniquely and allow us to quantize the integrals q_k . It turns out [38] that the Reggeon Hamiltonian can be rewritten in terms of Baxter Q –operator (3.15). Therefore, combining together the solutions of the Baxter equations and the conditions for q_k with the Schrödinger equation we can calculate the energy spectrum (3.24). Moreover, we are able to determine the quasimomentum of the eigenstates (3.20), i.e. the observable which defines the properties of the state with respect to the cyclic permutation symmetry (2.68).

One can solve the Baxter equations (3.3)–(3.4) using the quasi-classical approach (4.3). Following Refs. [21] we have presented the WKB approximation for the quantized values of q_k (4.18) and explained the structure of their spectrum (4.21). Applying this approximation, one introduces a small parameter η and performs expansion of the Baxter function for large values of q_k . The single-valuedness requirement of the Baxter function gives conditions for q_k in a form of Bohr-Sommerfeld integrals (4.15). Adding the condition coming from the possible values of the quasimomentum (4.16) one obtains the relations between the quantized values of q_k (4.18). However, not all quantization conditions can be obtained from (4.18). It turns out that in the leading order of the WKB approximation for a given value of ν_h the quantized values of $q_N^{1/N}$ correspond to vertices of equilateral lattices (4.21). For lower conformal charges the conditions are underdetermined, i.e. in the $N = 4$ case one has only one of two required conditions (7.23).

In order to obtain the exact values of q_k we have used the method [21, 23] which makes it possible to calculate numerically the spectrum of the conformal charges as well as other observables, i.e. the energy (6.14) and the quasimomentum (6.24). The exact method consists in rewriting the Baxter equations and the other conditions for Q –operator eigenvalues as the N –order differential equation (6.2). This equation can be solved similarly to the q_3 –eigenequation (5.16). Thus, one obtains the conditions for quantized q_k (6.27) and the formulae for the energy (6.14) and the quasimomentum (6.24).

We have applied this exact method for states with $N = 2, \dots, 8$ particles. The quantum values of q_k form continuous trajectories, Fig. 7.3. This fact is related to the dependence of q_2 on the real parameter ν_h (5.2). The energy is a continuous function of ν_h so the energy spectrum is gapless. This energy continuity leads to additional logarithmic dependence of the scattering amplitude (7.3) on the total energy s . The energy changes continuously along the trajectory (7.2) and reaches the lowest value in the vicinity of $\nu_h = 0$. Moreover, since the q_k spectrum possesses symmetries, (7.4) and (7.5), the energy for some cases is degenerated.

For $N = 3$ we have calculated the behaviour of the q_3 -spectrum for the conformal Lorentz spins $n_h = 0, 1, 2, 3$ and the scaling dimension $1 + 2i\nu_h$. Some results for $n_h > 0$ were presented before in Ref. [27] for $n_h = 1$ and Refs. [50] for $n_h = 3$. The quantized values of $q_3^{1/3}$ for given n_h and fixed ν_h exhibit the WKB lattice structure (4.21), which for $N=3$ takes a form an equilateral-triangle lattice (7.11), Figs. 7.1-7.5. The non-leading WKB corrections move the quantized value of q_3 away from the lattice and cause that the quantized values of q_3 lie outside a disk located around the origin of the lattice, i.e. near $q_3 = 0$. However, for odd n_h there are states with $q_3 = 0$. They are called descendent states because their wave-function is effectively built of $N = 2$ Reggeon states. The non-descendent state with the lowest energy belongs to $n_h = 0$ sector and its energy is positive (7.15). This state is double-degenerated and it appears to be the nearest one to the origin of the $q_3^{1/3}$ lattice. However, the ground state for $N = 3$ is the descendent one with $n_h = 1$ and energy $E_3 = 0$ (7.16). Having found the exact values of q_3 we are able to calculate corrections to the WKB approximation (7.20), Table 7.2. These corrections differ from the corrections obtained earlier in Ref. [21]. The difference seems to be caused by using only one expansion parameter η for two various conformal charges, q_2 and q_3 . The obtained corrections are subleading to the WKB approximation [21] which is an expansion for large values of conformal charges, i.e. $1 \ll |q_2^{1/2}| \ll |q_3^{1/3}|$.

In the case with $N = 4$ particles we have constructed the spectrum for $n_h = 0$ depicting complicated interplay between the conformal charges: q_3 and q_4 . Such a complete analysis has been performed here for the first time. Earlier, for $N = 4$ full spectrum of q_4 was shown in Ref. [23] (however the corresponding q_3 spectrum was not discussed) and some values of q_4 were found in Ref. [27]. The spectrum of $q_4^{1/4}$ has a structure of square-like lattice (7.24), Fig. 7.7. In this case the spectrum of q_3 is more complicated. It turns out that it has a few possible forms. Firstly, there are simple states with $q_3 = 0$, Fig. 7.8. Moreover, we have found the $q_3^{1/2}$ -lattices whose distribution of vertices is similar to the distribution of vertices of $q_4^{1/4}$ -lattice. We have called this structures as resemblant lattices, Figs 7.10-7.13. The next $q_3^{1/2}$ -lattices are called winding lattices. They wind around the origin and in course of this winding the distance between vertices increases and also the lattice goes away from the origin, Figs. 7.14-7.16. The WKB approximation does not describe these structures (7.23) exactly because one quantization condition is missing. Finally, we have also considered the descendent states with $q_4 = 0$, Fig. 7.8. They have quasimomentum $\theta_4 = \pi$ and the structure of their $q_3^{1/3}$ -lattices is the same as for $q_3^{1/3}$ -lattices (7.11) in the three-Reggeon case with $\theta_4 = 0$. For the $N = 4$ Reggeon

states with $q_3 = 0$ we have calculated corrections to the WKB approximation (7.30), Table 7.4. Similarly to the $N = 3$ case they come from the fact of using only one expansion parameter η for two different conformal charges, q_4 and q_2 . One has to notice that these corrections are subleading in comparison to the WKB limit [21].

For $N > 4$ we have more conformal charges so their spectrum is more complicated. Therefore, in these cases we have been concentrating only on the ground states, Table 7.5. Thus, we have shown the dependence of the ground state energy as a function of particle number $N = 2, \dots, 8$ (7.38)–(7.37) [22], Fig. 7.17. When we enlarge number of particles N the energy seems to go to zero as $1/N$. For even N the energy of the ground state is negative so the contribution of the even ground states to the scattering amplitude increases with the total energy s . For odd N we have to consider separately the descendent states with $q_N = 0$ and non-descendent ones. For the latter states the energy is positive so the contribution to the scattering amplitude decreases with s . For the states with $q_N = 0$ the lowest energy $E_N = 0$. Therefore, the descendent states include the ground states for odd N . Additionally, we have calculated the energy along the ground state trajectories for $N = 2, \dots, 8$ as a function of ν_h , Fig. 7.18. These functions are symmetric in ν_h . The minimum energy is in $\nu_h = 0$. The order of these energy levels tell us that the system for $\nu_h = 0$ is anti-ferromagnetic one. Increasing ν_h we have observed reordering of the energy levels which makes the system for a large ν_h ferromagnetic.

Next we have made comments on the approach of the Baxter Q –operator method presented in Ref. [28, 27]. The authors of this approach solve the Baxter equation by using the pole ansatz (8.1) whereas the quantization conditions come from the normalization requirement and condition of equality of holomorphic energies (8.9) for different holomorphic solutions to the Baxter equation. We claim the the latter condition is too strong because the Reggeon system is two dimensional so the holomorphic energy is not a physical observable.

At the end, we have passed to the deep inelastic scattering region where Reggeon states allow us to investigate properties of the structure function (9.3) of the scattered hadron [24]. Performing analytical continuation of the energy into complex ν_h we have calculated the anomalous dimensions as functions of the strong coupling constant (9.7) and the respective twists (9.21) [26] which have been determined for each N separately. The case with $N = 2$ was discussed in Refs. [24, 25]. It turns out that after the analytical continuation the energy for $N > 2$ is multi-valued function defined on the complicated Riemann surfaces and possesses branching points and poles [70, 71, 72, 26], Fig. 9.2. The poles (9.30) occur on imaginary axis of ν_h and their positions correspond to the twist n of the structure functions while expansion coefficients of the energy around the poles (9.18) are related to expansion coefficients of anomalous dimensions $\gamma(\overline{\alpha}_s)$ in the strong coupling constant $\overline{\alpha}_s$ (9.19). Thus, we have found [26] that for N Reggeon system the minimal twist $n = N$. However, for even N it is formed by the states belonging to the $n_h = 0$ sector while for odd N it corresponds to the $n_h = 1$ sector.

Thus, we have become convinced that although the Q –Baxter method is complicated it

is a powerful tool. It allows us to solve the reggeized gluon state problem for more than $N = 3$ particles. The above calculations are of interest not only for perturbative QCD but also to statistical physics as the $SL(2, \mathbb{C})$ non-compact XXX Heisenberg spin magnet model [68, 44, 69].

One has to mention that in this work we have not calculated all pieces of an elastic scattering amplitude but only the part that is responsible for the dependence on the total energy s (7.3), which is determined by the intercept $j = 1 - \bar{\alpha}_s E_N/4$. Similarly, in the deep inelastic scattering processes we have only identified exponents of the operator product expansion (OPE) series which are related to the twists and anomalous dimensions of the structure function $F_2(x, Q^2)$ (9.3). In order to find the full scattering amplitude one has to calculate the impact factors (9.9), i.e. overlaps between the Reggeon wave function and the wave functions of the scattered particles. These impact factors strongly depend on the scattered system and they are hard to calculate due to a large number of integrations. Therefore, with more than $N = 2$ Reggeons only overlaps of the simplest Reggeon states were calculated, i.e. in the $\eta_c \rightarrow \gamma^*(q)$ diffractive process [59, 60, 61], the double-diffractive production of J/ψ [73], photon-photon processes [74, 75, 76, 77] as well as the proton-proton scattering process [78] and other similar processes.

One has to remember that apart from the GLLA method presented in this work there are other techniques which also make use of the reggeized gluons. Firstly, one may use the extended leading logarithm approximation (EGLLA) [35, 36, 79] where the number of gluons in the t -channel may fluctuate. Moreover, Balitsky and Kovchegov [80, 81, 82] derived a non-linear differential (BK) equation that for the two-Reggeon Pomeron contains the linear BFKL equation and additionally the non-linear terms which for higher energy s describe the saturation effect [82, 83, 84, 70]. Furthermore, one can use the dipole model [85, 86, 87, 88, 56], the colour glass model [89, 90, 91, 92] or the Wilson loop operators model [93, 94] in order to derive or explain diagrammatically the BK equation. All these methods seem to be equivalent in the leading order to the BFKL. However, they include different non-leading corrections which cause that the different approaches better describe the scattering processes in different kinematical regions [34].

This work opens the way for further studies related to the multi-Reggeon states. Using the method presented in Refs. [21, 22, 23] it will be interesting to calculate the spectrum of the conformal charges for $N = 4$ and $n_h \neq 0$ and compare them to results obtained in Refs. [27, 28]. Additionally, increasing precision one may try to find the energy of the ground states for $N > 8$ and confirm the dependence $E_N \sim 1/N$. It is also of interest to perform analytical continuation of the energy for the states which have not been considered here and calculate their twist and anomalous dimensions. Moreover, we have mentioned that there are attempts to calculate the scattering processes with Reggeon exchange where a number of exchanging reggeized gluons varies in the t -channel, i.e. Extended GLLA method [35, 36, 79]. These diagrams start to be important at higher energy s [34] and describe saturation which might allow to unitarize the scattering amplitude. To complete this picture one should also include the diagrams with $N > 2$

Reggeon states and the diagrams containing vertices of N Reggeons going into M Reggeons for any N and M . These diagrams would allow to calculate the DIS processes as well as the elastic scattering processes, i.e. onium-onium or proton-proton scattering. Furthermore, we can go beyond the multi-colour approximation and try to calculate NLO BKP diagrams. The next-to-leading order corrections to the BFKL kernel (NLO BFKL) was calculated by Fadin and Lipatov in Ref. [95] and seems to play an important role for really high energy s . This calculation needs further studies. One has to notice the analysis of the multi-colour limit seems to be interesting for the anomalous dimensions of the structure functions in DIS processes and compare to Ref. [96]. At the end we have to say that there is a connection between the GLLA approach and $\mathcal{N} = 2$ SUSY gauge theories presented in Ref. [97]. It is very impressive and this topic also needs more research.

Acknowledgements

I would like to warmly thank to Michał Przaszłowicz for fruitful discussions and help during writing this dissertation. I am very grateful to G.P. Korchemsky, A.N.Manashov and S.É. Derkachov I could work with them in early state of this project and without whom this work couldn't be written. I also thank to Jacek Wosiek for illuminating discussions. This work was supported by KBN-PB-2-P03B-43-24 and KBN-PB-0349-P03-2004-27.

Appendix A

$SL(2, \mathbb{C})$ invariants and other variables

Let us consider a difference of coordinates $(z_1 - z_2)$. It changes under the $SL(2, \mathbb{C})$ transformation (2.27) as

$$(z'_1 - z'_2) = \left(\frac{az_1+b}{cz_1+d} - \frac{az_2+b}{cz_2+d} \right) = (cz_1+d)^{-1}(cz_2+d)^{-1}(z_1 - z_2) . \quad (\text{A.1})$$

One can see that during the transformation (A.1) the factors $(cz_i + d)^{-1}$ appear in front of the difference. These factors also exist in the transformation law of the wave-function (2.55). In order to cancel these factors one can construct a fraction where the same additional factors appear in the denominator and numerator of the constructed fraction variable.

The fraction variable

$$x = \frac{(z_1 - z_2)(z_3 - z_0)}{(z_1 - z_0)(z_3 - z_2)} \equiv (z_1 z_2 z_3 z_0) \quad (\text{A.2})$$

is invariant under the $SL(2, \mathbb{C})$ transformations (2.27). It is only one independent invariant for four coordinates [39, 98]. One can see that the fractions coming from the $SL(2, \mathbb{C})$ transformation simplified because:

- the variable is a function of the coordinate differences (A.1),
- the coordinates in the numerator and denominator of the variable x are the same.

Therefore, simplifying the partial fractions we can obtain expression like $((az_i + b)(cz_j + d) - (az_j + b)(cz_i + d))$ which with making use of $ad - cb = 1$ goes to $(z_i - z_j)$. As we can see, we have to build our invariants from differences of the coordinates.

It is easy to see that performing permutations of coordinates we can construct six different dependent invariants

$$\begin{aligned} (z_1 z_2 z_3 z_0) &= x, & (z_3 z_2 z_1 z_0) &= 1/x, \\ (z_2 z_3 z_1 z_0) &= 1/(1-x), & (z_1 z_3 z_2 z_0) &= 1-x, \\ (z_3 z_1 z_2 z_0) &= (x-1)/x, & (z_2 z_1 z_3 z_0) &= x/(x-1). \end{aligned} \quad (\text{A.3})$$

Let us take another product of z_{ij}

$$w' = \frac{(z'_1 - z'_2)}{(z'_1 - z'_0)(z'_2 - z'_0)} = (cz_0 + d)^2 \frac{(z_1 - z_2)}{(z_1 - z_0)(z_2 - z_0)} = (cz_0 + d)^2 w . \quad (\text{A.4})$$

One can see that since in the denominator we have two additional z_0 variables after the transformation we obtain a multiplying factor $(cz_0 + d)^2$. Similarly for w^h we obtain

$$w^h = (cz_0 + d)^{2h} w^h. \quad (\text{A.5})$$

Now one can compare this transformation to the transformation of the $SL(2, \mathbb{C})$ wave-function (2.55).

For $N = 3$ the variables $w = \frac{(z_3 - z_2)}{(z_3 - z_0)(z_2 - z_0)}$ and $x = \frac{(z_1 - z_2)(z_3 - z_0)}{(z_1 - z_0)(z_3 - z_2)}$ transform under the cycling permutation (2.68) as

$$\begin{aligned} (x - 1) &\rightarrow \frac{(-x)}{(x-1)} \rightarrow \frac{1}{(-x)} \rightarrow (x - 1), \\ (-x) &\rightarrow \frac{1}{(x-1)} \rightarrow \frac{(x-1)}{(-x)} \rightarrow (-x), \\ w &\rightarrow w(x - 1) \rightarrow w(-x) \rightarrow w \end{aligned} \quad (\text{A.6})$$

while under the mirror permutation:

$$\begin{aligned} (x - 1) &\rightarrow \frac{(x-1)}{(-x)} \rightarrow (x - 1) \\ (-x) &\rightarrow \frac{1}{(-x)} \rightarrow (-x) \\ w &\rightarrow w x \rightarrow w \end{aligned} \quad (\text{A.7})$$

For higher N we have more invariants. All of them can be constructed [51] from

$$x_r = \frac{(z_{r-1} - z_r)(z_{r+1} - z_0)}{(z_{r-1} - z_0)(z_{r+1} - z_r)}; \quad \prod_{r=1}^N x_r = (-1)^N; \quad \sum_{r=1}^N (-1)^r \prod_{k=r+1}^N x_k = 0. \quad (\text{A.8})$$

Variables x_r are subject to the two conditions:

$$\prod_{r=1}^N x_r = (-1)^N \quad (\text{A.9})$$

and

$$\sum_{r=1}^N (-1)^r \prod_{k=r+1}^N x_k = 0. \quad (\text{A.10})$$

From (A.9) we have $x_1 = (-1)^N / \prod_{r=2}^N x_r$. From (A.10) we can calculate

$$x_2 = \frac{\sum_{r=2}^N (-1)^r \prod_{k=r+1}^N x_k}{\prod_{k=3}^N x_k}. \quad (\text{A.11})$$

Interchangeably, one can derive from (A.9) $x_N = (-1)^N / \prod_{r=1}^{N-1} x_r$ and next from (A.10)

$$x_{N-1} = \frac{(-1)^N}{\sum_{r=1}^{N-1} (-1)^r \prod_{k=r}^{N-2} x_k}. \quad (\text{A.12})$$

Thus, we can see that we have for N particles $N - 2$ independent invariants built of the particle coordinates z_i .

Appendix B

Solution of the q_2 eigenproblem

B.1 Case for $N = 2$

For two particles, i.e. $N = 2$, we do not have any invariant variables x_j , (A.8). Substituting (5.1) into the equation (5.3) we obtain

$$\hat{q}_2(z_{10})^{k_{10}}(z_{20})^{k_{20}}(z_{12})^{k_{12}} = (-h(h-1) + s_1(s_1-1) + s_2(s_2-1)) (z_{10})^{k_{10}}(z_{20})^{k_{20}}(z_{12})^{k_{12}}. \quad (\text{B.1})$$

Next, solving (B.1) for k_{ij} we get the eigenstates:

1. $\psi_1(z_{10}, z_{20}) = (z_{10})^{-h-s_1+s_2}(z_{20})^{-h+s_1-s_2}(z_{12})^{h-s_1-s_2},$
2. $\psi_2(z_{10}, z_{20}) = (z_{10})^{-1+h-s_1+s_2}(z_{20})^{-1+h+s_1-s_2}(z_{12})^{1-h-s_1-s_2}.$

The first solution transforms with the proper factor $(cz_0 + d)^{2h}(cz_1 + d)^{2s_1}(cz_2 + d)^{2s_2}$. The second one has $h \rightarrow 1 - h$.

A full eigenstate of \hat{q}_2 with $N = 2$ can be presented as a linear combination of the difference-coordinate products. It comes from the fact that during the $SL(2, \mathbb{C})$ transformation the factor $(cz_i + d)^{2s}$ have to be obtained (2.55). Thus, the eigenstate, up to some normalization factor, has a form [15, 4, 16]

$$\Psi(z_{10}, z_{20}) = (z_{10})^{-h-s_1+s_2}(z_{20})^{-h+s_1-s_2}(z_{12})^{h-s_1-s_2} = \left(\frac{z_{12}}{z_{20}z_{10}}\right)^h \left(\frac{z_{20}}{z_{12}z_{10}}\right)^{s_1} \left(\frac{z_{10}}{z_{12}z_{20}}\right)^{s_2}. \quad (\text{B.2})$$

For the homogeneous model, i.e. $s = s_i$,

$$\psi(z_{10}, z_{20}) = (z_{10})^{-h}(z_{20})^{-h}(z_{12})^{h-2s} = z_{12}^{-2s} \left(\frac{z_{12}}{z_{10}z_{20}}\right)^h. \quad (\text{B.3})$$

In the special case for $s = 0$ it leads to

$$\psi(z_{10}, z_{20}) = (z_{10})^{-h}(z_{20})^{-h}(z_{12})^h = \left(\frac{z_{12}}{z_{10}z_{20}}\right)^h \quad (\text{B.4})$$

while for $s = 1$ it gives

$$\psi(z_{10}, z_{20}) = (z_{10})^{-h}(z_{20})^{-h}(z_{12})^{h-2} = \frac{1}{z_{12}^2} \left(\frac{z_{12}}{z_{10}z_{20}}\right)^h = \frac{1}{z_{10}^2 z_{20}^2} \left(\frac{z_{12}}{z_{10}z_{20}}\right)^{h-2}. \quad (\text{B.5})$$

B.2 Case for $N = 3$

In this case, the solutions with z_0 can be reduced to one independent function

$$\begin{aligned}
\psi(z_{10}, z_{20}, z_{30}) &= (z_{10})^{-h+k_{32}-s_1+s_2+s_3} (z_{12})^{k_{12}} (z_{20})^{-k_{32}-k_{12}-2s_2} (z_{30})^{-h+k_{12}+s_1+s_2-s_3} \\
&\quad \times (z_{31})^{h-k_{32}-k_{12}-s_1-s_2-s_3} (z_{32})^{k_{32}} = \\
&= (z_{10})^{-h-s_1+s_2+s_3} (z_{20})^{-2s_2} (z_{30})^{-h+s_1+s_2-s_3} (z_{31})^{h-s_1-s_2-s_3} \left(\frac{-x}{x-1}\right)^{k_{12}} \left(\frac{1}{x-1}\right)^{k_{32}}
\end{aligned} \tag{B.6}$$

and to the other one with $h \rightarrow 1-h$. It is invariant under the cyclic permutation and contains two free parameters, k_{12} and k_{32} .

For $N = 3$, there is one independent invariant variable (A.2), e.g. $x = x_2$. Next, we multiply our wave-function by an arbitrary function of x , $F(x)$. There is only one pattern of the eigenfunction which satisfy the eigenequation for q_2 and the $SL(2, \mathbb{C})$ transformation (2.55) law. This eigenfunction looks like

$$\begin{aligned}
\Psi(z_{10}, z_{20}, z_{30}) &= (z_{10})^{-h-s_1+s_2+s_3} (z_{20})^{-2s_2} (z_{30})^{-h+s_1+s_2-s_3} (z_{31})^{h-s_1-s_2-s_3} F(x) = \\
&= \frac{1}{(z_{10})^{2s_1} (z_{20})^{2s_2} (z_{30})^{2s_3}} \left(\frac{z_{31}}{z_{10}z_{30}}\right)^{h-s_1-s_2-s_3} F(x).
\end{aligned} \tag{B.7}$$

For the homogeneous model ($s = s_i$) we have an ansatz

$$\Psi(z_{10}, z_{20}, z_{30}) = (z_{10})^{-h+s} (z_{20})^{-2s} (z_{30})^{-h+s} (z_{31})^{h-3s} F(x) = \frac{1}{(z_{10}z_{20}z_{30})^{2s}} \left(\frac{z_{31}}{z_{10}z_{30}}\right)^{h-3s} F(x) \tag{B.8}$$

Substituting $s = 0$ we have

$$\Psi(z_{10}, z_{20}, z_{30}) = (z_{10})^{-h} (z_{30})^{-h} (z_{31})^h F(x) = \left(\frac{z_{31}}{z_{10}z_{30}}\right)^h F(x), \tag{B.9}$$

whereas for $s = 1$, it is

$$\Psi(z_{10}, z_{20}, z_{30}) = (z_{10})^{-h+1} (z_{20})^{-2} (z_{30})^{-h+1} (z_{31})^{h-3} F(x) = \frac{1}{(z_{10}z_{20}z_{30})^2} \left(\frac{z_{31}}{z_{10}z_{30}}\right)^{h-3} F(x). \tag{B.10}$$

B.3 Case for $N = 4$

Here, like in the previous cases, we have also four 2×2 solutions. When we take solutions with z_0 they reduce into two functions:

$$\begin{aligned}
\Psi(z_{10}, z_{20}, z_{30}, z_{40}) &= (z_{10})^{-k_{12}-k_{31}-k_{14}-2s_1} (z_{12})^{k_{12}} (z_{20})^{-h+k_{31}+k_{34}+k_{14}+s_1-s_2+s_3+s_4} (z_{24})^{k_{24}} \\
&\quad \times (z_{30})^{-h+k_{24}+k_{12}+k_{14}+s_1+s_2-s_3+s_4} (z_{34})^{k_{34}} (z_{40})^{-k_{24}-k_{34}-k_{14}-2s_4} \\
&\quad \times (z_{14})^{k_{14}} (z_{31})^{k_{31}} (z_{32})^{-h-k_{24}-k_{12}-k_{31}-k_{34}-k_{14}-s_1-s_2-s_3-s_4}
\end{aligned} \tag{B.11}$$

and the other one is with $h \rightarrow 1-h$. The function (B.11) is invariant under cyclic permutation and contains two free parameters.

In the $N = 4$ case we have $N - 2 = 2$ independent invariant variables. Let us take $x_1 = \frac{(z_4 - z_1)(z_2 - z_0)}{(z_4 - z_0)(z_2 - z_1)}$ and $x_2 = \frac{(z_1 - z_2)(z_3 - z_0)}{(z_1 - z_0)(z_3 - z_2)}$. We multiply our wave-function by an arbitrary function of these variables, $F(x_1, x_2)$. Considering (2.55), we obtain a solution for the q_2 -eigenequation

$$\begin{aligned}\Psi(z_{10}, z_{20}, z_{30}, z_{40}) &= (z_{10})^{-k_{12}-k_{31}-k_{14}-2s_1} (z_{12})^{k_{12}} (z_{20})^{-h+k_{31}+k_{34}+k_{14}+s_1-s_2+s_3+s_4} (z_{24})^{k_{24}} \\ &\quad \times (z_{30})^{-h+k_{24}+k_{12}+k_{14}+s_1+s_2-s_3+s_4} (z_{34})^{k_{34}} (z_{40})^{-k_{24}-k_{34}-k_{14}-2s_4} \\ &\quad \times (z_{14})^{k_{14}} (z_{31})^{k_{31}} (z_{32})^{-h-k_{24}-k_{12}-k_{31}-k_{34}-k_{14}-s_1-s_2-s_3-s_4} f(x_1, x_2) = \\ &= \frac{1}{(z_{10})^{2s_1} (z_{20})^{2s_2} (z_{30})^{2s_3} (z_{40})^{2s_4}} \left(\frac{z_{31}}{z_{10} z_{30}} \right)^{h-s_1-s_2-s_3-s_4} F(x_1, x_2).\end{aligned}\tag{B.12}$$

For the homogeneous model ($s = s_i$) we have an ansatz

$$\Psi(z_{10}, z_{20}, z_{30}, z_{40}) = \frac{1}{(z_{10} z_{20} z_{30} z_{40})^{2s}} \left(\frac{z_{31}}{z_{10} z_{30}} \right)^{h-4s} F(x_1, x_2).\tag{B.13}$$

For $s = 0$

$$\Psi(z_{10}, z_{20}, z_{30}, z_{40}) = (z_{10})^{-h} (z_{30})^{-h} (z_{31})^h F(x_1, x_2) = \left(\frac{z_{31}}{z_{10} z_{30}} \right)^h F(x_1, x_2)\tag{B.14}$$

and for $s = 1$

$$\begin{aligned}\Psi(z_{10}, z_{20}, z_{30}, z_{40}) &= (z_{10})^{-h+2} (z_{20})^{-2} (z_{30})^{-h+2} (z_{40})^{-2} (z_{31})^{h-4} F(x_1, x_2) = \\ &= \frac{1}{(z_{10} z_{20} z_{30} z_{40})^2} \left(\frac{z_{31}}{z_{10} z_{30}} \right)^{h-4} F(x_1, x_2).\end{aligned}\tag{B.15}$$

Appendix C

Solutions for $N = 3$

C.1 Solutions for $s = 0$ around $x = 0^+$

C.1.1 Solutions for $q_3 \neq 0$ and $h \notin \mathbb{Z}$

The eigenequation for \hat{q}_3 (5.15) is a differential equation of the third order so around each singular point, $x = 0, 1, \infty$, it has three independent solutions. Around $x = 0^+$ we have an indicial equation

$$(h - n - r)(r + n - 1)(n + r) = 0, \quad (\text{C.1})$$

so its solutions are given by $r_1 = h$, $r_2 = 1$ and $r_3 = 0$. As we can see we have two cases when $h \notin \mathbb{Z}$ (one solution with $\text{Log}(x)$) and $h \in \mathbb{Z}$ (one solution with $\text{Log}(x)$ and one solution with $\text{Log}^2(x)$). As we will see below we have to consider separately solutions with $q_3 = 0$. In the first case

$$\begin{aligned} u_1(x) &= x^{r_1} \sum_{n=0}^{\infty} a_{n,r_1} x^n, \\ u_2(x) &= x^{r_2} \sum_{n=0}^{\infty} a_{n,r_2} x^n, \\ u_3(x) &= x^{r_3} \sum_{n=0}^{\infty} b_{n,r_3} x^n + x^{r_2} \sum_{n=0}^{\infty} a_{n,r_2} x^n \text{Log}(x), \end{aligned} \quad (\text{C.2})$$

where $a_{0,r}$ is arbitrary (e.g. equal to 1)

$$a_{1,r} = \frac{(iq_3 - (h - 2r)(h - r)r)}{(h - 1 - r)r(1 + r)} a_{0,r} \quad (\text{C.3})$$

and $m = n + r$

$$\begin{aligned} a_{n,r} &= \frac{(h - m + 1)(h - m + 2)(m - 2)}{(h - m)(m - 1)m} a_{n-2,r} + \\ &\quad + \frac{(iq_3 - (1 + h - m)(m - 1)(h - 2(m - 1)))}{(h - m)(m - 1)m} a_{n-1,r}, \end{aligned} \quad (\text{C.4})$$

whereas $b_{0,r_3} = \frac{(h-1)}{iq_3} a_{0,r_2}$ and b_{1,r_3} is arbitrary. One can notice that coefficient b_{0,r_3} is well defined only for $q_3 \neq 0$. Moreover,

$$b_{2,r_3} = \frac{2+(h-3)h-iq_3}{2(2-h)} b_{1,r_3} + \frac{3h-8}{2(2-h)} a_{1,r_3} + \frac{6+h(h-6)}{2(2-h)} a_{0,r_3} \quad (\text{C.5})$$

and

$$\begin{aligned}
b_{n,r_3} = & \frac{(h+1-m)(h-m+2)(m-2)}{(h-m)(m-1)m} b_{n-2,r_3} + \frac{iq_3-(1+h-m)(m-1)(h-2(m-1))}{(h-m)(m-1)m} b_{n-1,r_3} + \\
& + \frac{h^2+h(7-4m)+(m-2)(3m-4)}{(h-m)(m-1)m} a_{n-3,r_3} - \frac{h^2-6h(m-1)+6(m-1)^2}{(h-m)(m-1)m} a_{n-2,r_3} + \\
& - \frac{2m-3m^2+h(2m-1)}{(h-m)(m-1)m} a_{n-1,r_3} ,
\end{aligned} \tag{C.6}$$

where $m = r_3 + n$.

C.1.2 Solution with $q_3 = 0$

In this case $a_{0,r}$ defined in (C.2) is arbitrary (e.g. equal to 1). For the first solution with $r_1 = h$ we have $a_{1,r_1} = 0$ whereas for the third one a_{1,r_3} is arbitrary (let us take 0). It turns out that we do not need Log-solutions. The second solution is more complicated. One can derive an exact formula for

$$a_{n,r_2} = a_{0,r_2} \prod_{k=1}^n \frac{k-h}{k+1} = \frac{\Gamma(1-h+n)}{\Gamma(1-h)\Gamma(n+2)} a_{0,r_2} \tag{C.7}$$

and performing summations

$$\begin{aligned}
u_1(x) &= x^{r_1} \sum_{n=0}^{\infty} a_{n,r_1} x^n = x^h a_{0,r_1} , \\
u_2(x) &= x^{r_2} \sum_{n=0}^{\infty} a_{n,r_2} x^n = a_{0,r_2} x \sum_{n=0}^{\infty} \frac{\Gamma(1-h+n)}{\Gamma(1-h)\Gamma(n+2)} x^n = -a_{0,r_2} \frac{1}{h} ((1-x)^h - 1) , \\
u_3(x) &= x^{r_3} \sum_{n=0}^{\infty} a_{n,r_3} x^n = a_{0,r_3} .
\end{aligned} \tag{C.8}$$

Gathering together this all solutions we have

$$u(x) = A + B(-x)^h + C(x-1)^h \tag{C.9}$$

where A, B, C are arbitrary. The above solution was presented by Lipatov and Vacca in Refs . [51, 55].

C.1.3 Solution with $q_3 \neq 0$, $q_2 = 0$ and $h = 1$

For $h = 0$, i.e. $q_2 = 0$, and $q_3 \neq 0$ we have a different set of solutions. Here we have three solutions of the indicial equation (C.1) which are integer $r_1 = 1$, $r_2 = 1$, $r_3 = 0$ so the solutions are given by

$$\begin{aligned}
u_1(x) &= x^{r_1} \sum_{n=0}^{\infty} a_{n,r_1} x^n , \\
u_2(x) &= x^{r_2} \sum_{n=0}^{\infty} b_{n,r_2} x^n + x^{r_1} \sum_{n=0}^{\infty} a_{n,r_1} x^n \text{Log}(x) , \\
u_3(x) &= x^{r_3} \sum_{n=0}^{\infty} c_{n,r_3} x^n + 2x^{r_2} \sum_{n=0}^{\infty} b_{n,r_2} x^n \text{Log}(x) + x^{r_1} \sum_{n=0}^{\infty} a_{n,r_1} x^n \text{Log}^2(x) ,
\end{aligned} \tag{C.10}$$

where $a_{0,r}$ is arbitrary (e.g. equal 1)

$$a_{1,r} = \frac{r+r^2(2r-3)}{r^2(1+r)-iq_3} a_{0,r} \tag{C.11}$$

and $m = n + r$

$$a_{n,r} = -\frac{(m-3)(m-2)^2}{(m-1)^2 m} a_{n-2,r} + \frac{(m-2)(m-1)(2m-3)-iq_3}{(m-1)^2 m} a_{n-1,r} , \tag{C.12}$$

whereas

$$b_{1,r_2} = \frac{1}{2}(-iq_3 b_{0,r_2} + a_{0,r_1} - 5a_{1,r_1}) \quad (\text{C.13})$$

$$\begin{aligned} b_{n,r_2} = & -\frac{(n-1)^2(n-2)}{n^2(n+1)}b_{n-2,r_2} + \frac{(2m^3-3m^2+m-iq_3)}{n^2(n+1)}b_{n-1,r_2} + \frac{1+6n(n-1)}{n^2(n+1)}a_{n-1,r_1} + \\ & + \frac{(n-1)(5-3n)}{n^2(n+1)}a_{n-2,r_1} - \frac{(2+3n)}{n(n+1)}a_{n,r_1} \end{aligned} \quad (\text{C.14})$$

while $c_{0,r_3} = \frac{-2}{iq_3}a_{0,r_1}$, c_{1,r_3} is arbitrary and

$$c_{2,r_3} = -\frac{1}{2}iq_3 c_{1,r_3} + b_{0,r_2} - 5b_{1,r_2} + 3a_{0,r_1} - 4a_{1,r_1}, \quad (\text{C.15})$$

$$\begin{aligned} c_{n,r_3} = & -\frac{(n-2)^2(n-3)}{n(n-1)^2}c_{n-2,r_3} + \frac{-iq_3-6+n(13+n(2n-9))}{n(n-1)^2}c_{n-1,r_3} - \frac{2(n-2)(3n-8)}{n(n-1)^2}b_{n-2,r_2} + \\ & + \frac{26-36n+12n^2}{n(n-1)^2}b_{n-1,r_2} - \frac{6n^2-8n+2}{n(n-1)^2}b_{n,r_2} + \frac{2(7-3n)}{n(n-1)^2}a_{n-3,r_1} - \frac{6(3-2n)}{n(n-1)^2}a_{n-2,r_1} + \\ & + \frac{2(2-3n)}{n(n-1)^2}a_{n-1,r_1}. \end{aligned} \quad (\text{C.16})$$

C.1.4 Solution with $q_2 = q_3 = 0$ and $h = 1$

In this case $a_{0,r}$ is arbitrary (e.g. equal to 1). For the first solution with $r_1 = (h = 1)$ we have $a_{1,r_1} = 0$ and for the third one a_{1,r_3} with $r_3 = 0$ is arbitrary (let us take 0). The second solution is more complicated. We need Log-solutions

$$u_2(x) = x^{r_2} \sum_{n=0}^{\infty} b_{n,r_2} x^n + x^{r_1} \sum_{n=0}^{\infty} a_{n,r_1} x^n \text{Log}(x). \quad (\text{C.17})$$

Using recurrence relations with $b_{1,r_2} = \frac{1}{2}a_{0,r_1}$ (and $a_{n,r_1} = 0$ for $n > 0$)

$$\begin{aligned} b_{2,r_2} &= \frac{1}{3}b_{1,r_2}, \\ b_{n,r_2} &= -\frac{(n-1)^2(n-2)}{n^2(n+1)}b_{n-2,r_2} + \frac{(n-1)n(2n-1)}{n^2(n+1)}b_{n-1,r_2} \end{aligned} \quad (\text{C.18})$$

one can derive an exact formula for $b_{n,r_2} = b_{1,r_2} \frac{2}{(n+1)n}$ and performing summations with arbitrary $b_{0,r_2}(=0)$ we have $x \sum_{n=0}^{\infty} b_{n,r_2} x^n = 2b_{1,r_2}(x + \text{Log}(1-x) - x\text{Log}(1-x))$, so that

$$\begin{aligned} u_1(x) &= x^{r_1} \sum_{n=0}^{\infty} a_{n,r_1} x^n = a_{0,r_1} = xa_{0,r_1}, \\ u_2(x) &= a_{0,r_1}(x + \text{Log}(1-x) - x\text{Log}(1-x) + x\text{Log}(x)), \\ u_3(x) &= x^{r_3} \sum_{n=0}^{\infty} a_{n,r_3} x^n = a_{0,r_3}. \end{aligned} \quad (\text{C.19})$$

Gathering together all this solutions we have

$$u(x) = A + B(-x) + C((x-1)\text{Log}(x-1) + (-x)\text{Log}(-x)), \quad (\text{C.20})$$

where A, B, C are arbitrary. See also Ref. [27].

C.1.5 Solution with $q_3 \neq 0$, $q_2 = 0$ and $h = 0$

For $h = 0$, i.e. $q_2 = 0$, and arbitrary $q_3 \neq 0$ we have three solutions

$$\begin{aligned} u_1(x) &= x^{r_1} \sum_{n=0}^{\infty} a_{n,r_1} x^n \\ u_2(x) &= x^{r_2} \sum_{n=0}^{\infty} b_{n,r_2} x^n + x^{r_1} \sum_{n=0}^{\infty} a_{n,r_1} x^n \text{Log}(x) \\ u_3(x) &= x^{r_3} \sum_{n=0}^{\infty} c_{n,r_3} x^n + 2x^{r_2} \sum_{n=0}^{\infty} b_{n,r_2} x^n \text{Log}(x) + x^{r_1} \sum_{n=0}^{\infty} a_{n,r_1} x^n \text{Log}^2(x) \end{aligned} \quad (\text{C.21})$$

where $r_1 = 1$, $r_2 = 0$ and $r_3 = 0$. Here $a_{0,r}$ is arbitrary (e.g. 1)

$$a_{1,r} = \frac{-iq_3 + 2r^2}{r(1+r)^2} a_{0,r} \quad (\text{C.22})$$

and $m = n + r$

$$a_{n,r} = -\frac{(m-2)^2}{m^2} a_{n-2,r} + \frac{-iq_3 + 2(m-1)^3}{(m-1)m^2} a_{n-1,r}, \quad (\text{C.23})$$

whereas $b_{0,r_2} = -\frac{1}{iq_3} a_{0,r_1}$ and b_{1,r_2} is arbitrary while

$$b_{2,r_2} = \frac{1}{4}((2 - iq_3)b_{1,r_2} + 6a_{0,r_1} - 8a_{1,r_1}), \quad (\text{C.24})$$

$$\begin{aligned} b_{n,r_2} &= -\frac{(n-2)^2}{n^2} b_{n-2,r_2} + \frac{-iq_3 + 2(n-1)^3}{n^2(n-1)} b_{n-1,r_2} - \frac{(n-2)(3n-4)}{n^2(n-1)} a_{n-3,r_1} + \\ &+ \frac{6(n-1)}{n^2} a_{n-2,r_1} + \frac{2-3n}{n^2(n-1)} a_{n-1,r_1}. \end{aligned} \quad (\text{C.25})$$

The coefficient $c_{0,r_3} = \frac{2}{iq_3}(2a_{0,r_1} + b_{1,r_2})$ and c_{1,r_3} is arbitrary and

$$c_{2,r_3} = \frac{1}{4}(2 - iq_3)c_{1,r_3} + 3b_{1,r_2} - 4b_{2,r_2} + 3a_{0,r_1} - \frac{5}{2}a_{1,r_1}, \quad (\text{C.26})$$

$$\begin{aligned} c_{n,r_3} &= -\frac{(n-2)^2}{n^2} c_{n-2,r_3} + \frac{-iq_3 + 2(n-1)^3}{n^2(n-1)} c_{n-1,r_3} - \frac{2(n-2)(3n-4)}{n^2(n-1)} b_{n-2,r_2} + \\ &+ \frac{12(n-1)}{n^2} b_{n-1,r_2} + \frac{2(2-3n)}{n(n-1)} b_{n,r_2} + \frac{2(5-3n)}{n^2(n-1)} a_{n-3,r_1} + \frac{12}{n^2} a_{n-2,r_1} + \\ &+ \frac{2(1-3n)}{n^2(n-1)} a_{n-1,r_1}. \end{aligned} \quad (\text{C.27})$$

C.1.6 Solution with $h = 0$ and $q_2 = q_3 = 0$

In this case $a_{0,r}$ is arbitrary. For the first solution with $r_1 = 1$ we have recurrence relations with $a_{1,r_1} = \frac{1}{2}a_{0,r_1}$

$$\begin{aligned} a_{2,r_1} &= \frac{1}{3}a_{1,r_1}, \\ a_{n,r_1} &= -\frac{(n-1)^2}{n+1} a_{n-2,r_1} + \frac{2n^2}{n+1} a_{n-1,r_1}. \end{aligned} \quad (\text{C.28})$$

Summing series up we derive an exact formula for

$$u_1(x) = x^{r_1} \sum_{n=0}^{\infty} a_{n,r_1} x^n = x \sum_{n=0}^{\infty} x^n a_{0,r_1} \frac{1}{n+1} = -\text{Log}(1-x). \quad (\text{C.29})$$

In the second solution, with $r_2 = 0$, we have arbitrary a_{1,r_2} (let us take 0) and solution is $u_2(x) = a_{0,r_2}$. The third one is with Log-solutions

$$u_3(x) = x^{r_3} \sum_{n=0}^{\infty} b_{n,r_3} x^n + x^{r_2} \sum_{n=0}^{\infty} a_{n,r_2} x^n \text{Log}(x). \quad (\text{C.30})$$

Using recurrence relations with arbitrary b_{0,r_3}

$$\begin{aligned} b_{2,r_3} &= \frac{1}{2}b_{1,r_3} \\ b_{n,r_3} &= -\frac{(n-2)^3}{n^2}b_{n-2,r_3} + \frac{2(n-1)^2}{n^2}b_{n-1,r_3} \end{aligned} \quad (C.31)$$

one can derive an exact formula for $b_{n,r_3} = b_{1,r_3} \frac{1}{n}$ and performing summations with arbitrary $b_{0,r_3}(=0)$ we have $\sum_{n=0}^{\infty} b_{n,r_3} x^n = -b_{0,r_3} \text{Log}(1-x)$. All these solutions look like

$$\begin{aligned} u_1(x) &= x^{r_1} \sum_{n=0}^{\infty} a_{n,r_1} x^n = -a_{1,r_3} \text{Log}(1-x), \\ u_2(x) &= x^{r_2} \sum_{n=0}^{\infty} a_{n,r_2} x^n = a_{0,r_2}, \\ u_3(x) &= x^{r_3} \sum_{n=0}^{\infty} b_{n,r_3} x^n + a_{0,r_2} \text{Log}(x) = -b_{0,r_3} \text{Log}(1-x) + a_{0,r_2} \text{Log}(x). \end{aligned} \quad (C.32)$$

Gathering together all this solutions we obtain

$$u(x) = A + B \text{Log}(-x) + C \text{Log}(x-1), \quad (C.33)$$

where A, B, C are arbitrary. See also Ref. [27].

C.1.7 Solution with $q_3 \neq 0$ and $h = 2$

For $h = 2$ and $q_3 \neq 0$ we have three solutions

$$\begin{aligned} u_1(x) &= x^{r_1} \sum_{n=0}^{\infty} a_{n,r_1} x^n, \\ u_2(x) &= x^{r_2} \sum_{n=0}^{\infty} b_{n,r_2} x^n + x^{r_1} \sum_{n=0}^{\infty} a_{n,r_1} x^n \text{Log}(x), \\ u_3(x) &= x^{r_3} \sum_{n=0}^{\infty} c_{n,r_3} x^n + 2x^{r_2} \sum_{n=0}^{\infty} b_{n,r_2} x^n \text{Log}(x) + x^{r_1} \sum_{n=0}^{\infty} a_{n,r_1} x^n \text{Log}^2(x) \end{aligned} \quad (C.34)$$

with $r_1 = 2, r_2 = 1, r_3 = 0$. Here a_{0,r_1} is arbitrary (e.g. 1)

$$a_{1,r_1} = \frac{-iq_3 + 2r(r-1)(r-2)}{r(r^2-1)} a_{0,r_1} \quad (C.35)$$

and $m = n + r_1$

$$a_{n,r_1} = -\frac{(m-3)(m-4)}{m(m-1)} a_{n-2,r_1} + \frac{-iq_3 + 2(m-1)(m-2)(m-3)}{(m-2)(m-1)m} a_{n-1,r_1}, \quad (C.36)$$

whereas $b_{0,r_2} = -\frac{2}{iq_3} a_{0,r_1}$ and b_{1,r_2} is arbitrary while

$$b_{2,r_2} = \frac{1}{6}(-iq_3 b_{1,r_2} + 4a_{0,r_1} - 11a_{1,r_1}), \quad (C.37)$$

$$\begin{aligned} b_{n,r_2} &= -\frac{(n-2)(n-3)}{n(n+1)} b_{n-2,r_2} + \frac{-iq_3 + 2(n-2)(n-1)n}{n(n^2-1)} b_{n-1,r_2} - \frac{11+3(n-4)n}{n(n^2-1)} a_{n-3,r_1} + \\ &+ \frac{6(n-2)n+4}{n(n^2-1)} a_{n-2,r_1} + \frac{1-3n^2}{n(n^2-1)} a_{n-1,r_1}. \end{aligned} \quad (C.38)$$

Moreover, $c_{0,r_3} = \frac{2}{iq_3} b_{0,r_2}$ and $c_{1,r_3} = -\frac{4(b_{0,r_2} + b_{1,r_2})}{iq_3} - \frac{6a_{0,r_1}}{iq_3}$ and c_{2,r_3} is arbitrary while

$$c_{3,r_3} = \frac{1}{6}(-iq_3 c_{2,r_3} + 2b_{0,r_2} + 8b_{1,r_2} - 22b_{2,r_2} + 12a_{0,r_1} - 12a_{1,r_1}), \quad (C.39)$$

$$\begin{aligned} c_{n,r_3} &= -\frac{(n-3)(n-4)}{n(n-1)} c_{n-2,r_3} + \frac{-iq_3 + 2(n-3)(n-2)(n-1)}{n(n-1)(n-2)} c_{n-1,r_3} + \frac{2(3n(6-n)-26)}{n(n-1)(n-2)} b_{n-3,r_2} + \\ &+ \frac{4(11-12m+3m^2)}{n(n-1)(n-2)} b_{n-2,r_2} - \frac{2(2-6m+3m^2)}{n(n-1)(n-2)} b_{n-1,r_2} - \frac{6(n-3)}{n(n-1)(n-2)} a_{n-4,r_1} + \frac{12}{n(n-1)} a_{n-3,r_1} + \\ &- \frac{6}{n(n-2)} a_{n-2,r_1}. \end{aligned} \quad (C.40)$$

C.1.8 Solution with $q_3 = 0$ and $h = 2$

In this case $a_{0,r}$ is arbitrary (e.g. equal to 1). For the first solution with $r_1 = 2$ we have remaining coefficients $a_{n>0,r_1} = 0$. The second solution, with $r_2 = 1$, has an arbitrary a_{1,r_2} (we can take it as 0), $a_{2,r_2} = 0$ and third one with arbitrary a_{1,r_3} , a_{2,r_3} (we also set them to 0). All these solutions look like

$$\begin{aligned} u_1(x) &= x^{r_1} \sum_{n=0}^{\infty} a_{n,r_1} x^n = x^2 a_{0,r_3}, \\ u_2(x) &= x^{r_2} \sum_{n=0}^{\infty} a_{n,r_2} x^n = x a_{0,r_2}, \\ u_3(x) &= x^{r_3} \sum_{n=0}^{\infty} a_{n,r_3} x^n = a_{0,r_3}. \end{aligned} \quad (\text{C.41})$$

Gathering together this all solutions we have

$$u(x) = A + B(-x)^2 + C(x-1)^2, \quad (\text{C.42})$$

where A, B, C are arbitrary. As we can see this solution corresponds to the solution with $q_3 = 0$ and arbitrary $h \notin \{0, 1\}$. For other integer $h \notin \{0, 1\}$ we can observe the same correspondence.

C.2 Solutions for $s = 0$ around $x = 1^-$

C.2.1 Solutions for $q_3 \neq 0$ and $h \notin \mathbb{Z}$

Similarly to the case $x = 0$ for $x = 1^-$ we have independent solutions where an indicial equation has a form

$$(h - n - r)(r + n - 1)(n + r) = 0. \quad (\text{C.43})$$

Its solutions have following values: $r_1 = h$, $r_2 = 1$ and $r_3 = 0$. As we can see we have two cases when $h \notin \mathbb{Z}$ (one solution with $\text{Log}(x)$) and $h \in \mathbb{Z}$ (one solution with $\text{Log}(x)$ and one solution with $\text{Log}^2(x)$). We will see below that we have to consider solutions with $q_3 = 0$, separately.

In this case, for $q_3 \neq 0$:

$$\begin{aligned} u_1(x) &= (1-x)^{r_1} \sum_{n=0}^{\infty} a_{n,r_1} (1-x)^n, \\ u_2(x) &= (1-x)^{r_2} \sum_{n=0}^{\infty} a_{n,r_2} (1-x)^n, \\ u_3(x) &= (1-x)^{r_3} \sum_{n=0}^{\infty} b_{n,r_3} (1-x)^n + (1-x)^{r_2} \sum_{n=0}^{\infty} a_{n,r_2} (1-x)^n \text{Log}(1-x), \end{aligned} \quad (\text{C.44})$$

where $a_{0,r}$ is arbitrary (e.g. 1) and

$$a_{1,r} = \frac{(iq_3 + (h-2r)(h-r)r)}{(h-1-r)r(1+r)} a_{0,r} \quad (\text{C.45})$$

and $m = n + r$

$$a_{n,r} = \frac{(h-m+1)(h-m+2)(m-2)}{(h-m)(m-1)m} a_{n-2,r} - \frac{(iq_3 + (1+h-m)(m-1)(h-2(m-1)))}{(h-m)(m-1)m} a_{n-1,r}, \quad (\text{C.46})$$

whereas $b_{0,r_3} = \frac{(1-h)}{iq_3} a_{0,r_2}$ (one can notice that coefficient b_{0,r_3} is valid only for $q_3 \neq 0$) and b_{1,r_3} is arbitrary

$$b_{2,r_3} = \frac{iq_3 + (h-2)(h-1)}{2(2-h)} b_{1,r_3} - \frac{8-3h}{2(2-h)} a_{1,r_3} + \frac{6+h(h-6)}{2(2-h)} a_{0,r_3} \quad (\text{C.47})$$

and

$$\begin{aligned}
b_{n,r_3} = & \frac{(h+1-m)(h-m+2)(m-2)}{(h-m)(m-1)m} b_{n-2,r_3} - \frac{iq_3+(1+h-m)(m-1)(h-2(m-1))}{(h-m)(m-1)m} b_{n-1,r_3} + \\
& + \frac{h^2+h(7-4m)+(m-2)(3m-4)}{(h-m)(m-1)m} a_{n-3,r_3} - \frac{h^2-6h(m-1)+6(m-1)^2}{(h-m)(m-1)m} a_{n-2,r_3} + \\
& - \frac{2m-3m^2+h(2m-1)}{(h-m)(m-1)m} a_{n-1,r_3}
\end{aligned} \tag{C.48}$$

where $m = r_3 + n$.

We can easily see that above coefficients correspond to coefficients for solution around $x = 0^-$ with $q_3 \rightarrow -q_3$.

C.2.2 Solution with $q_3 = 0$

Here $a_{0,r}$ is arbitrary (e.g. equal to 1). For the first solution with $r_1 = h$ we have $a_{1,r_1} = 0$ and for the third one a_{1,r_3} is arbitrary (let us take 0). We do not need Log solutions. The second solution is more complicated. One can derive an exact formula for

$$a_{n,r_2} = a_{0,r_2} \prod_{k=1}^n \frac{k-h}{k+1} = \frac{\Gamma(1-h+n)}{\Gamma(1-h)\Gamma(n+2)} a_{0,r_2} \tag{C.49}$$

and performing summations

$$\begin{aligned}
u_1(x) &= (1-x)^{r_1} \sum_{n=0}^{\infty} a_{n,r_1} (1-x)^n = (1-x)^h a_{0,r_1}, \\
u_2(x) &= (1-x)^{r_2} \sum_{n=0}^{\infty} a_{n,r_2} (1-x)^n = a_{0,r_2} (1-x) \sum_{n=0}^{\infty} \frac{\Gamma(1-h+n)}{\Gamma(1-h)\Gamma(n+2)} (1-x)^n \\
&= -a_{0,r_2} \frac{1}{h} (x^h - 1), \\
u_3(x) &= (1-x)^{r_3} \sum_{n=0}^{\infty} a_{n,r_3} (1-x)^n = a_{0,r_3}.
\end{aligned} \tag{C.50}$$

Gathering together all these solutions we have

$$u(x) = A + B(-x)^h + C(x-1)^h, \tag{C.51}$$

where A, B, C are arbitrary. The above solution was presented by Lipatov and Vacca in Refs. [53, 51].

C.2.3 Solution with $q_3 \neq 0$, $q_2 = 0$ and $h = 1$

For $h = 1$, i.e. $q_2 = 0$, and $q_3 \neq 0$ we have three solutions to the indicial equation (C.43) which are integer $r_1 = 1$, $r_2 = 1$, $r_3 = 0$ so solutions are

$$\begin{aligned}
u_1(x) &= (1-x)^{r_1} \sum_{n=0}^{\infty} a_{n,r_1} (1-x)^n, \\
u_2(x) &= (1-x)^{r_2} \sum_{n=0}^{\infty} b_{n,r_2} (1-x)^n + x^{r_1} \sum_{n=0}^{\infty} a_{n,r_1} (1-x)^n \text{Log}(1-x), \\
u_3(x) &= (1-x)^{r_3} \sum_{n=0}^{\infty} c_{n,r_3} (1-x)^n + 2(1-x)^{r_2} \sum_{n=0}^{\infty} b_{n,r_2} (1-x)^n \text{Log}(1-x) + \\
&\quad + (1-x)^{r_1} \sum_{n=0}^{\infty} a_{n,r_1} (1-x)^n \text{Log}^2(1-x),
\end{aligned} \tag{C.52}$$

where $a_{0,r}$ is arbitrary (e.g. equal to 1)

$$a_{1,r} = \frac{iq_3 + r + r^2(2r-3)}{r^2(1+r)} a_{0,r} \tag{C.53}$$

and $m = n + r$

$$a_{n,r} = -\frac{(m-3)(m-2)^2}{(m-1)^2m}a_{n-2,r} + \frac{(iq_3 + (m-2)(m-1)(2m-3))}{(m-1)^2m}a_{n-1,r}, \quad (\text{C.54})$$

whereas

$$b_{1,r_2} = \frac{1}{2}(iq_3b_{0,r_2} + a_{0,r_1} - 5a_{1,r_1}), \quad (\text{C.55})$$

$$\begin{aligned} b_{n,r_2} = & -\frac{(n-1)^2(n-2)}{n^2(n+1)}b_{n-2,r_2} + \frac{(iq_3+2n^3-3n^2+n)}{n^2(n+1)}b_{n-1,r_2} + \frac{1+6n(n-1)}{n^2(n+1)}a_{n-1,r_1} + \\ & + \frac{(n-1)(5-3n)}{n^2(n+1)}a_{n-2,r_1} - \frac{(2+3n)}{n(n+1)}a_{n,r_1}. \end{aligned} \quad (\text{C.56})$$

Moreover, $c_{0,r_3} = \frac{2i}{q_3}a_{0,r_1}$ c_{1,r_3} is arbitrary and

$$c_{2,r_3} = \frac{1}{2}iq_3c_{1,r_3} + b_{0,r_2} - 5b_{1,r_2} + 3a_{0,r_1} - 4a_{1,r_1}, \quad (\text{C.57})$$

$$\begin{aligned} c_{n,r_3} = & -\frac{(n-2)^2(n-3)}{n(n-1)^2}c_{n-2,r_3} + \frac{iq_3-6+n(13+n(2n-9))}{n(n-1)^2}c_{n-1,r_3} - \frac{2(n-2)(3n-8)}{n(n-1)^2}b_{n-2,r_2} + \\ & + \frac{2(13+6(n-3)n)}{n(n-1)^2}b_{n-1,r_2} - \frac{2(1+n(3n-4))}{n(n-1)^2}b_{n,r_2} + \frac{2(7-3n)}{n(n-1)^2}a_{n-3,r_1} - \frac{6(3-2n)}{n(n-1)^2}a_{n-2,r_1} + \\ & + \frac{2(2-3n)}{n(n-1)^2}a_{n-1,r_1}. \end{aligned} \quad (\text{C.58})$$

C.2.4 Solution with $q_2 = q_3 = 0$ and $h = 1$

In this case $a_{0,r}$ is arbitrary (e.g. 1). For the first solution with $r_1 = (h = 1)$ we have $a_{1,r_1} = 0$ and for the third one a_{1,r_3} with $r_3 = 0$ is arbitrary (let us take 0). The second solution is more complicated. We need Log-solutions

$$u_2(x) = (1-x)^{r_2}, \sum_{n=0}^{\infty} b_{n,r_2}(1-x)^n + x^{r_1}, \sum_{n=0}^{\infty} a_{n,r_1}(1-x)^n \text{Log}(1-x). \quad (\text{C.59})$$

Using recursive relations with $b_{1,r_2} = \frac{1}{2}a_{0,r_1}$ (and $a_{n,r_1} = 0$ for $n > 0$)

$$\begin{aligned} b_{2,r_2} &= \frac{1}{3}b_{1,r_2}, \\ b_{n,r_2} &= -\frac{(n-1)^2(n-2)}{n^2(n+1)}b_{n-2,r_2} + \frac{(n-1)n(2n-1)}{n^2(n+1)}b_{n-1,r_2} \end{aligned} \quad (\text{C.60})$$

one can derive an exact formula for $b_{n,r_2} = b_{1,r_2} \frac{2}{(n+1)n}$ and performing summations with arbitrary $b_{0,r_2}(=0)$ we have

$$x \sum_{n=0}^{\infty} b_{n,r_2}(1-x)^n = 2b_{1,r_2}((1-x) + \text{Log}(x) - (1-x)\text{Log}(x)) \quad (\text{C.61})$$

what gives us

$$\begin{aligned} u_1(x) &= (1-x)^{r_1} \sum_{n=0}^{\infty} a_{n,r_1}(1-x)^n = a_{0,r_1} = (1-x)a_{0,r_1}, \\ u_2(x) &= a_{0,r_1}((1-x) + \text{Log}(x) - (1-x)\text{Log}(x) + (1-x)\text{Log}(1-x)), \\ u_3(x) &= (1-x)^{r_3} \sum_{n=0}^{\infty} a_{n,r_3}(1-x)^n = a_{0,r_3}. \end{aligned} \quad (\text{C.62})$$

Gathering together all this solutions we have

$$u(x) = A + B(-x) + C((x-1)\text{Log}(x-1) + (-x)\text{Log}(-x)), \quad (\text{C.63})$$

where A, B, C are arbitrary. Here we have also obtained the consistent solution.

C.2.5 Solution with $q_3 \neq 0$, $q_2 = 0$ and $h = 0$

For $h = 0$, i.e. $q_2 = 0$, and $q_3 \neq 0$ we have three solutions

$$\begin{aligned} u_1(x) &= (1-x)^{r_1} \sum_{n=0}^{\infty} a_{n,r_1} (1-x)^n, \\ u_2(x) &= (1-x)^{r_2} \sum_{n=0}^{\infty} b_{n,r_2} (1-x)^n + (1-x)^{r_1} \sum_{n=0}^{\infty} a_{n,r_1} (1-x)^n \text{Log}(1-x), \\ u_3(x) &= (1-x)^{r_3} \sum_{n=0}^{\infty} c_{n,r_3} (1-x)^n + 2(1-x)^{r_2} \sum_{n=0}^{\infty} b_{n,r_2} (1-x)^n \text{Log}(1-x) \\ &\quad + (1-x)^{r_1} \sum_{n=0}^{\infty} a_{n,r_1} (1-x)^n \text{Log}^2(1-x), \end{aligned} \quad (\text{C.64})$$

where coefficients $r_1 = 1$, $r_2 = 0$, $r_3 = 0$ are integer while $a_{0,r}$ is arbitrary (e.g. 1)

$$a_{1,r} = \frac{iq_3 + 2r^2}{r(1+r)^2} a_{0,r} \quad (\text{C.65})$$

and $m = n + r$

$$a_{n,r} = -\frac{(m-2)^2}{m^2} a_{n-2,r} + \frac{iq_3 + 2(m-1)^3}{(m-1)m^2} a_{n-1,r}, \quad (\text{C.66})$$

whereas $b_{0,r_2} = \frac{1}{iq_3} a_{0,r_1}$ and b_{1,r_2} is arbitrary while

$$b_{2,r_2} = \frac{1}{4} ((2 + iq_3) b_{1,r_2} + 6a_{0,r_1} - 8a_{1,r_1}), \quad (\text{C.67})$$

$$\begin{aligned} b_{n,r_2} &= -\frac{(n-2)^2}{n^2} b_{n-2,r_2} + \frac{iq_3 + 2(n-1)^3}{n^2(n-1)} b_{n-1,r_2} - \frac{(n-2)(3n-4)}{n^2(n-1)} a_{n-3,r_1} + \\ &\quad + \frac{6(n-1)}{n^2} a_{n-2,r_1} + \frac{2-3n}{n(n-1)} a_{n-1,r_1}. \end{aligned} \quad (\text{C.68})$$

Moreover, $c_{0,r_3} = \frac{2}{iq_3} (2a_{0,r_1} + b_{1,r_2})$, c_{1,r_3} is arbitrary and

$$c_{2,r_3} = \frac{1}{4} (2 + iq_3) c_{1,r_3} + 3b_{1,r_2} - 4b_{2,r_2} + 3a_{0,r_1} - \frac{5}{2} a_{1,r_1}, \quad (\text{C.69})$$

$$\begin{aligned} c_{n,r_3} &= -\frac{(n-2)^2}{n^2} c_{n-2,r_3} + \frac{iq_3 + 2(n-1)^3}{n^2(n-1)} c_{n-1,r_3} - \frac{2(n-2)(3n-4)}{n^2(n-1)} b_{n-2,r_2} + \\ &\quad + \frac{12(n-1)}{n^2} b_{n-1,r_2} + \frac{2(2-3n)}{n(n-1)} b_{n,r_2} + \frac{2(5-3n)}{n^2(n-1)} a_{n-3,r_1} + \frac{12}{n^2} a_{n-2,r_1} + \\ &\quad + \frac{2(1-3n)}{n^2(n-1)} a_{n-1,r_1}. \end{aligned} \quad (\text{C.70})$$

C.2.6 Solution with $q_2 = q_3 = 0$ and $h = 0$

In this case $a_{0,r}$ is arbitrary (e.g. 1). For the first solution with $r_1 = 1$ we have recurrence relations with $a_{1,r_1} = \frac{1}{2} a_{0,r_1}$

$$\begin{aligned} a_{2,r_1} &= \frac{1}{3} a_{1,r_1}, \\ a_{n,r_1} &= -\frac{(n-1)^2}{n+1} a_{n-2,r_1} + \frac{2n^2}{n+1} a_{n-1,r_1}. \end{aligned} \quad (\text{C.71})$$

Summing series up we derive an exact formula for

$$u_1(x) = (1-x)^{r_1} \sum_{n=0}^{\infty} a_{n,r_1} (1-x)^n = (1-x) \sum_{n=0}^{\infty} (1-x)^n a_{0,r_1} \frac{1}{n+1} = -\text{Log}(x). \quad (\text{C.72})$$

In the second solution, with $r_2 = 0$, we have an arbitrary a_{1,r_2} (let us take 0) so the solution is $u_2(x) = a_{0,r_2}$. The third one is with Log solutions

$$u_3(x) = (1-x)^{r_3} \sum_{n=0}^{\infty} b_{n,r_3} (1-x)^n + (1-x)^{r_2} \sum_{n=0}^{\infty} a_{n,r_2} (1-x)^n \text{Log}(1-x). \quad (\text{C.73})$$

Using recurrence relations with arbitrary b_{0,r_3}

$$\begin{aligned} b_{2,r_3} &= \frac{1}{2} b_{1,r_3}, \\ b_{n,r_3} &= -\frac{(n-2)^3}{n^2} b_{n-2,r_3} + \frac{2(n-1)^2}{n^2} b_{n-1,r_3} \end{aligned} \quad (\text{C.74})$$

one can derive an exact formula for $b_{n,r_3} = b_{1,r_3} \frac{1}{n}$ and performing summations with arbitrary $b_{0,r_3}(=0)$ we have $\sum_{n=0}^{\infty} b_{n,r_3} (1-x)^n = -b_{0,r_3} \text{Log}(x)$. All these solutions look like

$$\begin{aligned} u_1(x) &= (1-x)^{r_1} \sum_{n=0}^{\infty} a_{n,r_1} (1-x)^n = -a_{1,r_3} \text{Log}(x), \\ u_2(x) &= (1-x)^{r_2} \sum_{n=0}^{\infty} a_{n,r_2} (1-x)^n = a_{0,r_2}, \\ u_3(x) &= (1-x)^{r_3} \sum_{n=0}^{\infty} b_{n,r_3} (1-x)^n + a_{0,r_2} \text{Log}(1-x) = -b_{0,r_3} \text{Log}(x) + a_{0,r_2} \text{Log}(1-x). \end{aligned} \quad (\text{C.75})$$

Gathering together all this solutions we have

$$u(x) = A + B \text{Log}(-x) + C \text{Log}(x-1), \quad (\text{C.76})$$

where A, B, C are arbitrary.

C.2.7 Solution with $q_3 \neq 0$ and $h = 2$

For integer $h = 2$ and $q_3 \neq 0$ we have three solutions to the indicial equation (C.43) which are integer $r_1 = 2, r_2 = 1, r_3 = 0$ so solutions are

$$\begin{aligned} u_1(x) &= (1-x)^{r_1} \sum_{n=0}^{\infty} a_{n,r_1} (1-x)^n, \\ u_2(x) &= (1-x)^{r_2} \sum_{n=0}^{\infty} b_{n,r_2} (1-x)^n + (1-x)^{r_1} \sum_{n=0}^{\infty} a_{n,r_1} (1-x)^n \text{Log}(1-x), \\ u_3(x) &= (1-x)^{r_3} \sum_{n=0}^{\infty} c_{n,r_3} (1-x)^n + 2(1-x)^{r_2} \sum_{n=0}^{\infty} b_{n,r_2} (1-x)^n \text{Log}(1-x) + \\ &\quad + (1-x)^{r_1} \sum_{n=0}^{\infty} a_{n,r_1} (1-x)^n \text{Log}^2(1-x), \end{aligned} \quad (\text{C.77})$$

where a_{0,r_1} is arbitrary (e.g. 1)

$$a_{1,r_1} = \frac{iq_3 + 2r(r-1)(r-2)}{r(r^2-1)} a_{0,r_1} \quad (\text{C.78})$$

and $m = n + r_1$

$$a_{n,r_1} = -\frac{(m-3)(m-4)}{m(m-1)} a_{n-2,r_1} + \frac{iq_3 + 2(m-1)(m-2)(m-3)}{(m-2)(m-1)m} a_{n-1,r_1}, \quad (\text{C.79})$$

whereas $b_{0,r_2} = \frac{2}{iq_3} a_{0,r_1}$ and b_{1,r_2} is arbitrary while

$$b_{2,r_2} = \frac{1}{6} (iq_3 b_{1,r_2} + 4a_{0,r_1} - 11a_{1,r_1}), \quad (\text{C.80})$$

$$\begin{aligned}
b_{n,r_2} = & -\frac{(n-2)(n-3)}{n(n+1)}b_{n-2,r_2} + \frac{iq_3+2(n-2)(n-1)n}{n(n^2-1)}b_{n-1,r_2} - \frac{11+3(n-4)n}{n(n^2-1)}a_{n-3,r_1} + \\
& + \frac{6(n-2)n+4}{n(n^2-1)}a_{n-2,r_1} + \frac{1-3n}{n(n^2-1)}a_{n-1,r_1} .
\end{aligned} \tag{C.81}$$

Therefore, $c_{0,r_3} = -\frac{2}{iq_3}b_{0,r_2}$ and $c_{1,r_3} = \frac{4(b_{0,r_2}+b_{1,r_2})}{iq_3} + \frac{6a_{0,r_1}}{iq_3}$ and c_{2,r_3} is arbitrary while

$$c_{3,r_3} = \frac{1}{6}(iq_3c_{2,r_3} + 2b_{0,r_2} + 8b_{1,r_2} - 22b_{2,r_2} - 12a_{0,r_1} + 12a_{1,r_1}), \tag{C.82}$$

$$\begin{aligned}
c_{n,r_3} = & -\frac{(n-3)(n-4)}{n(n-1)}c_{n-2,r_3} + \frac{iq_3+2(n-3)(n-2)(n-1)}{n(n-1)(n-2)}c_{n-1,r_3} + \frac{2(3n(6-n)-26)}{n(n-1)(n-2)}b_{n-3,r_2} + \\
& + \frac{4(11-12m+3m^2)}{n(n-1)(n-2)}b_{n-2,r_2} - \frac{2(2-6m+3m^2)}{n(n-1)(n-2)}b_{n-1,r_2} - \frac{6(n-3)}{n(n-1)(n-2)}a_{n-4,r_1} + \frac{12}{n(n-1)}a_{n-3,r_1} + \\
& - \frac{6}{n(n-2)}a_{n-2,r_1} .
\end{aligned} \tag{C.83}$$

C.2.8 Solution with $q_3 = 0$ and $h = 2$

In this case $a_{0,r}$ is arbitrary (e.g. 1). For the first solution with $r_1 = 2$ we have other coefficients $a_{n>0,r_1} = 0$. The second solution, with $r_2 = 1$, has arbitrary a_{1,r_2} (we can take it as 0) and $a_{2,r_2} = 0$. The third one is with arbitrary a_{1,r_3}, a_{2,r_3} (we also set them to 0). All these solutions look like

$$\begin{aligned}
u_1(x) &= (1-x)^{r_1} \sum_{n=0}^{\infty} a_{n,r_1} (1-x)^n = (1-x)^2 a_{0,r_3}, \\
u_2(x) &= (1-x)^{r_2} \sum_{n=0}^{\infty} a_{n,r_2} (1-x)^n = (1-x) a_{0,r_2}, \\
u_3(x) &= (1-x)^{r_3} \sum_{n=0}^{\infty} a_{n,r_3} (1-x)^n = a_{0,r_3}.
\end{aligned} \tag{C.84}$$

Gathering together all this solutions we have

$$u(x) = A + B(-x)^2 + C(x-1)^2, \tag{C.85}$$

where A, B, C are arbitrary. As we can see this solution corresponds to the solution with $q_3 = 0$ and arbitrary $h \notin \{0, 1\}$. For other integer $h \notin \{0, 1\}$ we can observe the same correspondence.

C.3 Solutions for $s = 0$ around $x = \infty^-$

C.3.1 Solutions for $q_3 \neq 0$ and $h \notin \mathbb{Z}$

When $x = \infty^+$ we have an indicial equation

$$(h+n+r)(h-1+r+n)(n+r) = 0 \tag{C.86}$$

so its solutions are $r_1 = 0$, $r_2 = 1-h$ and $r_3 = h$. As we can see we have to cases when $h \notin \mathbb{Z}$ (one solution with $\text{Log}(x)$) and $h \in \mathbb{Z}$ (one solution with $\text{Log}(x)$ and one solution with $\text{Log}^2(x)$). As we will see below we have to consider solutions with $q_3 = 0$, separately. In the first case

$$\begin{aligned}
u_1(x) &= (1/x)^{r_1} \sum_{n=0}^{\infty} a_{n,r_1} (1/x)^n, \\
u_2(x) &= (1/x)^{r_2} \sum_{n=0}^{\infty} a_{n,r_2} (1/x)^n, \\
u_3(x) &= (1/x)^{r_3} \sum_{n=0}^{\infty} b_{n,r_3} (1/x)^n + (1/x)^{r_2} \sum_{n=0}^{\infty} a_{n,r_2} (1/x)^n \text{Log}(1/x),
\end{aligned} \tag{C.87}$$

where $a_{0,r}$ is arbitrary (e.g. 1)

$$a_{1,r} = \frac{(iq_3 + r(h+r)(h+2r))}{(1+r)(h+r)(h+1+r)} a_{0,r} \quad (\text{C.88})$$

and $m = n + r$

$$a_{n,r} = \frac{(m-2)(m-1)(2-h-m)}{(h+m)(h+m-1)m} a_{n-2,r} + \frac{iq_3 + (h-1+m)(m-1)(h+2(m-1))}{(h+m)(h+m-1)m} a_{n-1,r}, \quad (\text{C.89})$$

whereas $b_{0,r_3} = \frac{(1-h)}{iq_3} a_{0,r_2}$ (one can notice that coefficient b_{0,r_3} is valid only for $q_3 \neq 0$) and b_{1,r_3} is arbitrary

$$b_{2,r_3} = \frac{iq_3+2+(h-3)h}{2(2-h)} b_{1,r_3} - \frac{8-3h}{2(2-h)} a_{1,r_3} + \frac{6+h(h-6)}{2(2-h)} a_{0,r_3} \quad (\text{C.90})$$

and

$$\begin{aligned} b_{n,r_3} = & \frac{(h+1-m)(h-m+2)(m-2)}{(h-m)(m-1)m} b_{n-2,r_3} - \frac{iq_3+(1+h-m)(m-1)(h-2(m-1))}{(h-m)(m-1)m} b_{n-1,r_3} + \\ & + \frac{h^2+h(7-4m)+(m-2)(3m-4)}{(h-m)(m-1)m} a_{n-3,r_3} - \frac{h^2-6h(m-1)+6(m-1)^2}{(h-m)(m-1)m} a_{n-2,r_3} + \\ & - \frac{2m-3m^2+h(2m-1)}{(h-m)(m-1)m} a_{n-1,r_3}, \end{aligned} \quad (\text{C.91})$$

where $m = r_3 + n$.

C.3.2 Solution with $q_3 = 0$

In this case $a_{0,r}$ is arbitrary (e.g. 1). For the first solution with $r_1 = 0$ we have $a_{1,r_1} = 0$ and for the third one a_{1,r_3} is arbitrary (let us take 0). Here it also turns out that we do not need Log solutions. The second solution is more complicated. One can derive exact formula for

$$a_{n,r_2} = a_{0,r_2} \prod_{k=1}^n \frac{k-h}{k+1} = \frac{\Gamma(1-h+n)}{\Gamma(1-h)\Gamma(n+2)} a_{0,r_2} \quad (\text{C.92})$$

and performing summations

$$\begin{aligned} u_1(x) &= (1/x)^{r_1} \sum_{n=0}^{\infty} a_{n,r_1} (1/x)^n = a_{0,r_1}, \\ u_2(x) &= (1/x)^{r_2} \sum_{n=0}^{\infty} a_{n,r_2} (1/x)^n = a_{0,r_2} (1/x)^{1-h} \sum_{n=0}^{\infty} \frac{\Gamma(1-h+n)}{\Gamma(1-h)\Gamma(n+2)} (1/x)^n \\ &= -a_{0,r_2} \frac{1}{h} ((x-1)^h - x^h), \\ u_3(x) &= (1/x)^{r_3} \sum_{n=0}^{\infty} a_{n,r_3} (1/x)^n = a_{0,r_3} (1/x)^{-h}. \end{aligned} \quad (\text{C.93})$$

Gathering together all this solutions we have

$$u(x) = A + B(-x)^h + C(x-1)^h, \quad (\text{C.94})$$

where A, B, C are arbitrary. The above solution was presented by Lipatov and Vacca in Refs. [53, 51].

C.3.3 Solution with $q_3 \neq 0$, $q_2 = 0$ and $h = 1$

For integer $h = 1$, i.e. $q_2 = 0$, and $q_3 \neq 0$ we have three solutions to the indicial equation (C.86) which are integer $r_1 = 0$, $r_2 = 0$, $r_3 = -1$ so solutions are

$$\begin{aligned} u_1(x) &= (1/x)^{r_1} \sum_{n=0}^{\infty} a_{n,r_1} (1/x)^n \\ u_2(x) &= (1/x)^{r_2} \sum_{n=0}^{\infty} b_{n,r_2} (1/x)^n + (1/x)^{r_1} \sum_{n=0}^{\infty} a_{n,r_1} (1/x)^n \text{Log}(1/x) \\ u_3(x) &= (1/x)^{r_3} \sum_{n=0}^{\infty} c_{n,r_3} (1/x)^n + 2(1/x)^{r_2} \sum_{n=0}^{\infty} b_{n,r_2} (1/x)^n \text{Log}(1/x) + \\ &\quad + (1/x)^{r_1} \sum_{n=0}^{\infty} a_{n,r_1} (1/x)^n \text{Log}^2(1/x), \end{aligned} \quad (\text{C.95})$$

where $a_{0,r}$ is arbitrary (e.g. 1)

$$a_{1,r} = \frac{iq_3 + r(1+r)(1+2r)}{(1+r)^2(2+r)} a_{0,r} \quad (\text{C.96})$$

and $m = n + r$

$$a_{n,r} = -\frac{(m-2)(m-1)^2}{(m+1)m^2} a_{n-2,r} + \frac{iq_3 + (m-1)m(2m-1)}{(m+1)m^2} a_{n-1,r}, \quad (\text{C.97})$$

whereas

$$b_{1,r_2} = \frac{1}{2} (iq_3 b_{0,r_2} + a_{0,r_1} - 5a_{1,r_1}), \quad (\text{C.98})$$

$$\begin{aligned} b_{n,r_2} &= -\frac{(n-1)^2(n-2)}{n^2(n+1)} b_{n-2,r_2} + \frac{(iq_3 + 2m^3 - 3m^2 + m)}{n^2(n+1)} b_{n-1,r_2} + \frac{1+6n(n-1)}{n^2(n+1)} a_{n-1,r_1} + \\ &\quad + \frac{(n-1)(5-3n)}{n^2(n+1)} a_{n-2,r_1} - \frac{(2+3n)}{n(n+1)} a_{n,r_1} \end{aligned} \quad (\text{C.99})$$

and $c_{0,r_3} = \frac{2}{iq_3} a_{0,r_1}$ c_{1,r_3} is arbitrary while

$$c_{2,r_3} = \frac{1}{2} iq_3 c_{1,r_3} + b_{0,r_2} - 5b_{1,r_2} + 3a_{0,r_1} - 4a_{1,r_1}, \quad (\text{C.100})$$

$$\begin{aligned} c_{n,r_3} &= -\frac{(n-2)^2(n-3)}{n(n-1)^2} c_{n-2,r_3} + \frac{-6+n(13+n(2n-9))-iq_3}{n(n-1)^2} c_{n-1,r_3} - \frac{2(n-2)(3n-8)}{n(n-1)^2} b_{n-2,r_2} + \\ &\quad + \frac{2(13+6(n-3)n)}{n(n-1)^2} b_{n-1,r_2} - \frac{2(3n-1)}{n(n-1)} b_{n,r_2} + \frac{2(7-3n)}{n(n-1)^2} a_{n-3,r_1} - \frac{6(3-2n)}{n(n-1)^2} a_{n-2,r_1} + \\ &\quad - \frac{2(3n-2)}{n(n-1)} a_{n-1,r_1}. \end{aligned} \quad (\text{C.101})$$

C.3.4 Solution with $q_2 = q_3 = 0$ and $h = 1$

In this case $a_{0,r}$ is arbitrary (e.g. 1). For the first solution with $r_1 = 0$ we have $a_{1,r_1} = 0$ and for the third one a_{1,r_3} with $r_3 = 0$ is arbitrary (let us take 0). The second solution is more complicated. We need Log-solutions

$$u_2(x) = (1/x)^{r_2} \sum_{n=0}^{\infty} b_{n,r_2} (1/x)^n + (1/x)^{r_1} \sum_{n=0}^{\infty} a_{n,r_1} (1/x)^n \text{Log}(1/x). \quad (\text{C.102})$$

Using recurrence relations with $b_{1,r_2} = \frac{1}{2} a_{0,r_1}$ (and $a_{n,r_1} = 0$ for $n > 0$)

$$\begin{aligned} b_{2,r_2} &= \frac{1}{3} b_{1,r_2}, \\ b_{n,r_2} &= -\frac{(n-1)^2(n-2)}{n^2(n+1)} b_{n-2,r_2} + \frac{(n-1)n(2n-1)}{n^2(n+1)} b_{n-1,r_2} \end{aligned} \quad (\text{C.103})$$

one can derive an exact formula for $b_{n,r_2} = b_{1,r_2} \frac{2}{(n+1)n}$ and performing summations with arbitrary $b_{0,r_2}(=0)$ we have $\sum_{n=0}^{\infty} b_{n,r_2} (1/x)^n = 2b_{1,r_2} (1 - \text{Log}(1 - 1/x) + x \text{Log}(1 - 1/x))$, so that

$$\begin{aligned} u_1(x) &= (1/x)^{r_1} \sum_{n=0}^{\infty} a_{n,r_1} (1/x)^n = a_{0,r_1}, \\ u_2(x) &= a_{0,r_1} (1 - \text{Log}(1 - 1/x) + x \text{Log}(1 - 1/x) + \text{Log}(1/x)), \\ u_3(x) &= (1/x)^{r_3} \sum_{n=0}^{\infty} a_{n,r_3} (1/x)^n = (1/x)^{-1} a_{0,r_3}. \end{aligned} \quad (\text{C.104})$$

Gathering together all this solutions we have

$$u(x) = A + B(-x) + C((x-1)\text{Log}(x-1) + (-x)\text{Log}(-x)), \quad (\text{C.105})$$

where A, B, C are arbitrary.

C.3.5 Solution with $q_3 \neq 0$, $q_2 = 0$ and $h = 0$

For $h = 0$, i.e. $q_2 = 0$, and $q_3 \neq 0$ we have three solutions of the indicial equation (C.86) which are integer $r_1 = 1$, $r_2 = 0$, $r_3 = 0$ so solutions are

$$\begin{aligned} u_1(x) &= (1/x)^{r_1} \sum_{n=0}^{\infty} a_{n,r_1} (1/x)^n, \\ u_2(x) &= (1/x)^{r_2} \sum_{n=0}^{\infty} b_{n,r_2} (1/x)^n + (1/x)^{r_1} \sum_{n=0}^{\infty} a_{n,r_1} (1/x)^n \text{Log}(1/x), \\ u_3(x) &= (1/x)^{r_3} \sum_{n=0}^{\infty} c_{n,r_3} (1/x)^n + 2(1/x)^{r_2} \sum_{n=0}^{\infty} b_{n,r_2} (1/x)^n \text{Log}(1/x) + \\ &\quad + (1/x)^{r_1} \sum_{n=0}^{\infty} a_{n,r_1} (1/x)^n \text{Log}^2(1/x), \end{aligned} \quad (\text{C.106})$$

where $a_{0,r}$ is arbitrary (e.g. 1)

$$a_{1,r} = \frac{iq_3 + 2r^2}{r(1+r)^2} a_{0,r} \quad (\text{C.107})$$

and $m = n + r$

$$a_{n,r} = -\frac{(m-2)^2}{m^2} a_{n-2,r} + \frac{iq_3 + 2(m-1)^3}{(m-1)m^2} a_{n-1,r}, \quad (\text{C.108})$$

whereas $b_{0,r_2} = \frac{1}{iq_3} a_{0,r_1}$ and b_{1,r_2} is arbitrary while

$$b_{2,r_2} = \frac{1}{4} ((2 + iq_3)b_{1,r_2} + 6a_{0,r_1} - 8a_{1,r_1}), \quad (\text{C.109})$$

$$\begin{aligned} b_{n,r_2} &= -\frac{(n-2)^2}{n^2} b_{n-2,r_2} + \frac{iq_3 + 2(n-1)^3}{n^2(n-1)} b_{n-1,r_2} - \frac{(n-2)(3n-4)}{n^2(n-1)} a_{n-3,r_1} + \\ &\quad + \frac{6(n-1)}{n^2} a_{n-2,r_1} + \frac{2-3n}{n(n-1)} a_{n-1,r_1}. \end{aligned} \quad (\text{C.110})$$

Furthermore, $c_{0,r_3} = \frac{2}{iq_3} (2a_{0,r_1} + b_{1,r_2})$ and c_{1,r_3} is arbitrary and

$$c_{2,r_3} = \frac{1}{4} (2 + iq_3)c_{1,r_3} + 3b_{1,r_2} - 4b_{2,r_2} + 3a_{0,r_1} - \frac{5}{2}a_{1,r_1}, \quad (\text{C.111})$$

$$\begin{aligned} c_{n,r_3} &= -\frac{(n-2)^2}{n^2} c_{n-2,r_3} + \frac{iq_3 + 2(n-1)^3}{n^2(n-1)} c_{n-1,r_3} - \frac{2(n-2)(3n-4)}{n^2(n-1)} b_{n-2,r_2} + \\ &\quad + \frac{12(n-1)}{n^2} b_{n-1,r_2} + \frac{2(2-3n)}{n(n-1)} b_{n,r_2} + \frac{2(5-3n)}{n^2(n-1)} a_{n-3,r_1} + \frac{12}{n^2} a_{n-2,r_1} + \\ &\quad + \frac{2(1-3n)}{n^2(n-1)} a_{n-1,r_1}. \end{aligned} \quad (\text{C.112})$$

C.3.6 Solution with $q_2 = q_3 = 0$ and $h = 0$

In this case $a_{0,r}$ is arbitrary (e.g. 1). For the first solution with $r_1 = 1$ we have recurrence relations with $a_{1,r_1} = \frac{1}{2}a_{0,r_1}$

$$\begin{aligned} a_{2,r_1} &= \frac{1}{3}a_{1,r_1}, \\ a_{n,r_1} &= -\frac{(n-1)^2}{n+1}a_{n-2,r_1} + \frac{2n^2}{n+1}a_{n-1,r_1}. \end{aligned} \quad (\text{C.113})$$

Summing series up we derive an exact formula for

$$u_1(x) = (1/x)^{r_1} \sum_{n=0}^{\infty} a_{n,r_1} (1/x)^n = (1/x) \sum_{n=0}^{\infty} (1/x)^n a_{0,r_1} \frac{1}{n+1} = -\text{Log}(1 - 1/x). \quad (\text{C.114})$$

In the second solution, with $r_2 = 0$, we have arbitrary a_{1,r_2} (let us take 0) so the second solution is $u_2(x) = a_{0,r_2}$. The third one is with Log solutions

$$u_3(x) = (1/x)^{r_3} \sum_{n=0}^{\infty} b_{n,r_3} (1/x)^n + (1/x)^{r_2} \sum_{n=0}^{\infty} a_{n,r_2} (1/x)^n \text{Log}(1/x). \quad (\text{C.115})$$

Using recurrence relations with arbitrary b_{0,r_3}

$$\begin{aligned} b_{2,r_3} &= \frac{1}{2}b_{1,r_3}, \\ b_{n,r_3} &= -\frac{(n-2)^3}{n^2}b_{n-2,r_3} + \frac{2(n-1)^2}{n^2}b_{n-1,r_3} \end{aligned} \quad (\text{C.116})$$

one can derive an exact formula for $b_{n,r_3} = b_{1,r_3} \frac{1}{n}$ and performing summations with arbitrary $b_{0,r_3}(=0)$ we have $\sum_{n=0}^{\infty} b_{n,r_3} (1/x)^n = -b_{0,r_3} \text{Log}(1 - (1/x))$. All these solutions look like

$$\begin{aligned} u_1(x) &= (1/x)^{r_1} \sum_{n=0}^{\infty} a_{n,r_1} (1/x)^n = -a_{1,r_3} \text{Log}(1 - 1/x), \\ u_2(x) &= (1/x)^{r_2} \sum_{n=0}^{\infty} a_{n,r_2} x^n = a_{0,r_2}, \\ u_3(x) &= (1/x)^{r_3} \sum_{n=0}^{\infty} b_{n,r_3} (1/x)^n + a_{0,r_2} \text{Log}(1/x) = -b_{0,r_3} \text{Log}(1 - 1/x) + a_{0,r_2} \text{Log}(1/x). \end{aligned} \quad (\text{C.117})$$

Gathering together this all solutions we have

$$u(x) = A + B \text{Log}(-x) + C \text{Log}(x - 1), \quad (\text{C.118})$$

where A, B, C are arbitrary.

C.3.7 Solution with $q_3 \neq 0$ and $h = 2$

For $h = 2$ and $q_3 \neq 0$ we have three solutions to the indicial equation (C.86) which are integer $r_1 = 0, r_2 = -1, r_3 = -2$ so solutions are

$$\begin{aligned} u_1(x) &= (1/x)^{r_1} \sum_{n=0}^{\infty} a_{n,r_1} (1/x)^n, \\ u_2(x) &= (1/x)^{r_2} \sum_{n=0}^{\infty} b_{n,r_2} (1/x)^n + (1/x)^{r_1} \sum_{n=0}^{\infty} a_{n,r_1} (1/x)^n \text{Log}(1/x), \\ u_3(x) &= (1/x)^{r_3} \sum_{n=0}^{\infty} c_{n,r_3} (1/x)^n + 2(1/x)^{r_2} \sum_{n=0}^{\infty} b_{n,r_2} (1/x)^n \text{Log}(1/x) + \\ &\quad + (1/x)^{r_1} \sum_{n=0}^{\infty} a_{n,r_1} x^n \text{Log}^2(1/x), \end{aligned} \quad (\text{C.119})$$

where a_{0,r_1} is arbitrary (e.g. 1)

$$a_{1,r_1} = \frac{iq_3 + 2r(r+1)(r+2)}{(r+1)(r+2)(r+3)} a_{0,r_1} \quad (C.120)$$

and $m = n + r_1$

$$a_{n,r_1} = -\frac{(m-1)(m-2)}{(m+1)(m+2)} a_{n-2,r_1} + \frac{iq_3 + 2m(m^2-1)}{(m+2)(m+1)m} a_{n-1,r_1}, \quad (C.121)$$

whereas $b_{0,r_2} = \frac{2}{iq_3} a_{0,r_1}$ and b_{1,r_2} is arbitrary while

$$b_{2,r_2} = \frac{1}{6} (iq_3 b_{1,r_2} + 4a_{0,r_1} - 11a_{1,r_1}), \quad (C.122)$$

$$\begin{aligned} b_{n,r_2} = & -\frac{(n-2)(n-3)}{n(n+1)} b_{n-2,r_2} + \frac{iq_3 + 2(n-2)(n-1)n}{n(n^2-1)} b_{n-1,r_2} - \frac{11+3(n-4)n}{n(n^2-1)} a_{n-3,r_1} + \\ & + \frac{6(n-2)n+4}{n(n^2-1)} a_{n-2,r_1} + \frac{1-3n}{n(n^2-1)} a_{n-1,r_1}. \end{aligned} \quad (C.123)$$

Moreover, $c_{0,r_3} = -\frac{2}{iq_3} b_{0,r_2}$ and $c_{1,r_3} = \frac{4(b_{0,r_2} + b_{1,r_2})}{iq_3} + \frac{6a_{0,r_1}}{iq_3}$ and c_{2,r_3} is arbitrary while

$$c_{3,r_3} = \frac{1}{6} (iq_3 c_{2,r_3} + 2b_{0,r_2} + 8b_{1,r_2} - 22b_{2,r_2} - 12a_{0,r_1} + 12a_{1,r_1}), \quad (C.124)$$

$$\begin{aligned} c_{n,r_3} = & -\frac{(n-3)(n-4)}{n(n-1)} c_{n-2,r_3} + \frac{iq_3 + 2(n-3)(n-2)(n-1)}{n(n-1)(n-2)} c_{n-1,r_3} + \frac{2(3n(6-n)-26)}{n(n-1)(n-2)} b_{n-3,r_2} + \\ & + \frac{4(11-12m+3m^2)}{n(n-1)(n-2)} b_{n-2,r_2} - \frac{2(2-6m+3m^2)}{n(n-1)(n-2)} b_{n-1,r_2} - \frac{6(n-3)}{n(n-1)(n-2)} a_{n-4,r_1} + \frac{12}{n(n-1)} a_{n-3,r_1} + \\ & - \frac{6}{n(n-2)} a_{n-2,r_1}. \end{aligned} \quad (C.125)$$

C.3.8 Solution with $q_3 = 0$ and $h = 2$

In this case $a_{0,r}$ is arbitrary (e.g. 1). For the first solution with $r_1 = 0$ we have other coefficients $a_{n>0,r_1} = 0$. The second solution, with $r_2 = -1$, has arbitrary a_{1,r_2} (we can take it as 0) and $a_{2,r_2} = 0$. and third one with arbitrary a_{1,r_3} , a_{2,r_3} (we also set them to 0). All these solutions look like

$$\begin{aligned} u_1(x) &= (1/x)^{r_1} \sum_{n=0}^{\infty} a_{n,r_1} (1/x)^n = a_{0,r_3}, \\ u_2(x) &= (1/x)^{r_2} \sum_{n=0}^{\infty} a_{n,r_2} (1/x)^n = x a_{0,r_2}, \\ u_3(x) &= (1/x)^{r_3} \sum_{n=0}^{\infty} a_{n,r_3} (1/x)^n = x^2 a_{0,r_3}. \end{aligned} \quad (C.126)$$

Gathering together all this solutions we have

$$u(x) = A + B(-x)^2 + C(x-1)^2, \quad (C.127)$$

where A, B, C are arbitrary. As we can see this solution corresponds to the solution with $q_3 = 0$ and arbitrary $h \notin \{0, 1\}$. For other integer $h \notin \{0, 1\}$ we can observe the same correspondence.

Appendix D

Coefficients in the eigenequations for $N = 4$

Coefficients for the eigenequations of \hat{q}_3 and \hat{q}_4 for $N = 4$ presented in (5.55) and (5.56) look like

$$t_{0,0} = \frac{1}{x_2-1} (i(-h + s_1 + s_2 + s_3 + s_4)((s_2 - s_4)(1 - h + s_1 + s_2 - s_3 + s_4) + (s_2^2 - s_2(-1 + h + s_1 - s_3 + 2s_4 - 2s_4x_1) + s_4(1 + s_1 - s_3 + s_4 - 2(1 + s_4)x_1 + h(-1 + 2x_1)))x_2)) - q_3, \quad (D.1)$$

$$t_{1,0} = -i((s_1 + s_2)(1 - h + s_1 + s_2 - s_3 + s_4) - (2 + h - h^2 + s_1(3 + s_1) - s_2 + 4hs_2 - 3s_2^2 - 3s_3 - 2s_2s_3 + s_3^2 + s_4 + s_4^2 - 2s_1(s_2 + s_3 + s_4(x_1 - 1)) + -2s_2s_4x_1)x_2 - (s_2 + s_3 - 2)(1 + h + s_1 - s_2 - s_3 + s_4 - 2s_4x_1)x_2^2), \quad (D.2)$$

$$t_{0,1} = \frac{1}{(x_2-1)x_2} (i((h - s_1 - s_2 + s_3 - s_4)(s_1 + s_4 + (s_1 + s_2 - 2)x_1) + ((s_1 + s_4)(1 - 2h + 2s_1 - 2s_3 + 2s_4) - 2(1 + h^2 + s_2 + s_2^2 - s_3 + s_2s_3 - s_3^2 + (4 + s_2)s_4 + 2s_4 + s_1(2 + s_2 + s_3 + 2s_4) - h(2 + s_1 + 2s_2 + 3s_4))x_1 + -(s_1 + s_2 - 2)(1 + 2s_4)x_1^2)x_2 + (-(s_1 + s_4)(1 - h + s_1 - s_2 - s_3 + s_4) + (2 + h^2 + s_1^2 + s_2 + s_3 - 2(s_2 + s_3)^2 + h(-3 - 2s_1 + s_2 + s_3 - 6s_4) + 7s_4 + (s_3 - s_2)s_4 + 5s_4^2 + s_1(3 - s_2 + s_3 + 6s_4))x_1 + (-2 - h^2 - 2s_2 + s_2^2 - 3s_3 + s_2s_3 + s_1(-2 + s_2 - 3s_4) + -(7 + 2s_2 + 5s_3)s_4 - 5s_4^2 + h(3 + s_1 + s_3 + 6s_4))x_1^2)x_2^2)), \quad (D.3)$$

$$t_{2,0} = -\frac{1}{x_2(x_2-1)} (i(x_1 - 1)x_1(h - s_1 - s_2 + s_3 - s_4 + (2 - 2h + 3s_1 - 2s_3 + 3s_4 + (-4 + s_1 + s_2 - s_4)x_1)x_2 + (-2 + h - 2s_1 + s_2 + s_3 - 2s_4 - 2hx_1 + (4 + s_1 + s_2 + 2s_3 + 4s_4)x_1)x_2^2)), \quad (D.4)$$

$$t_{0,2} = -i(x_2 - 1)x_2(h - 2 - 2s_1 - 2s_2 + s_3 - s_4 + (4 + h + s_1 - 2s_2 - 2s_3 + s_4 - 2s_4x_1)x_2), \quad (D.5)$$

$$t_{1,1} = -i(x_1(2h - 3s_2 + (2h - 4(s_2 + s_3) + (s_2 - 2)x_1)x_2 + (s_2 + s_3 - 2)(x_1 - 1)x_2^2 + 2(s_3 + x_2)) + s_1(x_2 - 1 + x_1(x_1x_2 - 3)) + s_4(x_2 - 1 - 2x_1(1 + 2x_1x_2))), \quad (D.6)$$

$$t_{3,0} = -i(x_1 - 1)^2 x_1^2, \quad (D.7)$$

$$t_{0,3} = -i(x_2 - 1)^2 x_2^2, \quad (D.8)$$

$$t_{2,1} = i(x_1 - 1)x_1(x_2 - 1 + 2x_1x_2), \quad (D.9)$$

$$t_{1,2} = ix_1(x_2 - 1)x_2((x_1 - 1)x_2 - 2) \quad (D.10)$$

and where

$$\begin{aligned} f_{1,0} = & \frac{1}{(x_2-1)^2 x_2} ((-h + s_1 + s_2 - s_3 + s_4)((s_2 - 1)(s_1 + s_4) - (-2 + s_1 + \\ & + s_2)(1 + s_4)x_1) + (-s_1 + s_4)(-h(-2 + s_2) + s_1(s_2 - 2) + 3s_3 + \\ & - 2s_4 + s_2(-2 + s_2 - 3s_3 + s_4)) + (-5s_2 + 3s_1^2 s_2 + s_2^2 + s_3^3 + 5s_3 + \\ & - 2s_2 s_3 + s_3^2 - s_2 s_3^2 + h^2(-1 + s_2 - s_4) + (-5 + 4s_2^2 + s_2(5 + s_3) + \\ & - s_2(7 + 3s_3))s_4 + 2(s_2 - 4)s_4^2 - s_4^3 + h(5 + s_1 - 4s_1 s_2 - 2s_2^2 + \\ & + (9 + s_1 - 3s_2)s_4 + 2s_4^2) + s_1(-5 + s_2 + 4s_2^2 + 6s_2 s_4 - 3s_3(1 + s_4) + \\ & - s_4(8 + s_4)))x_1 - (-2 + s_1 + s_2)(-h + s_1 + s_2 + s_4)(1 + 2s_4)x_1^2)x_2 + \\ & + (-s_1 + s_4)(s_1 + s_2 - h(1 + s_2) - 3s_3 + s_4 + s_2(s_1 + s_2 + 3s_3 + s_4)) + \\ & + (3s_2 - 5s_3 + 2(s_2^2 + s_2(1 - s_2)s_3 + (-1 + s_2)s_3^2) + 3s_4 + 2(s_2^2 + \\ & + 4s_2(1 + s_3) - s_3(4 + s_3))s_4 + (6 + 3s_2 - s_3)s_4^2 + s_4^3 + h^2(1 + s_4) + \\ & + s_1^2(1 - 2s_2 + s_4) + s_1(3 - 2s_2^2 + s_3 + (7 + s_3)s_4 + 2s_4^2 + s_2(3 + \\ & + 4s_3 + s_4)) + h(-3 + s_3 + 2s_1(-1 + s_2 - s_4) + (-7 + s_3)s_4 - 2s_4^2 + \\ & - s_2(3 + 2s_3 + 3s_4)))x_1 + (2s_1^2 s_2 + s_3 + s_2(-3 + s_2^2 + (-2 + s_2)s_3) + \\ & + h^2(-1 + s_2 - 2s_4) - 3s_4 + (s_3 - s_2(7 + 5s_3))s_4 - (7 + 3s_2 + 2s_3)s_4^2 + \\ & - 2s_4^3 + h(3 + s_1 + s_2 - 3s_1 s_2 - 2s_2^2 + s_3 - s_2 s_3 + 2(4 + s_1 + s_2 + s_3)s_4 + \\ & + 4s_4^2) + s_1(3s_2^2 + s_2(2s_3 + s_4) - (3 + 2s_3 + s_4)(1 + 2s_4)))x_1^2)x_2^2 + \\ & + ((s_1 + s_4)(-h + s_1 + s_2 + s_3 + s_4)) - (h^2 s_2 + 2s_1 s_2 + s_1^2 s_2 + 2s_2^2 + \\ & + s_2^3 - 2s_3 - s_1 s_3 + s_2 s_3 + 4s_1 s_2 s_3 + 2s_2^2 s_3 - s_3^2 + s_2 s_3^2 + \\ & + (5s_2^2 - s_3(5 + s_1 + s_3) + s_2(2 + 5s_1 + 6s_3))s_4 + (4s_2 - s_3)s_4^2 + \\ & + h(s_3 - 2s_2(1 + s_1 + s_2 + s_3) + (-5s_2 + s_3)s_4))x_1 + \\ & + (h^2 s_2 + 2s_2^2 + s_2^3 - 2s_3 + 2s_2 s_3 + \\ & + 3s_2^2 s_3 - s_3^2 + 2s_2 s_3^2 + (2s_2(1 + 2s_2) + 5(-1 + s_2)s_3 - 2s_3^2)s_4 + \\ & + (3s_2 - 2s_3)s_4^2 + s_1 s_2(2 + s_2 + 2s_3 + 3s_4) + \\ & - h(-s_3 + s_2(2 + s_1 + 2s_2 + 3s_3) + 4s_2 s_4 - 2s_3 s_4))x_1^2)x_2^3), \end{aligned} \quad (D.11)$$

$$\begin{aligned}
f_{0,0} = & \frac{1}{(x_2-1)^2} (s_2 s_4 (h^2 - h + s_1 - 4h s_1 + 3s_1^2 + s_2 - 2h s_2 + 4s_1 s_2 + s_2^2 + s_3 + \\
& - s_3^2 + s_4 - 2h s_4 + 4s_1 s_4 + 2s_2 s_4 + s_4^2 + 2(h s_1 - s_1^2 - s_1 s_2 - h s_3 + \\
& + 2s_1 s_3 + s_2 s_3 + s_3^2 - s_1 s_4 + s_3 s_4 + (1 - h + 2s_1 + s_2 + s_4) \\
& (-h + s_1 + s_2 + s_3 + s_4) x_1) x_2 + \times (-s_1^2 - s_1(1 + 2s_2 + 4s_3 + 2s_4) + \\
& + 2s_1(1 + s_2 + 2s_3 + s_4) x_1 + h^2(2x_1 - 1) + \\
& + (s_2 + s_3 + s_4)(-1 - s_2 - s_3 - s_4 + 2(1 + s_2 + 2s_3 + s_4) x_1) + \\
& + h(1 + 2s_1 + 2s_2 + 2s_3 + 2s_4 - 2(1 + s_1 + 2s_2 + 3s_3 + 2s_4) x_1) x_2^2)) - q_4, \tag{D.12}
\end{aligned}$$

$$\begin{aligned}
f_{0,1} = & -\frac{1}{x_2-1} (s_4(s_1^2(1 + 2x_1 x_2 - x_2^2) + s_1(1 - h + 2s_2 - s_3 + s_4 + (-2 - h + \\
& + 4s_2 + 3s_3 + s_4 + 2(1 - h + 2s_2 + s_4) x_1) x_2 - (1 + 5s_2 + s_3 + 2s_4 + \\
& + 2h(x_1 - 1) - 2(-2 + 4s_2 + 2s_3 + s_4) x_1) x_2^2 - (-2 + s_2 + s_3) x_2^3) + \\
& + s_2^2(1 + (2x_1 - 1) x_2)(1 + x_2(3 + x_2)) + (1 + h - s_3 - s_4) x_2 \\
& \times (h + h(2x_1 - 1) x_2 - (2 + s_4 - 2x_2)(1 - x_2 + 2x_1 x_2) + \\
& + s_3(1 + x_2(-2 + x_2 - 2x_1 x_2))) + \\
& + s_2((1 + (-1 + 2x_1) x_2)(1 + s_4 + x_2 + 4s_4 x_2 + (-3 + s_4) x_2^2) + \\
& - h(1 + (2x_1 - 1) x_2(1 + x_2(4 + x_2))) + \\
& + s_3(-1 + x_2(3 - 2x_2^2 + 4x_1 x_2(2 + x_2))))), \tag{D.13}
\end{aligned}$$

$$\begin{aligned}
f_{2,0} = & \frac{1}{(x_2-1)^2 x_2} (x_1((h - s_1 - s_2 + s_3 - s_4)(2 + s_1 - s_2 + s_4 + \\
& + (-4 + s_1 + s_2 - s_4) x_1) + (-4h + 4s_1 - 2h s_1 + 2s_1^2 + 4s_2 + s_1 s_2 - s_2^2 + \\
& - 6s_3 - 3s_1 s_3 + 3s_2 s_3 + 4s_4 - 2h s_4 + 4s_1 s_4 + s_2 s_4 - 3s_3 s_4 + 2s_4^2 + \\
& - (h^2 - s_1 s_2 - s_2^2 + 3s_1 s_3 + 3s_2 s_3 - s_3^2 + 5s_1 s_4 + 4s_2 s_4 - 3s_3 s_4 + 5s_4^2 + \\
& + 11(s_1 + s_2 - s_3 + s_4) - h(11 + s_1 + 6s_4)) x_1 + \\
& - (-h + s_1 + s_2 + s_4)(s_1 + s_2 - 2(2 + s_4)) x_1^2) x_2 - (s_1^2 + 2s_1 s_2 + s_2^2 + \\
& - 3s_1 s_3 + 3s_2 s_3 + 2s_1 s_4 + 2s_2 s_4 - 3s_3 s_4 + s_4^2 - h(2 + s_1 + s_2 + s_4) + \\
& + 2(s_1 + s_2 - 3s_3 + s_4) + h(7 + 2s_1 + 3s_2 - s_3 + 5s_4) x_1 + \\
& - (s_1^2 + 2s_2^2 - s_3(13 + 2s_3) + 7s_4 - 6s_3 s_4 + 4s_4^2 + \\
& + s_1(7 + 3s_2 + s_3 + 5s_4) + s_2(7 + 4s_2 + 6s_4)) x_1 + h^2(x_1 - 1) x_1 + \\
& - h(5 + s_1 + 2s_2 + s_3 + 4s_4) x_1^2 + (s_2^2 - 3s_3 + 5s_4 - s_3 s_4 + 3s_4^2 + \\
& + s_1(5 + s_2 + 2s_3 + 3s_4) + s_2(5 + 3s_3 + 4s_4)) x_1^2) x_2^2 + \\
& - (x_1 - 1)(-h s_2 + s_1 s_2 + s_2^2 - 2s_3 - s_1 s_3 + s_2 s_3 + s_2 s_4 - s_3 s_4 + \\
& - (s_1 s_2 + s_2^2 - 4s_3 + s_2 s_3 - s_3^2 + h(s_3 - s_2) + s_2 s_4 - 3s_3 s_4) x_1) x_2^3), \tag{D.14}
\end{aligned}$$

$$\begin{aligned}
f_{0,2} = & s_4 x_2 (2 - h + 2s_1 + 2s_2 - s_3 + s_4 + (-6 - s_1 + 3s_3 + \\
& + 2(-h + 2(1 + s_1 + s_2) + s_4) x_1) x_2 + \\
& - (s_1 + h(2x_1 - 1) - (2(-2 + s_2 + s_3) + s_4)(-1 + 2x_1)) x_2^2), \tag{D.15}
\end{aligned}$$

$$\begin{aligned}
f_{1,1} = & \frac{1}{x_2-1}(hs_1 - s_1^2 - 2s_1s_2 + s_1s_3 + hs_4 - 2s_1s_4 - 2s_2s_4 + s_3s_4 - s_4^2 - 2hx_1 + \\
& + 2s_1x_1 + hs_1x_1 - s_1^2x_1 + 2s_2x_1 + hs_2x_1 - 2s_1s_2x_1 - s_2^2x_1 - 2s_3x_1 + \\
& + s_1s_3x_1 + 2s_4x_1 - 2hs_4x_1 + 2s_1s_4x_1 + 2s_2s_4x_1 - 2s_3s_4x_1 + 2s_4^2x_1 + \\
& -(-(s_1 + s_4)(2 - 2h + 2s_1 + 3s_2 + 3s_3 + 2s_4) + (h^2 + s_1 + 3s_2 + \\
& + 4s_1s_2 + 2s_2^2 - 3s_3 + 3s_1s_3 + 3s_2s_3 - s_3^2 + (5 + 6s_1 + 10s_2 - 6s_3)s_4 + \\
& + 5s_4^2 - h(3 + s_1 + 3s_2 + 6s_4))x_1 + ((-2 + s_1 + s_2)(-h + s_1 + s_2) + \\
& + (-2 + 4h - 5s_1 - 5s_2)s_4 - 4s_4^2)x_1^2)x_2 + (-(s_1 + s_4)(4 - h + s_1 + \\
& - 3s_3 + s_4) + (h^2 + s_1 + s_1^2 + 3s_2 + 5s_1s_2 + 2s_2^2 + s_3 + s_1s_3 - 2s_3^2 + \\
& + h(-3 - 2s_1 - 3s_2 + s_3 - 4s_4) + 11s_4 + 4(s_1 + s_2 - 2s_3)s_4 + 3s_4^2)x_1 + \\
& + (-h^2 + s_1 - s_2 - 4s_1s_2 - 3s_2^2 + s_3 - 2s_1s_3 - 4s_2s_3 - 5s_4 + \\
& - 3s_1s_4 - 4s_2s_4 + 5s_3s_4 - s_4^2 + h(1 + s_1 + 4s_2 + s_3 + 2s_4))x_1^2)x_2^2 + \\
& + (-2 + s_2 + s_3)(x_1 - 1)(s_1 + s_4 - (-h + s_2 + s_3 + 3s_4)x_1)x_2^3), \tag{D.16}
\end{aligned}$$

$$\begin{aligned}
f_{3,0} = & \frac{1}{x_2(1-x_2)}x_1^2(x_1 - 1)(-h + s_1 + s_2 - s_3 + s_4 - (s_1 + s_2 - 2s_3 + s_4 + \\
& + h(x_1 - 1) - (s_1 + s_2 + s_4)x_1)x_2 + s_3(x_1 - 1)x_2^2), \tag{D.17}
\end{aligned}$$

$$t_{0,3} = -s_4(x_2 - 1)x_2^2(1 + (2x_1 - 1)x_2), \tag{D.18}$$

$$\begin{aligned}
f_{2,1} = & \frac{1}{x_2-1}(x_1(1 - 2s_2 + s_3 - 2x_1 + (3s_1 + 3s_2 - 2s_3 + s_4)x_1 + \\
& + (s_3(6x_1 - 3) + x_1(3 - 4s_1 + s_4 - 2x_1 + 3s_1x_1) + \\
& + s_2(3 + x_1(-5 + 3x_1)))x_2 + (x_1 - 1)(3 + 3s_3(x_1 - 1) - s_1x_1 + 2s_4x_1)x_2^2 + \\
& -(-2 + s_2 + s_3)(x_1 - 1)^2x_2^3 - h(x_2 + 2x_1 - 1)(1 + (x_1 - 1)x_2))), \tag{D.19}
\end{aligned}$$

$$\begin{aligned}
f_{1,2} = & x_2(-(h - 2s_2 + s_3)x_1 + s_1(1 + 2x_1 - x_2)(1 + (x_1 - 1)x_2) + \\
& + x_1x_2(-3 + 3s_3 - hx_1 + 2s_2x_1 - (3 + h - 2s_2 - 2s_3)(x_1 - 1)x_2) + \\
& + s_4(x_1 - 1)(x_2 - 1)(1 + (-1 + 3x_1)x_2)), \tag{D.20}
\end{aligned}$$

$$f_{3,1} = (x_1 - 1)x_1^2(1 + (x_1 - 1)x_2), \tag{D.21}$$

$$f_{1,3} = -x_1(x_2 - 1)x_2^2(1 + (x_1 - 1)x_2), \tag{D.22}$$

$$f_{2,2} = x_1(1 + x_1(x_2 - 2) - x_2)x_2(1 + (x_1 - 1)x_2), \tag{D.23}$$

$$f_{4,0} = f_{0,4} = 0. \tag{D.24}$$

If we take homogeneous spins $s = s_1 = s_2 = \dots s_N$ our equations simplify and the coefficients for \hat{q}_3 look like

$$t_{0,0} = \frac{2i}{1-x_2}(h - 1)(h - 4s)s(x_1 - 1)x_2 - q_3, \tag{D.25}$$

$$\begin{aligned}
t_{1,0} = & \frac{1}{x_2(x_2-1)}(i(2(h-2s)(s+(s-1)x_1) - 2(-s(1-2h+2s)+ \\
& +(-1+h-4s)(-1+h-2s)x_1 + (s-1)(1+2s)x_1^2)x_2 + \\
& -((h-2)(h-1)(x_1-1)x_1 + 4s^2x_1(3x_1-1) - 2s(h-1+ \\
& -3(h-2)x_1 + (4h-7)x_1^2))x_2^2)), \tag{D.26}
\end{aligned}$$

$$\begin{aligned}
t_{0,1} = & -i((1+h)x_2(-2+h+2x_2) + 4s^2(1+x_2)(1+x_1x_2) - 2s(-1+h+ \\
& +2hx_2 + (1+h+2x_1)x_2^2)), \tag{D.27}
\end{aligned}$$

$$\begin{aligned}
t_{2,0} = & \frac{i}{x_2(x_2-1)}(x_1-1)x_1(-h+2s+2(-1+h-2s+2x_1)x_2+ \\
& +(2-h+2s+2(h-2-4s)x_1)x_2^2), \tag{D.28}
\end{aligned}$$

$$t_{0,2} = -i(x_2-1)x_2(-2+h-4s+(h-2(s-2+sx_1))x_2), \tag{D.29}$$

$$\begin{aligned}
t_{1,1} = & -2i(x_1(1+x_2)(h+x_2-x_1x_2) + s(-1+x_2+ \\
& +x_1^2(x_2-1)x_2 - x_1(1+x_2)(3+x_2))), \tag{D.30}
\end{aligned}$$

$$t_{3,0} = -i(x_1-1)^2x_1^2, \tag{D.31}$$

$$t_{0,3} = -i(x_2-1)^2x_2^2, \tag{D.32}$$

$$t_{2,1} = i(x_1-1)x_1(2x_1x_2+x_2-1), \tag{D.33}$$

$$t_{1,2} = ix_1(x_2-1)x_2(x_2(x_1-1)-2) \tag{D.34}$$

and for \hat{q}_4

$$\begin{aligned}
f_{0,0} = & \frac{1}{(x_2-1)^2} (s^2(h^2(1+x_2)(1+(2x_1-1)x_2)+ \\
& -h(1+8s)(1+x_2)(1+(2x_1-1)x_2) + 2s(2(1+x_2)(1-x_2+2x_1x_2)+ \\
& +s(7+x_2(2-9x_2+16x_1(x_2+1)))))) - q_4, \tag{D.35}
\end{aligned}$$

$$\begin{aligned}
f_{1,0} = & \frac{1}{(x_2-1)^2x_2} (h^2x_1x_2(-1+(x_1-1)(-1+s(x_2-1))x_2) + h(x_1(3x_2-2) \\
& \times(1+(x_1-1)x_2) - 2s^2(x_1-1)(x_2-1)(1+2x_1x_2+(4x_1-1)x_2^2)+ \\
& +s(2+x_2(2(x_2-2)+x_1(x_2-10)(x_2-1)-x_1^2(2+(x_2-11)x_2))))+ \\
& +2s(2s^2(x_1-1)(x_2-1)(1+x_2+3x_1x_2+(5x_1-2)x_2^2)+ \\
& +s(-2+x_2(3+10x_1(x_2-1)-x_2^2+x_1^2(3+(x_2-12)x_2))))+ \\
& +x_1(2+x_2(-5+x_2(2+x_2)-x_1(-3+x_2(4+x_2))))), \tag{D.36}
\end{aligned}$$

$$\begin{aligned}
f_{0,1} = & \frac{1}{x_2-1} (s(-(1+h)x_2(h-2+2x_2)(1+(2x_1-1)x_2) - 4s^2(1+x_2(4+x_2 \\
& \times(3+2x_2)+x_1(3+x_2)(1+3x_2))) + 2s(-1+h(1+(2x_1-1)x_2)(1+ \\
& +x_2(4+x_2))+x_2(-1+(7-5x_2)x_2+2x_1(-1+x_2(4x_2-1))))), \tag{D.37}
\end{aligned}$$

$$\begin{aligned}
f_{2,0} = & \frac{1}{(x_2-1)^2 x_2} (x_1(-4s - h^2 x_1 x_2 (1 + (x_1 - 1)x_2) + 2s(3x_2 - x_2^3 + \\
& -2x_1^2 x_2 (x_2(3 + x_2)) + x_1(x_2 - 1))(-4 + x_2(7 + 3x_2)) + \\
& -s(-(x_2 - 1)^3 + 8x_1^2 x_2^2 + x_1(1 + x_2(7 + (x_2 - 9)x_2)))) + \\
& + h((1 + (x_1 - 1)x_2)(2 - 2x_2 + x_1(5x_2 - 4)) + s(-(x_2 - 1)^3 + \\
& + 8x_1^2 x_2^2 + x_1(1 + x_2(7 + (x_2 - 9)x_2))))), \tag{D.38}
\end{aligned}$$

$$\begin{aligned}
f_{0,2} = & s x_2 (-h(1 + x_2)(1 + (2x_1 - 1)x_2) + 2(1 - 3x_2 + 2x_2(x_1 + x_2 - 2x_1 x_2) + \\
& + s(2 + x_2(1 - 3x_2 + 5x_1(1 + x_2))))), \tag{D.39}
\end{aligned}$$

$$\begin{aligned}
f_{1,1} = & \frac{1}{(x_2-1)} (-h^2 x_1 x_2 (1 + (x_1 - 1)x_2) + 2s(-3s + 2x_1 + s x_1 + (2 + 3(x_1 - 1)x_1 + \\
& + s(4 + x_1(5x_1 - 13)))x_2 - (2(2 + (x_1 - 4)x_1) + s(-1 + x_1(8x_1 - 5)))x_2^2 + \\
& - (s - 1)(x_1 - 1)(5x_1 - 2)x_2^3) + h(-x_1(1 + (x_1 - 1)x_2)(2 + x_2(2x_2 - 1)) + \\
& + 2s(1 + x_2(-2 + x_2 + x_1(5 - x_1 + 4(x_1 - 1)x_2 + (x_1 - 1)x_2^2))))), \tag{D.40}
\end{aligned}$$

$$f_{3,0} = \frac{1}{x_2(x_2-1)} (x_1 - 1)x_1^2 (h + h(x_1 - 1)x_2 + s(-2 + x_2(1 + x_2 - x_1(3 + x_2))))), \tag{D.41}$$

$$f_{0,3} = -s(x_2 - 1)x_2^2(1 + (2x_1 - 1)x_2), \tag{D.42}$$

$$\begin{aligned}
f_{2,1} = & \frac{1}{x_2-1} (x_1(1 - s - 2x_1 + 5s x_1 + x_1(3 - 2x_1 + s(6x_1 - 2)))x_2 + \\
& + (x_1 - 1)(3 + s(4x_1 - 3))x_2^2 - 2(s - 1)(x_1 - 1)^2 x_2^3 + \\
& - h(x_2 + 2x_1 - 1)(1 + (x_1 - 1)x_2)), \tag{D.43}
\end{aligned}$$

$$\begin{aligned}
f_{1,2} = & x_2(-x_1(h + (3 + h)x_2)(1 + (x_1 - 1)x_2) + s(2 + 2x_1 - 4x_2 + \\
& x_1(7 + x_1)x_2 + (x_1 - 1)(7x_1 - 2)x_2^2)), \tag{D.44}
\end{aligned}$$

$$f_{3,1} = (x_1 - 1)x_1^2(1 + (x_1 - 1)x_2), \tag{D.45}$$

$$f_{1,3} = -x_1(x_2 - 1)x_2^2(1 + (x_1 - 1)x_2), \tag{D.46}$$

$$f_{2,2} = x_1(1 + x_1(x_2 - 2) - x_2)x_2(1 + (x_1 - 1)x_2), \tag{D.47}$$

$$f_{4,0} = f_{0,4} = 0. \tag{D.48}$$

Bibliography

- [1] M. Gell-Mann, M.L. Goldberger, F.E. Low, E. Marx, F.Zachariasen. Elementary particles of Conventional Field Theory as Regge poles. III. *Phys. Rev. B*, 133:145, 1964.
- [2] M. Gell-Mann, M.L. Goldberger, F.E. Low, E. Marx, F.Zachariasen. Elementary particles of Conventional Field Theory as Regge poles. IV. *Phys. Rev. B*, 133:161, 1964.
- [3] V. N. Gribov. A Reggeon diagram technique. *Sov. Phys. JETP*, 26:414–422, 1968.
- [4] V. S. Fadin, E. A. Kuraev, and L. N. Lipatov. On the Pomeranchuk singularity in asymptotically free theories. *Phys. Lett.*, B60:50–52, 1975.
- [5] J. Bartels. High-Energy behavior in a nonabelian gauge field theory. *Phys. Lett.*, B68:258, 1977.
- [6] H. Cheng and C. Y. Lo. High-energy amplitudes of Yang-Mills theory in arbitrary perturbative orders. 1. *Phys. Rev.*, D15:2959, 1977.
- [7] J. Bartels. High-energy behavior in a nonabelian gauge theory. 2. First corrections to $T(n \rightarrow m)$ beyond the leading $\ln s$ approximation. *Nucl. Phys.*, B175:365, 1980.
- [8] J. Kwiecinski and M. Praszalowicz. Three gluon integral equation and odd C singlet Regge singularities in QCD. *Phys. Lett.*, B94:413, 1980.
- [9] T. Jaroszewicz. Infrared divergences and Regge behavior in QCD. *Acta Phys. Polon.*, B11:965, 1980.
- [10] G. 't Hooft. A planar diagram theory for strong interactions. *Nucl. Phys.*, B72:461, 1974.
- [11] L. N. Lipatov. Pomeron and odderon in QCD and a two-dimensional conformal field theory. *Phys. Lett.*, B251:284–287, 1990.
- [12] L. N. Lipatov. High-energy asymptotics of multicolor QCD and two- dimensional conformal field theories. *Phys. Lett.*, B309:394–396, 1993.
- [13] L. N. Lipatov. High-energy asymptotics of multicolor qcd and exactly solvable lattice models. *JETP Lett.*, 59:596–599, 1994.

- [14] L. D. Faddeev and G. P. Korchemsky. High-energy QCD as a completely integrable model. *Phys. Lett.*, B342:311–322, 1995.
- [15] L. N. Lipatov I. I. Balitsky. The Pomeranchuk singularity in Quantum Chromodynamics. *Sov. J. Nucl. Phys.*, 28:822–829, 1978.
- [16] E. A. Kuraev, L. N. Lipatov, and V. S. Fadin. The Pomeranchuk singularity in nonabelian gauge theories. *Sov. Phys. JETP*, 45, 1977.
- [17] T. Jaroszewicz. High-energy multi - gluon exchange amplitudes. Triest preprint IC/80/175.
- [18] R. A. Janik and J. Wosiek. Solution of the odderon problem. *Phys. Rev. Lett.*, 82:1092–1095, 1999.
- [19] P. Gauron, B. Nicolescu, and L. Szymanowski. A possible field theoretical description of the odderon. IPNO/TH 87-53.
- [20] L. Lukaszuk and B. Nicolescu. A possible interpretation of p p rising total cross- sections. *Nuovo Cim. Lett.*, 8:405–413, 1973.
- [21] S. E. Derkachov, G. P. Korchemsky, and A. N. Manashov. Noncompact Heisenberg spin magnets from high-energy QCD. III: Quasiclassical approach. *Nucl. Phys.*, B661:533–576, 2003.
- [22] G. P. Korchemsky, J. Kotanski, and A. N. Manashov. Compound states of reggeized gluons in multi-colour QCD as ground states of noncompact Heisenberg magnet. *Phys. Rev. Lett.*, 88:122002, 2002.
- [23] S. E. Derkachov, G. P. Korchemsky, J. Kotanski, and A. N. Manashov. Noncompact Heisenberg spin magnets from high-energy QCD. II: Quantization conditions and energy spectrum. *Nucl. Phys.*, B645:237–297, 2002.
- [24] T. Jaroszewicz. Gluonic Regge singularities and anomalous dimensions in QCD. *Phys. Lett.*, B116:291, 1982.
- [25] L. N. Lipatov. The bare Pomeron in Quantum Chromodynamics. *Sov. Phys. JETP*, 63:904–912, 1986.
- [26] G. P. Korchemsky, J. Kotanski, and A. N. Manashov. Multi-Reggeon compound states and resummed anomalous dimensions in QCD. *Phys. Lett.*, B583:121–133, 2004.
- [27] H. J. De Vega and L. N. Lipatov. Interaction of reggeized gluons in the Baxter-Sklyanin representation. *Phys. Rev.*, D64:114019, 2001.
- [28] H. J. De Vega and L. N. Lipatov. Exact resolution of the Baxter equation for reggeized gluon interactions. *Phys. Rev.*, D66:074013, 2002.

- [29] M. A. Braun. *The interaction of reggeized gluons and Lipatov's hard pomeron*. – lectures. University of Santiago de Compostela, 17506 Santiago de Compostela, Spain, 1994.
- [30] R. J. Baxter. *Exactly Solved Models in Statistical Mechanics*. Academic Press, London, 1982.
- [31] E. A. Kuraev, L. N. Lipatov, and V. S. Fadin. Multi - Reggeon processes in the Yang-Mills theory. *Sov. Phys. JETP*, 44:443–450, 1976.
- [32] J. Bartels. A field - theoretic study of the Regge - eikonal model. 1. *Ann. Phys.*, 94:1, 1975.
- [33] A. B. Kaidalov. The quark - gluon structure of the Pomeron and the rise of inclusive spectra at high-energies. *Phys. Lett.*, B116:459, 1982.
- [34] Yu. V. Kovchegov. High energy QCD and the large N_c limit. 2002. hep-ph/0202238.
- [35] J. Bartels and M. G. Ryskin. Absorptive corrections to structure functions at small x . *Z. Phys.*, C60:751–756, 1993.
- [36] J. Bartels and M. Wusthoff. The triple Regge limit of diffractive dissociation in deep inelastic scattering. *Z. Phys.*, C66:157–180, 1995.
- [37] A. H. Mueller. Limitations on using the operator product expansion at small values of x . *Phys. Lett.*, B396:251–256, 1997.
- [38] S. E. Derkachov, G. P. Korchemsky, and A. N. Manashov. Noncompact Heisenberg spin magnets from high-energy QCD. I: Baxter Q-operator and separation of variables. *Nucl. Phys.*, B617:375–440, 2001.
- [39] P. Di Francesco, P. Mathieu, D. Sénéchal. *Conformal Field Theory*. Springer, New York, 1982.
- [40] J. B. Zuber. An introduction to Conformal Field Theory. *Acta Phys. Polon.*, B26:1785–1813, 1995.
- [41] E. K. Sklyanin. Quantum inverse scattering method. Selected topics. 1991. hep-th/9211111.
- [42] L. D. Faddeev. Algebraic aspects of Bethe Ansatz. *Int. J. Mod. Phys.*, A10:1845–1878, 1995.
- [43] L. D. Faddeev. How Algebraic Bethe Ansatz works for integrable model. 1996. hep-th/9605187.

- [44] L. D. Faddeev, E. K. Sklyanin, and L. A. Takhtajan. The quantum inverse problem method. 1. *Theor. Math. Phys.*, 40:688–706, 1980.
- [45] C. Ewerz. The odderon in Quantum Chromodynamics. 2003. hep-ph/0306137.
- [46] G. P. Korchemsky. Quasiclassical QCD Pomeron. *Nucl. Phys.*, B462:333–388, 1996.
- [47] G. P. Korchemsky. WKB quantization of Reggeon compound states in high-energy QCD. 1997. hep-ph/9801377.
- [48] J. Wosiek and R. A. Janik. Solution of the odderon problem for arbitrary conformal weights. *Phys. Rev. Lett.*, 79:2935–2938, 1997.
- [49] M. Praszalowicz and A. Rostworowski. Spectrum of the odderon charge for arbitrary conformal weights. *Acta Phys. Polon.*, B30:349–357, 1999.
- [50] J. Kotanski and M. Praszalowicz. Solutions of the quantization conditions for the odderon charge q_3 and conformal weight h . *Acta Phys. Polon.*, B33:657–682, 2002.
- [51] L. N. Lipatov. Duality symmetry of Reggeon interactions in multicolour QCD. *Nucl. Phys.*, B548:328–362, 1999.
- [52] H. Navelet and R. Peschanski. Conformal invariance and the exact solution of BFKL equations. *Nucl. Phys.*, B507:353–366, 1997.
- [53] J. Bartels, L. N. Lipatov, and G. P. Vacca. A new odderon solution in perturbative QCD. *Phys. Lett.*, B477:178–186, 2000.
- [54] J. Bartels, M. A. Braun, D. Colferai, and G. P. Vacca. Diffractive η_c photo- and electro-production with the perturbative QCD odderon. *Eur. Phys. J.*, C20:323–331, 2001.
- [55] G. P. Vacca. Properties of a family of n reggeized gluon states in multicolour QCD. *Phys. Lett.*, B489:337–344, 2000.
- [56] Yu. V. Kovchegov, L. Szymanowski, and S. Wallon. Perturbative odderon in the dipole model. *Phys. Lett.*, B586:267–281, 2004.
- [57] G. P. Korchemsky. Bethe ansatz for QCD pomeron. *Nucl. Phys.*, B443:255–304, 1995.
- [58] G. P. Korchemsky and J. Wosiek. New representation for the odderon wave function. *Phys. Lett.*, B464:101–110, 1999.
- [59] R. Engel, D. Yu. Ivanov, R. Kirschner, and L. Szymanowski. Diffractive meson production from virtual photons with odd charge-parity exchange. *Eur. Phys. J.*, C4:93–99, 1998.

- [60] J. Czyzewski, J. Kwiecinski, L. Motyka, and M. Sadzikowski. Exclusive η_c photo- and electroproduction at HERA as a possible probe of the odderon singularity in QCD. *Phys. Lett.*, B398:400–406, 1997.
- [61] J. Bartels, M. A. Braun, and G. P. Vacca. The process $\gamma^* + p \rightarrow \eta_c + X$: A test for the perturbative QCD odderon. *Eur. Phys. J.*, C33:511–521, 2004.
- [62] G. P. Korchemsky. Integrable structures and duality in high-energy QCD. *Nucl. Phys.*, B498:68–100, 1997.
- [63] C. M. Bender and T. T. Wu. Anharmonic oscillator. *Phys. Rev.*, 184:1231–1260, 1969.
- [64] A. V. Turbiner and A. G. Ushveridze. Spectral singularities and quasiexactly solvable quantal problem. *Phys. Lett.*, A126:181, 1987. ITEP-87-55.
- [65] C. M. Bender and A. V. Turbiner. Analytic continuation of eigenvalue problems. *Phys. Lett.*, A173:442, 1993. WU-HEP-92-13.
- [66] V. M. Braun, S. E. Derkachov, G. P. Korchemsky, and A. N. Manashov. Baryon distribution amplitudes in QCD. *Nucl. Phys.*, B553:355–426, 1999.
- [67] A. V. Belitsky. Integrability and WKB solution of twist-three evolution equations. *Nucl. Phys.*, B558:259–284, 1999.
- [68] L. A. Takhtajan and L. D. Faddeev. The quantum method of the inverse problem and the heisenberg xyz model. *Russ. Math. Surveys*, 34:11–68, 1979.
- [69] N. M. Bogolyubov, A. G. Izergin, and V. E. Korepin. *Quantum inverse scattering method and correlation functions*. Univ. Press, Cambridge, 1993.
- [70] E. Levin and K. Tuchin. Nonlinear evolution and saturation for heavy nuclei in DIS. *Nucl. Phys.*, A693:787–798, 2001.
- [71] J. Bartels. Unitarity corrections to the Lipatov pomeron and the small x region in deep inelastic scattering in QCD. *Phys. Lett.*, B298:204–210, 1993.
- [72] J. Bartels. Unitarity corrections to the lipatov pomeron and the four gluon operator in deep inelastic scattering in qcd. *Z. Phys.*, C60:471–488, 1993.
- [73] A. Schafer, L. Mankiewicz, and O. Nachtmann. Double diffractive J/ψ and phi production as a probe for the odderon. *Phys. Lett.*, B272:419–424, 1991.
- [74] V. V. Barakhovsky, I. R. Zhitnitsky, and A. N. Shelkovenko. Odderon: A Sharp signal at HERA. *Phys. Lett.*, B267:532–534, 1991.

- [75] I. F. Ginzburg, D. Yu. Ivanov, and V. G. Serbo. Pomeron and odderon in photon initiated reactions and jet production in gamma gamma collisions. *Phys. Atom. Nucl.*, 56:1474–1480, 1993.
- [76] I. F. Ginzburg and D. Yu. Ivanov. Semihard production of tensor mesons in gamma gamma collisions and the perturbative odderon. *Nucl. Phys. Proc. Suppl.*, 25B:224–233, 1992.
- [77] L. Motyka and J. Kwiecinski. Possible probe of the QCD odderon singularity through the quasidiffractive eta/c production in gamma gamma collisions. *Phys. Rev.*, D58:117501, 1998.
- [78] H. G. Dosch, C. Ewerz, and V. Schatz. The odderon in high energy elastic p p scattering. *Eur. Phys. J.*, C24:561–571, 2002.
- [79] J. Bartels, L. N. Lipatov, and G. P. Vacca. Interactions of Reggeized gluons in the Moebius representation. *Nucl. Phys.*, B706:391–410, 2005.
- [80] I. Balitsky. Operator expansion for high-energy scattering. *Nucl. Phys.*, B463:99–160, 1996.
- [81] Yu. V. Kovchegov. Small- x F_2 structure function of a nucleus including multiple pomeron exchanges. *Phys. Rev.*, D60:034008, 1999.
- [82] Yu. V. Kovchegov. Unitarization of the BFKL pomeron on a nucleus. *Phys. Rev.*, D61:074018, 2000.
- [83] E. Levin and K. Tuchin. Solution to the evolution equation for high parton density QCD. *Nucl. Phys.*, B573:833–852, 2000.
- [84] E. Levin and K. Tuchin. New scaling at high energy DIS. *Nucl. Phys.*, A691:779–790, 2001.
- [85] A. H. Mueller. Soft gluons in the infinite momentum wave function and the BFKL pomeron. *Nucl. Phys.*, B415:373–385, 1994.
- [86] A. H. Mueller and B. Patel. Single and double BFKL pomeron exchange and a dipole picture of high-energy hard processes. *Nucl. Phys.*, B425:471–488, 1994.
- [87] A. H. Mueller. Unitarity and the BFKL pomeron. *Nucl. Phys.*, B437:107–126, 1995.
- [88] Z. Chen and A. H. Mueller. The Dipole picture of high-energy scattering, the BFKL equation and many gluon compound states. *Nucl. Phys.*, B451:579–604, 1995.
- [89] L. D. McLerran and R. Venugopalan. Gluon distribution functions for very large nuclei at small transverse momentum. *Phys. Rev.*, D49:3352–3355, 1994.

- [90] L. D. McLerran and R. Venugopalan. Computing quark and gluon distribution functions for very large nuclei. *Phys. Rev.*, D49:2233–2241, 1994.
- [91] L. D. McLerran and R. Venugopalan. Green’s functions in the color field of a large nucleus. *Phys. Rev.*, D50:2225–2233, 1994.
- [92] Y. Hatta, E. Iancu, K. Itakura, and L. McLerran. Odderon in the color glass condensate. 2005. hep-ph/0501171.
- [93] I. Balitsky. Factorization and high-energy effective action. *Phys. Rev.*, D60:014020, 1999.
- [94] I. Balitsky. High-energy QCD and Wilson lines. 2001. hep-ph/0101042.
- [95] V. S. Fadin and L. N. Lipatov. BFKL pomeron in the next-to-leading approximation. *Phys. Lett.*, B429:127–134, 1998.
- [96] E. M. Levin, M. G. Ryskin, and A. G. Shuvaev. Anomalous dimension of the twist four gluon operator and pomeron cuts in deep inelastic scattering. *Nucl. Phys.*, B387:589–616, 1992.
- [97] A. Gorsky, I. I. Kogan, and G. Korchemsky. High energy QCD: Stringy picture from hidden integrability. *JHEP*, 05:053, 2002.
- [98] A. Staruszkiewicz. *Algebra i Geometria*. NKF, Kraków, 1993.